Understanding and Exploring the Diverse Potential of Natural Products

Sannia Farooque

Submitted in accordance with the requirements for the degree of Doctor of Philosophy

School of Chemistry

Faculty of Mathematical and Physical Sciences

The University of Leeds

November 2019

The candidate confirms that the work submitted is her own, except where work has formed part of jointly authored publications has been included. The contribution of the candidate and the other authors of this work has been explicitly indicated below. The candidate confirms that appropriate credit has been given within the thesis where reference has been made to the work of others.

This copy has been supplied on the understanding that it is copyright material and that no quotation from the thesis may be published without proper acknowledgement.

The right of Sannia Farooque to be identified as Author of this work has been asserted by her in accordance with the Copyright, Designs and Patents Act 1988.

Acknowledgements

I am very much grateful for this opportunity to Prof Chris Rayner, Dr Richard Blackburn and Dr Alex O'Neill. A special thanks to Chris for allowing me to work flexibly so that I could manage my parental responsibilities whilst doing my PhD.

I would like to thank Simon Barrette, Martin Huscroft, Dr Mark Howard and Dr Stuart Warriner for keeping the analytical equipment up and running. I am grateful to them for their technical assistance.

I had much fun working with Dr Nada Nass, Zeyad AlZeyadi, Dr Asma Akhter and Luiza Galarion from O'Neill group and learnt a bit of microbiology.

I would like to thank past and present members of Rayner group for their support and constructive criticism, especially Dr Meryem Benohoud. I really enjoyed working with Muhammad Wathon and Laurent Octavia, you guys are some of the best people to work with. I will miss my coffee and lunch dates with Heather and Ravi so much, you guys are awesome.

I would like to dedicate this thesis to my sister Hina, my brother-in-law Jason and my daughter Perniyan. You guys give me strength and inspire me to be a better version of myself every day. Thank you for being there for me whenever I needed you.

Abstract

In this thesis, the diverse potential of natural products for their use in consumer products and as therapeutics has been explored. The importance of design of extraction experiments has been highlighted; a well-developed method not only allows targeted extraction of natural products from biological matrices but can also reduces the number of purification steps significantly. This in turn makes processes more environmentally friendly as well as cost and time-effective. During literature research, it was noted that natural product extracts and isolated compounds were often not fully characterised which can lead to error. In this project, all extracts and the isolated compounds were monitored and analysed using a range of analytical techniques to facilitate reliable and reproducible characterisation of the extracts.

In first part of this thesis, blackcurrant extract was fully characterised and a scalable method for extraction of polyphenols and generation of three product streams was developed. Fourteen polyphenols were isolated and fully characterised using mass spectrometry, IR, UV/Vis and NMR spectroscopy. Extinction coefficients were calculated for all compounds. The extract was quantified using HPLC and external standards. Total monomeric anthocyanin content assay (TMAC) was evaluate for its efficiency of estimating percentage of anthocyanins in natural extracts and compared with HPLC. The effect of organic solvents and co-occurring flavonoids on the assay results was studied. The stability of anthocyanins during extraction and purification processes was also studied.

Second part of this thesis was focussed on discovery of antibacterial compounds from microbial extracts. This project was further divided into two areas of research: revisiting previously discarded antibiotic compounds and exploration of novel sources of antibiotic compounds. These projects were done in close collaboration with Dr Alex O'Neill and his PhD students. Previously discarded actinorhodin family of compounds were revisited and extracellular γ-actinorhodin with strong antistaphylococcal activity was identified. Targeted scalable method of extraction and purification was developed. γ-Actinorhodin was isolated in 19 wt./wt.% yield and fully characterised using mass spectrometry, IR, UV/Vis and NMR spectroscopy. A TLC–bioautography assay was developed which allowed efficient screening of active crude extracts. VF48A and P5-25 extracts with strong activity against *S. aureus* SH1000 and MDR *E. coli* CMR400 were chosen to take to next stage. Seventeen 2,5-diketopiperazines were isolated from these extracts altogether. These DKPs showed selective activity against targeted organisms. Thirteen DKPs were synthesised to confirm assignments and bioactivity.

Table of Contents

List of Tables

List of Figures

XII

List of Schemes

Abbreviations

δ	Chemical shift
ε	Molar extinction coefficient
λ	Wavelength
J	Coupling constant
A	Absorbance
ATCC	American Type Culture Collection
COG	Cyanidin-3-*O*-glucoside
COR	Cyanidin-3-*O*-rutinoside
CA	Caffeic acid
DOG	Delphinidin-3-*O*-glucoside
DOR	Delphinidin-3-*O*-rutinoside
Eq.	Equivalent
FA	Formic acid
Gly.	Glycoside
HPLC	High performance liquid chromatography
Kg	Kilogram
LC-MS	Liquid chromatography-mass spectrometry
Mg	Milligram
M_w	Molecular weight
MOG	Myricetin-3-*O*-glucoside
MOR	Myricetin-3-*O*-rutinoside
NF	Nigrumin ferulate
NMR	Nuclear magnetic resonance
p-CA	*p*-Coumaric acid
p-NC	*p*-nigrumin coumarate
PA	Polymeric anthocyanins
ppm	Parts per million
QOG	Quercetin-3-*O*-glucoside
QOR	Quercetin-3-*O*-rutinoside
SPE	Solid phase extraction
TFA	Trifluoroacetic acid
v/v %	Volume per volume %
wt./wt.%	Weight per weight %

Chapter 1 Introduction to the Blackcurrant Project

1.1 Role of Colour

Colour plays an important role in nature facilitating pollination, protection and function.[1] The versatility of colour in plant kingdom stems from two major families of molecules namely anthocyanins and carotenoids. Anthocyanins are known for red to blue shades while the latter incorporates yellow and orange hues into fruits, vegetables and flowers; more than 700 carotenoids have been identified in nature.[2] Anthocyanins are the largest group of polyphenolic pigments in the plant kingdom.[3] They are non-toxic, water-soluble phenolic compounds responsible for the red, purple and blue coloration of fruits, vegetables and flowers.[4] Their colour is determined by the number of hydroxyl groups (and degree of methylation) and the nature, number and position of glycosyl moieties including associated aliphatic or aromatic acids attached to the glycosides.[5,6,7]

Drawing inspiration from nature humans have long used colour in textiles, food and cosmetics. For example, indigo and alizarin are natural colorants that had great economic value as textile dyes.[5] There is a desire across industries to replace synthetic dyes with natural renewable sources of colorants; anthocyanins are widely permitted as natural sources as food/beverage colorants within Europe (E163), Japan, the US, and many other countries.[3,8] Grape skin extract has been used as a colorant for more than 100 years, first being applied to enhance wine colour.[2] In the US, "Grape-color extract" is obtained as a by-product in processing Concord grapes (*Vitus labruscana*), but its application is limited by the FDA to non-beverage food use.[3] Practical sources of anthocyanins are limited by overall economic considerations and availability of suitable raw material.[9]

1.2 Anthocyanins

The discovery of the structure and synthesis of anthocyanins took place during the first years of the 20th century. However, as early as 1664, Robert Boyle was already curious about the properties of these compounds, which led him to report on the colour changes that take place when extracts of flowers are treated with acids and alkalis.[5] The word anthocyanin has its origin in Greek: Anthos = flower and kyanos = blue, it was used to describe the pigment in blue cornflower.[6] Anthocyanin **1** (Figure 1.1) backbones are constructed from anthocyanidin **2** (the aglycone) and at least one sugar moiety. The

glycosidic substitution imparts stability to anthocyanidin and facilitates aqueous solubility which allows easy transport within biological systems.[6] The anthocyanin sugars are represented by one or more units of glucose (most common), galactose, rhamnose, arabinose, xylose and glucuronic acid. Several apiose containing anthocyanins have recently been isolated from the African milk bush (*Synadenium grantii*).[6] The glycosyl moieties are connected to the aglycone at position 3, and sometimes also to the 5-, 7-, 3'-, 4'- or 5 '-hydroxyl groups. Nearly all anthocyanins have a glycosyl substitution at position-3 except for the 3-deoxyanthocyanins.

Anthocyanins are usually found in solution in the vacuole in plant cells. In some plant families, anthocyanins have also been reported to occur in intensively coloured bodies recently called AVIs (anthocyanic vacuolar inclusions) but the structures of AVIs have not been yet fully characterised. Anthocyanins are synthesised on the cytoplasmic surface of rough endoplasmic reticulum *in vivo* and then transported to vacuoles.[6] The exact mechanism for the latter is not known yet, however, the biosynthetic pathway has been probed extensively (*vide infra*).

Anthocyanin **(1)**

Anthocyanidin **(2)**

Flavylium cation **(3)**

3-Deoxyanthocyanin **(4)**
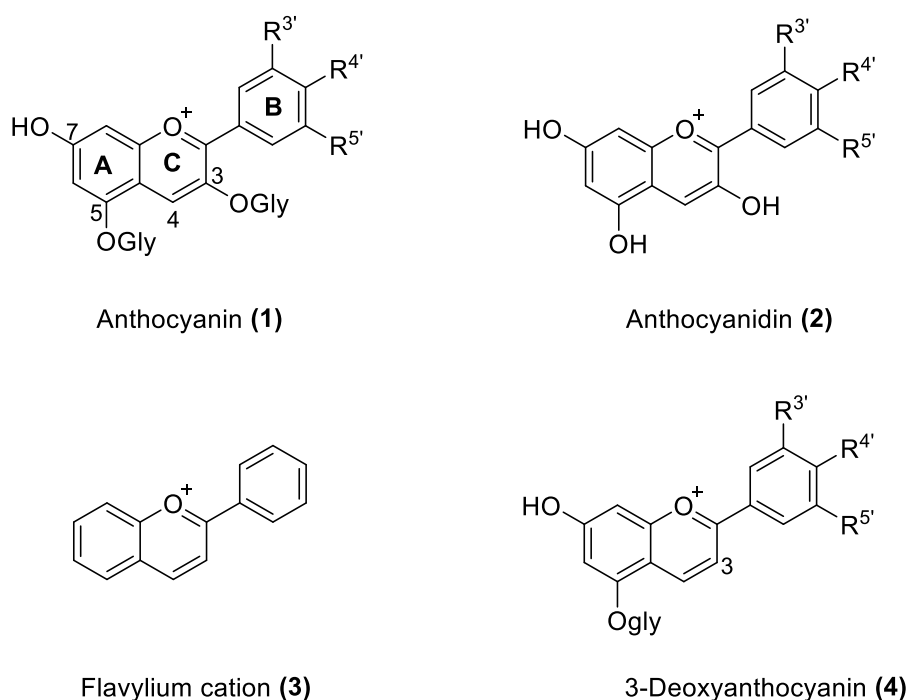
Figure 1.1. Generic forms of flavylium cations in nature (Gly = glycoside).[5]

The main chemical motif that exhibits interesting chemistry is the flavylium cation **3**.[5,10] Anthocyanidins **2** (aglycones) have been found to be relatively unstable on their own. It is worthy to note that chemists synthesised flavylium cationic compounds significantly

sooner than anthocyanins; they served as a guide to solve anthocyanins' structures and to achieve complete synthesis of anthocyanins. Moreover, the study of the kinetics and thermodynamics of the network of chemical reactions involving synthetic flavylium compounds has been very useful to the comprehension of the chemical behaviour of anthocyanins, since both groups follow an identical network of chemical reactions. 3-Deoxyanthocyanins **4** lack glycosidic and hydroxy substitution at position 3; they have a limited distribution in angiosperms and are found in ferns and mosses as well as hybrids of sorghum and purple corn.[5] The fact that anthocyanidins and deoxyanthocyanins are not found as commonly as anthocyanins in nature may suggest crucial role of C-3 substitution on the flavylium cation.[5]

1.3 Equilibria Framework of Anthocyanins

Anthocyanins exhibit a remarkable framework of reactions with varying pH. It took decades to figure out all the equilibrium forms using synthetic flavylium salts.[5] It is generally agreed that anthocyanins and synthetic partners take part in acid-base equilibria in aqueous solutions. A general scheme of reactions has been put together in Scheme 1.1 to highlight important equilibria forms. At pH 3 and below they exist mainly as red flavylium cations **AH$^+$**, however as pH is raised there is a competition between kinetic and thermodynamic processes. Deprotonation of **AH$^+$** leads to formation of kinetic product **A$_{4'}$** (quinoidal base, violet). Further deprotonation of the quinonoidal bases can take place at pH 6–7 with the formation of more bluish resonance-stabilised quinonoidal anions **A$^-$**.

Thermodynamics favours formation of colourless hemiketal **B$_2$** *via* hydration at position 2 (followed by proton loss); the ring opening leads to the formation of yellow *cis*-chalcone **C$_E$**. However, this step is relatively slow compared to the hydration and deprotonation. The hydration can also occur at position 4 but it is more common at position 2. The isomerisation of *cis*-chalcone **C$_E$** into *trans*-chalcone **C$_Z$** is activated by UV absorption. It has been suggested that these set of reactions can be viewed as single acid-base equilibrium between the flavylium cation **AH$^+$** and a conjugate base **C$_B$** which is defined as sum of the concentrations of all the species at equilibrium.[5]

$$[CB] = [A_{4'/7}] + [B_{2/4}] + [C_E] + [C_Z]$$

3

Although anthocyanins can take on all the forms (on the R.H.S of the equation) in aqueous solutions, it has been reported that colourless hemiketal **B$_{2/4}$** dominates in **[CB]** for most of 3-substituted anthocyanins at pH > 4.[5] However, anthocyanins in red cabbage were found to exist mainly in violet quinoidal form **A$_{4'}$** at pH 4.3.[11] Andersen *et al.* demonstrated that 3-glucosides of pelargonidin, peonidin and malvidin (all have one OH on B ring) exhibit intense blue colours and stability at pH 8–9.[12] The exact mole fraction of these species and the rate of their interconversion varies with number and nature of the substituents. For instance, quinoidal base **A** has the largest mole fraction for 4-, 5-substituted flavylium cations and deoxyanthocyanins.[5] In conclusion anthocyanins are most stable at pH < 3, therefore extraction, purification and processing should be performed below pH 3 to avoid degradation.
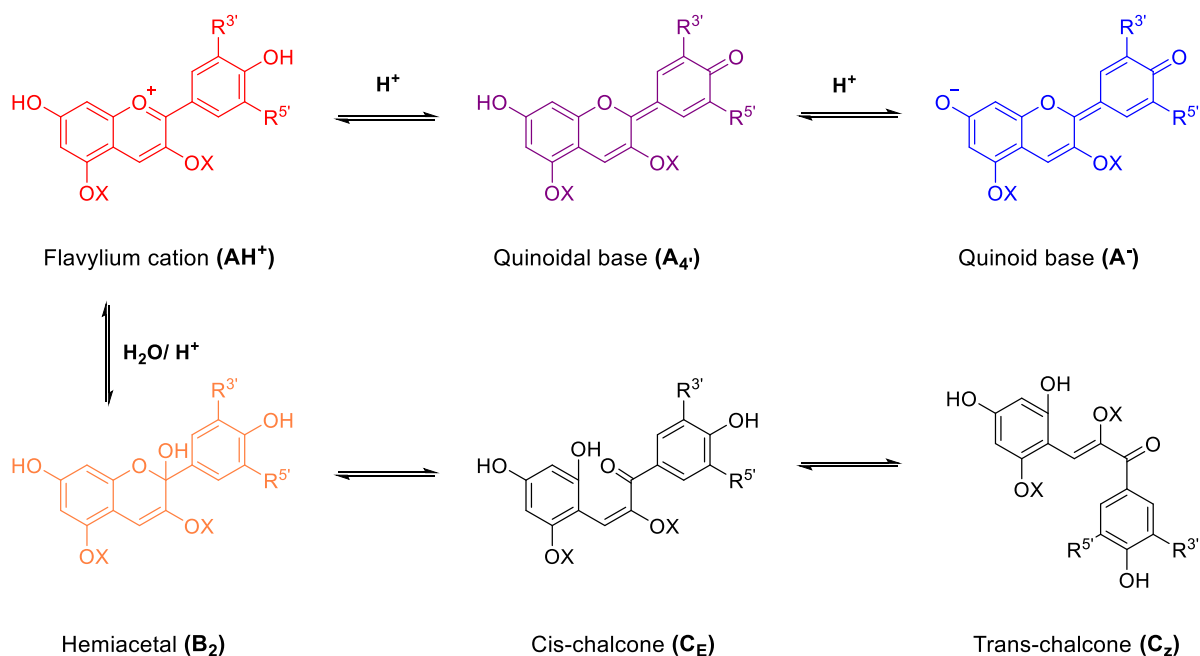
Scheme 1.1. General scheme for anthocyanidin equilibrium forms. X= glycoside or OH. [6]

1.4 Co-pigmentation

Anthocyanins can exist in monomeric form but also associate non-covalently with auxiliary molecules (co-pigments) such as flavonoids, metals and organic acids such as benzoic acid and cinnamic acid, or self-associate when present in higher amounts.[6] Co-pigmentation of anthocyanins is one of the most important factors in determining the final anthocyanin colour in plants. More than 66% of the reported anthocyanins contain one or more acyl moieties which may participate in inter-/intramolecular co-pigmentation of the anthocyanidin nucleus with significant impact on the colours of plants, especially in

flowers. For example, the pH of the cell sap is around 4–6 and most un-substituted monomeric anthocyanins exist as colourless hemiketal B_2 or chalcone $C_{E/Z}$ forms at this pH. In contrast, *mono-* or *di-*acylated anthocyanins display colours in this pH region since these anthocyanins mainly exist as reddish flavylium cations AH^+ or blue quinonoidal bases $A_{4'}$ at these pH values (Scheme 1.1). The acyl groups of these latter anthocyanins hinder hydrolysis of the flavylium cationic form, and thus formation of the colourless hemiketal/chalcone forms of the anthocyanin. The interaction between the acyl groups and the anthocyanidin of the same anthocyanin is an example of intramolecular co-pigmentation.

A similar mechanism involving stacked complexes is proposed for intermolecular co-pigmentation of anthocyanins with other flavonoids and similar planar compounds. Cultivars with different colours but the same anthocyanin have been found to contain different co-pigments or altered molar proportions of anthocyanin to co-pigment. When pigment concentrations become relatively high, anthocyanins themselves may act as co-pigments and participate in self-association reactions.[6] The colour intensity (absorbance) will then increase more than proportionally to anthocyanin concentration. The magnitude of the co-pigmentation has been shown to be influenced by the nature of the anthocyanidin and the co-pigment, the concentration of the anthocyanin, the copigment:anthocyanin molar ratio, as well as pH and temperature.[6] The exact mechanisms for co-pigmentation of anthocyanins are, however, often inadequately known. It is difficult to differentiate between intramolecular association between different moieties of the same anthocyanin molecule, and intermolecular association of two or more anthocyanin molecules. The exact orientation of the co-pigment in relation to the anthocyanidin chromophore in the associated complexes is only rarely measured experimentally.[6]

1.5 Biosynthesis of Anthocyanins

Anthocyanins are synthesised on the cytoplasmic surface of the rough endoplasmic reticulum and then carried to the vacuoles in plant cells.[6] The mechanism behind this initial transport is not fully understood, however genes involved in the biosynthesis of anthocyanins have been probed extensively which has facilitated unravelling of the biosynthetic network.[13,14,15,16] Intense pigmented cellular bodies have been identified in some plants namely anthocyanic vacuolar inclusions (AVIs).[17] It has been suggested that AVIs may find their use in the food industry, however, the pH inside AVIs is higher than food formulations. This can be challenging due to behaviour of anthocyanins at different pH environments (*vide supra*).

The synthesis of anthocyanins is facilitated by a network of enzymes *in vivo*. Anthocyanins as well as other flavanoids are synthesised from precursors: malonyl-CoA and *p*-coumaroyl-CoA **5** (Scheme 1.2). The first step involves stepwise chalcone synthase-catalysed (CHS) condensation of the acetate moieties from three malonyl and one *p*-coumaroyl molecule into 4, 2', 4', 6'-tetrahydroxychalcone **6** (yellow). This is then isomerised by chalcone isomerase to give colourless naringenin **7**. The hydroxylation of naringenin **7** into dihydrokaempferol **8** is catalysed by flavanone-3-hydroxylase (F3H). At this stage, the path can branch out to give different types of anthocyanins and flavonoids. The example of cyanidin has been presented in Scheme 1.2. Dihydrokaempferol **8** is hydroxylated to give dihydroquercetin **9**. Dihydroflavanol-4-reductase, anthocyanin synthase and glucosyltransferase then catalyse the transformation of dihydroquercetin into the final product. The resulting anthocyanidin **10** can then be further decorated with glycosyl, acetyl and/or methyl groups depending on plant's needs and the enzymes that it carries.
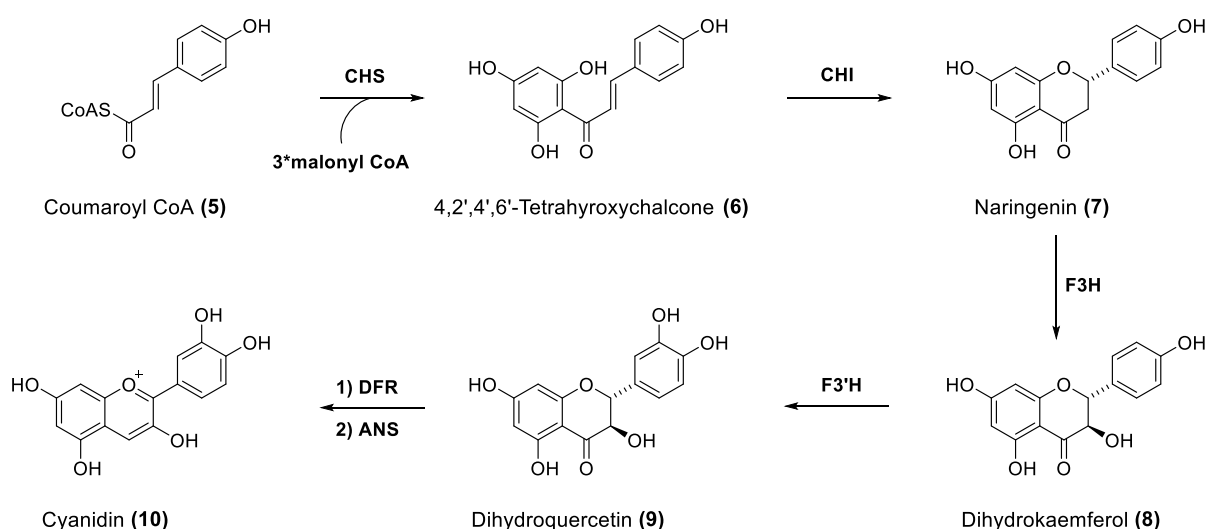
Scheme 1.2. The biosynthetic pathway to cyanidin **10**.[13] CHS = chalcone synthase; CHI = chalcone isomerase; F3H = flavanone-3-hydroxylase; DFR = dihydroflavanol-4-reductase; ANS = anthocyanin synthase.

1.6 Sources of Major Anthocyanins

More than 600 anthocyanins have been discovered in plants, flowers and fruits.[6] Despite the diversity exhibited by anthocyanins, there are six common anthocyanidins lending their core structure to this pool of molecules (Table 1.1); these are cyanidin **10** (50%), pelargonidin **11** (12%), peonidin **12** (12%), delphinidin **13** (12%), petunidin **14** (7%) and malvidin **15** (7%). Cyanidin and glucoside are the most commonly found anthocyanidin

and glycoside respectively.[18] Anthocyanins have been reported in blackcurrants,[19,20,21,22,23] strawberries,[12,24] chokeberries,[25] black carrot,[26] black beans,[27,28] blueberries,[12,29] and black mulberries[30]. The types and distribution of anthocyanins vary widely between angiosperms. Cyanidin-3-*O*-glucoside has been isolated from blackberry [31] and black rice.[32] Black beans have been reported to contain 3-*O*-glucosides of delphinidin, petunidin and malvidin.[28] Berry fruits are predominantly comprised of 3-glycosidic substituted anthocyanidins whereas sophisticated motifs have been reported in flowers.[6,33]

Table 1.1. The most common anthocyanidins found in nature.[3]
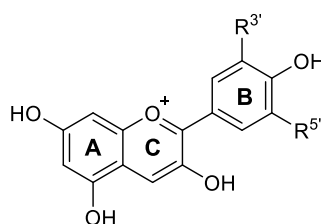
Anthocyanidin	$R^{3'}$	$R^{5'}$	Number
Pelargonidin	H	H	**11**
Cyanidin	OH	H	**10**
Peonidin	OCH_3	H	**12**
Delphinidin	OH	OH	**13**
Petunidin	OCH_3	OH	**14**
Malvidin	OCH_3	OCH_3	**15**

1.7 Anthocyanins and Neutral Polyphenols in Anthocyanin-rich Foods

Chandler and Harper first reported aglycones (**10** & **13**), monoglucosides and rutinosides of cyanidin and delphinidin **16-19** in blackcurrant fruits in 1962 (Figure 1.2).[19] Subsequent research groups have also found these four major anthocyanins (predominantly by comparison of literature with mass spectral data and relative retention times on HPLC systems), however accounts of minor anthocyanins vary markedly in these studies.[34,35,36] In general, these four anthocyanins contribute to about 97% of the total monomeric anthocyanin content in blackcurrants.[21] It is worth noting that this figure is not indicative of their overall amount as it does not take into account rest of the polyphenols present in blackcurrants.

The qualitative data on blackcurrant extracts in the literature is in general agreement, however, there is a significant difference in the quantification data. Although some variation in chemical profile of different cultivars is expected due to the habitat and nutrient profile, the discrepancy in data surpasses the expected variation. Many studies employ total monomeric anthocyanin content (TMAC) assay to estimate the amount of anthocyanins in blackcurrant fruits, juices and extracts.[8,37] However, this method lacks accuracy and leads to inconsistency in the literature (*vide infra*). Quantitative HPLC is a more reliable technique for quantification of natural product than assays. Cyboran *et al.* found blackcurrant fruit extract to contain 419.8 mg g^{-1} of dry matter which is considerably higher than other reports (where TMAC was employed).[38] The team used standard samples to obtain external calibration graphs to quantify the monomeric anthocyanins in the extract. In another interesting study, Aneta *et al.* screened four cultivars from organic and conventional cultivation and found organic cultivars to have higher anthocyanic profile (1272 mg kg^{-1} of dry fruit weight) than the conventional ones (1162 mg kg^{-1} of dry fruit weight).[39]

Delphinidin-3-*O*-glucoside (**16**)

Cyanidin-3-*O*-glucoside (**18**)

Delphinidin-3-*O*-rutinoside (**17**)

Cyanidin-3-*O*-rutinoside (**19**)
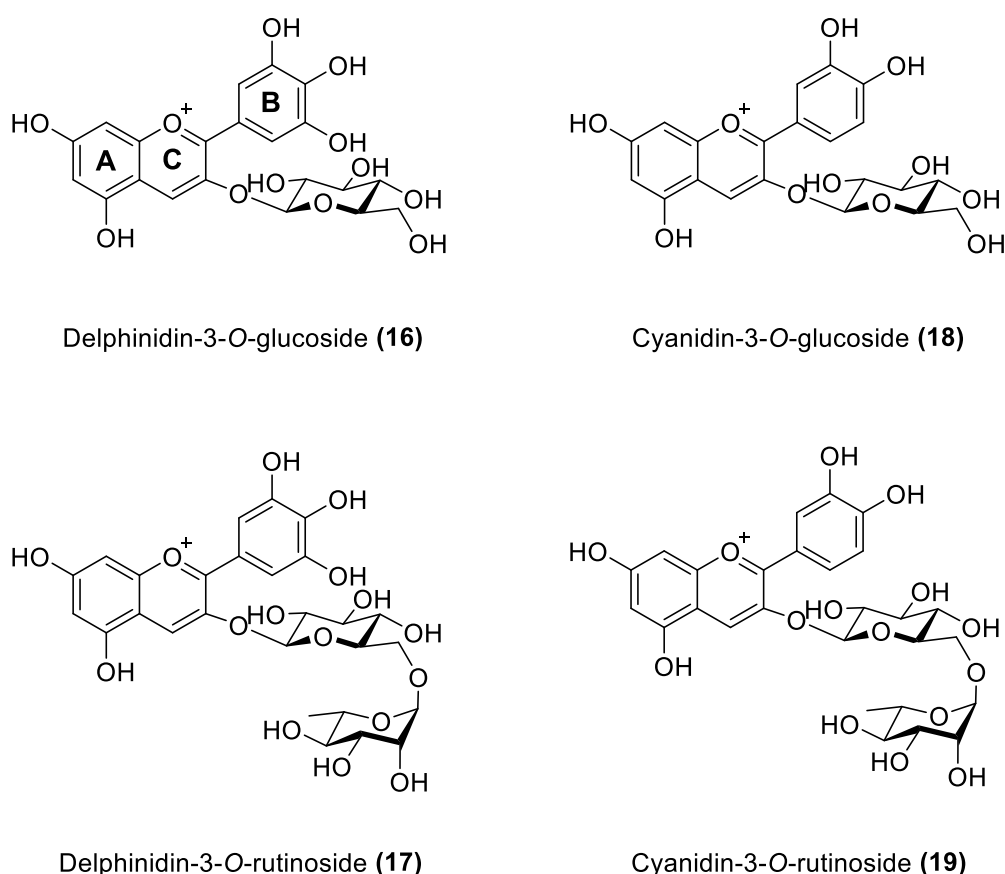
Figure 1.2. Predominant anthocyanins reported in blackcurrant extracts.[20]

Frøytlog, Slimestad and Andersen found six anthocyanins in blackcurrant extract with delphinidin-3-*O*-rutinoside **17** being the predominant one as previously reported by Harper and Chandler; this was the first account of rutinosides of malvidin and peonidin in blackcurrant extract.[20] In contrast, Aneta *et al.* found cyanidin-3-*O*-rutinoside **19** to contribute the most [39] and Kahkohnen *et al.* discovered both rutinosides to exist in competing amounts.[40] Fifteen anthocyanins were reported from blackcurrants by Slimestad and Solheim with eleven being present in very small amounts.[21] The team isolated acylated glucosides of delphinidin and cyanidin as a mixture and tentatively assigned them. This was the first report of acylated anthocyanins in blackcurrant fruit extract.

Most studies on blackcurrant and other berry extracts, juices and fruit tend to focus on anthocyanic profile whereby the extract is monitored and characterised at 520 nm (λ_{max}).[41,42] However, this may lead to inconsistency as many neutral polyphenols do not absorb at this wavelength and will go undetected. There have been some accounts of neutral polyphenols in blackcurrant extracts and juices based on comparison with mass spectral data bank; the range and number of polyphenols reported vary markedly.[34,38,43] For instance, Anita *et al.* is the only group who not only found myricetin-3-*O*-galactoside, but it was also the main flavonoid in the extracts, whereas, Corbyn *et al.* reported myricetin-3-*O*-rutinoside **23** (Figure 1.3) to be the predominant flavonoid (16.5 mg g^{-1}). The data on neutral polyphenols in blackcurrants and other anthocyanin-rich foods is scarce and inconsistent. The structures of the most commonly reported flavonoids have been presented in Figure 1.3; these are glucosides and rutinosides of kaempferol (**20** & **21**), myricetin (**22** & **23**) and quercetin (**24** & **25**).

Another important sub-class of neutral polyphenols called proanthocyanidins are widespread throughout the plant kingdom, where they accumulate in different organs and tissues to provide protection against predation. At the same time, they impart astringency and flavour to beverages such as wines,[44] fruit juices and teas. They have been reported in *Prunus amygdalus* (almonds), *Rheum palmatum* (rhubarb), *Vaccinium macrocarpon* (cranberry),[45] *Prunus armeniaca* (apricots), *Vitis vinifera* (grape skins) [46] among others.[47] Proanthocyanidins in blackcurrant extracts or juices have not been reported in the literature. The chemistry of proanthocyanidins has been studied for many decades. Their structures depend upon the nature (stereochemistry and hydroxylation pattern) of the flavan-3-ol starter and extension units, the position and stereochemistry of the linkage to the "lower" unit, the degree of polymerisation,[48] and the presence or absence of modifications such as esterification of the 3-hydroxyl group. On acid hydrolysis, the extension units are broken down to coloured monomeric anthocyanidins.[47]

R$^{3'}$= R$^{5'}$ = H **(20)**

R$^{3'}$ = R$^{5'}$ = OH **(22)**

R$^{3'}$; R$^{5'}$ = H; OH **(24)**

R$^{3'}$= R$^{5'}$ = H **(21)**

R$^{3'}$= R$^{5'}$ = OH **(23)**

R$^{3'}$; R$^{5'}$ = H; OH **(25)**
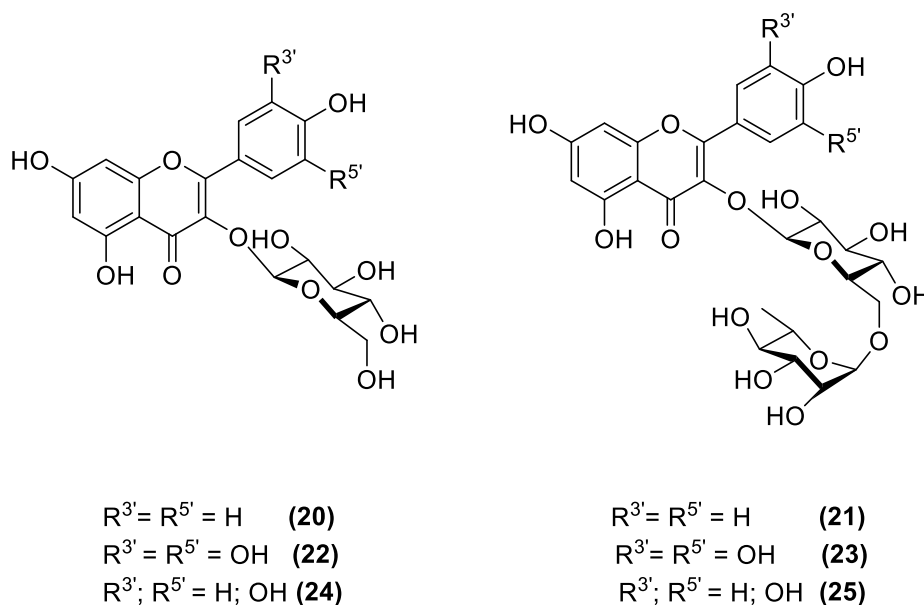
Figure 1.3. Flavonoids identified in blackcurrant extracts by HPLC–DAD–ESI–MS.[36,38,39]

There are two main types of proanthocyanidins: A-type and B-type. Most proanthocyanidins are built from the flavan-3-ols (+)-catechin (2,3-*trans*-) and (-)-epicatechin (2,3-*cis*). The linkage between successive monomeric units in proanthocyanidins is usually between the position-4 of the "upper" unit and the position-8/6 of the "lower" or "starter" unit and may be either α- or β-. Anthocyanins have also been considered as potential substrates for proanthocyanidin polymerisation. Condensation between anthocyanins and proanthocyanidins monomers (flavan-3-ols), oligomers or polymers is one of the main processes contributing to the changes in colour and astringency as wines age. The debate concerning the operation of an enzymatic or non-enzymatic mechanism for proanthocyanidin condensation continues.[47]
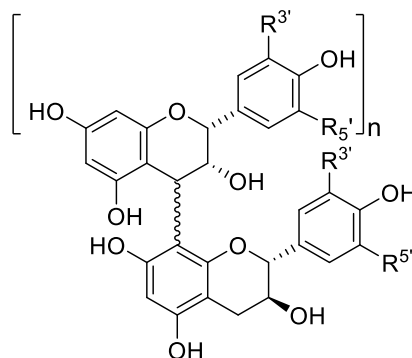
Proanthocyanidin **(26)**

Figure 1.4. The structure of a generic proanthocyanidin.

10

1.8 Extraction Methods

Solvent extraction has been the most common method for extraction of a wide range of compounds found in fruits.[49] The method in general involves drying or lyophilising plant material followed by grinding and then solvent extraction.[18] This method is slightly different to solvent-solvent extractions in a typical organic chemistry laboratory; the plant materials are stirred in a solvent of choice over a certain length of time and then solids are filtered off leaving behind the liquid extract. Anthocyanins and other glycosylated polyphenols are soluble in polar solvents.[50] Methanol,[32] ethanol,[42] acetone[51] and water[52] are the most commonly used solvents for extraction of anthocyanins; water and alcoholic solvents are acidified with small amount of acids (0.01–0.5% *v/v*). It has been suggested that acidification not only stabilises anthocyanins by keeping pH < 3 but also breaks down cell walls.[41] Acid hydrolyses of acylated anthocyanins has been a cause of concern when using acidified alcoholic solvents; this results in difficulty establishing true chemical profile of the extracts.

Brouillard *et al.* noted acetone to be a better solvent as it can extract anthocyanins efficiently without the need for acidification.[50] However, Lu and Foo discovered unusual oxidative addition of the extracting solvent acetone to anthocyanins to form pyranoanthocyanins (Scheme 1.1).[53] The team noted that the pyranoanthocyanins were present in acetone but absent in the alcohol extracts, and their amount increased gradually with the duration of the extraction.

In one interesting study, Meyer and Landbo treated blackcurrant pomace with four pectinolytic enzymes to allow cell wall breakdown under milder conditions. Each of the tested enzyme preparations except Grindamyl pectinase significantly enhanced the yields of polyphenols extracted from the pomace. In contrast, the effect was either neutral or negative for the extraction of anthocyanins.[9] These results further confirm the role of acid in stabilising the anthocyanins during extraction process.

Heffels, Weber and Schieber compared the influence of accelerated solvent extraction (ASE) and ultrasound-assisted extraction (UAE) on the anthocyanin profile of bilberries, lowbush blueberries and American cranberries.[54] UAE is based on the principle of cavitation, which means the production, growth, and collapse of bubbles in the extraction solvent and sample material. In contrast, ASE uses high pressure to keep solvents liquid above their boiling point which facilitates the extractability of the analytes. The group concluded that the results for different fruits were not completely consistent regarding the resulting profile differences after ASE and UAE and, hence, do not inevitably demonstrate systematic differences between the investigated extraction methods. It is

possible that the nature of the anthocyanins in these extracts affected the yields; some anthocyanins are more unstable and can easily degrade at temperature > 40 °C. In conclusion extraction methods should be devised based on end use of anthocyanins and/or neutral polyphenols rather than a generic method from the literature.

Cyanidin-3-*O*-glucoside **(18)**   Pyranoanthocyanin **(27)**
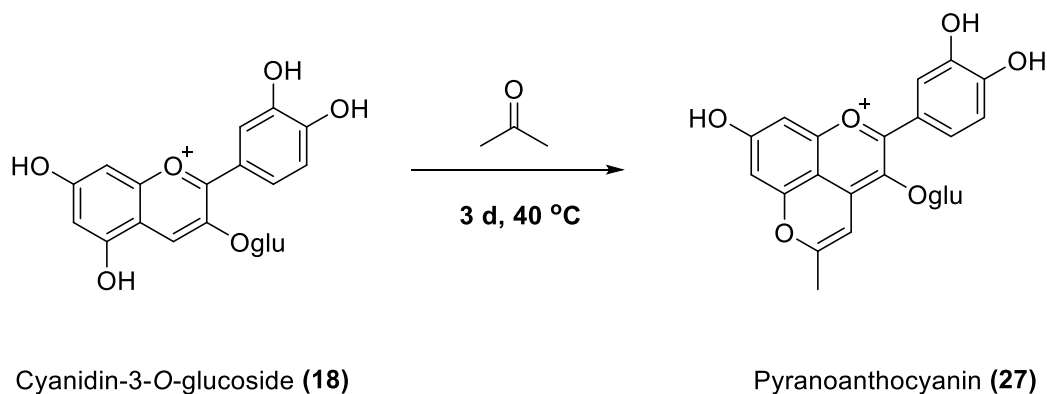
Scheme 1.3. Oxidative addition of acetone to anthocyanins.[53]

1.9 Characterisation of Polyphenols in Blackcurrant

There have been many reports on characterisation of blackcurrant extracts, fruits and juices, however much of the focus has been on establishing anthocyanic profile. Harper and Chandler confirmed identity of the anthocyanins in 1962 for the first time.[19] They employed a series of hydrolysis, oxidation and purification steps to achieve this. Similar methods were used by other groups. [55,13] Briefly, the extract was refluxed in concentrated formic or hydrochloric acid for couple of hours, thereafter the glycosidic components were characterised by comparison with standard samples using paper chromatography. The molar concentration of each sugar in the hydrolysate was determined by comparison of the optical density at λ_{max} (365 nm). Similarly, the resulting aglycones were identified by comparison with the respective anthocyanidins.

In recent years, HPLC chromatography has become the method of choice for characterisation of anthocyanins in blackcurrants. HPLC is a powerful technique, however, these published methods are less accurate as they rely on comparison of spectroscopic and mass data of the extracts with the literature. [21,34,36,37,56] Flavonoids and hydroxycinnamic acids have similar spectroscopic and chromatographic properties especially when they are substituted; these polyphenols alongside anthocyanins also have similar molecular weights. Therefore, there is a significant chance of inaccuracy if assignments are made merely based on comparison of mass data with the literature. For example, the anthocyanins petunidin-3-*O*-rutinoside, petunidin-3-O-(6''-coumaroyl)-

glucoside, and flavonoids myricetin-3-O-rutinoside and myricetin hexose-deoxyhexoside all have molecular weight of 626 g mol^{-1}. Similarly, hydroxycinnamic acids and flavonoids both absorb at 350 and 325 nm; acylated flavonoids and hydroxycinnamates cannot be distinguished based on their absorbance at 325 nm. HPLC is a powerful technique for efficient characterisation of natural product extracts, however external standards must be used for unambiguous characterisation.

Some research groups have attempted full characterisation of blackcurrant extracts using HPLC, and combination of external standards and comparison with the literature.[38,39,57] Anthocyanin and flavonoid standards are expensive which might render full characterisation of the extracts using standards. While these studies are good at highlighting the type of compounds in blackcurrant extracts, they lack rigor of research required to fully characterise a complex natural product extract. A combination of analytical techniques must be utilised to overcome these barriers and identify the compounds unambiguously.

1.10 Blackcurrant as a Commercial Source of Anthocyanins

Practical sources of anthocyanins are limited by overall economic considerations and availability of suitable raw material, however blackcurrant pomace is available in substantial consistent quantities.[9] Preparative isolation of anthocyanins from blackcurrants has been reported which would be impractical for any commercial application. Unrefined simple extracts or tinctures, which although often coloured, contain only low levels of anthocyanins and limited applications. Neither of these forms are suitable for large scale and high value applications where high-quality extracts are required. These extracts should be fully characterised and carefully monitored during extraction and purification processes to ensure quality control.

1.11 Conclusion

Anthocyanins are intensely pigmented natural colorants responsible for red, purple and blue coloration of fruits, vegetables and flowers. They are pH, temperature and light sensitive (certain equilibrium forms). Anthocyanins exhibit a remarkable framework of reactions with varying pH; it is generally agreed that anthocyanins and synthetic partners take part in acid-base equilibria in aqueous solutions. They can exist as monomers, polymers, or co-pigment with other polyphenols and metals which can help stabilise them in solutions. Anthocyanins have been reported in blackcurrants,[19,20,21,22,23]

strawberries,[12,24] chokeberries,[25] black carrot,[26] black beans,[27,28], blueberries,[12,29] and black mulberries[30].

The qualitative data on blackcurrant extracts in the literature is in general agreement, however, there is a significant difference in the quantification data. This arises from two factors; the method of extraction and the method of characterisation of the extracts. As mentioned earlier anthocyanins are sensitive to hydrolysis and temperature (50 °C); this is even of more significance for esterified anthocyanins and flavonoids. Therefore, if extraction conditions are not chosen and monitored carefully, degradation of anthocyanins and acylated flavonoids is inevitable which would result in unreliable and irreproducible data.

Similarly, the purification and analytical techniques play a significant role. In the literature, typically, a routine analysis may consist of just one high-performance liquid chromatographic (HPLC) injection (5 µL) of 0.5 mg crude extract and then comparison of the spectroscopic profile with the literature. However, complete structure elucidation demands extraction of approximately 200 g plant material with acidified alcoholic solvent, followed by purification and separation using various chromatographic techniques before structure elucidation by spectroscopy and sometimes chemical degradation.[6] A series of purification techniques and a set of analytical methods are required to accurately characterise a complex natural product extract.

1.12 Aims of the Blackcurrant Project

Due to the growing needs of the population, the food industry is expanding faster than ever before. This evidently results in tons of waste which needs treatment; it is costly both to the company and the environment. This project was done in collaboration with Keracol Ltd. who developed a patented extraction method for extraction of anthocyanins from blackcurrant waste left after the production of the blackcurrant cordial Ribena. The aim of this project was to review the original protocol developed by the Keracol team by monitoring and characterising the chemical profile and yield of the extract at every stage of the process. Furthermore, a series of solvents was screened for the extraction of polyphenols from blackcurrant pomace and their performance was compared with the original protocol. The efficiency and efficacy of each step was revisited and the possibility of having multiple product streams was explored to improve overall economic and environmental value of the process. The stability of anthocyanins under various solvent and experimental conditions was also probed.

Furthermore, the aim of this project was to characterise the blackcurrant extract by using a series of analytical techniques to determine the overall composition of the extract. All analytical techniques have their strengths and weaknesses, therefore use of combination

of analytical techniques facilitates production of reliable data. For example, NMR spectroscopy is not a commonly used technique in this area of research, however, it is a powerful technique and can give us insight into the nature of the extract by identifying key features of the compounds. The polyphenols including anthocyanins were purified from the blackcurrant extract and characterised using NMR, IR, UV/Vis spectroscopy and mass spectrometry. These samples were used as external standards to determine the composition of blackcurrant extract and quantify monomeric anthocyanins in the extract using HPLC. The efficacy of total monomeric anthocyanin content (TMAC) assay was probed and compared with HPLC method of quantification.

Chapter 2 Results and Discussion for the Blackcurrant Project

2.1 Introduction

HPLC–DAD and HPLC–ESI–MS are the most commonly used techniques in characterisation of blackcurrant extracts. Whilst these are powerful techniques, there are several issues concerning sole use of them. Anthocyanins have maximum absorbance at 520 nm which is why the extracts are monitored at this wavelength in the reported literature.[29] However neutral polyphenols such as flavonoids, flavanols and hydroxycinnamic acids do not absorb at this wavelength. Therefore, if an anthocyanin-rich extract is analysed using only HPLC–DAD at 520 nm, it is likely to incur an error. HPLC is a useful technique to determine number as well as relative ratio of compounds in an extract providing, they are separated well. It is often challenging to find a method that works for different classes of compounds present in an extract.

Qualitative and quantitative HPLC analyses of the extract is possible with the help of external standards. However, anthocyanins and neutral polyphenols are costly and not always commercially available. This could be the reason why many researchers characterise the extracts by comparing spectroscopic or mass data with the literature. The nature and polarity of many polyphenols, especially from the same class, is very similar which can lead to overlapping of bands in the chromatograms. Therefore, when the assignments are made solely based on comparison of retentions times or mass data with the literature values, it can lead to error. Moreover, some compounds ionise better than the others in HPLC–ESI–MS method which can overestimate or underestimate their amounts in the extract.

NMR spectroscopy is not a commonly used technique in this area of research. The NMR spectra for natural product mixtures are complex and difficult to decipher. Moreover, purified samples are required to be able to assign the compounds accurately. NMR spectroscopy is a powerful and reliable technique; analysis of characteristic chemical shifts and relative ratios of the integrated peaks in a spectrum can give basic information about chemical profile of the extract. However, the compounds belonging to a family of natural products can give overlapping peaks in ^{1}H NMR spectrum too. Some researchers have reported indication of impurities in the ^{1}H NMR spectra of samples that showed high purity on HPLC–DAD. It is likely that the impurities did not absorb at the wavelength the samples were monitored at on HPLC.[32]

Andersen and his research group have done pioneering work in characterisation of anthocyanins in various flowers and berries using NMR spectroscopy.[58] Briefly, their protocol starts with extraction of plant materials with slightly acidified alcoholic solvents (0.1%-0.5% acid *v/v*); The dried extract is dissolved in water and partitioned against ethyl acetate to remove neutral polyphenols. The aqueous layer is partially purified on exchange resin (XAD-7) before subjecting it to preparative HPLC to isolate individual anthocyanins. These anthocyanins are then fully characterised using NMR spectroscopy.[28]

All analytical techniques have their strengths and weaknesses; therefore, a combination of techniques should be used in characterisation of a complex extract for accuracy and reproducibility. Drawing inspiration from Andersen's work one of the aims of this project was to characterise the blackcurrant extract by thorough investigation using a variety of analytical techniques including but not limited to NMR spectroscopy. The analytical protocol would then be used to build a complete picture of the extract by qualitative as well as quantitative analysis of all the families of compounds in the extract and not just the anthocyanins. The identification and characterisation of all the compounds would enable a systemic approach to design a scalable extraction and purification method leading to multiple product streams.

Initially, the chemical profile of Keracol Ltd. blackcurrant extract was probed using NMR spectroscopy, analytical HPLC, LC-MS and total monomeric anthocyanin content (TMAC) assay. Thereafter, fresh extractions from blackcurrant pomace using a variety of solvent systems were performed and analysed to develop a dynamic picture of the extract as it goes through different stages of extraction and purification. The blackcurrant extract was then subjected to preparative HPLC to obtain pure samples of the polyphenols including anthocyanins for full characterisation; this was a lengthy process owing to development of ideal HPLC system which would allow isolation of all the compounds (belonging to different classes) from the extract and not just the anthocyanins. It became clear that an additional purification step was required prior to preparative HPLC for optimum chromatographic separation of the compounds. In the literature natural extracts are often subjected to a series of chromatographic steps to isolate a compound in high purity. This can often lead to poor yield and in some case degradation of the product. Anthocyanins are pH and temperature sensitive therefore minimum chromatographic steps were desired.

Fourteen polyphenols were isolated and fully characterised using mass spectrometry, 1-D and 2-D NMR, UV/Vis and IR spectroscopy. Anthocyanins in the blackcurrant extract were quantified using isolated as well as commercial samples of delphinidin-3-*O*-glucoside as standards. Total monomeric anthocyanin content (TMAC) assay was probed for its inaccuracy and extinction coefficients for all the isolated anthocyanins were

determined experimentally. Finally, an improved extraction and purification system was devised for Keracol Ltd. which would allow access to three complementary product streams as opposed to one (anthocyanins).

2.2 Preliminary Analysis of Blackcurrant Extract

2.2.1 HPLC Analysis of Blackcurrant Extract

Anthocyanins are pH sensitive (Section 1.3) and each anthocyanin can exist in up to eight equilibrium forms. Therefore, it was crucial to maintain pH below 3 to form red flavylium cationic species. The extract was dissolved in acidified water/ethanol mixture (9:1, 0.1% *v/v* HCl), filtered following general procedure and analysed immediately. The sample was subjected to analytical HPLC using method 7.5.1 in experimental section. Anthocyanins, flavonoids and hydroxycinnamates have maximum absorbance at 520, 350 and 325 nm respectively, therefore the extract was monitored at these wavelengths. The chromatogram A (Figure 2.1) at 520 nm showed four peaks with two predominant peaks; the retention times and relative peak area is given in Table 2.1. The order of elution of four anthocyanins was in agreement with that reported by Andersen *et al.*;[20] delphinidin-3-*O*-glucoside **16** and delphinidin-3-*O*-rutinoside **17** eluted before cyanidin-3-*O*-glucoside **18** and cyanidin-3-*O*-rutinoside **19** (Figure 2.1).

Delphinidin has an additional hydroxyl group substituted on ring B making it more polar than cyanidin. The relative peak areas were 44% and 35% for delphinidin-3-*O*-rutinoside **17** and cyanidin-3-*O*-rutinoside **19** respectively, making them the predominant anthocyanins in the extract; whereas, cyanidin-3-*O*-glucoside **18** was present in smallest amount (6%) and delphinidin-3-*O*-glucoside **16** was significant (15%). It was not possible to conclude at this stage if the rutinosides were naturally more abundant in the blackcurrant extract or they were extracted in larger amount due to their greater solubility in water (disaccharide vs monosaccharide). Moreover, it can be argued that the disaccharides provide increased stability to these anthocyanidins so that they can survive the extraction and semi-purification processes better than their monosaccharide counterparts. Therefore, further investigation was warranted.

The chromatograms were more complex at 350 (Figure 2.1, chromatogram B), 325 and 285 nm. Hydroxycinnamic acids are more polar than anthocyanins and so they are expected to elute before anthocyanins. The two major peaks at 4.7 and 7.3 min (λ_{max} 325 nm) were likely to belong to hydroxycinnamic acids; however, further work was required to explicitly assign these peaks. At 350 nm, the compound eluting at 11.4 min had a retention time in between delphinidin-3-*O*-glucoside **16** and cyanidin-3-*O*-glucoside **18**,

coeluting with delphinidin-3-*O*-rutinoside **17** (11.7 min); it had λ_{max} at 350 nm which indicated it was probably a flavonoid.
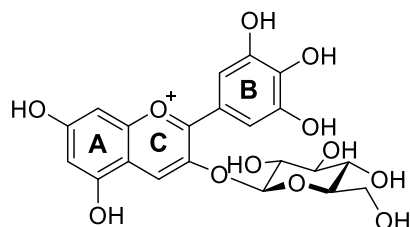
Delphinidin-3-*O*-glucoside **(16)**
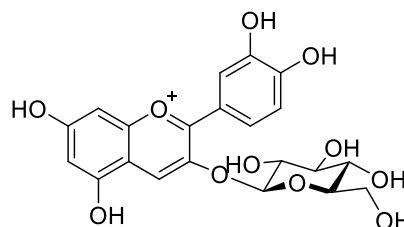
Cyanidin-3-*O*-glucoside **(18)**
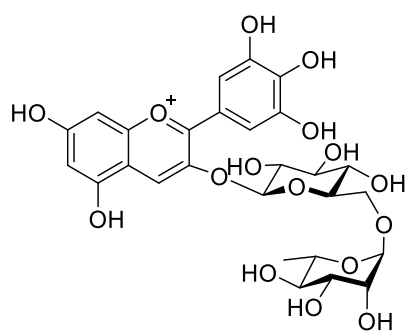
Delphinidin-3-*O*-rutinoside **(17)**
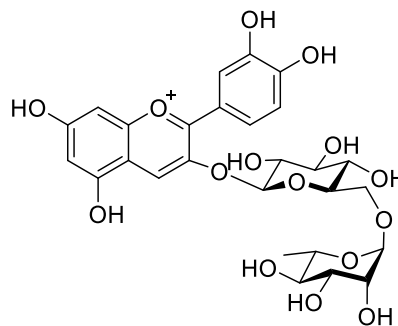
Cyanidin-3-*O*-rutinoside **(19)**
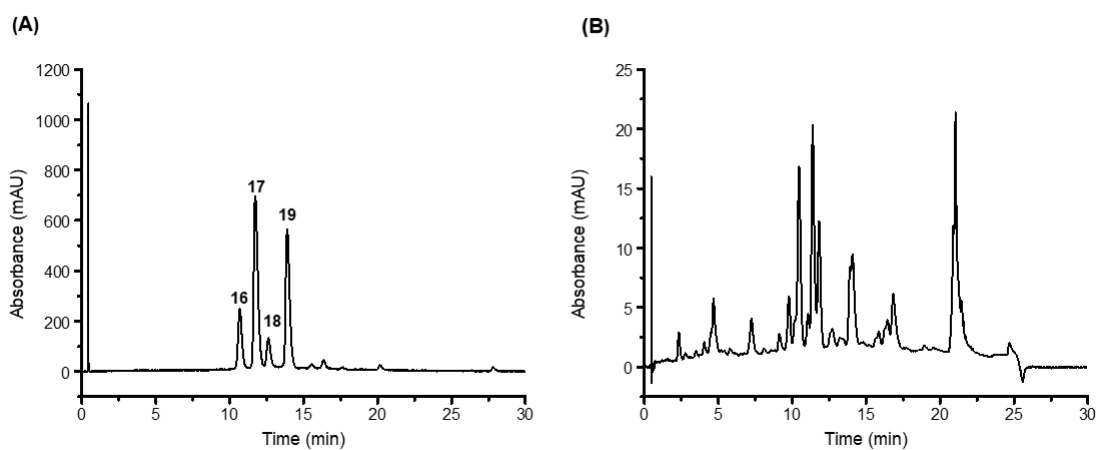
Figure 2.1. The HPLC chromatograms of blackcurrant extract: (A) 520 nm; (B) 350 nm.

19

These results highlighted the challenge of purifying the blackcurrant extract; in general, only one wavelength can be chosen to monitor the extract on preparative HPLC. Therefore, if the extract was monitored at 520 nm, the flavonoid peaks would not be present as they do not absorb at 520 nm and incidentally lead to co-elution of the compounds. Furthermore, higher amount of acid in the mobile phase, often required for anthocyanins, could lead to degradation of neutral polyphenols. Indeed, when the extract was eluted with 0.1% and 0.5% TFA in mobile phase in two different experiments, the chromatogram at 520 nm was more resolved at 0.5% TFA. In contrast, degradation of neutral polyphenols was observed at 0.5% TFA indicated by low intensity peaks at 350 nm (Appendix A1 & 2). HPLC-ESI-MS was not an ideal method for purification of this extract due to the similarity in molecular weights and preferred ionisation mode of different polyphenols in mass spectrometry.

Table 2.1. Relative percentage of anthocyanins found in blackcurrant extract.

Number	t_R (min)	Peak area (%)	Anthocyanin
16	10.7	15	Delphinidin-3-*O*-glucoside
17	11.7	44	Delphinidn-3-*O*-rutinoside
18	12.6	6	Cyanidin-3-*O*-glucoside
19	13.9	35	Cyanidin-3-*O*-rutinoside

2.2.2 NMR Analysis of Blackcurrant Extract

The blackcurrant extract was tested for its solubility in various NMR solvents and was found to be sufficiently soluble in deuterated methanol. The anthocyanins can exist in several equilibrium forms depending on pH (Scheme 1.1). For example, when anthocyanidin-3-*O*-glucosides are dissolved in pure methanol, they exist as three species: the flavylium cationic form and two epimeric hemiketal forms.[22] This in turn affects the chemical shifts and integration ratio of the protons. The existence of anthocyanins in several equilibrium forms would make the analysis of an already complicated spectrum much more difficult. Therefore, the extract was dissolved in acidified methanol (CD_3OD/CF_3COOD 95:5) to maintain low pH and keep anthocyanins predominantly in flavylium cationic form.[12] The samples were sonicated and filtered through cotton wool prior to transfer to NMR tubes and analysed straight away.

Monomeric anthocyanins, in flavylium cationic forms, have diagnostic peaks at 8.8–9.4 ppm; a downfield shift is observed when anthocyanins are acylated. Four peaks were

found in the diagnostic region in ^{1}H NMR spectrum; these were at 9.01, 8.96, 8.93 and 8.88 ppm (Figure 2.2). This was in agreement with the four peaks previously identified at 520 nm in HPLC analysis. The relative integrated area of these peaks was in good agreement with HPLC results: delphinidin-3-*O*-rutinoside (1) > cyanidin-3-*O*-rutinoside (0.96) > delphinidin-3-*O*-glucoside (0.34) > cyanidin-3-*O*-rutinoside (0.17). The relative ratio of delphinidin-3-*O*-rutinoside **17** and delphinidin-3-*O*-glucoside **16** was estimated to be 2.94 by both HPLC as well as ^{1}H NMR. For the cyanidin glycosides, these values only differed by 0.1. This implied that extinction coefficient values for these major anthocyanins were not significantly different and it was potentially possible to quantify the extract using one standard sample of anthocyanin rather than four (*vide infra*).
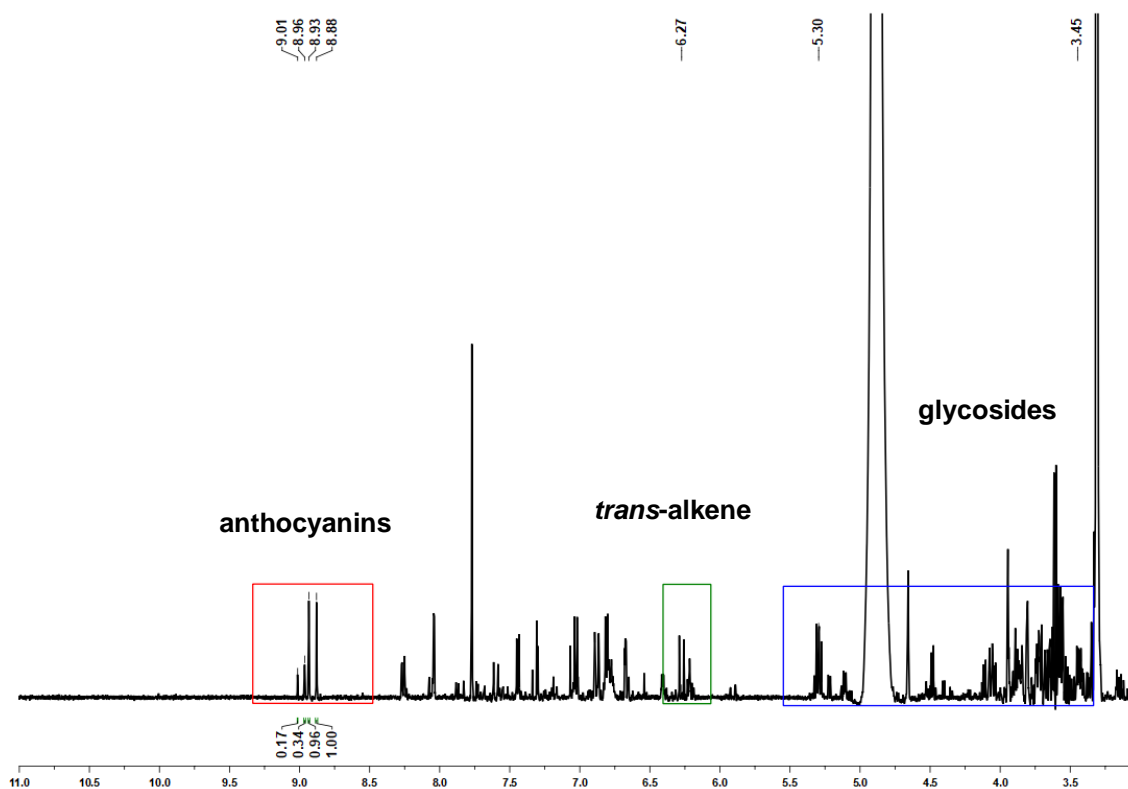
Figure 2.2. ^{1}H NMR of blackcurrant extract in MeOD/CF$_3$OD (95:5).

There were several peaks in the region of 6–8 ppm suggesting presence of polyphenols. Although it was not possible to assign all these peaks due to overlap, preliminary analysis of the aromatic region gave insight into the nature of compounds in the extract. The peak around 6.20 ppm had coupling constant of 16.0 Hz which is characteristic of a *trans* double bond; this could be a hydroxycinnamic acid. The overlapping peaks at 3–4 ppm were indicative of glycosides; these were likely to be substituted glycosides as free sugar

molecules are removed by solid-phase extraction earlier in the process. In summary, NMR results were in agreement with HPLC results and confirmed presence of four anthocyanins. However, the extract was far more complex than initially anticipated and needed further work for full characterisation.

2.2.3 Total Monomeric Anthocyanin Assay

Total monomeric anthocyanin content assay (TMAC) is a commonly used technique in quantification of monomeric anthocyanins in berry fruit juices and extracts. The protocol was first reported by Lee *et al.* and allows quantification of monomeric anthocyanins without the need for standard samples.[59] Many researchers have reported discrepancies in data where extracts are quantified using HPLC (and external standards) and TMAC assay (*vide infra*). Nevertheless, TMAC was done at this stage to estimate the percentage of monomeric anthocyanins in the blackcurrant extract.

The method makes use of the two equilibrium forms of anthocyanins; the flavylium cation and hemiketal dominate at pH 1 and 4.5 respectively (Scheme 1.1). Furthermore, the method uses cyanidin-3-*O*-glucoside as a reference because it is the most common anthocyanin in nature.[6] The method used for this calculation is given in equation 1. Molecular weight (595 g mol^{-1}) and extinction coefficient (23600 M^{-1} cm^{-1}) for cyanidin-3-*O*-glucoside **18** is substituted in the equation; the final absorbance value (A) is obtained by taking the difference in absorbance value measured at pH 1.0 and 4.5 at 520 nm (corrected for haze at 700 nm). Dilution factor (DF) and path length (1 cm) are also included in the calculation (section 7.9).

$$Anthocyanin \text{ content (mg/L)} = \frac{A \times MW \times DF \times 10^3}{\varepsilon \times l} \qquad (1)$$

The blackcurrant extract (10 mg) was dissolved in buffers at pH 1.0 and 4.5 to give concentration of 1 mg mL^{-1}, thereafter several dilutions were prepared to obtain absorbance range of 0.2–1.2 at 520 nm. The measurements were made in triplicate and TMAC was found to be 8% in the extract using this method. This was inconsistent with the NMR and HPLC data which predicted anthocyanins to be present in much greater amount. It should be noted that cyanidin-3-*O*-glucoside, conventionally used as a reference for TMAC calculations, is present in smallest amount in this extract (Table 2.1). This was further investigated at a later stage (section 2.7.2).

2.2.4 LC-MS Analysis of Blackcurrant Extract

The blackcurrant extract (4 mg) was dissolved in acidified water/ethanol mixture (9:1, 0.1% *v/v* conc. HCl), filtered following the general procedure and analysed immediately. The aqueous extract was loaded onto a UHPLC column (general procedure), eluted with 5–95% acetonitrile (0.1% TFA) and ionised under negative mode. The run time was 3 minutes and four peaks were observed at 1.15, 1.22, 1.31 and 1.35 min (Table 2.2). The peaks at 1.15 and 1.22 min gave *m/z* values of 610.5 and 594.5 which matched with (ionised) molecular weights of dephinidin-3-*O*-rutinoside **17** and cyanidin-3-*O*-rutinoside **19**.

The minor peaks at 1.31 and 1.35 min showed *m/z* values of 625.5 and 609.5 which matched with (ionised) molecular weights of myricetin-3-*O*-rutinoside **23** (626.5 g mol^{-1}) and quercetin-3-*O*-rutinoside **25** (610.5 g mol^{-1}). These peaks were assigned tentatively, and further analysis was required. Moreover, ^{1}H NMR for the extract presented far more complex picture than the LC-MS data.

Table 2.2. The LC-MS data for blackcurrant extract under negative ionisation mode.

t_R (min)	[M-H]$^-$	Compound	M_W (g mol^{-1})
1.15	610.5	Dephinidin-3-*O*-rutinoside	611.5
1.22	594.5	Cyanidin-3-*O*-rutinoside	595.5
1.31	625.5	Myricetin-3-*O*-rutinoside	626.5
1.35	610.5	Quercetin-3-*O*-rutinoside	610.5

2.2.5 Conclusion to Analysis of Keracol Extract

The Keracol blackcurrant extract was analysed using HPLC, ^{1}H NMR, LC-MS and TMAC assay. The strengths and weaknesses of these techniques came to the forefront highlighting the need for a holistic approach; the data collected from each technique acts as a piece of the jigsaw and should be treated accordingly rather than in isolation. To characterise an extract accurately, a combination of techniques should be used rather than relying on one technique solely.

2.3 Evaluation of Extraction Methods

The nature of extraction solvents influences the chemical profile of the extract; this is partly due to solubility of the compounds in a specific solvent as well as their polarity. Acetone, methanol, ethanol and water are commonly used solvents for extraction of anthocyanins in the literature. In this study water, methanol, ethanol isopropylacetate and ethyl acetate were screened for the extraction of anthocyanins from blackcurrant pomace; the effect of acid on yield and anthocyanin profile was also investigated. The difference in polarity of these solvents was expected to influence the nature and amount of compounds being extracted. Extraction time, solvent-to-biomass ratio, temperature and resin-to-biomass ratio were kept the same for consistency.

The detailed method for extraction has been described in experimental (section 7.4.1). Briefly, blackcurrant pomace was added to the solvent of choice (solvent to biomass ratio of 20, e.g. 10 g in 200 mL) and stirred gently in the dark at room temperature for two hours. Then plant material was removed by filtration using a sieve and the liquid extract was either evaporated or loaded onto solid-phase resin (XAD-7HP polymeric resin) directly to remove free sugar and small organic acids. The percentage yields were calculated as final amount of the extract obtained from initial amount of blackcurrant pomace (% *wt./wt.*) and have been summarised in Table 2.3. The extracts were monitored using HPLC and ^{1}H NMR at all stages of the process.

2.3.1 Effect of Acid on Extraction of Polyphenols

A small amount of acid is used in extraction of anthocyanins to stabilise their flavylium cationic form.[28] Some researchers have suggested that acid helps break down cell walls allowing efficient extraction of anthocyanins which in turn gives higher yield; the use of 0.5% *v/v* HCl, TFA or formic acid have been reported in the literature. Initially two types of extraction systems were compared, the extraction solvent (water) was acidified with hydrochloric acid (12.5 M) to give 0.1 and 0.01% *v/v* (Keracol Ltd. method) solutions. The yields (1.9% *wt./wt.*) and anthocyanin profile was almost identical for the two systems (Table 2.3).

A tenfold increase in acid did not facilitate higher yield and/or higher anthocyanin content. Therefore, the role of acid in extraction of anthocyanins is likely to stabilise them in flavylium cationic form rather than enabling efficient extraction by cell wall breakdown. If acid was required to degrade cell walls to allow extraction of anthocyanins and other polyphenols, then higher amounts of acid should have led to higher yield and polyphenolic content. This observation was further strengthened when blackcurrant

pomace was extracted with ethyl acetate in the presence (0.1% *v/v*) and absence of acid. The polyphenolic profile was in good agreement for the two systems and the yield was in fact higher when no acid was used; 52 mg (0.6% *wt./wt.)* and 65 mg (0.7% *wt./wt.)* for acidified and non-acidified systems respectively. It should be noted that ethyl acetate only extracted neutral polyphenols from blackcurrant pomace and not the anthocyanins.

2.3.2 Effect of Solvent on Extraction of Polyphenols

Water, methanol, ethanol, ethyl acetate and isopropyl acetate were screened for their efficiency as extracting solvents; the yields have been summarised in Table 2.3. All extracts were monitored using analytical HPLC and ^{1}H NMR spectroscopy to identify the family and relative ratio of the compounds being extracted. Methanol was found to be the best solvent for yield as well as higher polyphenolic content (Appendix A3 & A4). Although the amount of solid-phase resin XAD-7HP (20 g) was kept constant throughout this study for consistency, almost double the amount of resin (35 g) was required for methanolic extract owing to the higher anthocyanin content. In contrast, the extraction with acidified ethanol (0.1% *v/v*) gave lowest yield of 0.6% *wt./wt.* and anthocyanin content (Table 2.3).

Table 2.3. The percentage yields (% wt./wt. of dry plant material) of blackcurrant extracts using different solvents.

Solvent	HCl (% *v/v*)	Yield (% *wt./wt.*)
Isopropylacetate	×	0.9
Isopropylacetate	0.1	0.9
Ethyl acetate	×	0.7
Ethyl acetate	0.1	0.6
Methanol	0.1	2.6
Ethanol	0.1	0.7
Water	0.01	1.9
Water	0.1	1.9

Bordonaba and Terry compared aqueous methanol (30 & 70%), aqueous ethanol (30% & 70%) and pure water (all acidified with 0.5% HCl *v/v*) for extraction of anthocyanins and found 70% methanol to give highest anthocyanin content.[41] They did not screen pure

ethanol or methanol therefore a direct comparison was difficult. However, it can be concluded that higher methanolic content leads to higher anthocyanin content which is in agreement with this work. Moreover, the researchers found 50% and 70% acidified aqueous ethanol to perform better than acidified water implying higher ethanolic amount gives higher anthocyanin content. This contrasted with our work; acidified water (yield1.9% *wt./wt.*) was better extracting solvent than acidified ethanol (yield 0.3% *wt./wt.*) and gave higher anthocyanin content indicated by HPLC and ^{1}H NMR.

Ethyl acetate and isopropylacetate were also screened for extraction of anthocyanins and neutral polyphenols from blackcurrant pomace (Appendix A5). They are relatively less polar than water, ethanol and methanol, therefore the chemical profile of the extracts was expected to change as compared to more polar solvents. The experiments were done in a sequential manner whereby blackcurrant pomace (10 g) was first extracted with isopropylacetate (2 h), then ethyl acetate (2 h) and finally water (2 h) both in presence (0.1% *v/v* HCl 12.5 M) and absence of acid. It was noted that acidified ethyl acetate and isopropyl solvents led to more sticky extracts indicating presence of higher content of free sugar molecules. Acidified as well as non-acidified isopropylacetate extracted predominantly tannins, flavonoid and hydroxycinnamic acids which were tentatively assigned by their characteristic features in HPLC and ^{1}H NMR.

Ethyl acetate selectively extracted flavonoids and hydroxycinnamates alongside small amounts of tannins. ^{1}H NMR spectra for the extracts obtained from ethyl acetate and acidified water (0.1% *v/v* HCl) in two different experiments have been overlaid in Figure 2.3. Common peaks were observed in these two extracts in the aromatic region (characteristic for polyphenols); for example, peaks at 6.28, 6.81, 7.30, 7.34, 7.45 and 7.60 ppm were observed in both spectra. The peaks at 7.34 and 6.88 were more intense in ethyl acetate extract (Figure 2.3B). Moreover, no peaks for anthocyanins (8.8–9.4 ppm) were observed in the ethyl acetate extract. Therefore, it can be concluded that ethyl acetate selectively extracted neutral polyphenols whereas water extracted anthocyanins as well as neutral polyphenols.

Based on these results it is possible to devise a sequential extraction solvent system whereby tannins and polymeric phenolic compounds are extracted from blackcurrant pomace using isopropylacetate first. Then the neutral polyphenols and anthocyanins are sequentially extracted using ethyl acetate and acidified water respectively. This system would allow production of three complementary product streams with different chemical profile; anthocyanins as natural colourants, tannins as raw material and an antioxidant-rich polyphenolic extract. Flavonoids and hydroxycinnamates have been reported to show excellent antioxidant activity.[60]
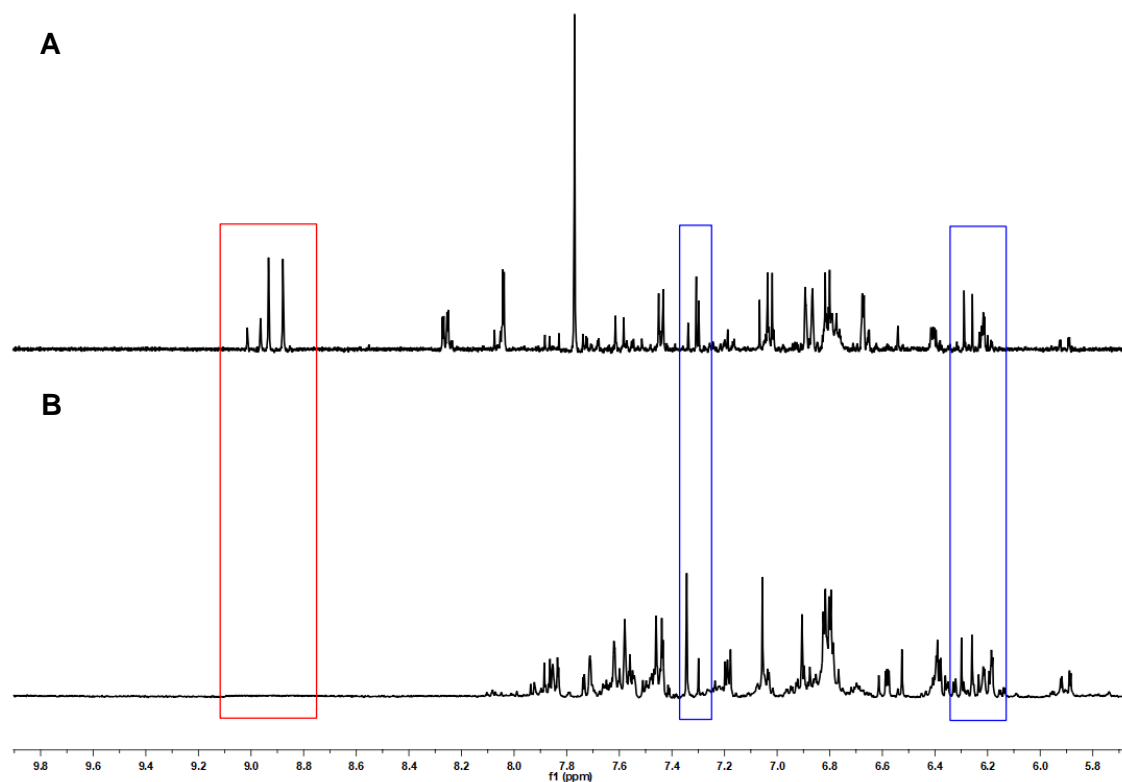
Figure 2.3. Stacked ^{1}H NMR spectra for blackcurrant pomace extracted with solvents: (A) acidified water; (B) ethyl acetate.

2.4 Preparative HPLC Method Development

After developing extraction conditions, the next step was to purify the blackcurrant extract using preparative HPLC for full characterisation. The aim of this part of the research was to build a complete chemical profile of the extract using a combination of analytical techniques. Pure anthocyanin samples were also required for quantification of anthocyanins in the original Keracol extract. Most studies on blackcurrants have been solely focussed on anthocyanic profile by monitoring the extract at 520 nm. While anthocyanins might be predominant class of polyphenols in blackcurrants, it is highly likely that other compounds can be found too (indicated by ^{1}H NMR). This is particularly important when an extract is being evaluated for its functional and/or biological properties. A simple solid-phase extraction (using resins) does not facilitate high purification required for the biological analysis. Indeed, some of the studies reporting potent biological activity of anthocyanins in natural extracts lack rigor of analysis required for such an evaluation.[61,62,63,64] It is highly likely that the reported activity is either a synergistic effect of anthocyanins and neutral polyphenols or solely coming from the latter.

Anthocyanins are temperature and pH sensitive, they are most stable at pH < 3 and temperature < 50 ºC. However, neutral polyphenols can behave differently depending on the nature of the compound. During initial HPLC analysis of the extract, reduced intensity of peaks at 350 and 325 nm was observed when 0.5% TFA was added to the mobile phase as opposed to 0.1% TFA (Appendix A1 & 2); the separation of anthocyanins was better at higher acid content though. The analytical HPLC system was different to the preparative HPLC system available therefore method development of the latter was warranted.

The blackcurrant extract (20 mg) was dissolved in acidified water/ethanol mix (9:1, 2 mL, 0.1% HCl *v/v*) and filtered before loading on to the column. A summary of all the methods has been given in Table 2.4 and detailed protocols can be found in experimental section (Section 7.6). The HPLC method **1** (Table 2.4) constituted of gradient solvent system on a standard size preparative column, XBridge™ Prep C18 OBD™, 100 × 19 mm × cm, 5 µm column. The elution profile consisted of linear gradient from 5% B to 20% B in the first 20 min, then linear increase to 100% B (20–23 min), isocratic elution (100% B) at 23–24 minutes, and then linear decrease to 5% B at 24–25 min followed by 5%B isocratic elution at 25–30 minutes; where solvent A: water with 0.1% formic acid and solvent B: acetonitrile. There was poor separation of the anthocyanins between 9–13 minutes; two peaks rather than four peaks were observed (Figure 2.4A). However, they were separated from the rest of the compounds in the extract.

Table 2.4. Summary of method development for HPLC purification of blackcurrant extract.

Method	Time (min)	Column (mm × cm)	Solvent B	Additive (%)
1	30	19 × 100	Acetonitrile	0.1% FA
2	30	19 × 100	Methanol	0.1% FA
3	30	21.2 × 250	Acetonitrile	0.1% FA
4	30	10 × 50	Acetonitrile	0.1% FA
5	40	10 × 50	Acetonitrile	0.1% FA
6	40	10 × 50	Acetonitrile	0.5% FA
7	40	10 × 50	Acetonitrile	0.1% TFA

The substitution of acetonitrile with methanol (method **2** in Table 2.4), whilst keeping the rest of the parameters same as method 1, led to elution of all the phenolics together at

21–23 min (Figure 2.4B). Acetonitrile is considered a stronger eluent than methanol when the ratio of organic solvent to aqueous is low in the mobile phase. This was certainly the case in this gradient system (5–20% organic solvent). However, if organic solvent is > 90% in the mobile phase, then methanol is the stronger eluent. Therefore, methanol did not perform well on this system.

In HPLC method **3** (Table 2.4), the column was substituted with a bigger column (21.2 × 250 mm × cm) to allow better separation of the anthocyanins, however, it led to broadening of the peaks (Figure 2.4C). Anthocyanins can exist in various neutral equilibrium forms at pH > 3 (Scheme 1.1). It is possible when the extract was loaded on to the bigger column a small amount of these neutral equilibrium forms interacted with the resin strongly causing the equilibrium to shift which resulted in broadening of the peaks. Furthermore, the retention time increased from 11.1 min on the smaller column (19 × 100 mm × cm) to 16.2 min on the bigger column (21.2 × 250 mm × cm). The longer the anthocyanins from the extract spend on the column the more the chances of equilibrium shift in the favour of neutral forms, and consequent peak broadening.

Semi-preparative chromatography is a good compromise between analytical and preparative HPLC chromatography. It enables preparative isolation of small amount of material using an analytical column. When the aqueous extract (1.5 mg) was loaded on to a semi-prep XBridge^{TM} C18, 10 × 50 mm × cm, 5 µm column (method **4**, Table 2.4), four peaks were visible at 520 nm (corresponding to anthocyanins) but they were not well resolved (rest of the parameters same as method **1**). The resolution improved significantly when 0.1% TFA (method **7**, Table 2.4) was used as an additive (Figure 2.4D) instead of 0.1% or 0.5% formic acid. Anthocyanins are pH sensitive and behave better at pH < 2. Trifluoroacetic acid is a stronger acid than formic acid, therefore it facilitated formation and maintenance of the flavylium cationic form of anthocyanins during the chromatographic separation; the peaks were base resolved and higher in intensity.

However, it was also important to consider the amount of the acid used to avoid any damage to the column and rest of the neutral polyphenols present in the extract. The neutral polyphenols in the extract did not respond positively to the strongly acidic conditions and exhibited very low absorbance at λ_{max} 350 and 325 nm when eluted with 0.1% TFA. Better peak intensity was achieved when no acid or 0.1% formic acid was added to the mobile phase, however these conditions were not suitable for the anthocyanins. In conclusion, due to the striking difference in nature of anthocyanins and neutral polyphenols in blackcurrant extract, it was not possible to find one ideal HPLC system that would work to isolate all these compounds in pure forms. Therefore, a semi-purification step prior to preparative HPLC purification was required.
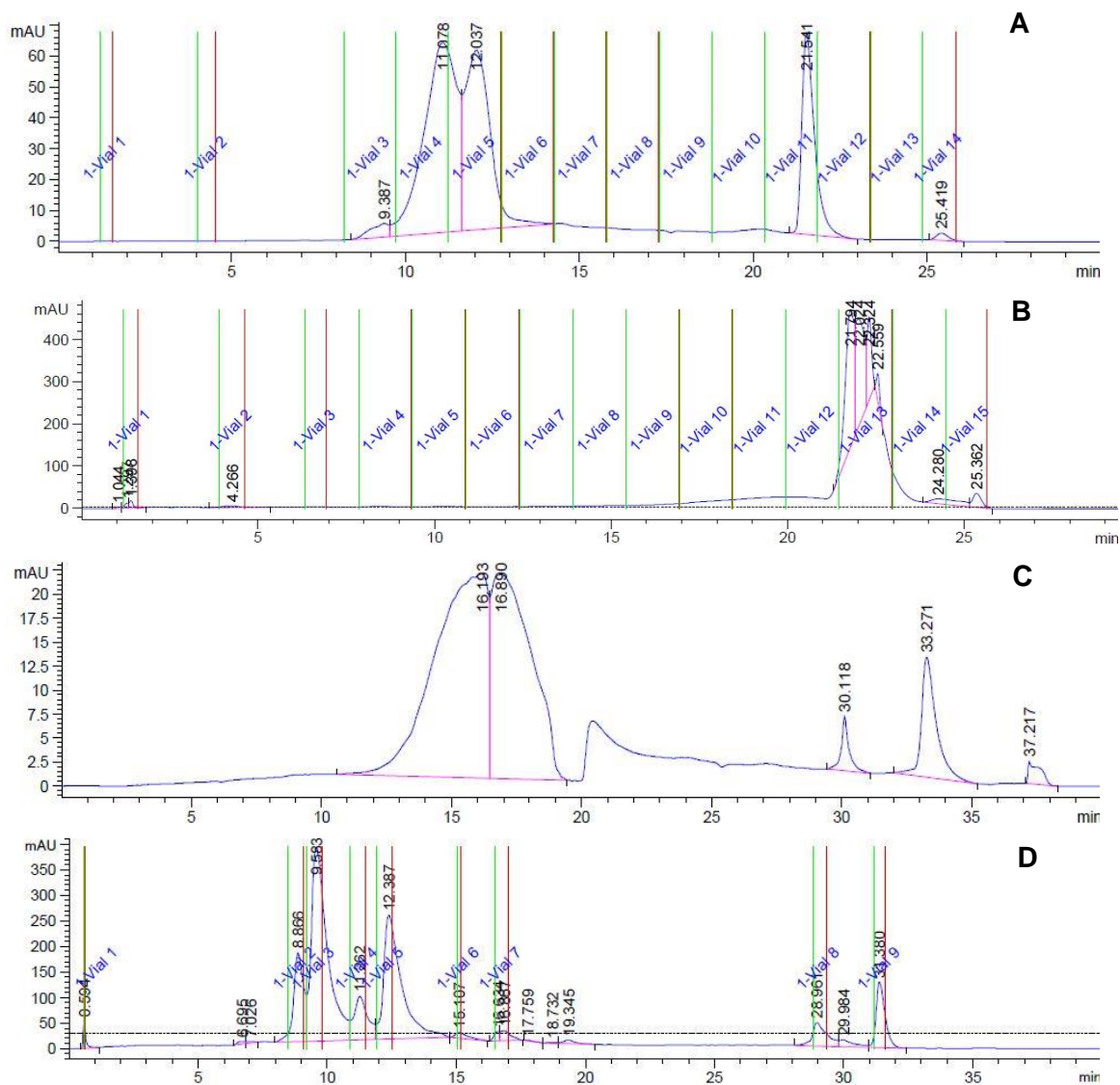
Figure 2.4. The chromatograms for preparative separation of anthocyanins at 520 nm: (A) Method 1; (B) Method 2; (C) Method 3; (D) Method 7.

2.5 Liquid-Liquid Partitioning Experiments

Liquid-liquid partitioning is a useful technique for semi-purification of natural product extracts. In principle, it can be scaled up with relative ease at an affordable cost. Andersen *et al.* semi-purified black bean aqueous extract by partitioning it against ethyl acetate prior to HPLC purification.[28] Anthocyanins and neutral polyphenols in blackcurrant extract were expected to have different solubility in aqueous and polar organic solvents. Anthocyanins, in the flavylium cationic form, should have highest solubility in water due to it being a charged species. Neutral polyphenols are less polar than anthocyanins, therefore their migration into an organic solvent was highly likely.

However, substitution of glucosyl moieties on these neutral polyphenols can also impart water solubility. Therefore, investigation of differential solubility of anthocyanins and neutral polyphenols was warranted.

2.5.1 Choice of Organic Solvents for Partitioning Experiments

Ethyl acetate, isopropylacetate and chloroform were selected due to their polar nature and phase separation from water; pH was kept below 3 to maintain flavylium cationic form of anthocyanins. Three experiments were done in a sequential manner whereby aqueous blackcurrant extract (10 mg mL^{-1}) was partitioned against hexane, followed by ethyl acetate, isopropyl acetate or chloroform. This resulted in three sub-extracts in each experiment: (1) hexane, (2) ethyl acetate, isopropyl acetate or chloroform and (3) aqueous extract; the percentage yields have been summarised in Table 2.5. The aqueous extract was red-coloured in all cases indicating presence of anthocyanins.

Table 2.5. The percentage yields of aqueous and organic blackcurrant extracts.

Layer	Yield (wt./wt.%)	Layer	Yield (wt./wt.%)	Layer	yield (wt./wt.%)
Hexane	0.2	Hexane	0.2	Hexane	0.2
Ethyl acetate	19.8	Chloroform	11.8	^{i}Propylacetate	17.8
Aqueous	80	Aqueous	88	Aqueous	82
Total	100		100		100

Around 80–88% of the extract remained in the aqueous phase which suggested that bulk of the extract was made up of very polar components. Around 11.8–19.8% of the extract migrated into the organic layer. Ethyl acetate extracted highest amount of neutral polyphenols and chloroform only extracted 11.8%. The hexane layer constituted only a minute amount of the extract.

2.5.2 LC–MS Analysis of Aqueous and Organic Blackcurrant Extracts after Partitioning Experiments

The aqueous and organic extracts from 2.5.1 were analysed on LC-MS; the method and column described in general procedures (7.1) was employed. The masses of four anthocyanins were identified in all three aqueous blackcurrant extracts after the partitioning experiments by comparing *m/z* values (positive mode) with the calculated molecular weights; these were rutinosides and glucosides of cyanidin and delphinidin. Neutral polyphenols were tentatively assigned by comparing mass data with the literature. LC–MS data on these semi-purified extracts was much better resolved than it was for the original Keracol extract. This result highlights the limitations of LC–MS for analysis of complex crude extracts. Although the original Keracol extract had been through one round of purification (SPE on XAD 7HP polymeric resin) to remove free sugar and acid molecules, it was not enough considering complexity the of the extract.

The masses for the rutinosides of myricetin **23** and quercetin **25** (Figure 2.6) were also found in LC-MS spectra (negative mode) of aqueous extracts. Interestingly, the substitution of a disaccharide moiety onto quercetin and myricetin aglycones imparted onto them a competing solubility to that of anthocyanins; therefore, these compounds did not migrate into the polar organic solvents and stayed in aqueous layer alongside anthocyanins. In ethyl acetate layer, the glucosides and aglycones of myricetin and quercetin were identified (by comparison with mass data) along with hydroxycinnamic acids (caffeic acid **30** and *p*-coumaric acid **31** Figure 2.6). However, a full characterisation of the extract was still required as most of these polyphenols differ by only one mass unit and so mass data alone was not enough.

2.5.3 ¹H NMR Analysis of Aqueous and Organic Blackcurrant Extracts after Partitioning Experiments

^{1}H NMR spectra were recorded for dried organic and aqueous extracts (freeze-dried) at 500 MHz and tentatively assigned by comparing data with characteristic peaks for polyphenols. The diagnostic region for anthocyanins (8.8–9.1 ppm) and aromatic region (6–8 ppm) were analysed for all the dried extracts. The ^{1}H NMR spectra for three organic extracts have been put together in Figure 2.5. Chloroform was not as selective as acetate solvents; anthocyanins (8.8–9.4 ppm) along with small number of neutral polyphenols migrated into chloroform (Figure 2.5A). This can be explained based on dielectric constants for these solvents; chloroform has a higher dielectric constant (8.93) than the

acetate solvents but it is significantly less polar than water (80.4). Consequently, it facilitated migration of small amount of both charged as well as neutral polyphenols.
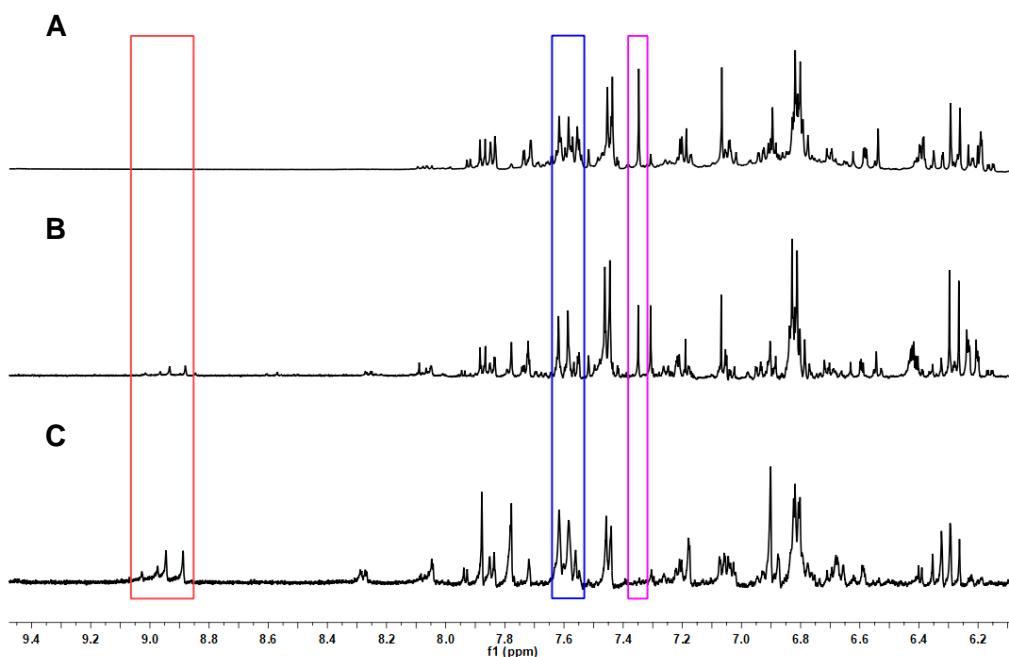
Figure 2.5. Stacked ^{1}H NMR spectra for the organic blackcurrant extracts after partitioning experiments: (A) isopropylacetate extract; (B) ethyl acetate extract; (C) chloroform extract.

The acetate solvents were selective and extracted neutral polyphenols predominantly. Ethyl acetate removed almost all the neutral polyphenols from aqueous blackcurrant extract (Figure 2.5B). Both glucosides as well as aglycones of myricetin (singlets at 7.35 and 7.31 ppm) and quercetin migrated into ethyl acetate along with hydroxycinnamic acids (indicated by doublets around 6.20 and 7.60 ppm). Small amounts of anthocyanins were also found in ethyl acetate extract which is likely to be caused by solubility of ethyl acetate in water and vice versa. All the structures have been summarised in Figure 2.6.

Isopropylacetate was more selective than ethyl acetate; the dielectric constant values for these two acetate solvents only differed by 0.62 with ethyl acetate being slightly more polar. However, this subtle difference and hydrophobicity of isopropylacetate was enough to enable selectivity. Hydroxycinnamic acids and aglycones of quercetin as well myricetin selectively migrated into isopropylacetate (Figure 2.5C). However, glucosides of quercetin and myricetin stayed in the aqueous layer.

The ^{1}H NMR spectra of the aqueous layers indicated presence of four anthocyanins (8.90–9.4 ppm) as well as rutinosides of myricetin (7.30 ppm) and quercetin (Figure 2.6).

33

The substitution of a disaccharide moiety on myricetin and quercetin aglycone imparts onto them high solubility in water despite of their nature as neutral polyphenols. ^{1}H NMR for hexane extract did not show any peaks indicating absence of non-polar compounds in the extract. Therefore, a hexane wash was not necessary for purification for further experiments.

A method has been developed for the separation of neutral polyphenols from anthocyanins in aqueous blackcurrant extract. Based on this data, a sequential extraction of aqueous blackcurrant extract with isopropylacetate followed by ethyl acetate would allow selective uptake of neutral polyphenols. This is potentially very useful for a large-scale semi-purification of the extract and in providing access to multi-product streams. In principle, these processes are scalable with relative ease and useful for the purification of similar natural product extracts.

2.5.4 Sequential Liquid-Liquid Partitioning of Blackcurrant Extract

After initial screen of organic solvents isopropylacetate and ethyl acetate were chosen for semi-purification of blackcurrant extract. Acidified (0.1% *v/v* HCl) aqueous blackcurrant, 50 mL, 10 mg mL^{-1}) was partitioned against isopropylacetate (1 × 70 mL) followed by ethyl acetate (3 × 50). The two organic extracts were dried with magnesium sulphate and then in *vacuo*; the aqueous layer was freeze dried. All extracts were analysed by HPLC (Figure 2.7) and ^{1}H NMR; the structures have been presented in Figure 2.6.

The highly polar, water-soluble anthocyanins **16−19** (Figure 2.6) were exclusively found in the aqueous layer (Figure 2.7A), alongside myricetin-3-*O*-rutinoside **23** and quercetin-3-*O*-rutinoside **25** (Figure 2.7B). Polymeric anthocyanins were also present in this layer. Isopropylacetate achieved selective extraction of caffeic acid (CA) **30**, *p*-coumaric acid (*p*-CA) **31**, myricetin **28**, and quercetin **29** (Figure 2.7C). Myricetin-3-*O*-glucoside **22**, quercetin-3-*O*-glucoside **24**, nigrumin-*p*-coumarate **32**, and nigrumin ferulate **33** were extracted from the remaining aqueous fraction using ethyl acetate (Figure 2.7D).

Hence, these solubility differences allowed the preparation of three distinctly different polyphenol fractions. The first is a highly coloured aqueous fraction dominated by anthocyanins alongside rutinoside of neutral polyphenols. The combination of a cationic anthocyanin and a monosaccharide would appear to confer a similar degree of aqueous solubility to the presence of the rutinoside disaccharide on a neutral polyphenol. The isopropylacetate extract was a relatively nonpolar fraction containing neutral flavonoids and phenolic acids, whereas the ethyl acetate extract gave an intermediate polarity

fraction containing various monosaccharides of neutral polyphenols. Hence, starting from one aqueous blackcurrant extract, three distinct potentially useful fractions were obtained which had significantly different well-defined chemical constituents and properties and hence potential applications as colorants or antioxidants.[3]

R = OH Delphinidin-3-*O*-glucoside **(16)**
R = H   Cyanidin-3-*O*-glucoside **(18)**

R = OH Delphinidin-3-*O*-rutinoside **(17)**
R = H   Cyanidin-3-*O*-rutinoside **(19)**

R = OH Myricetin-3-*O*-glucoside **(22)**
R = H   Quercetin-3-*O*-glucoside **(24)**

R = OH Myricetin **(28)**
R = H   Quercetin **(29)**

R = OH Caffeic acid **(30)**
R = H   *p*-Coumaric acid **(31)**

R = OH Myricetin-3-*O*-rutinoside **(23)**
R = H   Quercetin-3-*O*-rutinoside **(25)**

R = H   Nigrumin-*p*-coumarate **(32)**
R = OMe Nigrumin ferulate **(33)**

Figure 2.6. The structures of anthocyanins and neutral polyphenols isolated from blackcurrant extract in this work.

Myricetin **28**, quercetin **29**, caffeic **30** and *p*-coumaric acid **31** (Figure 2.6) in the isopropylacetate extract has been reported to exhibit potent antioxidant activity.[65,66] Myricetin-3-*O*-glucoside **22** and quercetin-3-*O*-glucoside **24** in the ethyl acetate layer have also been for their bioactivity.[67] Upon literature search it was found that nigrumin-*p*-coumarate **32** and nigrumin ferulate **33** found in the ethyl acetate extract were patented

for their therapeutic or nutritive use in management of impaired mitochondrial functions in 2015.[68] The antioxidant activity of quercetin **28**, quercetin-3-*O*-glucoside **24** and quercetin-3-*O*-rutinoside **25** has been extensively investigated by Dr Elizabeth Dufton (former Rayner group PhD student) among other research groups.[60]
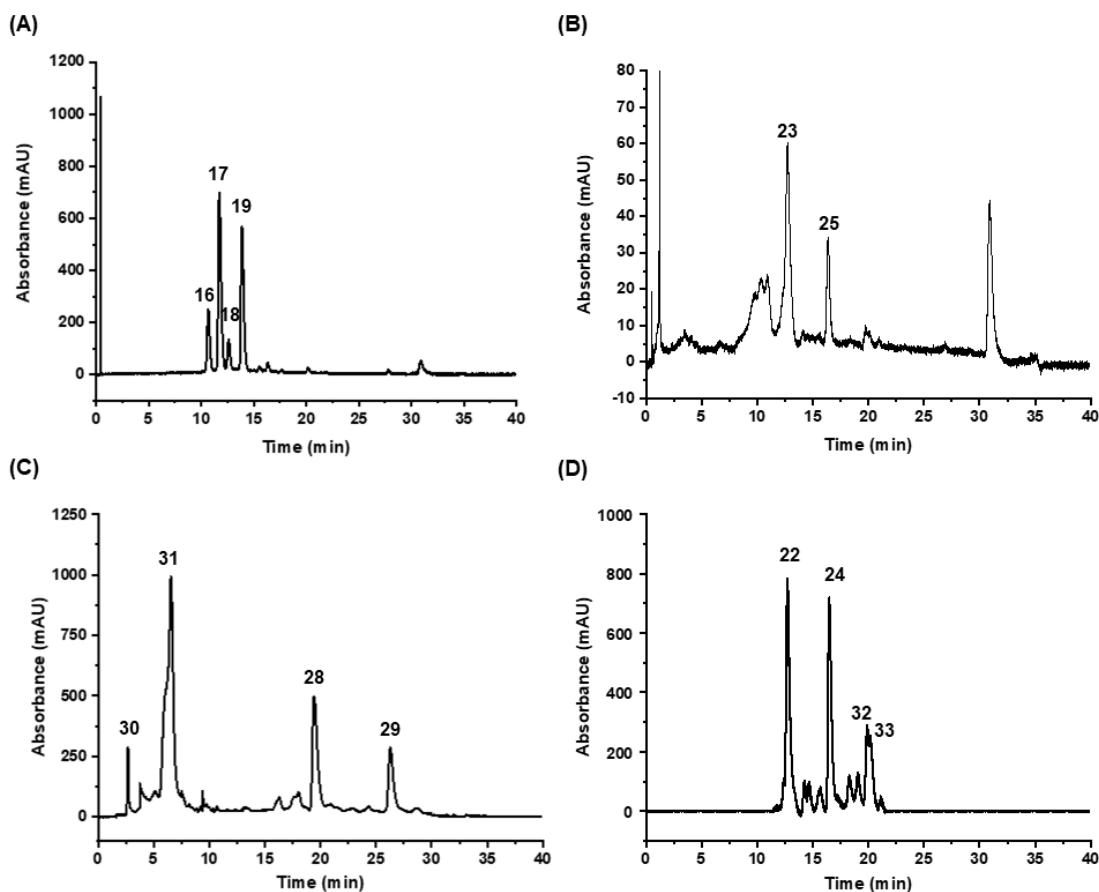
Figure 2.7. HPLC chromatograms of all the fractions after sequential solvent−solvent extractions: (A) aqueous fraction at 520 nm; (B) aqueous fraction at 350 nm; (C) isopropylacetate fraction at 325 nm; (D) ethyl acetate fraction at 350 nm. Peak numbers refer to structures presented in Figure 2.6.

2.6 Purification and Characterisation of Anthocyanins and Neutral Polyphenols from Aqueous and Organic Extracts

Aqueous, isopropylacetate and ethyl acetate extracts were obtained using the method described in Section 2.5.4. This semi-purification step was necessary as the neutral polyphenols were not previously found to respond well to strongly acidic conditions that were necessary for isolation of anthocyanins during preparative HPLC method development (Section 2.4). Having developed a method for preparative separation of

anthocyanins as well as neutral polyphenols in the blackcurrant extracts the next step was to isolate and characterise them. All the compounds isolated from aqueous and organic extracts have been summarised in Figure 2.6.

2.6.1 Purification and Characterisation of Aqueous Blackcurrant Extract

Freeze-dried aqueous blackcurrant extract (described in section 2.5.4) was dissolved (20 mg) in acidified H_2O/EtOH (9:1, 0.1% *v/v* HCl, 2 mL) solvent mixture and filtered. It was then loaded onto a semi-preparative column and eluted using method 8 (described in section 7.6.8) with 0.5% TFA in mobile phase. Five compounds were collected at 520 nm to give delphinidin-3-*O*-glucoside **16** (1.6 mg), delphinidin-3-*O*-rutinoside **17** (4.5 mg), cyanidin-3-*O*-glucoside **18** (0.8 mg) cyanidin-3-*O*-rutinoside **19** (4.1 mg), and polymeric anthocyanins (4.5 mg). Myricetin-3-*O*-*β*-rutinoside **23** (0.8 mg)[69] and quercetin-3-*β*-*O*-rutinoside **25** (0.8 mg)[69] were also isolated (monitored at 350 nm) using 0.1% formic acid. All compounds were characterised using ^{1}H NMR, [1]H−^{1}H COSY, HRMS, UV/vis, IR, and ^{13}C, DEPT135, [1]H−^{13}C HMBC, and [1]H−^{13}C HSQC spectroscopy.

The full assignment of delphinidin-3-*O*-rutinoside **17** is discussed here in detail and rest of anthocyanins were characterised using the same methodology. The proton in position 4 (Table 2.6) for these anthocyanins, in the flavylium cationic form, has a diagnostic chemical shift (8.7–9.2 ppm). Therefore, H-4 was assigned the singlet at 8.90 ppm. The singlet at 7.79 ppm which integrated to two protons was unambiguously assigned to the two protons on the B ring (H-2', 6'). The two meta-coupled protons (H-6/8) on the A ring were assigned based on ^3J (C, H) correlation of C-10 with H-6. The [1]H−[1]H coupling constants for the anomeric protons were 7.5 Hz (J_{ax-ax}) and 1.5 Hz (J_{ax-eq}) for the β and α protons respectively; this result was as expected for a rutinose sugar. The remainder of the glycosidic protons were assigned based on their chemical shifts and coupling constants.

Once all the protons were assigned, the corresponding carbon signals could be deduced from the HSQC spectrum. The cross-peak at δ 5.30/145.8 (H-1''/C-3) confirmed 3-*O*-substitution of the sugar moiety. The quaternary signals were assigned with the help of long range HMBC experiments (Table 2.6). The diagnostic proton H-4 was a good starting point as it correlated with five carbon centres (C-2, 3, 5, 8a and 4a). The assignment of C-2 at 164.2 ppm was deduced from its ^3J(C-H) couplings to H-4 and H-2'; whereas ^2J(C-H) couplings of H-4 to the signals at 145.8 and 112.8 ppm and cross-peak at δ 6.68/112.8 (H-6/C-4a) facilitated their assignments to C-3 and C-4a respectively. Similarly, the signals at 157.6 and 159.1 ppm showed ^3J(C-H) correlations

to H-4 and so they were assigned to C-8a and C-5 respectively. The quaternary signals on the B ring were assigned based on their cross-peaks with H-2'.

Table 2.6. ^{1}H–^{13}C correlations found in the long range (HMBC) heteronuclear correlation experiment for delphinidin-3-*O*-rutinoside **17**.
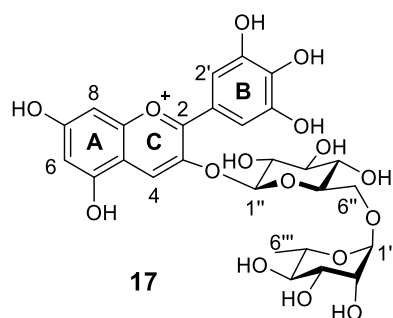
Proton	^{13}C correlations (HMBC)
H-4	C-2, 3, 5, 9, 10
H-2'	C-2, 3', 4', 5'
H-1"	C-2", 3"
H-6"	C-5", C-4"
H-6	C-10

Cyanidin-3-*O*-rutinoside **19** was assigned following same protocol with exception of protons on B ring; it does not have a symmetrical proton system on B ring, therefore COSY experiments were carried to confirm the assignments for these protons. The glucosides of cyanidin as well as delphinidin only presented one anomeric proton each in ^{1}H NMR spectra (as expected) and the coupling constants (~8.0 Hz) predicted *β* configurations for the substituted sugar moieties.

^{1}H NMR spectrum for polymeric anthocyanin fraction (PA) showed a broad aromatic and sugar region; this was indicative of a polymeric species. The presence of proanthocyanidins have been reported in grape skins and wines.[70,71,46] However, no accounts of their presence or characterisation in the blackcurrant extract were found. Degradation studies are commonly used to analyse such polymeric species; this was beyond the scope of this project.

2.6.2 Purification and Characterisation of Organic Blackcurrant Extracts

The isopropylacetate extract (15 mg) and ethyl acetate extract (10 mg) prepared previously (described in section 2.5.4) were both dissolved in methanol (2 ml) and purified on a semi-preparative column using method 9 (described in section 7.6.9). The peaks were monitored at 325 nm for isopropylacetate extract and 350 nm for ethyl acetate extract. Caffeic acid **30** (3.3 mg),[72] *p*-coumaric acid **31** (5.5 mg), myricetin **27** (2.7 mg)[73] and quercetin **28** (3.5 mg)[74] were purified from isopropylacetate extract. The glucosides of myricetin **22** (4.7 mg) and quercetin **24** (3.0 mg) alongside nigrumin-*p*-coumarate **32** (1.5 mg)[75] and nigrumin ferulate **33** (0.7 mg)[75] were isolated from ethyl acetate extract. Most of these polyphenols have been found in nature previously, however, full characterisation data on them is scarce.

Hydroxycinnamates were characterised with the aid of 1-D and 2-D NMR experiments; the assignments for *p*-coumaric acid has been described here. The doublets at 7.60 and 6.28 ppm exhibited coupling of 16.0 Hz which is characteristic of a *trans*-cinnamate system. However, HMBC correlations were acquired to confirm the assignment of these protons (Table 2.7). The doublet at 7.45 ppm was assigned to the chemically equivalent protons H-5 & 9 due to their *ortho* and *meta* positions to the allylic and hydroxyl functional groups. By default, the doublet at 6.81 ppm was assigned to H-6 and H-8. The assignments for the corresponding carbon atoms for these protons were made using HSQC spectra.

HMBC correlations were used to unambiguously assign tertiary signals (Table 2.7); this was also helpful in distinguishing between the allylic protons. The peak at 171.0 downfield of TMS was assigned to carbonyl carbon due to its characteristically high value as well its correlations to the alkene protons 2 and 3. The assignment of C-7 was deduced from its downfield position and ^3J(C-H) correlation to H-5. The signal at 146.6 ppm was assigned to C-3 as it correlated (^3J) with H-5; this interaction was not found for the C-H signal at 115.7 ppm which was then assigned to C-2. The quaternary signal at 127.3 ppm showed a 3-bond interaction with H-6 and the H-2, therefore it was assigned position 4. Other hydroxycinnamates and flavonoids were assigned using same protocol.

Although the presence of glycosylated caffeic acid and *p*-coumaric acid has been reported in some cases, these compounds were not found in this study. It is likely that such compounds are removed during the juicing process due to their small size and polar nature. No accounts of nigrumin-*p*-coumarate **32** and nigrumin ferulate **33** in blackcurrant skin extracts were found in the literature, however they have been previously identified

by one group in blackcurrant seeds.[76] Therefore, this is the first time their presence has been reported in blackcurrant skin extract.

Table 2.7. ^{1}H–^{13}C correlations found in the long range (HMBC) heteronuclear correlation experiment for *p*-coumaric acid **31**.
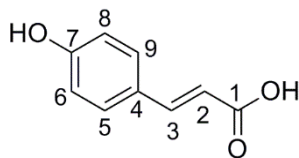
Proton	^{13}C correlations
H-2	C-1, 4
H-3	C-1, 5
H-6	C-4, 7
H-5	C-3, 7

2.7 Quantification of Post-SPE Blackcurrant Extract

Quantitative HPLC (q-HPLC) is the most reliable commonly used method for quantification of compounds in a sample. This requires having access to HPLC equipment and standard samples for external calibration.[77] In the case of anthocyanins, these standards are often not readily available and when available, are expensive. As an alternative, the total monomeric anthocyanin content (TMAC) assay has been reported, which is used to quantify the total amount of anthocyanins in wines, juices and plant extracts.[78,79] It is a pH differential method, and exploits the variation of UV/vis spectra of the different equilibrium forms of anthocyanins and the Beer-Lambert law ($A = \varepsilon cl$) for quantification (method discussed in 2.2.3).

Whilst the TMAC assay is easier to perform than q-HPLC and does not require standard samples, it has significant limitations. It does not take into consideration the effect of other polyphenols that are present in the sample, which may absorb at the wavelength used for the assay or be involved in co-pigmentation with the anthocyanins. The co-pigmentation phenomenon is observed as a bluing effect (bathochromic shift) since the visible absorption wavelengths (around λ_{max}) are shifted to longer wavelengths compared to similar absorptions of the anthocyanin without co-pigment.[6] In most cases the colour is also intensified (hyperchromic effect). Anthocyanins in the blackcurrant extracts were

quantified using q-HPLC and TMAC and both methods were compared for their accuracy.

2.7.1 HPLC Quantification of Blackcurrant Extract (q-HPLC)

Anthocyanins were quantified using q-HPLC, whereas the flavonoids and hydroxycinnamic acids were based on their isolated yields which was also reflective of their ^{1}H NMR quantification (relative to anthocyanins) in the extract. Delphinidin-3-*O*-glucoside (DOG) **16** was isolated in pure form from blackcurrant extract (*vide supra*) and was used as standard for quantitative HPLC analysis of all anthocyanins in the extract and compared with a commercial sample.

q-HPLC allows estimation of all the anthocyanins using only one standard sample. Although, it does not consideration the potentially different extinction coefficients for all the anthocyanins in a sample, it was found that there was a very good agreement between relative ratios of DOG **16** and individual anthocyanin peaks in the HPLC chromatogram and ^{1}H NMR (characteristic peaks at 8.8–9.2 ppm). For example, the relative ratio of delphinidin-3-*O*-rutinoside (DOR) **17** and delphinidin-3-*O*-glucoside (DOG) **16** given by HPLC and ^{1}H NMR was 2.8 and 2.7, respectively. Therefore, the amount of DOG in the extract was calculated using external calibration graphs (from isolated as well as a commercial sample) and then the relative ratio of the other anthocyanins was used to predict amount of DOR **17**, COG **18** (cyaninidin-3-*O*-glucoside) and COR **19** (cyaninidin-3-*O*-rutinoside) in the extract.

The chemical composition of the blackcurrant extract is summarised in Figure 2.8 (the structures have been presented previously in Figure 2.6). Anthocyanins constituted the largest class of polyphenols in the extract (54.7%) followed by neutral flavonoids (17.1%) and hydroxycinnamates (9.5%). The percentage of individual anthocyanins in this blackcurrant extract was found to be: DOR **17** (22.6%) > COR **19** (20.4%) > DOG **16** (7.7%) > COG **18** (4%). *p*-Coumaric acid (*p*-CA) **31** was the predominant (5%) hydroxycinnamate followed by caffeic acid **30** (CA, 3%). The flavonoids namely myricetin-3-*O*-glucoside **22**, myricetin-3-*O*-rutinoside **23**, myricetin **28**, quercetin-3-*O*-glucoside **24**, quercetin-3-*O*-rutinoside **25** and quercetin **29** were found in competing amount (2-3% each). Nigrumin-*p*-coumarate **32** (NCA**,** 1%) and nigrumin ferulate NF **33** (0.5%) were also present in small amounts.

Polymeric anthocyanins (PA, 18%) were isolated as purple amorphous solid. They were analysed by ^{1}H NMR and UV/vis spectroscopy. They gave broad peaks in the aromatic region of polyphenols (6-8 ppm) and glycosidic region of 4-5 ppm in ^{1}H NMR spectra

which is consistent with their generic structure in the literature (Figure 1.4). This was further supported by their maximum absorbance at 520, 350, 325 and 254 nm in UV/Vis spectra. Polymeric anthocyanins are also referred to as proanthocyanidins in the literature. Their structures depend upon the nature (stereochemistry and hydroxylation pattern) of the flavan-3-ol starter and extension units, the position and stereochemistry of the linkage to the "lower" unit, the degree of polymerisation, and the presence or absence of modifications such as esterification of the 3-hydroxyl group.[47] On acid hydrolysis, the extension units are converted to coloured anthocyanidins. The characterisation of polymeric anthocyanins was outside the scope of this project and has the potential to form basis for a separate research project in the future.
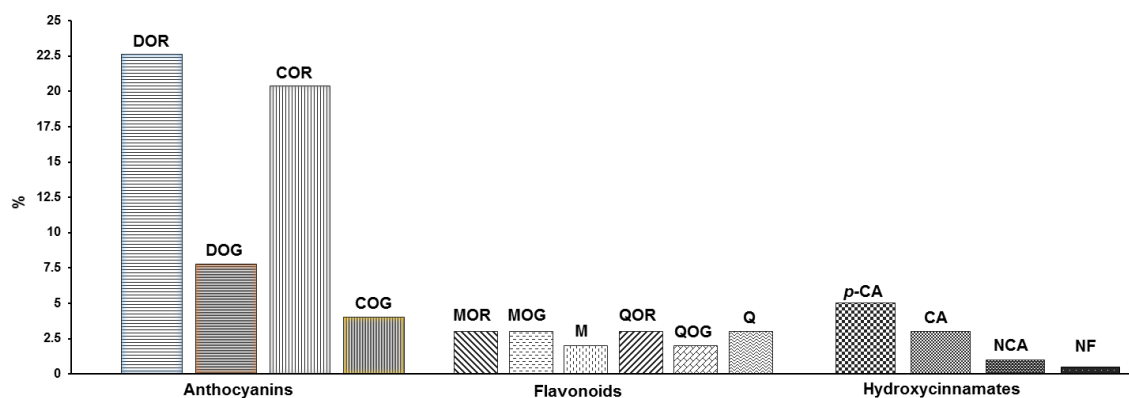
Figure 2.8. Summary of the chemical composition of the blackcurrant post-SPE extract.

2.7.2 Evaluation of Total Monomeric Anthocyanin Content (TMAC) Assay

An initial assessment of the TMAC of post-SPE blackcurrant extract using the pH-differential method (COG was used as standard, ε = 26900 M^{-1} cm^{-1})[59] suggested surprisingly low levels of monomeric anthocyanins (10%), particularly when compared with data obtained using q-HPLC (54.7%). NMR analysis of the extract clearly identified the four anthocyanins as the major components of the extract, rather than the low levels suggested by TMAC. This was further confirmed by isolation of purified anthocyanins (~50% recovery) from the extract using preparative HPLC.

Several studies have reported discrepancies between the total anthocyanin (TA) amount estimated by the TMAC assay and q-HPLC,[77,79] and many underestimated TA content significantly when compared with q-HPLC method[23,80,81] and found q-HPLC to be more reliable.

2.7.2.1 Effect of Extinction Coefficients on TMAC Assay

The original protocol (discussed in 2.2.3) uses the molecular weight (595 g mol^{-1}) and extinction coefficient (ε = 26900 M^{-1} cm^{-1}) for cyanidin-3-O-glucoside (COG) in the equation 1. This is because COG is the most common anthocyanin in nature. However, COG is not always present in the anthocyanin-rich extracts, for example in this study COG was the minor anthocyanin.

$$Anthocyanin \text{ content (mg/L)} = \frac{A \times MW \times DF \times 10^3}{\varepsilon \times l} \qquad (1)$$

Herein, extinction coefficients for all the anthocyanins isolated (*vide supra*) from the blackcurrant extract alongside a commercial sample of DOG were measured in buffer pH 1.0 (calibration graphs are in Appendix 8) The extinction coefficients for DOG **16**, DOR **17**, COG **18** and COR **19** were measured at 520 nm (commonly used for TMAC assay) as well as at their $\lambda_{vis-max}$. These values (Table 2.8) were in practice very similar; for example, for commercial DOG sample they were 7352 and 7398 M^{-1} cm^{-1} at 520 and 516 nm ($\lambda_{vis-max}$) respectively. Therefore, the extinction coefficient values measured at 520 nm were used, which would correspond to the overall $\lambda_{vis-max}$ for the blackcurrant extract. There was a good agreement between extinction coefficients for the isolated DOG **16** (ε 7068 M^{-1} cm^{-1}) and the commercial DOG **16** sample (ε 7352 M^{-1} cm^{-1}).

Extinction coefficients observed herein were notably lower than the literature values (Table 2.8), however there is considerable discrepancy between the existing literature values, making a direct comparison very difficult. The direct relationship between the extinction coefficient used and the TMAC result means it should be chosen particularly carefully if results are to be meaningful. Andersen raised the issue of discrepancy in the extinction coefficient values for anthocyanins in the literature in his critical review on anthocyanins;[6] however he did not comment on the root cause of this problem.

Cyanidin-3-O-glucoside **18** is the commonly used anthocyanin in TMAC calculation as it has been reported to be the most commonly found anthocyanin in nature. Therefore, it was suggested in the original protocol that COG can be representative of total anthocyanin content in an anthocyanin-rich extract, juices or wines. However, in this study COG was found to be present in lowest amount of all the anthocyanins found in blackcurrant extract (by ^{1}H NMR and HPLC); therefore, DOR **17**, the predominant anthocyanin, was used in the TMAC calculation instead. When total monomeric anthocyanin content (TMAC) was calculated using the experimental extinction coefficient data for DOR **17**, the percentage of anthcyanins in the extract (40%) was in much better agreement with q-HPLC (55%), however, further investigation was warranted.

Table 2.8. Experimental extinction coefficients for predominant anthocyanins found in this study (at 520 nm) compared with the literature values.

	ε (M^{-1} cm^{-1})		
Anthocyanin	Isolated sample	Commercial sample	Literature value
DOG	7068[a]	7352[a]	13000[b], 19055[c]
DOR	7699[a]		15135[d]
COG	6151[a]		10300[e], 12023[c]
COR	7452[a]		1560[f]

[a]buffer pH 1.0; [b]buffer (KCl/HCl) pH 1.0;[12] [c]0.01% HCl/methanol;[44] [d]MeOH/HCl;[44] [e]Ethanol/HCl;[82] [f]Methanol/HCl.[83]

2.7.2.2 The Effect of Solvents on TMAC Assay

The TMAC assay is based on the Beer-Lambert law which has some limitations; the absorption spectrum of an analyte can be affected by the presence of other chemical species (especially if co-pigmentation is possible) as well as the nature and pH of the solvent and concentration. To understand the limitations of using these methods, further studies were carried out under carefully controlled conditions to determine the potential significance of any variations.

TMAC is often used to measure total anthocyanin content of wine, juices and anthocyanin-rich extracts; these extracts are often alcoholic too. Stock solutions containing alcohol are then diluted with buffer pH 1.0 and 4.5 following the protocol. The alcohol content in the diluted samples would vary and can affect the absorbance measurements. Moreover, the extinction coefficients reported in the literature are often measured in ethanol or methanol. Therefore, if these extinction coefficient values are used in TMAC assay calculations which is a buffer-based assay, there is a possibility of error.

The UV/Vis spectra for DOG **16** were measured in aqueous buffer at pH 1.0 and acidified ethanol (99.9:0.1 v/v conc. HCl). There was a bathochromic shift of 31 nm (520 nm → 551 nm) when acidified ethanol (99.9:0.1 v/v conc. HCl) was used as the solvent system relative to the aqueous buffer at pH 1.0 (Figure 2.9); the extinction coefficient was also significantly higher (ε 9811 M^{-1} cm^{-1} at 551 nm in acidified ethanol, compared to ε 7352 M^{-1} cm^{-1} at 516 nm in buffer pH 1.0). This result shows presence of alcoholic solvents in the original extract (stock solution) directly affects the absorbance values and in turn would impact the assay results.
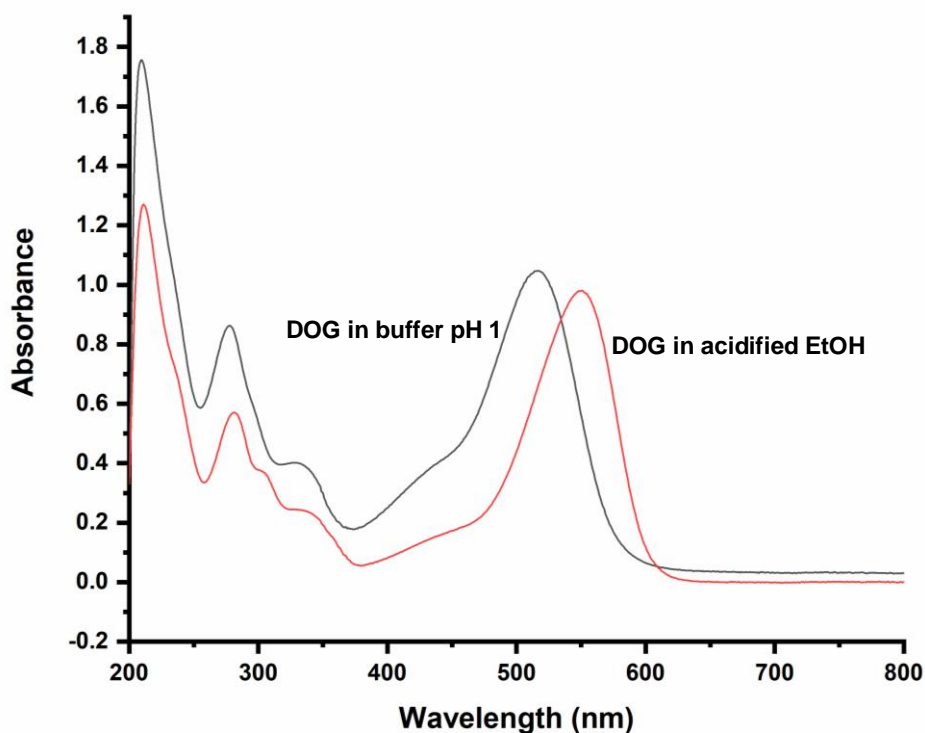
Figure 2.9. The Uv/vis spectra for delphinidin-3-*O*-glucoside (DOG) **16** in acidified ethanol (99.9:0.1 v/v conc. HCl) and aqueous buffer at pH 1.0.

2.7.2.3 The Effect of Co-pigments on TMAC Assay

Quercetin-3-*O*-rutinoside (QOR) **25** is a neutral flavonoid that remained in the aqueous blackcurrant extract after liquid-liquid partitioning experiments (2.5.4) and has been reported to co-pigment when in solution with anthocyanins. The effect of QOR **25** on the absorbance of DOG **16** was studied in aqueous buffer at pH 1.0 as well as at pH 4.5. Whilst the λ_{max} for DOG + QOR in buffer at pH 1.0 only shifted by 2 nm (Figure 2.10), there was a bathochromic shift of 27 nm at pH 4.5 which resulted in 5% decrease in the overall absorbance value at 520 nm which would correspond to 4% less TA content according to a TMAC assay.

Andersen and Jordheim eluded to the copigmentation phenomenon in their review; it is observed as a bluing effect (bathochromic shift) since the visible absorption wavelengths (λ_{max}) are shifted to longer wavelengths compared to similar absorptions of the anthocyanin without the co-pigment.[6] In most cases, the colour is also intensified (hyperchromic effect). Most anthocyanin-containing extracts and juices also contain other polyphenols such as hydroxycinnamic acids and flavonoids. These results strongly suggest that the presence of other polyphenols would significantly underestimate the TMAC quantification. This may at least in part help explain observations made in this

study and those of other researchers, and as such any photometric based assay needs to be treated with caution and does not provide accurate quantification data.
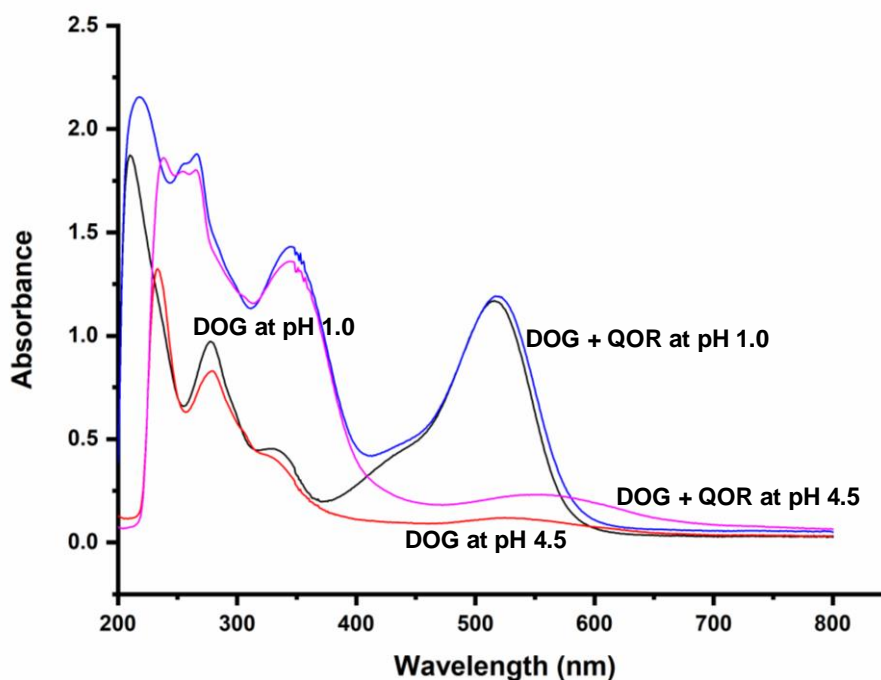
Figure 2.10. The UV/Vis absorption spectra for delphinidin-3-*O*-glucoside **16** (DOG) and mixtures of delphinidin-3-*O*-glucoside **16** with quercetin-3-*O*-rutinoside **25** in buffers at pH 1.0 and 4.5.

2.8 Stability of Anthocyanins

During the extraction protocol development, it was noticed that anthocyanin profile changed when the extract was dried *in vacuo* after solid-phase extraction (SPE) step. Anthocyanin rutinosides showed notable hydrolysis (Table 2.9)to the corresponding glucosides (88% and 93% hydrolysis for delphinidin-3-*O*-rutinoside **17** and cyanidin-3-*O*-rutinoside **19**, respectively) after only three hours at 40 °C through concentration on a standard laboratory rotovap. The rutinosides almost hydrolysed completely after 6 h. The aglycons of cyanidin **10** (7%) and delphinidin **13** (6%) were also observed after 9 hours under similar conditions, which were otherwise not present in the fresh extract. These aglycones started degrading after 12 and 15 h, whereas delphinidin-3-*O*-glucoside **16** and cyanidin-3-*O*-glucoside **18** remained stable through the process.

This hydrolysis is most likely due to the small amount of acid added to the eluent to retain low pH (and hence retain the more stable flavylium cationic form) becoming more concentrated, catalysing the hydrolysis of the most reactive glycosyl linkage by residual water still present. This is potentially a very important observation for related extraction

46

protocols, particularly if glycosylation ratios are important, which may be the case when using anthocyanin profiles for forensic analysis of source material. This in part could explain discrepancy in anthocyanic profile of blackcurrants reported in the literature.[44,84]

Table 2.9. Relative % of anthocyanins in post-SPE blackcurrant extract in time.

Anthocyanin	Relative % of anthocyanins					
	time (h)					
	0	3	6	9	12	15
DOG	15	53.7	55.7	50.6	50.6	50
DOR	44	5.3	2.3	1.9	1.9	0.9
COG	6	38.5	39	33.6	33.6	33
COR	35	2.5	1	0.7	0.7	0.2
Delphinidin	0	0	1	6.5	6.5	1.9
Cyanidin	0	0	1	6.7	6.7	2

One of the issues with the use of anthocyanin-rich extracts in commercial products is their instability. These results show the glucosides are highly stable and should be able to handle commercial processes. In a recent paper, Blackburn *et al* studied sorption properties of various anthocyanins onto hair fibres; they found cyanidin-3-*O*-glucoside **18** had higher sorption energy than cyanidin-3-*O*-rutinoside **19**.[85] Therefore, it was a better candidate for dyeing hair as a natural colorant.

Anthocyanin rutinosides can be selectively hydrolysed using enzymes.[86] Matsumoto *et al.* processed anthocyanins from blackcurrant concentrate utilising enzymes to increase yield. α-Rhamnosidase cleaved the disaccharides at α-position converting rutinosides into corresponding glucosides (Scheme 2.1).[86] As a result, the glucosides of cyanidin **18** and delphinidin **16** were enriched 7- and 4-fold respectively. This methodology is potentially very useful for obtaining a commercially useful anthocyanin glucoside-rich extract. Furthermore, enzymatic hydrolysis is better than acid hydrolysis due to specificity and environmental impact in general.
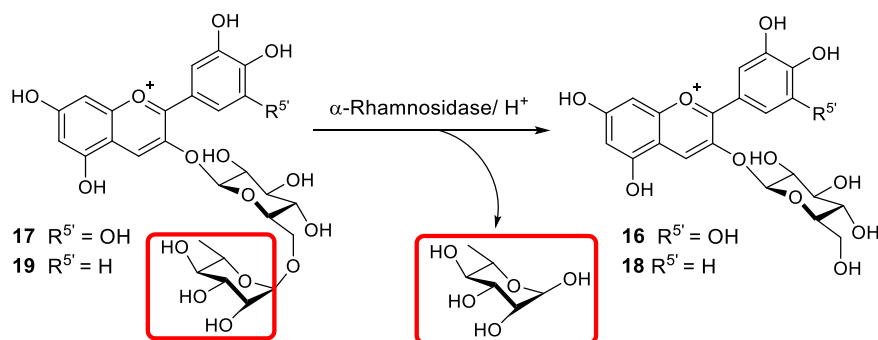
Scheme 2.1. The enzymatic cleavage/ acid hydrolysis of rutinosides of delphinidin and cyanidin by α-rhamnosidase (hesperidinase).[86]

2.9 Improved Method for Extraction of Polyphenols from Blackcurrant Pomace

The original Keracol Ltd. protocol for extraction of anthocyanins from blackcurrant waste has been presented in Figure 2.11; It starts with the extraction of blackcurrant skins (waste) with acidified hot water, the aqueous extract is then loaded onto the polymeric resin XAD-7HP (solid-phase extraction, SPE) to remove free sugar and small organic acid molecules. The polyphenols are adsorbed onto the resin and unwanted small molecules are washed off the column using slightly acidified water (0.01% *v/v* HCl). Then the polyphenols including anthocyanins are eluted using acidified ethanol (0.01% *v/v* HCl). The analysis of Keracol blackcurrant extract discussed in section 2.2 revealed that this extract did not only contain anthocyanins but also significant amount of other neutral polyphenols. Full chemical characterisation of the extract allowed better understanding of the physical and chemical properties of the compounds in the extract.

A series of solvents were screened for extraction of polyphenols including anthocyanins from blackcurrant skins (discussed in detail in section 2.3.2). When the blackcurrant skins were sequentially extracted with isopropylacetate, ethyl acetate and acidified water (0.1% HCl *v/v*), selective extraction of tannins and organic acids, neutral polyphenols and anthocyanins was observed. Non-acidified isopropylacetate extracted predominantly tannins, flavonoid and hydroxycinnamic acids. Ethyl acetate selectively extracted flavonoids and hydroxycinnamates alongside small amount of tannins (Figure 2.3). Acidified water extracted anthocyanins, disaccharide flavonoids and polymeric anthocyanins.
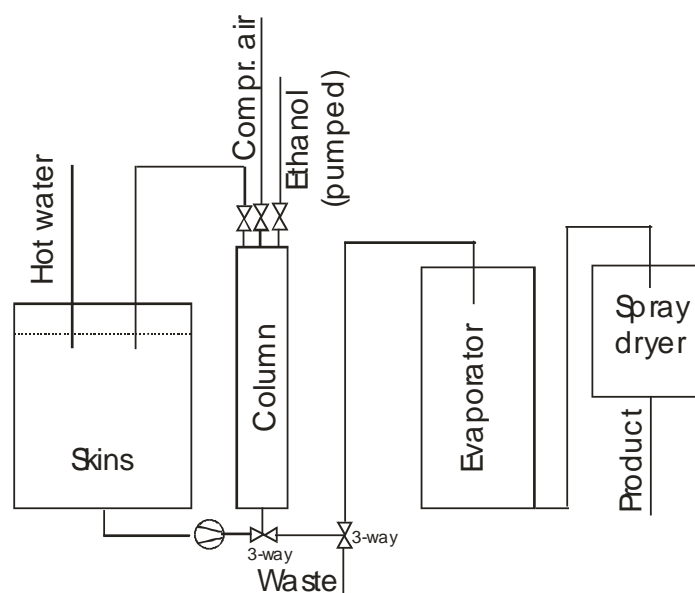
Figure 2.11. Schematic for industrial process of extraction of anthocyanins from blackcurrant skins developed by Keracol Ltd. Image is courtesy of Keracol Ltd.

Similar results were observed when post-SPE (eluted from XAD-7HP resin) aqueous extract was sequentially partitioned against isopropylacetate and ethyl acetate (discussed in detail in section 2.5.4). Isopropylacetate achieved selective extraction of caffeic acid (CA) **30**, *p*-coumaric acid (*p*-CA) **31**, myricetin **28**, and quercetin **29**. Ethyl acetate extracted myricetin-3-*O*-glucoside **22**, quercetin-3-*O*-glucoside **24**, nigrumin-*p*-coumarate **32**, and nigrumin ferulate **33**. The highly polar, water-soluble anthocyanins **16−19** were exclusively found in the aqueous layer, alongside myricetin-3-*O*-rutinoside **23** and quercetin-3-*O*-rutinoside **25**. Polymeric anthocyanins were also present in this layer.

It can be concluded based on these results that isopropylacetate, ethyl acetate and acidified water selectively extract different types of compounds regardless of whether it is done pre- or post-SPE (solid-phase extraction) step. An improved method is proposed here which would create three complementary product streams: intensely pigmented anthocyanins, antioxidant neutral polyphenolics and antioxidant glycosylated polyphenolics. In the new protocol, blackcurrant waste is extracted with acidified water (0.1% *v/v* HCl), then plant material is filtered off before loading the aqueous extract onto SPE resin (XAD-7HP).

At this stage, polyphenols are eluted with solvents of increasing polarity to give three fractions altogether; starting with one column wash of isopropylacetate that removes caffeic acid **29**, *p*-coumaric acid **30**, myricetin **27** and quercetin **28**. This is followed by one column wash of ethyl acetate which elutes myricetin-3-*O*-glucoside **22**, quercetin-3-

49

O-glucoside **24**, nigrumin-*p*-coumarate **31** and nigrumin ferulate **32**. Finally, four anthocyanins are eluted alongside rutinosides of myricetin and quercetin with slightly acidified ethanol (0.1% *v/v* HCl): namely delphinidin-3-*O*-glucoside **16**, delphinidin-3-*O*-rutinoside **17**, cyanidin-3-*O*-glucoside **18**, cyanidin-3-*O*-rutinoside **19**, myricetin-3-*O*-rutinoside **23** and quercetin-3-*O*-rutinside **25**.
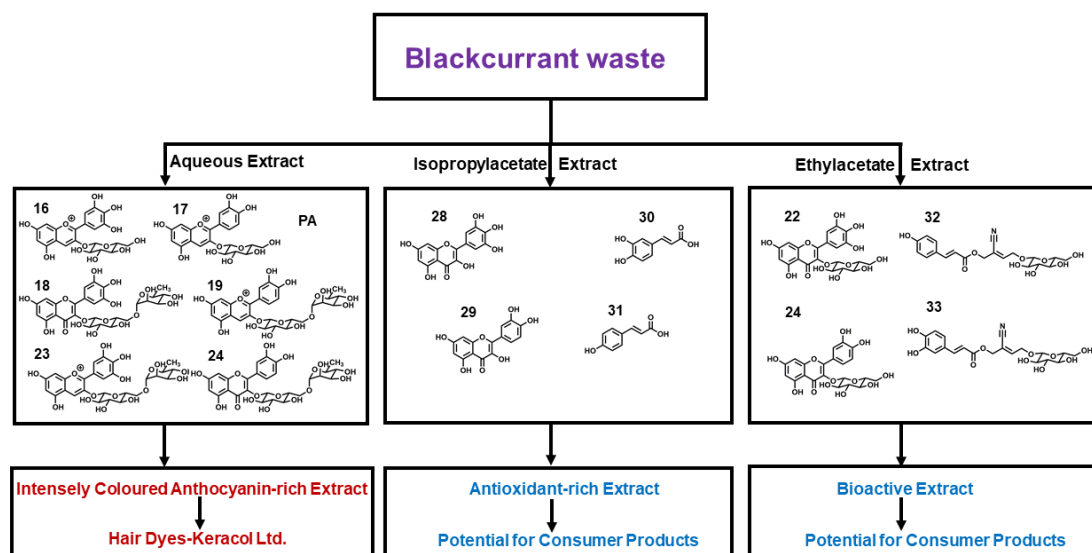
Figure 2.12. New Proposed Method for extraction of high valuable chemicals from blackcurrant waste.

Three product streams have been generated from blackcurrant waste and the method is potentially scalable (Figure 2.12). Intensely pigmented anthocyanin-rich extract has been formulated into commercial products by Keracol Ltd. Isopropylacetate extract is rich in known antioxidants. Myricetin **27**, quercetin **28**, caffeic **29** and *p*-coumaric acid **30** in the isopropylacetate extract has been reported to exhibit potent antioxidant activity in the literature.[65,66] Myricetin-3-*O*-glucoside **22** and quercetin-3-*O*-glucoside **24** in the ethyl acetate layer have also been reported for their bioactivity.[67] The antioxidant and absorbance properties of Quercetin-3-*O*-glucoside **24** and its aglycone quercetin **28** into the skin using different pickering emulsions has been extensively investigated by another Rayner group PhD student (now Dr Elizabeth Dufton).[60] Nigrumin coumarate **31** and nigrumin ferulate **32** found in the ethyl acetate layer were patented for their therapeutic or nutritive use in management of impaired mitochondrial functions in 2015.[68]

2.10 Conclusion

Anthocyanins are intensely pigmented natural colorants and form the largest group of polyphenols in the plant kingdom.[3] They have been reported in blackcurrants, strawberries, chokeberries, black carrot, black beans, blueberries and mulberries among others.[6] Much of the studies on characterisation of anthocyanin-rich food extracts, wines and juices have been solely focused on their analysis using HPLC-DAD at 520 nm.[3] However, anthocyanins are not the only group of polyphenols found in the plant kingdom and such narrow focus on one group when designing an analytical protocol can led to error. For example, neutral flavonoids do not absorb a 520 nm therefore HPLC analysis of an extract at this wavelength only can lead to false results on quality and purity of the extract.

A combination of analytical techniques was used in this project to gain full understanding of the nature of blackcurrant extract. Although NMR spectroscopy is an underused technique in this area of research, possibly due to the complex nature of natural extracts, it was proven to be a powerful technique. Water, methanol, ethanol, isopropylacetate and ethyl acetate (with and without acid) were screened for their efficiency at extracting polyphenols including anthocyanins from blackcurrant skins (waste). The extracts were monitored using HPLC-DAD, LC-MS, UV/Vis and ^{1}H NMR at different stages of the process to gain dynamic understanding of the chemical profile of the extracts.

Acidified methanol (0.1% *v/v* HCl) was found to be the best solvent for yield (2.6% *wt./wt.* of dry plant material) as well as higher polyphenolic content. It extracted anthocyanins: delphinidin-3-*O*-glucoside **16**, delphinidin-3-*O*-rutinoside **17**, cyanidin-3-*O*-glucoside **18**, cyanidin-3-*O*-rutinoside **19**; flavonoids**:** myricetin-3-*O*-glucoside **22**, myricetin-3-*O*-rutinoside **23**, quercetin-3-*O*-glucoside **24**, quercetin-3-*O*-rutinoside **25**, myricetin **28** and quercetin **29**; hydroxycinnamic acids: caffeic **30** and *p*-coumaric acid **31**. These compounds were assigned by co-eluting with their standard samples. The relative ratio of these polyphenolic groups in the blackcurrant extracts was same when extracted with acidified methanol (0.1% *v/v* HCl, yield 2.6% *wt./wt.*) or acidified water (0.1% *v/v* HCl, yield 1.9% *wt./wt.*); however, methanol extracted higher amount of polyphenols overall. Anthocyanins formed the largest group of extracted polyphenols followed by flavonoids and then hydroxycinnamic acids. Ethyl acetate and isopropylacetate showed selectivity towards flavonoids and hydroxycinnamic acids and did not extract anthocyanins. In conclusion, the extraction solvent should be chosen carefully depending on the final use of the extract as well desired chemical profile (yield *vs* selectivity).

Fourteen compounds were isolated from the blackcurrant extract and fully characterised using ^{1}H NMR, ^{1}H−^{1}H COSY, HRMS, UV/vis, IR, and ^{13}C, DEPT135, ^{1}H−^{13}C HMBC, and ^{1}H−^{13}C HSQC spectroscopy. It was found that a pre-clean up step was required prior to

purification on preparative HPLC due to the difference in physical and chemical properties of the compounds in the extract. The aqueous blackcurrant was partitioned against isopropylacetate and ethyl acetate in a sequential manner to generate three extracts; these extracts were dried and purified on preparative HPLC. The purified compounds were then used to quantify and characterise the blackcurrant extract. Anthocyanins constituted the largest class of polyphenols in the extract (54.7%) followed by neutral flavonoids (17.1%) and hydroxycinnamates (9.5%). Polymeric anthocyanins made up 18% of the extract.

Anthocyanins were quantified using quantitative HPLC (q-HPLC) and standard samples, whereas the flavonoids and hydroxycinnamic acids were based on their isolated yields which was also reflective of their ^{1}H NMR quantification (relative to anthocyanins) in the extract. This protocol was adapted due to the complexity of spectra at 350 nm (λ_{max} for flavonoids) and 325 nm (λ_{max} for hydroxycinnamates).[40] In contrast, the anthocyanins gave four well separated peaks at 520 nm therefore their quantification using standard samples was reliable. Polymeric anthocyanins were also isolated and tentatively characterised using UV/Vis and NMR spectroscopy. Their full characterisation was outside the scope of this project; however, they should be investigated in the future. The nature of the polymeric species would help us understand aggregation and co-pigmentation patterns of the blackcurrant extract.

Total monomeric anthocyanin content (TMAC) assay and quantification HPLC (q-HPLC) were compared for their efficacy in determining total amount of monomeric anthocyanins in the blackcurrant extract. There was a striking difference in the results obtained from TMAC (10%) and HPLC (55%). There have been several reports of inconsistency between these two techniques when used for quantification of anthocyanins.[79] An evaluation of the experimental conditions for the assay and commonly analysed extracts revealed limitations of the assay. Firstly, the experimentally determined extinction coefficients for the isolated and commercial anthocyanin samples were in agreement, however they were lower than the literature value. Andersen and Jordheim, among other researchers, have raised the issue of discrepancy in the published extinction values in their critical review;[6] this makes a direct comparison with the literature very difficult. Furthermore, the original protocol does not take into account the presence of small amount of alcohol (from the extraction process) and other polyphenols which would act as co-pigments to the anthocyanins in solution. There was a bathochromic shift of 31 nm (520 nm → 551 nm) when acidified ethanol (99.9:0.1 v/v conc. HCl) was used as the solvent system relative to the aqueous buffer at pH 1.0 (Figure 2.9); the extinction coefficient was also significantly higher (ε 9811 M^{-1} cm^{-1} at 551 nm in acidified ethanol, compared to ε 7352 M^{-1} cm^{-1} at 516 nm in buffer pH 1.0).

Furthermore, quercetin-3-*O*-rutinoside (QOR) in the assay led to bathochromic shift of 27 nm at pH 4.5 which resulted in 5% decrease in the overall absorbance value at 520 nm which would correspond to 4% less TA content according to a TMAC assay. Co-pigmentation of anthocyanins with other polyphenols (and self-association) is a well-known phenomenon and should not be overlooked when analysing anthocyanin-rich matrices.[6] These results strongly suggest that the presence of other polyphenols and solvents would significantly underestimate the TMAC quantification. This may at least in part help explain observations made in this study and those of other researchers, and as such any photometric based assay needs to be treated with caution and does not provide accurate quantification data.

Lastly, an improved method for the extraction of polyphenols including anthocyanins from blackcurrant waste has been proposed for Keracol Ltd. The new steps can be incorporated into the original protocol with relative ease. Once the aqueous blackcurrant extract is loaded onto the solid-phase extraction resin, the polyphenols are eluted with solvents of increasing polarity to give three fractions altogether; starting with one column wash of isopropylacetate followed by one column wash of ethyl acetate. These solvents elute neutral polyphenols from the resin then acidified ethanol is used to elute anthocyanins. Therefore, three complementary product streams are generated: intensely pigmented anthocyanin-rich extract, aglycosylated antioxidant-rich extract and glycosylated antioxidant-rich extract.

Chapter 3 Platforms for Antibiotic Drug Discovery

3.1 The Impact of Antibiotic Drug Discovery

Antibiotics have revolutionised modern medicine and have saved millions of lives since their discovery at the beginning of twentieth century.[87] These crucial drugs are invaluable owing to their ability to kill or inhibit the growth of bacteria without damaging host cells and tissues. They have contributed to an increase in the life expectancy; for instance, the average life expectancy of Canadians has increased by 22 years since the clinical introduction of antibiotics.[88] Antibiotics have not only saved lives by direct effect, but have also played a pivotal role in achieving major advances in medicine and surgery.[89]

Antibiotics have successfully prevented and/or treated infections that can occur in patients who are receiving chemotherapy treatments (as well as infections in healthy individuals); who have chronic diseases such as diabetes, end-stage renal disease, or rheumatoid arthritis; or who have had complex surgeries such as organ transplants, joint replacements, or cardiac surgery. Following their initial discovery in the early twentieth century, it was widely believed that antibiotic use would eventually eradicate bacterial diseases.[90] However, the emergence of bacterial resistance to antibiotic drugs undermines the therapeutic utility of existing agents, creating a requirement for the discovery of new antibacterial drugs.[91] Antibiotics remain one of the most commonly prescribed classes of drug, with more than 70 billion clinical doses administered globally in 2010, which represents a 36% increase in antibiotic consumption relative to 2000.[87]

3.2 Emergence of Resistance

Although the first antibiotics were synthetic compounds, most antibiotics are natural products or their derivatives.[87] Many antibiotics were recovered from cultured soil microorganisms; actinomycetes have been one of the most prolific sources of antibiotics including major classes of antibiotics such as β-lactams, tetracyclines, aminoglycosides, rifamycins, macrolides and glycopeptides (Figure 3.1).[92] As a result of the ubiquity of antibiotic production by environmental microorganisms, defence mechanisms against these antibiotics and thus resistance also seem to be inherent.[87] Multidrug-resistant genes have been detected by sequencing of DNA preserved in 30,000 old permafrost

sediments. Furthermore, direct screening of bacteria cultured from a cave that had no anthropogenic contact for the past four million years revealed extensive resistance against 14 distinct antibiotic classes.[87]
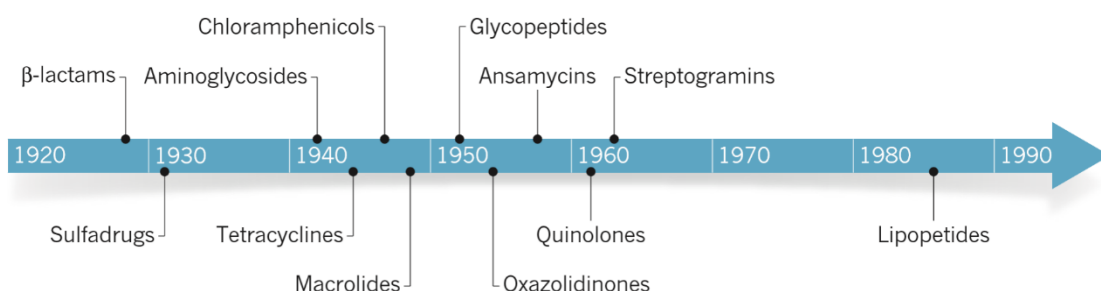
Figure 3.1. The antibiotic discovery timeline.[93]

The ancient origins of antibiotics and antibiotic resistance make it unsurprising that large-scale clinical and agricultural use of these compounds has resulted in rise in antibacterial resistance. Robust evidence for increasing environmental resistance exists in decades-old soil samples, in which increasing numbers of antibiotic resistance genes correlate with the industrial-scale production and use of these antibiotics.[87] In his Nobel address in 1945, Fleming warned of the potential of emergence of bacterial resistance to penicillin if used too little or for a too short period during treatment.[90,] The increasing frequency of multidrug-resistant (MDR) and pan-resistant strains like those of the ESKAPE pathogen group (*Enterococcus faecium*, *Staphylococcus aureus*, *Klebsiella pneumoniae*, *Acinetobacter baumannii*, *Pseudomonas aeruginosa*, and *Enterobacter spp.*) is now a major cause of concern which requires immediate action.

A recent report estimated that by 2050, 10 million lives a year and the grand total of US $100 trillion of economic output are at risk due to the rise of antibacterial resistant infections.[94] The problem has intensified following the emergence of resistance to the antibiotic colistin, creating an alarming situation by bringing an end to the last line of defence against multidrug-resistant Gram-negative bacterial infections.[95] A summary of the clinically useful antibiotics, year of introduction and resistance observed and mode of action has been given in Table 3.1.

Table 3.1. The summary of clinically useful antibiotics.[96]

Class	Discovery (y)	Introduction (y)	Resistance (y)	MOA	Activity
Sulfadrugs; prontosil	1932	1936	1942	Inhibition of dihydropteroate synthetase	Gram-positive
β-lactams; penicillin	1928	1938	1945	Cell wall biosynthesis Inhibition	Broad-spectrum
Aminoglycosides; streptomycin	1943	1946	1946	Binding of 30S ribosomal subunit	Broad-spectrum
Chloramphenicols; chloramphenicol	1946	1948	1950	Binding of 50S ribosomal subunit	Broad-spectrum
Macrolides; erythromycin	1948	1951	1955	Binding of 50S ribosomal subunit	Broad-spectrum
Tetracyclines; chlortetracycline	44	52	50	Binding of 30S ribosomal subunit	Broad-spectrum
Rifamycins; rifampicin	57	58	62	Binding of RNA polymerase β-subunit	Gram-positive
Glycopeptides; vancomycin	53	58	60	Cell wall biosynthesis Inhibition	Gram-positive
Quinolones; ciprofloxacin	61	68	68	Inhibition of DNA synthesis	Broad-spectrum
Streptogramins; streptogramin B	63	98	64	Binding of 50S ribosomal subunit	Gram-positive
Oxazolidinones; linezolid	55	2000	2001	Binding of 50S ribosomal subunit	Gram-positive
Lipopetides; daptomycin	86	2003	87	Depolarisation of cell membrane	Gram-positive
Fidaxomicin	48	2011	77	Inhibition of RNA polymerase	Gram-positive

One of the issues with antibiotic development and resistance in the past was our tunnel focus on pathogenic bacteria. Indeed, pathogenic bacteria are a cause of concern for human health, however bacteria exist in communities and therefore the role of commensal bacteria cannot be overlooked.[97] Over time, the study of antibiotic resistance has grown from focusing on single pathogenic organisms in axenic culture to studying antibiotic resistance in pathogenic, commensal and environmental bacteria at the level of microbial communities.[87] In bacteria, genes can be inherited from relatives or can be acquired from nonrelatives on mobile genetic elements such as plasmids. This horizontal gene transfer (HGT) can allow antibiotic resistance to be transferred among different species of bacteria.[89]

The rise of antibacterial resistance is a multi-faceted issue and therefore requires collaboration between governments, scientists, policy makers, doctors, farmers and general public: supply, demand and maintenance. Jim O'Neill recommended key steps in reducing demand for antibiotics in his exhaustive review of antimicrobial resistance. These are (1) massive global public awareness campaign, (2) improvement of hygiene, (3) reduction in unnecessary use of antimicrobials in agriculture, (4) improvement of global surveillance, (5) better diagnostics, (6) vaccine development and (7) better workforce.[94] Secondly, collaborations between academia and industry supported by government funding is required for reviving dried up antibiotic discovery pipeline. Lastly, antimicrobial resistance is an international problem, consequently a global action is required over long term to tackle this issue.

3.3 A Brief History of Antibiotic Discovery

The earliest history of antibacterial chemotherapeutic discovery was *via* screening dyestuffs and other chemicals for selective antibacterial activity, yielding salvarsan and the sulfa drugs.[98] The sulfa drugs, fluoroquinolones and oxazolidinones are examples of successful synthetic antibiotics; however the bulk of clinically relevant antibiotics are derived from microbial natural products. Following the discovery of penicillin **34** in 1928, the golden era for finding new antibiotics really began in the 1940s, when microbiologist Selman Waksman exploited soil bacteria's ability to produce their own antibiotics (which they use to out-compete each other) by systematically testing soil microbes–largely streptomycetes. This led to the discovery of streptomycin **35** in 1943, the first antibiotic used to treat tuberculosis (Figure 3.2). The so-called 'Waksman platform' of screening was widely adopted by the pharmaceutical industry and yielded the main classes of antibiotics over the following 20 years. However, overmining of soil bacteria resulted in diminishing returns – the same compounds were continuously rediscovered, and the platform collapsed.

Penicillin G **(34)**   Streptomycin **(35)**
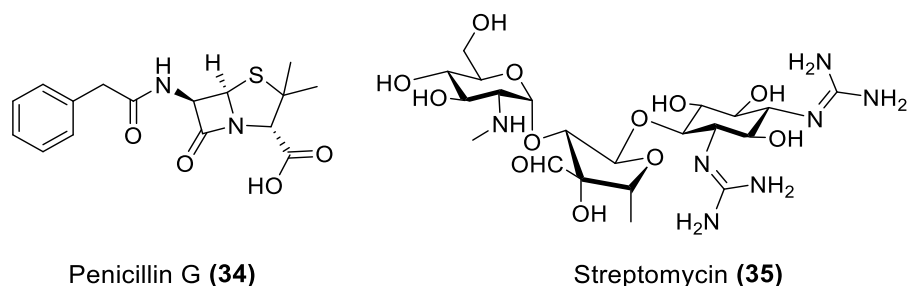
Figure 3.2. The structures of ground-breaking antibiotic drugs.

Natural product divisions in pharmaceutical companies were scaled down or shut down with emergence of large scale combinatorial synthesis and genome-influenced target-based drug discovery.[99] It was thought that essential bacterial proteins identified through genomics would serve as targets for high-throughput screening (HTS) and rational drug design with the aim of producing novel antibiotics. However, not a single drug with a reasonable spectrum of activity against important pathogens emerged from this platform.[96] Although inhibitors of targets were readily identified through *in vitro* HTS, it proved very challenging to produce compounds that were able to sufficiently penetrate the bacterial cell wall to reach their targets, especially in Gram-negative bacterial species. As a result, research and development on antibiotics went into severe decline and many larger pharmaceutical companies left the field altogether.

3.4 Discovery Void

The rise of antibiotic resistance in pathogenic bacteria is alarmingly affecting our ability to manage bacterial infection.[100] One of the effective strategies to deal with this growing problem would be the development of novel antibacterial drugs that display activity against multi-drug resistant bacteria. Unfortunately, progress in this area of research has been challenged by the extremely challenging nature of antibacterial drug discovery; the field is now 30 years into a 'Discovery Void', from which no novel drug class effective against the problematic ESKAPE pathogens (*E. faecium*, *S. aureus*, *K. pneumoniae*, *A. baumannii*, *P. aeruginosa*, and *Enterobacter* species) has emerged to reach the clinic.[100,98] The last clinically useful broad-spectrum antibiotic in a new class to be discovered was daptomycin (in 1986), a lipopeptide that acts against the bacterial cell membrane, but it was not approved until 2003.[96] The lack of new lead compounds led to resurrection of previously discarded daptomycin **36**, quinupristin–dalfopristin and fidaxomicin **37** (Figure 3.3).

58

Daptomycin **(36)**　　　　　　　　　　　Fidaxomicin **(37)**
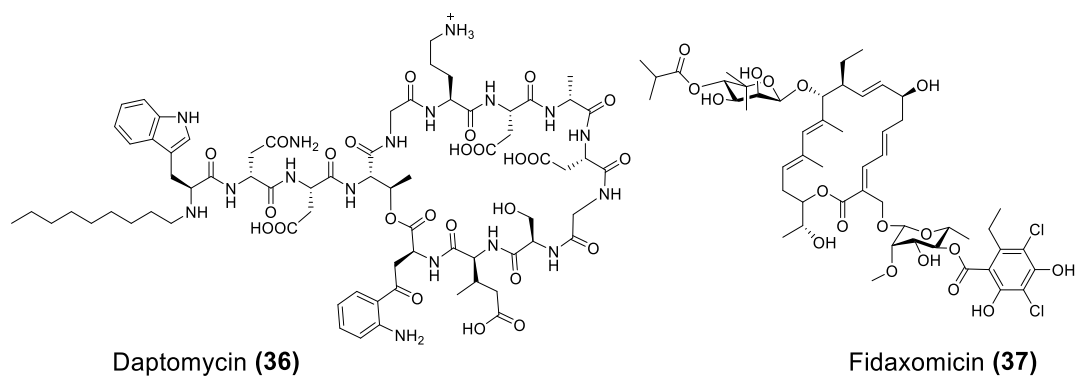
Figure 3.3. The examples of successful antibiotic drugs discovered by visiting previously discarded antibacterial compounds.

3.5 Recovering the Lost Art of Antibiotic Discovery

Considering the severity of the situation a multi-faceted approach is required for discovery of novel antibiotic compounds and rescuing of old antibiotic compounds.[99] The use of combination therapy and adjuvants can extend usefulness of current antibiotics. For efficient discovery and development of novel antibiotics, reliable discovery platforms are required.[101] Some of the examples of such platforms in the literature are prodrugs, species-specific antibiotics, silent operons, revisiting old antibiotics and investigating previously unexploited genera.[99] The usefulness of some of these platforms is discussed here.

3.5.1 Revisiting Old Antibiotics

Of the ~28000 natural product antibiotics that were discovered over the past decades, only a handful are in clinical use.[99] The rest of them were not thought to be useful as drugs due to unmanageable issues such as efficacy, toxicity, stability and lack of broad-spectrum activity.[99] Nevertheless, some of these compounds are worthy of reinvestigation. The availability of preliminary data on structure and antibacterial activity of previously discarded antibacterial compounds can potentially overcome pitfalls associated with early stages of drug discovery.[100] The successful launch of previously discarded antibiotics daptomycin **36**, fidaxomicin **37**, linezolid **38** and retapamulin **39** is an evidence of usefulness of this platform.[102]

In 1978, DuPont patented a series of oxazolidinones for the treatment of bacterial and fungal diseases in plants. Six years later efficacy of antibacterial treatment in mammals was confirmed. However, the development program was terminated owing to liver toxicity in 1987. In 1990s the researchers at Pharmacia and Upjohn (now part of Pfizer)

employed structure-activity relationships to generate a series of oxazolidinones leading to two drug candidates: eperezolid and linezolid. Zyvox (linezolid **38**, Figure 3.4) was approved by the FDA in 2000 for treatment of infections caused by Gram-positive bacteria.

Daptomycin **36** (Figure 3.3), a lipopeptide, was first isolated from soil bacteria (*Streptomyces roseosporus*) in 1987 by scientists at Eli Lilly and Company. Phase I and II clinical trials conducted in the late 1980s and early 1990s resulted in termination of the intravenous (IV) daptomycin clinical programs due to toxicological concerns.[100] Daptomycin **36** was then acquired by Cubist Pharmaceuticals in the mid-1990s, who focused their efforts on developing formulation for oral and topical clinical indications to limit the systemic exposure and re-deployed with alternate dosing for the IV treatment, and received FDA approval in 2003 for the treatment of skin and skin structure infections caused by Gram-positive pathogens.[102] Fidaxomicin **37** and retapamulin **39** (pleuromutilins, Figure 3.4), used for the treatment of bacterial intestinal and skin infections respectively, also came from this platform.

Linezolid **(38)**   Retapamulin **(39)**
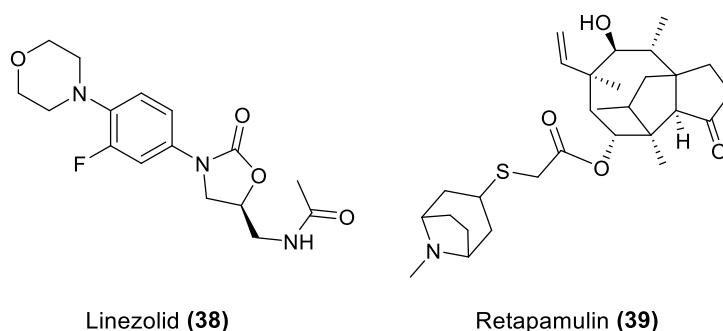
Figure 3.4. The structures of linezolid and retapamulin.

3.5.2 Species-specific Targets

During the golden age, hundreds of natural antibiotic compounds were screened for antimicrobial activity and mostly the compounds that did not exhibit broad spectrum activity were discarded. Although broad-spectrum antibiotic drugs are most commonly used by physicians, continuous improvement in diagnostics open doors for species-specific treatments of bacterial infections. This is a developing field, with molecular diagnostics replacing traditional plating techniques. This would allow selective therapy, using a pathogen-specific compound that would, in theory, have minimum impact on the body's natural protective flora.[93] A promising example is the approval of a rapid diagnostic to detect methicillin-resistant *Staphylococcus aureus* (MRSA) by MicroPhage,

which will enable the development of selective agents against this clinically important pathogen.[96]

The history of anti-tuberculosis drug discovery provides a compelling case for the development of species-specific antibiotics. The disease is caused by a single pathogen (*Mycobacterium tuberculosis*), the diagnosis is unambiguous and testing random compounds against *M. tuberculosis* has produced antimicrobials that act primarily against mycobacteria.[96] The first anti-tuberculosis compound to be discovered was streptomycin **35** which is a broad-spectrum natural antibiotic. Subsequent screening of synthetic compounds against *M. tuberculosis* resulted in the discovery of isoniazid, pyrazinamide, ethionamide and ethambutol, and all of these compounds turned out to be selective against mycobacteria.[96] Bedaquiline was obtained through high-throughput screening (HTS) of a commercially available library and was recently approved by the FDA for treatment of multi-drug resistant tuberculosis.

3.5.3 Novel Sources of Natural Antibiotic Compounds

Most of the clinically useful natural antibiotic compounds were isolated from soil bacteria. Actinomycetes have been one of the most prolific sources of antibiotics including major classes of antibiotics such as β-lactams, tetracyclines, aminoglycosides, rifamycins, macrolides and glycopeptides. A common, and probably correct, view among scientists working in the field of natural products is that chemical diversity follows biological diversity. Access to a database of known antibiotics (~3000), their producing strains and their targets would put this view into perspective. The relationship between biological and chemical novelty will be revealed by placing antibiotics on a taxonomically related tree of producers. [99]

Natural antibiotic products from Actinomycetes, together with their biosynthetic pathways, have been the subject of extensive study for many decades. In comparison, Gram-negative bacteria have received relatively little attention.[103] In recent years, however, they have become increasingly recognised as a rich and underexplored source of novel antimicrobial compounds with therapeutic potential. *Pseudomonas* species appear to be the most prolific producers of such metabolites, together with marine and terrestrial myxobacteria and cyanobacteria. Apart from these well-known producer organisms, Gram-negative bacteria from other diverse phylogenetic classes have also contributed to antimicrobial metabolite discovery. Teixobactin **40** [104] and Gladiolin **41** [105] are examples of the antibacterial compounds isolated from Gram-negative bacteria (Figure 3.6).[103]

Teixobactin **(40)**

Gladiolin **(41)**
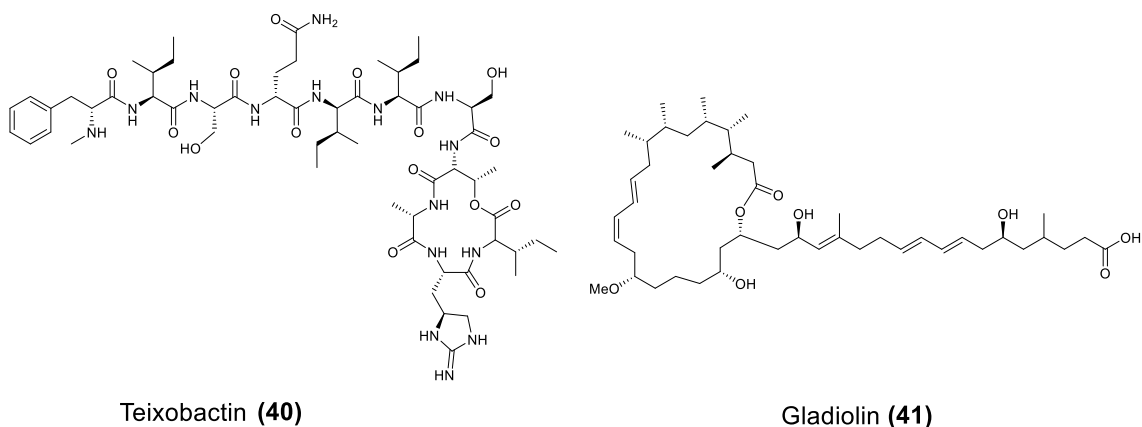
Figure 3.5. Antibacterial compounds isolated from Gram-negative bacteria.[104,105]

A plethora of secondary metabolites have been isolated from sponges and corals; interestingly, it appears that most of these compounds are actually synthesised by bacteria that are colonising these organisms. However, toxicity has been a problem for secondary metabolites derived from the sea, which has so far precluded their development as antibiotics.[96] Another potential source is human microbiota; the human microbiota is a dynamic collection of microbes that have existed within and on us, throughout our evolutionary history.[106] Microbes have been detected on most body sites, even those sites long-thought to be sterile, such as the brain, liver, pancreas, amniotic fluids, adipose tissues, and placenta. For example, lactic acid producing bacteria *L. reuteri* residing in the intestines produces a tetramic acid derivative, named reutericyclin **42** (Figure 3.6**)**, with activity against *S. aureus*, *Bacillus subtilis*, *B. cereus*, *Listeria innocua*, *Enterococcus faecalis*, and some other Lactobacilli.[106]

3.5.4 Silent Gene Clusters

Genome sequencing of actinomycetes reveals that each strain can produce 20–40 secondary metabolites, many of which have not yet been characterised and that may have some antibiotic activity. Most of these are not readily produced under standard laboratory conditions. Efforts to awaken these so-called 'cryptic' or 'silent' biosynthetic gene clusters have been pursued including altering the growth conditions, the overexpression of genetic regulators, the addition of chemical elicitors, and the capture of biosynthetic gene clusters for expression in heterologous hosts.

In one exemplary study, researchers from University of Warwick reported characterisation of a novel microbial natural product sceleric acid **43** (Figure 3.6) resulting from the rational derepression of a silent gene cluster.[107] A conserved set of five regulatory genes was used as a query to search genomic databases and identify

atypical biosynthetic gene clusters (BGCs). A 20-kb BGC from the genetically intractable *Streptomyces sclerotialus* bacterial strain was captured using yeast based homologous recombination and introduced into validated heterologous hosts. Scleric acid was shown to exhibit moderate inhibitory activity against *Mycobacterium tuberculosis*, as well as inhibition of the cancer-associated metabolic enzyme nicotinamide N-methyltransferase (NNMT).[107]

Reutericyclin **(42)**   Sceleric acid **(43)**
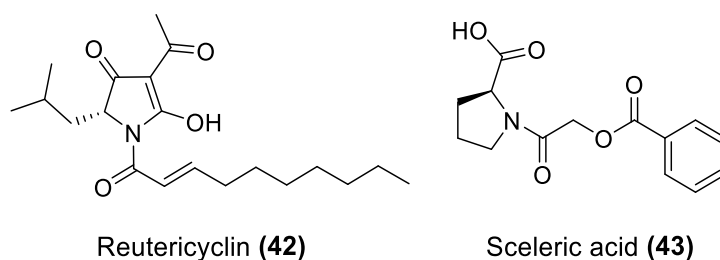
Figure 3.6. Antibacterial compounds isolated from human microbiota and silent gene clusters.[106,107]

3.6 Conclusion

Antibiotics are ranked amongst the most important classes of drugs by virtue of direct as well as indirect influence. Many modern day medical procedures would be ineffective in absence of useful antibiotics.[99] Natural product discovery holds a significant position in the history of antibiotic drug discovery. This is evidenced by Fleming's ground-breaking discovery of penicillin coupled with Waksman's platform that ushered us into the golden era where human health and life expectancy saw new horizons. Unfortunately overuse of antibiotics and absence of fruitful platforms for antibiotic discovery has brought us into discovery void of 30 years; no novel drug class effective against the problematic ESKAPE pathogens has emerged to reach the clinic.

Considering the severity of the situation a multi-faceted approach is required for discovery of novel antibiotic compounds and rescuing of old antibiotic compounds. The use of combination therapy and adjuvants can extend usefulness of current antibiotics. For efficient discovery and development of novel antibiotics, reliable discovery platforms are required. Some of the examples of such platforms in the literature are prodrugs, species-specific antibiotics, silent operons, revisiting old antibiotics and investigating previously unexploited genera for novel sources. Linezolid, daptomycin, retapamulin, fidaxomicin, teixobactin, gladiolin, reutericyclin and sceleric acid are some of the examples of antibacterial compounds that came through these platforms.

3.7 Aims of the Projects

Due to increasing prevalence of infections caused by multidrug-resistant bacteria and scarcity of novel antibiotics in development, this research aimed to identify potential candidates for use in the treatment of resistant bacterial infections. In two influential review papers on antibiotic drug discovery, Kim Lewis and Gerald Wright made recommendations for new discovery platforms:[99,102] revisiting previously discarded antibiotics, use of pro-drugs/adjuvants and combination therapy, triggering silent operons and investigation of previously uncultured bacterial species for production of species-specific antibiotics.[99,102]

These antimicrobial discovery projects were joint projects between the microbiology department (PhD students Dr Nada Nass, Zeyad alZeyadi and Luiza Galarion supervised by Alex O'Neill) and the chemistry department (Sannia Farooque supervised by Prof Chris Rayner) based at the University of Leeds; the work of other PhD students has been acknowledged in the relevant sections. Although the preliminary work on recovering antimicrobial activity from crude extracts was done by the microbiologists, they were unable to devise appropriate extraction systems and identify, isolate and characterise and if necessary, synthesise the active species.

The author initially analysed these extracts by mass spectrometry, UV/Vis and NMR spectroscopy to gain basic understanding of the nature of the extracts. Thereafter, a sequential solvent-solvent extraction system, in order of increasing polarity (diethyl ether, isopropylacetate, ethyl acetate and chloroform) was devised for the selective uptake of active species from cell cultures (broth or agar) leading to an increase in overall yield and the relative amount of targeted active species in the crude extracts; in some cases an additional acid-base work-up was done (discussed wherever necessary). The extracts were analysed at every stage of the process using ^{1}H NMR and UV/Vis spectroscopy to establish dynamic understanding of the extraction process. The ratio of the organic solvents to aqueous (cell cultures in broth or agar) had to be adjusted according to the nature of the compounds in each extract and project. This sequential solvent extraction system has been proven to be very useful for all natural product projects based in O'Neill lab; some of these projects have been discussed here.

In the first part of the project drawing inspiration from success of daptomycin, linezolid and fidaxomicin, a previously discarded class of antibacterial agents called the actinorhodins (ACTs) was revisited using whole-cell screening approach and *S. aureus* SH100 for specific Gram-positive activity. This class of compounds was originally discovered in 1940s however it was not pursued as an antibiotic drug candidate probably owing to its narrow spectrum activity. Only limited information exists regarding the

antibacterial properties of ACTs. Weak antibacterial activity has been reported against some Gram-positive bacteria, with an estimated MIC against *S. aureus* of 25–30 µg/ml.[100] To establish antibacterial profile of this class and to avoid the potential confounding associated with studying a mixture of ACTs, it was important to work with a single, defined species of ACTs.

Natural product analogues can vary considerably in respect of their antibacterial properties. Furthermore, mixtures can vary from batch to batch and their antibacterial property cannot be accurately evaluated. While HPLC chromatography is an excellent technique, it is not useful for generating large quantities of materials. A reliable method of extraction and purification of ACTs was developed; the method was economic, scalable and generated sufficient material for chemical and biological evaluation. A single species of actinorhodin, γ-actinorhodin, was identified and fully characterised using mass spectrometry, UV/Vis, NMR and IR spectroscopy. Lastly, γ-actinorhodin was evaluated for its antibacterial properties both *in vitro* and *in vivo* to establish its profile as a potential antibiotic drug (Dr Nada Nass).

The second part of the project had two aspects to it: (1) skin microbiota was probed for their potential to produce antibacterial compounds, (2) extracts were tested against specific pathogen strains (against Gram-positive *S. aureus* SH1000 by Zeyad alZeyadi and Gram-negative multi-drug-resistant *E. coli* CM400 by Luiza Galarion) to ensure species-specific activity using whole-cell screening approach. Chemical diversity follows biological diversity; this is a common and probably correct view among scientists working in the field of natural products.[96] Decades of research on human microbiota have revealed much of their taxonomic diversity and established their direct link in health and disease.[106] However, the breadth of bioactive natural products produced by these microbes remain unknown. Of particular interest are the antibiotics produced by our microbiota to ward off invasive pathogens. Herein, the potential of the human skin microbiota and microbiome as sources of antibiotics was probed.

Two approaches were employed in selection of antibacterial-producing strains from human microbiome. Firstly, the samples were collected from different parts of the body and tested against *S. aureus* SH1000 and multi-drug resistant *E. coli* CMR400 in parallel studies. The hit strains were then taken forward and cultured followed by extraction with organic solvents. Secondly, a collection of actinobacteria (long-standing source of antibiotics) were built from the collected samples; thereafter UV mutagenesis were employed to trigger expression of biosynthetic gene clusters (BGCs) for the production of antibacterial compounds (Dr Asma Akhter and Luiza Galarion); only hit strains were taken forward to the next step. The whole process of extraction and purification of a

natural product extract is a multi-step, laborious and resource-intensive task often with little to no returns. Therefore, a robust system for initial screen of the crude extracts was developed to ensure only promising extracts were taken to the next stage of purification and development. The successful extracts were then purified, and the active compounds were fully characterised.

Chapter 4 Reviving Old Antibiotics: the Case of γ-Actinorhodin

4.1 Introduction to Actinorhodins (ACT) Project

Of the ~28000 natural product antibiotics that were discovered in the 20th century, only a handful are in clinical use.[99] The rest of them were not thought to be useful as drugs due to unmanageable issues such as efficacy, stability and lack of broad-spectrum activity.[99] It is likely, that among these discarded compounds, there are antibiotic drug candidates that need systematic re-evaluation.[100] The availability of preliminary data on antibacterial activity of previously discarded antibacterial compounds can potentially overcome pitfalls associated with early stages of drug discovery. There are several examples of clinically-useful antibiotics that were dismissed as drug candidates following their discovery, but which were later successfully developed for therapeutic use (daptomycin, fidaxomicin, pleuromutilins).[108]

The actinorhodins (ACTs), a class that was first reported 70 years ago, but which remains poorly characterised has been investigated in this study. Actinorhodin **44** (ACT), a dimeric benzoisochromanequinone antibiotic produced by *Streptomyces coelicolor* A3(2), was first reported in the late 1940's.[109,110] It was later shown that *S. coelicolor* produces a series of closely-related compounds in addition to actinorhodin itself.[111,112] Most studies on this compound appear to have employed mixtures of ACTs, since the methods routinely used to purify and characterise actinorhodin are insufficient to resolve it from its closely-related analogues. ACTs are strongly pigmented and are pH sensitive; they undergo a reversible colour change from blue under alkaline conditions to red in acidic environment.

The structure of actinorhodin **44** was deduced from the fragments obtained during chemical degradation studies and mass spectrometry.[111,112] Other congeners γ-actinorhodin **46**, ε-actinorhodin **47**, actinorhodinic acid **48**, phenocyclinone **49**, α-actinorhodin **50** and β-actinorhodin **51** (Figure 4.1) were also isolated from the same strain.[112,113] The symmetrical nature of the two halves of actinorhodin was confirmed by obtaining NMR data on the esterified actinorhodin. Actinorhodin dimethyl ester tetraacetate and actinorhodin diethyl ester were isolated from *S. coelicolor* A3(2).[113,114],[115] The general protocol in all these studies constituted of an alkaline extraction of the cell cultures followed by acid-catalysed ester formation.
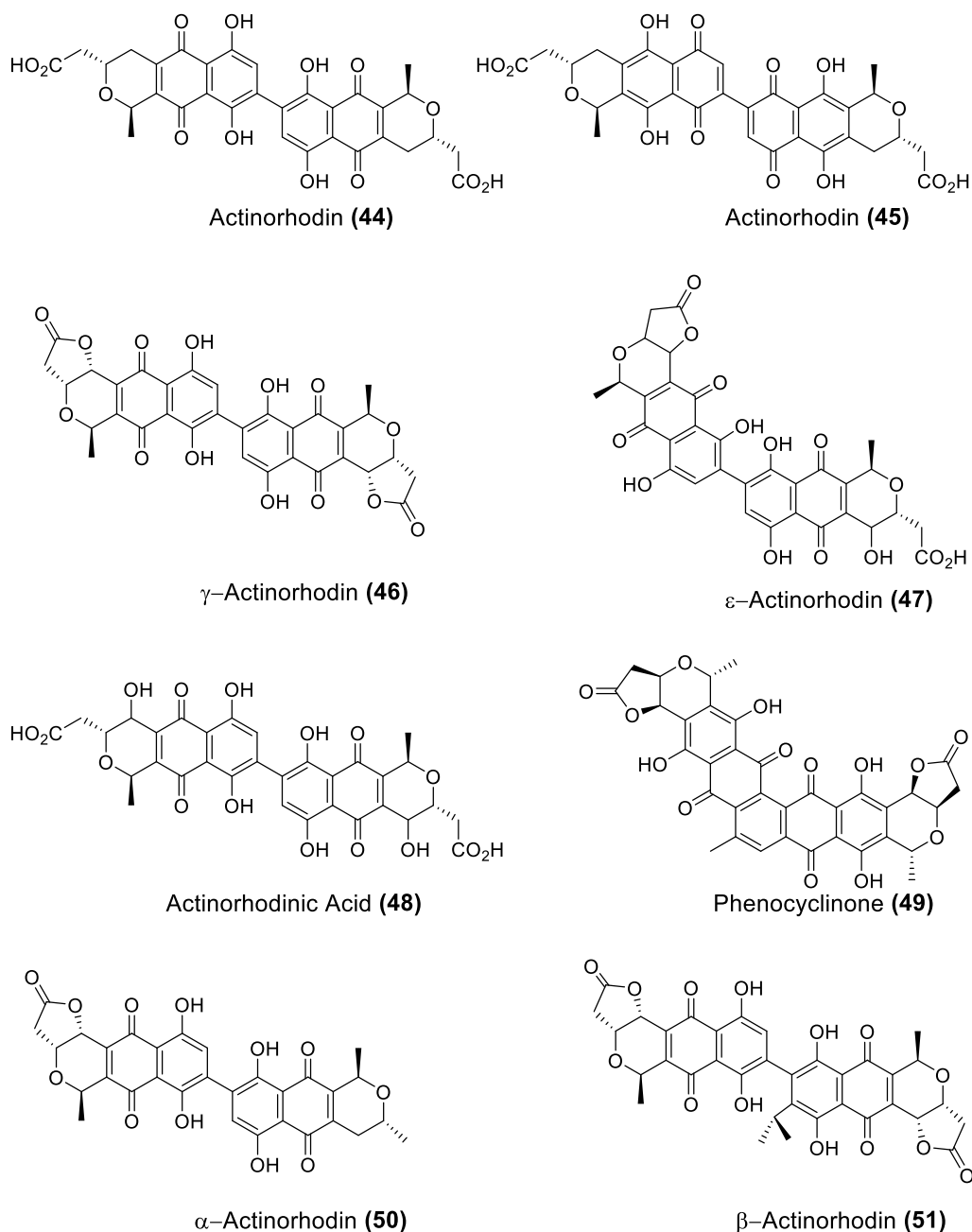
Figure 4.1. Actinorhodin and structurally related pigments produced by various *S. coelicolor* strains.[116]

Only limited information exists regarding the antibacterial properties of ACTs. Weak antibacterial activity has been reported against some Gram-positive bacteria, with an estimated MIC against *S. aureus* of 25–30 µg/ ml.[114] However, the experiments from which these results derive, involving measuring zones of inhibition around transplanted plugs of agar on which *S. coelicolor* had been grown, mean that these values must be considered approximate at best. There is also no clear understanding of the antibacterial mode of action of ACTs, although more than one hypothesis has been put forward. Naturally-occurring quinones, such as ACT, can function as bioreductive DNA-alkylating

agents, a property that could potentially explain ACT's antibacterial action.[117,118] Alternatively, a recent study proposed that ACT exerts its antibacterial effect by catalysing the production of toxic levels of hydrogen peroxide.[119]

In this work actinorhodins (ACTs) were revisited to explore their potential to form a basis for a new antibacterial class. For this purpose, a single compound from ACTs family was identified and isolated in its native form and not the esterified forms as published in the literature previously.[110] The bioactive extracellular form of actinorhodin, γ-actinorhodin, was initially identified, purified and fully characterised. A scalable and economic method for purification of γ-actinorhodin was then developed to generate sufficient material for full biological and chemical evaluation. The spectrum of bioactivity for the pure compound was assessed, with a particular emphasis on its antistaphylococcal activity against a number of clinical isolates; killing kinetics were also determined, and the mechanism of its antibacterial activity and any detrimental effects of the compound on eukaryotic cells were investigated (Dr Nada Nass).

Finally, to assess the potential for the compound to be used clinically, the rate of resistance development was also explored. To determine the bacterial specificity of γ-actinorhodin using *C. albicans* as a model eukaryote, followed by evaluating the activity against human cell line and *in vivo* infection model. These studies revealed that the ACT pharmacophore in fact displays potent antistaphylococcal activity and possesses many of the requisite properties of a useful antibacterial drug. This work has been published[100] and key biological results will be discussed here briefly, however for detailed methodology and biological evaluation results the reader may refer to Dr Nass's thesis.[108]

4.2 Extraction of γ-Actinorhodin 46

To explore the biological properties of ACTs family of antibiotics, it was important to isolate and purify a single active species of actinorhodin in its native form. *S. coelicolor* L646 strain was chosen for this work as this strain contains an integrated plasmid that overexpresses wild-type atrA, leading to hyperproduction of actinorhodins relative to the wild-type strain (M145).[108] In initial studies a range of media (YM broth, ISP2 agar, and R5 broth/agar) were screened to identify optimal conditions for growth of *S. coelicolor* L646 and the production of the blue pigments (Dr Nada Nass). ISP2 agar was found to best support the growth of *S. coelicolor* L646 and the production of diffusible blue pigments and was therefore used in subsequent studies.

Initially the blue pigment was extracted from agar using acidified water (pH 3) aiming to isolate actinorhodin **44** in its native form. The aqueous extract was neutralised before

extracting it with ethyl acetate and dried in *vacuo*. The dried extract was tested for antibacterial activity against *S. aureus* and analysed using LC-MS and ^{1}H NMR. Actinorhodins could not be detected in these spectra and no bacterial activity was recovered against *S. aureus* SH1000. In an effort to replicate the work done by Wright and Hopwood [114] the agar was extracted with acetone and the blue extract was dried in *vacuo*. The dried extract showed weak antibacterial activity against *S. aureus* SH1000; ^{1}H NMR spectrum of the crude extract was complex and did not show characteristic peaks for actinorhodin **44**. However, low intensity peaks for γ-actinorhodin **46** alongside unknown compounds were identified. The mass spectrum for crude extract also did not show peaks for actinorhodin **44** or γ-actinorhodin **46**.

Figure 4.2. *Streptomyces coelicolor* L646 colonies on ISP2 agar medium. After 4–6 days at 30 °C, dark blue diffusing pigment developed around the colonies and blue droplets appeared on the colony surface (Dr Nada Nass).

Preparative-TLC purification was attempted to obtain pure sample of γ-actinorhodin **46** from crude extract; ethyl acetate/hexane (4:1, 1:1, 1:4), dichloromethane/methanol (98:2, 95:5, 90:10) and chloroform/methanol (98:2, 95:5, 90:10) were screened for elution of the extract. Dichloromethane/methanol (9:1) enabled best chromatographic separation of the polar and relatively non-polar components of the extract. The crude extract (50 mg) was loaded onto the plates and eluted with DCM/MeOH (9:1). A purple band closest to the solvent front (R_f 0.29) was scraped off and extracted with $CHCl_3$/MeOH (9:1). The dried fraction (0.5 mg, 1% yield) was analysed by ^{1}H, ^{1}H-H COSY spectroscopy and mass spectrometry, and tentatively assigned as γ-actinorhodin **46**. γ-actinorhodin showed good activity against *S. aureus* SH1000, with MIC of 1 μg/ml. However, poor yield of γ-actinorhodin **46** necessitated targeted extraction of γ-actinorhodin to generate enough material for chemical and biological evaluation.

The chromatographic profile of the crude extract showed that γ-actinorhodin **46** was significantly less polar than rest of the unknown compounds in the extract. It was expected that extracting the blue pigment directly from the agar using an organic solvent of moderate polarity would recover γ-actinorhodin **46**, while more polar contaminants would remain associated with agar. Buffer (pH 3), DCM, DCM/MeOH (9:1), EtOAc and chloroform were screened for their efficiency as extraction solvents in small scale extraction experiments. Actinorhodins are intensely coloured and absorb at 530 nm. The organic extracts were monitored using UV/Vis spectroscopy at 530 nm (Table 4.1).

Table 4.1. The absorbance values for all the solvents screened for extraction of γ-actinorhodin **46** from *Streptomyces coelicolor* L646 colonies on ISP2 agar medium.

Solvent	Absorbance
Buffer (pH 3)	0.081
DCM	0.113
DCM/MeOH	0.561
EtOAc	0.379
Chloroform	0.171

Buffer pH 3 was the least ideal solvent with absorbance value of only 0.081 suggesting actinorhodins with acid group side chains, such as actinorhodin **44**, ε-actinorhodin **47** and actinorhodinic acid **48**, were either absent or present in traces. Dichloromethane (0.113) and chloroform (0.171) extracts showed higher absorbance than water and extracted competing amount of the blue pigment, whereas ethyl acetate looked promising with absorbance value of 0.379. DCM/MeOH (9:1) extract had highest absorbance of 0.561, however it showed less selectivity between polar (coloured non-actinorhodin compounds) and non-polar components of the extract (evidenced by ^{1}H NMR) which would make purification process lengthy.

Although DCM/MeOH mix showed highest absorbance, ethyl acetate was chosen due to its selective extraction of γ-actinorhodin **46** compared to other solvent systems. Based on previously attained chromatographic data ethyl acetate was expected to be more selective at extracting γ-actinorhodin **46** over polar components of the extract. Indeed ^{1}H NMR analysis of the ethyl acetate extract showed marked improvement in extraction of γ-actinorhodin when compared with acetone extract; the spectrum was far less complex

and the characteristic peaks for this compound could be clearly identified (Figure 4.3). The ethyl acetate extraction was scaled up to generate enough material for biological evaluation. Ethyl acetate was not only more selective than acetone but also afforded improved yield of γ-actinorhodin **46** from 1% to 20% *wt./wt.*

The method of extraction was also found to be crucial in determining the final yield of **46**. The agar was manually fragmented in all experiments; when it was extracted with ethyl acetate by giving it a quick shake (standard method), the yield was poor (5% *wt./wt.*). Two methods were tested next: (1) the fragmented agar was left shaking with ethyl acetate overnight (18 h) at 23 ºC; (2) the fragmented agar was shaken twice with ethyl acetate at 30 ºC for 1 hour each. Both methods gave competing yields for **46**, 20% and 21% *wt./wt.* for higher temperature and overnight extractions (18 h) respectively. Furthermore, the selective uptake of **46** compared to highly polar components of the extract was consistent in both methods. The overnight method (18 h) did not lead to extraction of higher amount of unwanted compounds as originally anticipated. Furthermore, the extraction at 30 ºC did not affect stability of **46**. These results suggest that kinetics play important role in extraction of natural products embedded in the biological matrices. The extraction of **46** with ethyl acetate reached equilibrium after 18 h giving 21% *wt./wt.* yield; therefore, longer extraction time can result in higher yield when designing natural product extractions. Temperature also plays a key role; the extraction time was reduced from 18 h to 2 h when fragmented agar was extracted with ethyl acetate at 30 ºC as compared with 23 ºC.

In conclusion, extraction of natural products with organic solvents requires careful planning; when the nature of organic solvent is compatible with the compound of desire and the method of extraction is compatible, it can result in selective extraction of the compound which would reduce the purification steps significantly. This is important for environmental considerations as multi-rounds of purification often generate large amount of waste organic solvents. Moreover, it may also ensure stability of the desired compound by minimising exposure to sunlight, acid/base systems (in chromatographic solvents), temperature and excessive organic solvents during multi-rounds of purification. Furthermore, the yields can be improved significantly by monitoring the kinetics of the extraction process. A small-scale extraction screen with solvents of varying polarity monitored by an analytical method (UV/Vis or HPLC) is recommended for future work.
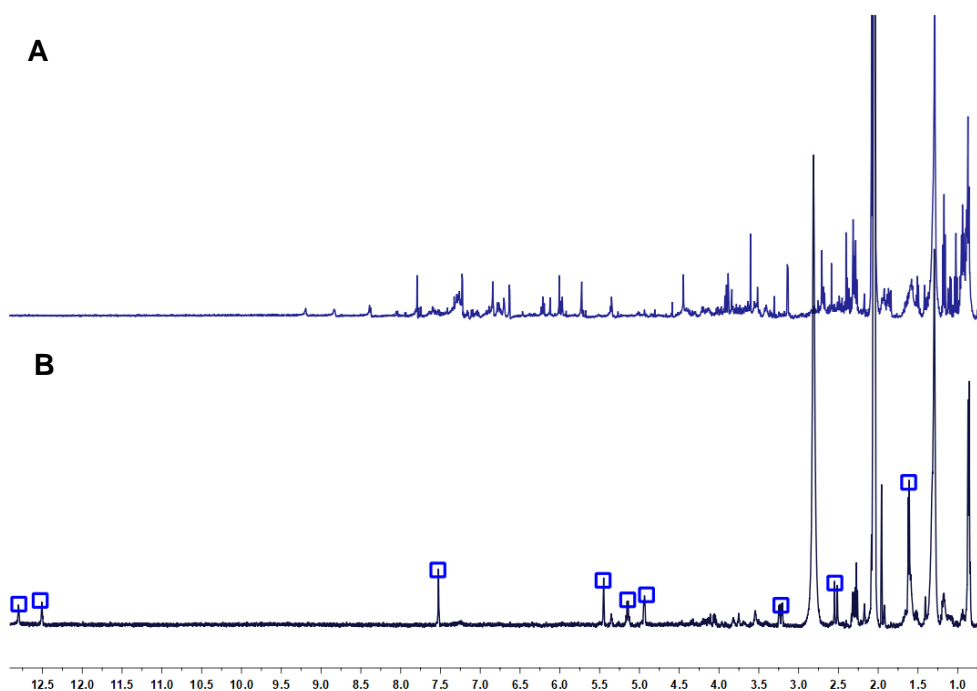
Figure 4.3. The stacked ¹H NMR spectra for crude extracts prepared from *Streptomyces coelicolor* L646 colonies on ISP2 agar medium using acetone and ethyl acetate: (A) Acetone extract; (B) ethyl acetate extract. The characteristic peaks for γ-actinorhodin **46** have been highlighted.

4.3 Purification of γ-Actinorhodin 46

After small scale purification of γ-actinorhodin on normal preparative-TLC plates, it was logical to attempt larger scale (500 mg extract) purification using flash chromatography. The crude extract was loaded onto normal-phase silica column and eluted with 5–20% MeOH in dichloromethane. Despite the higher content of methanol in eluting solvent, the bulk of the extract stayed adsorbed on silica and only 5 mg γ-actinorhodin was recovered. It is postulated that slightly acidic nature of silica degraded γ-actinorhodin which did not elute even with 20% methanol. In another attempt to purify γ-actinorhodin **46** using mass-directed reverse phase HPLC (50–95% acetonitrile) in absence of acid, merely 6 mg of product was isolated. Peak broadening is a common issue in HPLC chromatography in absence of acid as an additive which leads to poor separation and isolation of compounds. Furthermore **46** did not ionise very well which was indicated by low intensity *m/z* peak at 629.0929 in the mass spectrum.

It has been postulated that polyketide lactones are unstable at a high pH, degrading to a so-called acid form. Bystrykh *et al.* treated cell cultures (strain M145, cell cultures at neutral pH) with 1 M KOH and reported complete degradation of γ-actinorhodin **46**,

73

mainly to a single compound tentatively identified as actinorhodinic acid **48**.[110] The team used TLC chromatography to tentatively assign the degraded product as actinorhodinic acid **48** on the basis that its mobility on TLC plate was lower than that of actinorhodin **44** or γ-actinorhodin **46** when eluted with benzene/acetic acid (9:1); it remained almost at the origin.[110] However, the degraded product was not isolated and characterised, and no data was provided to support this hypothesis.

Building on this premise, the lactone moiety in γ-actinorhodin **46** was targeted; it was expected that at high pH (>10), **46** would ring-open to afford hydroxycarboxylate (the salt of actinorhodinic acid), which would have high water solubility. A small-scale purification was performed first, the red crude ethyl acetate extract was washed with aqueous sodium carbonate (pH 10.9) which resulted in a blue aqueous solution and a red ethyl acetate organic layer. The aqueous layer was then acidified with hydrochloric acid (6 M) to reform the lactone; a red precipitate was formed which was isolated by filtration. ^{1}H NMR analysis of this red precipitate showed major peaks for **46** and minor peaks in the aliphatic region (Figure 4.4C).
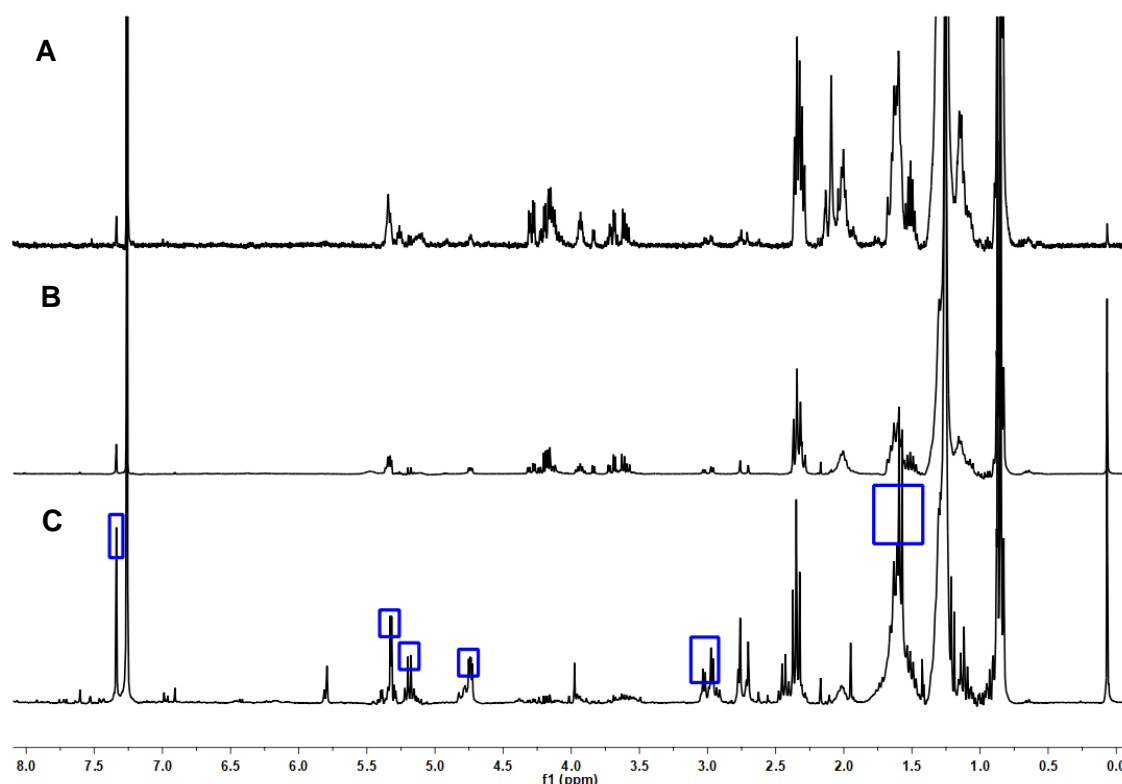
Figure 4.4. The stacked ^{1}H NMR spectra for acid/base semi-purification of γ-actinorhodin **46**: (A) crude ethyl acetate extract; (B) ethyl acetate organic layer after alkaline wash; (C) red precipitate isolated from the aqueous layer by acidification. The characteristic peaks for **46** have been highlighted.

The remaining ethyl acetate layer was dried in *vacuo* to give organic-layer extract and analysed by NMR spectroscopy; although this was red in colour similar to the actinorhodin family, the ^{1}H NMR spectrum showed major peaks in the aliphatic region (similar to minor peaks found in aliphatic region for the red precipitate isolated from the aqueous layer) and minor peaks at 3.5–4.5 ppm (Figure 4.4B). The red precipitate and organic-layer extract were tested against *S. aureus* SH1000 at 1 mg/ml and the red precipitate was found active; no activity was recovered for the organic-layer extract suggesting successful isolation of the active compound from the original ethyl acetate extract. During sample preparation for NMR analysis it was observed that the red precipitate, isolated from aqueous layer, was soluble in $CDCl_3$ and insoluble in MeOD, whereas the remaining organic-layer extract was highly soluble in MeOD. Therefore, pure γ-actinorhodin **46** was recrystallised from the red precipitate using DCM/MeOH in 19% *wt./wt.* overall yield; whereby dichloromethane was used as a good solvent and methanol as a bad solvent. The identity and purity (>95%) of γ-actinorhodin **46** were assessed using mass spectrometry, 1-D NMR, 2-D NMR and infrared spectroscopy and analytical HPLC (Appendix B).

4.4   Characterisation of γ-Actinorhodin 46

The structure of actinorhodin was originally assigned by extensive chemical degradation studies and mass spectrometry in 1950.[110] The substitution pattern of hydroxyl groups has been a subject of discussion in the literature. Brockmann and his co-workers initially proposed the structure of actinorhodin to be **45** (Figure 4.1) where ring **B** was dihydroxy-substituted. Two years later the team analysed esterified actinorhodin and model compounds to come to the conclusion that the hydroxyl substitution in fact occurred on ring **C** (structure **44** in Figure 4.1). However, Zeeck from the same group published NMR studies on a variety of actinorhodin congeners in 1987 and again referred to the structure of actinorhodin as **45** instead of **44**. Current work is in agreement with their proposed structure published in 1968; ring **C** rather than **B** is di-substituted with hydroxyl groups in actinorhodin and its congeners; γ-actinorhodin exists as **46** in its native form and not the redox isomer **52** (Figure 4.5).

Due to complexity of the structure of γ-actinorhodin **46**, 1-D and 2-D NMR spectroscopy were employed to decipher the structure. The protons were assigned based on their multiplicity, coupling constants and correlations observed in ^{1}H–^{1}H COSY spectrum. The peaks at 12.80 and 12.50 ppm were assigned to *para*-hydroxyl groups on ring C (Table 4.2). The coupling constants for the quartet and doublet at 5.19 and 1.59 ppm

respectively were 7.0 Hz, making their allocation to H-1 and the methyl group unequivocal. This was also confirmed by NOESY experiment (5% enhancement, Table 4.2). The doublet and doublet of doublet at 2.99 and 2.73 ppm coupled to each other with magnitude of 17.8 Hz which is characteristic of a geminal coupling (H-11).
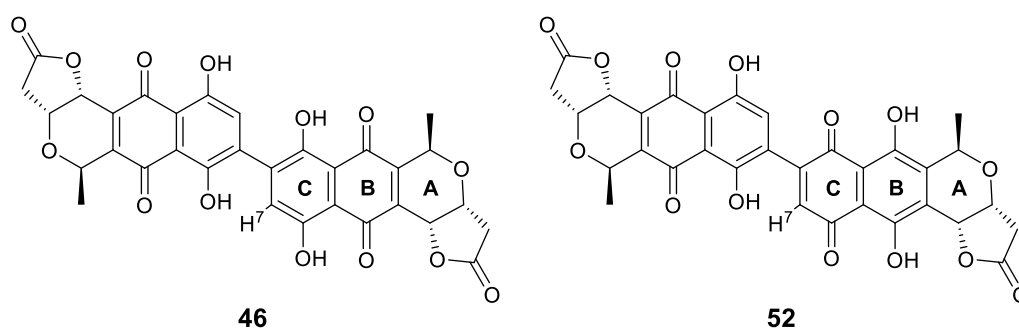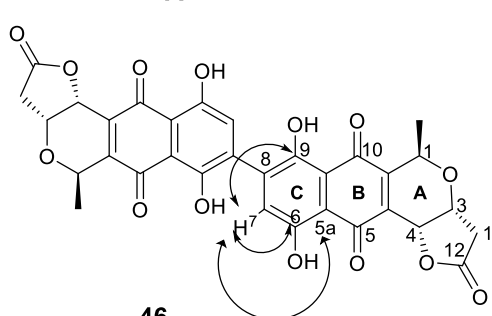
Figure 4.5. The isomers of γ-actinorhodin **46**. Refer to Table 4.2 for numbering.

In total seventeen signals were observed in ^{13}C spectrum for **46** which were assigned with the aid of HSQC, HMBC and NOESY experiments. The heteronuclear correlations found in HMBC experiment have been summarised in Table 4.2. The coupling of H-7 with C-6 and C-9 in HMBC experiment confirmed substitution of hydroxyl groups on ring **C** (Table 4.2, Figure 4.6) rather than ring **B**. There were no correlations found between H-7 and signals at 177.9 and 177.6 ppm (characteristic peaks for carbonyl carbon atoms) suggesting that they were not connected. This was further confirmed by nOe correlation between H-7 and OH-6 (Table 4.2). The signals at 148.9 and 133.4 ppm were assigned to carbon atoms on position 10a and 4a respectively due to their coupling to H-1. The assignment of the carbonyl-characteristic chemical shifts at 176.9, 176.6 and 174.1 ppm was deduced from their coupling to OH-9, OH-6 and H-11 respectively. X-ray crystallography is another powerful technique in characterisation of unknown compounds, unfortunately several attempts at crystallising γ-actinorhodin **46** from a combination of solvents were unsuccessful.
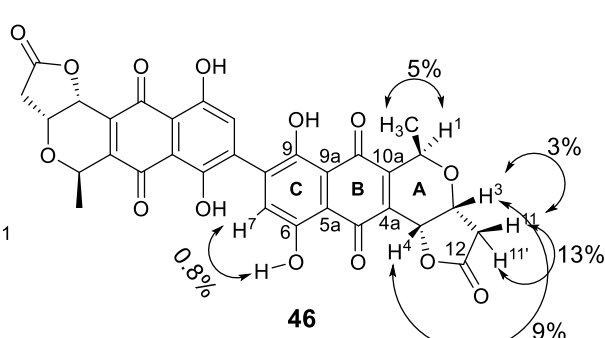
Table 4.2. [1]H–[13]C correlations found in the long range (HMBC) heteronuclear correlation experiment for γ-actinorhodin **46**: (A) The correlations found between H-7 and the carbon atoms in HMBC experiment; (B) nOe correlations found in the NOESY experiment.

A	B

Proton	[13]C correlations
OH-9	C-5,
OH-6	C-10
H-7	C-6, 8, 9, 5a
H-4	C-3, 4a
H-1	C-3, 4a, 10a & methyl
H-3	C-4, 12
H-11	C3, 4
Methyl	C-1, 10a
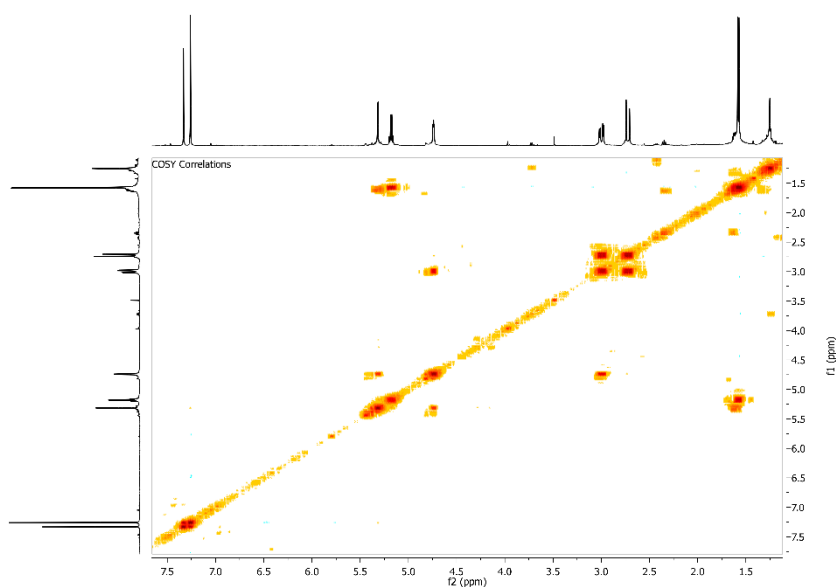
Figure 4.6. ^{1}H-^{1}H COSY correlations for γ-actinorhodin **46**.

4.5 Antibacterial Activity of γ-Actinorhodin 46

MICs were determined for γ-actinorhodin against clinically important Gram-positive and Gram-negative bacteria using standard CLSI broth microdilution methods by our collaborators (Dr Nada Nass). γ-actinorhodin **46** exhibited potent antibacterial activity against Gram-positive pathogens giving MIC values of 1-2 µg/ml (Table 4.3). However, it lacked clinically useful antibacterial activity against Gram-negative pathogens, with MICs of >256 µg/ml against representative *Enterobacteriaceae* and non-fermentative *Bacilli* (Table 4.3).

The antistaphylococcal activity of **46** was further investigated against a panel of clinical *S. aureus* isolates (70 isolates) including methicillin resistant *S. aureus* (MRSA) and vancomycin intermediate *S. aureus* (VISA) strains (Figure 4.7). The MIC_{90} and MICs for **46** were 2 µg/ml and 1–4 µg/ml respectively. Therefore γ-actinorhodin **46** possess potent antibacterial activity against two of the ESKAPE pathogens (*S. aureus* and *E. faecium*), with MIC values against members of these species, falling within the comparable range for systemically administrated antibacterial drugs in current clinical use. The MIC values for the clinically useful antibiotics, rifampicin, and fusidic acid for systemic use is often <1 µg/ml against *S. aureus*, whereas vancomycin and linezolid, often last resort antibiotics, display higher MIC values (e.g. values of 4 µg/ml) against susceptible *S. aureus* strains.[108]

Table 4.3. MICs of γ-actinorhodin **46** against a panel of Gram-positive and Gram-negative bacteria (courtesy of Dr Nada Nass).

Bacterial strains	MIC (µg/ml)
S. aureus SH100	1
S. epidermidis ATCC 14490	1
S. haemolyticus 41207	1
S. pyogenes ATCC 19615	1
S. pneumoniae ATCC R6	1
E. faecalis ATCC 29212	2
E. faecium 7634337	1
E. coli BW25113	>256
K. pneumoniae K25	>256
A. baumannii ATCC 19606	>256
P. aeruginosa PO1	>256

The antistaphylococcal activity of γ-actinorhodin **46** shown here is significantly greater than that originally published for actinorhodin **44** in 1976.[114] Hopwood and Wright reported antistaphylococcal MIC of 25-30 µg/ml measured by agar diffusion method; the MIC values were estimated using agar plug diffusion method which involves growing the antibiotic producer strain on a culture medium. Then an agar-plot is cut and placed on the surface of another agar plate and overlaid with the test microorganism. Furthermore, it was noted in the current study that γ-actinorhodin **46** appeared to have significantly reduced activity against *S. aureus* SH1000 (MIC of 16 µg/ml) when incorporated into agar medium. Therefore, the choice of culture media and/or method of testing may have contributed to the significant difference in the MIC values obtained in these studies. However, it is more likely that γ-actinorhodin **46** is a more potent antibacterial agent than actinorhodin **44** itself. Similar patterns have been observed and reported in antibacterial discovery whereby one analogue from a family of compounds exhibits higher bioactivity than the rest. For example, penicillin G **33** exhibited higher potency and broader spectrum of activity than rest of the natural congeners in the group.
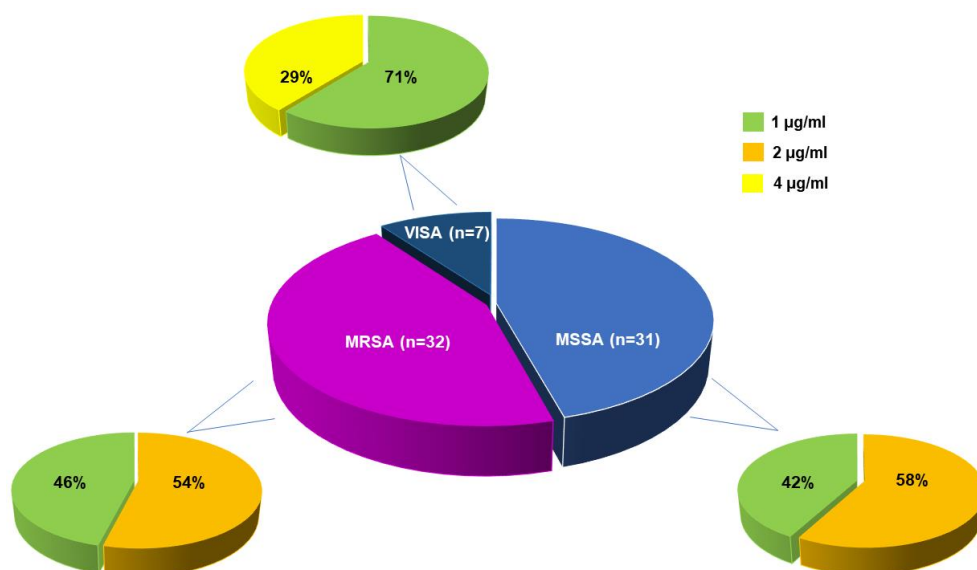
Figure 4.7. Distribution of *S. aureus* clinical isolates and MICs for γ-actinorhodin **46** in MSSA, MRSA, and VISA clinical isolates (n = 70, Dr Nada Nass).

Insusceptibility to antibiotics in Gram-negative bacteria often results from the permeability barrier offered by the outer membrane, or the action of the broad substrate range efflux pumps, such as AcrAB-TolC.[108] It has been demonstrated in O'Neill laboratory previously that most antistaphylococcal agents are active against Gram-

negative bacteria when they can surpass the outer barrier to reach their target.[120] To put this hypothesis to test in this study, γ-actinorhodin **46** susceptibility determinations were conducted against *E. coli* BW25113 in presence of an outer-membrane permeabilising agent (PMBN), and against derivatives of BW25113 deleted for components of the major efflux transporter, AcrAB-TolC. **46** exhibited higher activity against *E.coli* in presence of PMBN (MIC of 16 µg/ml), while no change in the activity against *E.coli* strains lacking AcrAB or TolC (MICs of >256 µg/ml) was found. At sub-inhibitory concentrations, PMBN is known to cause disruption and/or disorganisation of the outer membrane and enhanced antibiotic penetration. These results imply that the limited activity of **46** against Gram-negative bacteria like *E. coli* is, at least in part, a consequence of limited ingress across the outer membrane, and establishes that the target of **46** is present in Gram-negative bacteria.

4.6 Mode of Action and Scope of γ-Actinorhodin 46

In further studies by our collaborators, it was established that γ-actinorhodin **46** is selective against bacterial cell and possesses a mode of action (MOA) distinct from that of other agents in clinical use, an extremely low potential for the development of resistance, and a degree of *in vivo* efficacy in an invertebrate model of infection. For detailed studies and methods, the reader should refer to Dr Nada Nass's thesis and jointly authored paper as this is out of the scope of this work.[108, 100] In summary, to provide a preliminary indication of prokaryotic selectivity, the activity of **46** was evaluated against the eukaryotic microorganism, *Candida albicans*. Disc diffusion experiments revealed that **46** exerts little activity against this organism when compared with that observed against *S. aureus*, and in MIC determinations, no inhibition of *C. albicans* was observed even at the highest concentration tested (256 µg/ml); these results imply that **46** exhibits selectivity of action.

The antibacterial mechanism of **46** involves rapid dissipation of the proton motive force (PMF), prompting comprehensive shutdown of macromolecular biosynthesis, and ultimately, cell death. Several other antibacterial agents in use such as drugs (daptomycin, telavancin), antiseptics (CTAB) or food preservatives (nisin) also possess an MOA that involves disruption of membrane energetics.[121,122 ,123] However, in contrast to **46**, these agents additionally cause gross physical perturbation of the membrane, leading to detectable leakage of intracellular contents. Thus, the action of **46** on the bacterial membrane is apparently distinct from that of other membrane-perturbing agents in use. The antibacterial action of **46** is not restricted exclusively to effects at the

membrane. The dramatic sensitisation to **46** observed in *S. aureus* strains lacking superoxide dismutases, enzymes that constitute the major cellular defence against superoxide, strongly implicates this radical in the MOA of **46**.

Sensitisation to **46** was predominantly associated with loss of SodA, an enzyme that has been linked specifically with protection against internally-generated oxidative stress in *S. aureus*,[124] implying that **46** prompts the generation of endogenous, rather than exogenous, superoxide. It seems probable that these two antibacterial mechanisms observed for **46** (collapse of the PMF and the production of ROS) share a common root cause; both effects could be explained by γ-actinorhodin-mediated interference with correct functioning of the electron transport chain, a process that ordinarily not only acts to generate the PMF, but which also represents the primary source of superoxide in the bacterial cell.[125] Thus, it is speculated that **46** mediates oxidative damage to one or more components of the electron transport chain, which in turn acts both to compromise the bacterium's ability to maintain the PMF and yields a source of free electrons to drive the generation of superoxide.

4.7 Conclusion to Actinorhodins (ACT) Project

In this work the family of compounds called actinorhodins (ACTs) were revisited to explore their potential to form a basis for a new antibacterial class. For this purpose, a single compound from actinorhodin family was identified and isolated in its native form and not the esterified forms as published in the literature originally in 1940s.[109] The bioactive extracellular form of actinorhodin, γ-actinorhodin **46**, was initially identified, purified and fully characterised. Thereafter, a scalable and economic method for extraction and purification of **46** was developed to generate sufficient material for full biological and chemical evaluation. The spectrum of bioactivity for the pure compound was assessed, with a particular emphasis on its antistaphylococcal activity against a number of clinical isolates; killing kinetics were also determined, and the mechanism of its antibacterial activity and any detrimental effects of the compound on eukaryotic cells were investigated

.

Chapter 5 Investigation of Antibacterial Compounds from the Human Microbiota

5.1 Background

The human microbiota is a dynamic collection of microbes that have existed within and on us, throughout our evolutionary history. The human microbial composition is diverse across individuals and can also morph along individual lifetimes. Microbes have been detected in most of our body sites, even those sites long-thought to be sterile, such as brain, liver, pancreas, amniotic fluids, adipose tissues, and placenta.[126,127] The originally inherited microbial community is shaped through environmental acquisition, diet, and biological changes through life.[106] The metabolic products of the microbiota themselves are increasingly realised as mediators of cell–cell communication, xenobiotics, and antibiotics. It is thus interesting to speculate that commensal microbes inhabiting distinct body sites are an unexplored first line of defence against site-specific pathogens. In contrast to the in-depth studies of antibiotics produced from soil microbes, knowledge of the structural and mechanistic diversity of antibiotics within the microbiota is preliminary.

Distinct skin habitats are home to diverse microbial communities including bacteria, fungi, and viruses. Commensal microbes are believed to fight invading pathogens either by direct antibiosis through production of antibiotics or through modulation of the host immune response. Among the most dominant microbial genera in the skin are *Staphylococcus*, *Propionibacterium*, *Brevibacterium*, *Corynebacterium*, *Micrococcus*, *Streptococcus*, and *Acinetobacter*, in addition to a transitionary, low frequency of *Pseudomonas* and *Bacillus*.[128] A bioinformatics–metagenomics study revealed that the abundance of skin microbiota such as *S. pyogenes* and *G. vaginalis* is unique to each individual, much like a fingerprint.[129] *Propionibacterium acnes* and *Staphylococcus epidermidis* are among the most studied skin-inhabiting microbes either as commensal or opportunistic pathogens.[130,131]

S. aureus is a serious skin pathogen; interestingly, skin-associated *S. aureus* encodes for a non-ribosomal peptide synthetase responsible for the production of three non-ribosomal pyrazinone cyclic dipeptides (Figure 5.1) named tyrvalin/aureusimine A (**53**), phevalin/aureusimine B (**54**) and leuvalin (**55**).[132,133] Research has now delineated the impact of these agents on virulence as mediated through inhibition of host cell calpain proteases.[134] Furthermore, the aureusimine locus was shown to be essential for survival of *S. aureus* and death of the human host cell.[106] In another interesting study, analysis

of biosynthetic gene clusters in *Rhodococcus erythropolis* and *Rhodococcus equi* revealed that these species possess the genetic code required for the biosynthesis of humimycins (**56–57**), linear peptides with a broad antimicrobial spectrum, including against methicillin-resistant *S. aureus*. Humimycins were synthesised based on the primary sequence of gene clusters from *Rhodococcus*.[135] Considering the reports of novel antibiotics recently discovered, the skin microbiota and microbiome is a good source for discovery of antibacterial compounds.

Aureusimine A (**53**)   Aureusimine B (**54**)   Leuvalin (**55**)

R^1 = L-Phe, R^2 = L-Phe Humimycin A (**56**)
R^1 = L-Tyr, R^2 = L-Ile   Humimycin B (**57**)
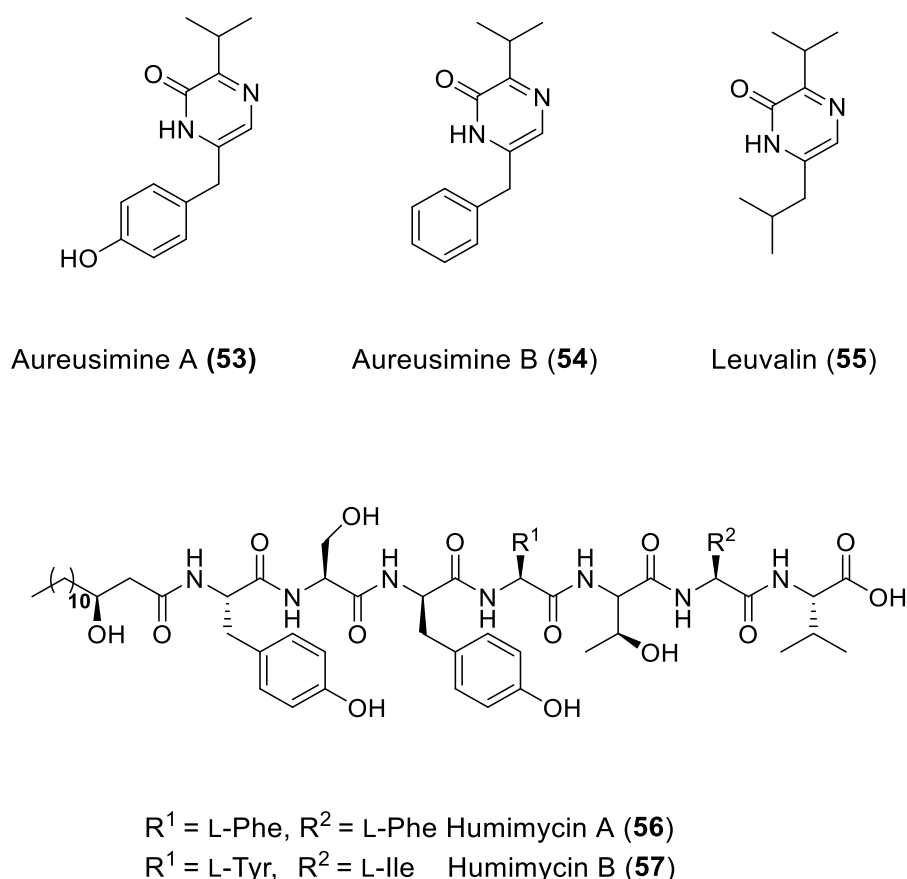
Figure 5.1. The secondary metabolites found in skin microbiome.[132,135]

5.2 Selection of Bacterial Strains

This part of the project was done by PhD students Luiza Galarion and Zeyad AlZeyadi in O'Neill group and is being included here for the sake of complete overview of the project. The project was approved by Faculty of Biological Sciences Research Ethics Committee of University of Leeds (Reference: LTSBIO-002). It was carried out in accordance with the Data protection, anonymisation, and storage and sharing of research data protocol; and Informed consent protocol for ethical research.

Table 5.1. Distribution and number of collected skin swabs and donated plates according to body site source, and active hits in brackets.

Body sites	No. of swabs (no. of active isolates against CM400)	No. of donated plates (no. of active isolates against CM400)
Armpit	17 (1)	29 (1)
Back of the ear	45 (1)	-
Back of the neck	27	-
Buccal mucosa	3	-
Collarbone	59 (2)	-
Elbow crease	27	-
External auditory canal	1	-
Fingertips	0	81 (4)
Forehead	52 (2)	21 (4)
Gums	3	-
Interdigital web space	16	26
Knee crease	6 (1)	-
Lower abdomen	4	-
Lower back 3	3	-
Nares	3	-
Palm	4 (1)	-
Roof of the mouth	4	-
Scalp	2	-
Side of the nose	34	-
Teeth	3	-
Tongue 3	3	-
Umbilicus	1 (1)	-
Volar forearm	37 (2)	32 (4)
Unknown	27	-
N = 570 (24)	n = 381 (11)	n = 189 (13)

Volunteers who are able to give informed consent (>18 y.o.) were recruited from microbiology teaching classes and laboratory members of the Antimicrobial Research Centre, Faculty of Biological Sciences, University of Leeds. They were asked to collect dry swabs from the body parts listed in Table 5.1. A total of 381 skin swabs and 189 previously plated swabs donated to this project were overlaid with *E. coli* CM400 to screen for antibiotic producers. Preliminary results show that approximately 2.8% of the plated swabs and 6.9% of the donated plates contained antibiotic producers. In sum, screening of 570 plates yielded a hit percentage of 4.2%.

From the 24 putative antibiotic producers, only 5 isolates retained their activity against *E. coli* CM400 in spot inoculation and spent medium assays (Table 5.2). The isolates VF48A, RC14, and MB32 exhibited more potent activities against *E. coli* CM400 than in *Candida albicans* CA6 (eukaryotic control). All confirmed antimicrobial producers were subjected to 16S rRNA gene sequencing for identification. Based on the analysed sequences, the top hit taxon and highest percentage of similarity from both NCBI and EzBioCloud are presented in Table 5.3. Isolate VF48A was 99% similar to *Bacillus sp.* while MB32 was 99% similar to an Uncultured *Bacillus*.

Table 5.2. Antimicrobial activity of hit isolates against *E. coli* CM400 and *C. albicans* CA6 measured by zone of inhibition (ZOI).

Isolates	Spot inoculation assay ZOI		Spent medium assay ZOI		Body site
	CM400	CA6	CM400	CA6	
VF48A	++	+	+++	-	Volar forearm
MB32	+++	++	+++	++	Collarbone
RC14	++	-	-	-	Back of the ear
MB5B	+	-	NA	NA	Collarbone

+ : 1 to 2 mm (or reduced growth); ++ : >2 to 4 mm; +++ : > 4 mm (Luiza Galarion).

For actinobacteria collection, all colony morphotypes growing on Bennett's agar were also identified through 16S rRNA gene sequencing and 84 isolates were confirmed to be actinobacteria. This project classified 16 cultivable genera from human skin and oral swabs. The most widely isolated genus was *Micrococcus sp.* comprising 21 of the total isolates, followed by *Kocuria sp.* (19), *Corynebacterium sp.* (11), *Dermacoccus sp.* (9), 5 of each: *Actinomyces sp.*, *Rothia sp.*, *Brevibacterium sp.* (5 each), and finally one of

each: *Knoellia sp.*, *Dietzia sp.*, *Streptomyces sp.*, *Cellulomonas sp.*, *Dermatophilus sp.*, *Dermabacter* sp., *Cutibacterium* sp., *Turicella* sp., and *Brachybacterium* sp.

Moreover, of the 22 body sites sampled, only 10 harboured isolates that are cultivable under the laboratory conditions employed in this project. Forehead, collarbone, and interdigital web spaces appear to have the most diverse isolates, and the collarbone had the highest number of actinobacteria isolates. A total of 18 selected actinobacteria isolates from the collection – all having no detectable antibiotic activity – were primarily UV irradiated at 24,000 µJ/cm^3 and then overlaid with *E. coli* CM400. This UV energy showed high mutation frequency and low survivability and allowed selection of "true mutants" among few isolates that lived after the radiation exposure. Of these isolates, only *Brevibacterium* MB5B showed activity against the test organism after irradiation (Table 5.2). *Brevibacterium* mutants were picked and isolated to confirm their activities employing the spot inoculation.

Table 5.3. Identity match for *E. Coli* CM400 active skin isolates in databases.

Isolates	NCBI	EzBioCloud
VF48A	*Bacillus* sp. 99%	*Bacillus amyloliquefaciens* 97.5%
MB32	Uncultured *Bacillus* 99%	*Bacillus circulans* 96.4%
RC14	*Bacillus subtilis* 96.86%	*Bacillus subtilis* 98.96%
MB5B	*Brevibacterium* sp. 99%	*Brevibacterium* sp. 99%

In a parallel study focussed on discovering antibacterial compounds active against *S. aureus* SH1000, another PhD student Zeyad Alzeyadi in Dr Alex O'Neill's group screened 2035 strains. Out of the 2035 *Staphylococcus spp.* skin isolates screened, 74 exhibited antibacterial activity against *Staph. aureus* SH1000. The screening collection comprised of various coagulase-positive and coagulase-negative *Staphylococcus* spp. obtained from human and animals infection sites. Since the aim of the project was to focus on small bioactive compounds, proteolytic enzymes and ferric chloride assay were employed to allow dereplication against peptidic and iron-chelating compounds. These hit producers were also tested for antibacterial activity against each other to identify cross-resistance and allow deprioritisation of the strains producing the same antibacterial compounds which led to five hit strains.

The concentrated freeze-dried supernatants (FDS) of the five producers NCTC11048, P5-25, DCM, G71, and CS808 were tested for activity against a range of clinical pathogens in well diffusion assay (Table 5.4). None of the FDS showed activity against the model Gram-negatives pathogens, *E. coli* BW25113 or *Haemophilus influenzae*. However, supernatants from strains P5-25, G71 and CS808 demonstrated moderate antibacterial activity against *Streptococcus pyogenes*, *Moraxella catarrhalis* and *Neisseria gonorrhoeae*, respectively. Moreover, P5-25, DCM and CS808 were weakly active against the eukaryotic yeast *Candida albicans*. Based on these results P5-25 was the most promising strain, therefore it was taken forward to the next step.

Table 5.4. Antibacterial activity of *staphylococcal* hit strains against a range of pathogens determined by well diffusion assay.

Pathogen	Producer strain				
	11048	P5-25	G71	DCM	CS808
S. aureus SH1000	+++	+++	++	+++	+++
S. aureus NR111	+++	+++	++	+++	+++
Streptococcus pyogenes	+	++	+	+	+
Moraxella catarrhalis	-	+	+	-	+
Neisseria gonorrhoeae	-	-	-	-	+
Haemophilus influenzae	-	-	-	-	-
Candida albicans C6	-	+	-	+	+

+: 1 to 2 mm (or reduced growth); ++: >2 to 4 mm; +++: > 4 mm (Zeyad AlZeyadi).

In conclusion, five hit strains were selected from various sources for further investigation. *Bacillus* sp. VF48A, MB32 and RC14 were collected from human skin commensals and exhibited activity against multi-drug resistant *E. coli* CM400; whereas MB5B, from actinobacteria collection, initially exhibited no activity against *E. coli* CM400. The UV mutagenesis method (developed in the O'Neill Lab) triggered expression of the gene cluster responsible for antibiotic production in this strain; mutant strain was active against the test organism. Lastly, P5-25 isolated from infected skin samples was active against *S. aureus* SH1000. Interestingly, the highest number of isolates were found in the samples collected from the collarbone.

5.3 TLC–Bioautography Assay Approach

The process of purifying a natural product extract is multi-step, time consuming, laborious and resource intensive often with little returns. A series of purification steps can lead to generation of only 1-3 mg of product on average which may not even be the

active compound. In this project, a robust strategy to screen the natural product extracts for their scope to generate enough purified material for biological evaluation and chemical characterisation was developed. Furthermore, the extracts containing sensitive (UV and temperature sensitive) and easily degradable compounds could also be ruled out.

Grzelak *et al.* developed a cutting edge (HP)TLC–bioautography–MS/NMR technique to accelerate anti-tuberculosis (TB) drug discovery from natural sources by acquiring structural information at a very early stage of the isolation process.[136] The team used established clinical agents and the avirulent, bioluminescent Mtb strain (mc^{2}7000 *luxABCDE*) to develop and optimise three variations of bioautography in detecting anti-TB agents of a wide range of polarities: (1) contact bioautography, (2)) agar-overlay bioautography, and (3) direct bioautography. The optimised method was applied to actinomycete and *Aspergillus* extracts for the identification and/or isolation as well as for the dereplication of anti-TB lead compounds. Previously identified anti-TB compounds ecumicin and gliotoxin were identified and isolated from *Nonomuraea* MJM5123 and *Aspergillus fumigatus*; no novel anti-TB compound was found using this approach.

Their strategy was modified to screen the five hit extracts in this project; however, the test organisms *E. coli* CM400 and *Staph. aureus* SH1000 strains were not bioluminescent. Therefore, a staining agent was required to be able to view the active zones of inhibition on TLC plates. 3-(4,5-Dimethylthiazol-2-yl)-2,5-diphenyl tetrazolium bromide (MTT) was a good candidate for this as the colourless MTT is reduced by viable cells to blue formazan. The assay showed a linear relationship between the number of viable bacteria and the ability to reduce MTT; dead bacterial cells were unable to reduce MTT.[137] Therefore zone of inhibition was observed as a colourless halo-like zone against a blue coloured background. Colistin was used as positive control as many commercial antibiotic drugs were not active against multi-drug resistant *E. coli* CM400 strain.

5.3.1 Development of TLC–Bioautography Assay

The TLC–Direct bioautography method was the method of choice to allow maximum contact between active compounds on the TLC plates and cell suspensions (with test organisms); a developed TLC plate is dipped in inoculated broth and incubated at 37 °C for 24 h. The quality of TLC-direct bioautography largely depends on the viscosity of the bacterial suspension. If the suspension density is too high or low, the resulting bacterial film is too uneven to yield clear inhibition zones. Furthermore, the amount and method of application of the staining agent MTT was another important factor. The viscosity of the cell suspension and amount of the staining agent needs to be compatible to yield a clear zone of inhibition.

Firstly, the method for application of staining agent MTT was evaluated using normal-phase TLC plates loaded with colistin (40 µg/ml). TLC plates loaded with colistin were developed in DCM/MeOH (9:1) and air dried before dipping it in *E. coli* CM400 or *S. aureus* SH1000 cell suspensions in MHB-II broth (OD 0.20) containing 0.05% agarose for 10 s. The plate was incubated at 37 ºC for 2 h and sprayed with 2% 2 mg/ml MTT solution in 0.01 M TES buffer (pH 7.2) followed by incubation at 37 ºC overnight. Where *S. aureus* SH1000 showed uniform growth on the plate, *E. coli* CM400 grew in patches making it very difficult to view clear zone of inhibition against dark blue background. The problem persisted even when plates coated with CM400 were sprayed 2 or 3 times with MTT (2% 2 mg/ml solution).

An improvement in the contrast was observed when the cell suspension density was doubled (OD 0.4). Moreover, addition of MTT solution directly in the cell suspensions led to significantly better results; 5%, 10% and 15% of 2 mg/ml MTT in buffer (0.01 M TES) were added to CM400 cell suspensions (OD 0.40). Developed TLC-plates loaded with colistin were dipped in these suspensions and incubated at 37 ºC overnight (Figure 5.2). The plate coated with 5% 2 mg/ml MTT in cell suspension showed homogenous growth, on the contrary 10% and 15% MTT led to streaky plates.
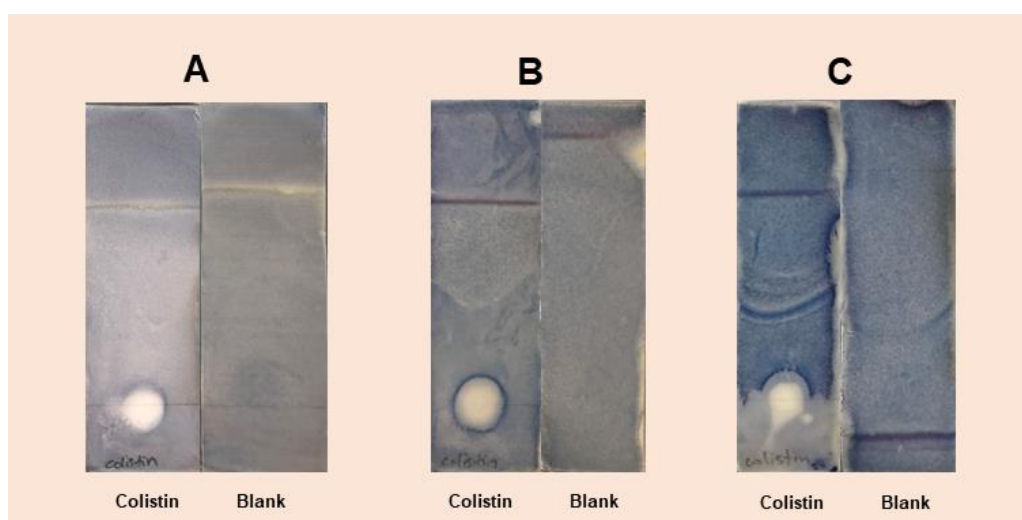
Figure 5.2. TLC-bioautography method development using colistin at 40 µg/ml: (A) 5% 2 mg/ml MTT in *E. coli* CM400 cell suspensions; (B) 10% 2 mg/ml MTT in *E. coli* CM400 cell suspensions; (C) 15% 2 mg/ml MTT in *E. coli* CM400 cell suspensions.

Additional factors to be optimised were incubation time and humidity. Insufficient incubation time of the inoculated TLC plates and a resulting low bacterial concentration can cause irregular inhibition zones, while excessive incubation times can lead to

decreased sensitivity to active compounds. Comparing incubation times of 12, 24 and 48 h resulted in well-defined inhibition zones for the shorter period of 12 h. Incubation in a humidified atmosphere achieved a more homogeneous bacterial layer compared to plates that were incubated in a non-humidified incubator.

5.3.2 Choice of Stationary Phase for TLC–Bioautography Assay

While TLC plates are commercially available in a variety of stationary phase materials, the selection of an ideal TLC sorbent can be challenge because both chromatographic and microbiological requirements need to be fulfilled. A limit of detection analysis was performed for colistin and the five hit extracts: *Bacillus* sp. VF48A, MB32, RC14, MB5B and *Staphylococcus* spp. P5-25. Alumina-backed plates coated with silica gel 60 (20 × 20 cm, Merck) and nanosilica gel C18-100 (10 × 10 cm, Merck) both with a fluorescence indicator were tested initially. All five extracts were dissolved in methanol (2 mL) and loaded onto normal-phase TLC plates using a micropipette. The plates were air-dried before eluting with DCM/MeOH (95:5) in a TLC chamber pre-saturated with the solvent system. The TLC plates were prepared in duplicates for each extract; one plate was subjected to bioautography, while the second was used for TLC–MS experiments. 600 µg/ml was found to be optimal amount for crude extracts whereas 40 µg/ml of colistin was enough to give a clear zone of inhibition.

The zones of inhibition were at the baseline for both colistin and *Bacillus* sp. VF48A extract suggesting the active compounds did not elute with DCM/MeOH (95:5). Addition of additives such as methanolic ammonia, formic acid, small amount of water and multiple elutions did not afford clear separation of the active compounds. Smudged zones of inhibition were observed when methanolic ammonia or water was added, whereas formic acid was not compatible with the bioassay altogether; no growth was visible on the entire plate.

Reverse-phase chromatography was employed next for colistin and *Bacillus* sp. VF48A (skin commensal from volar forearm) extract using methanol/water and acetonitrile/water in varying ratios (9:1, 1:1, 3:7, 1:9). Colistin could not be eluted using any of the solvent mixtures and stayed on the baseline even when methanolic ammonia was added. Addition of 0.1–0.3% TFA in the eluting solvents (MeCN/H_2O 1:1, 3:7, 6:4) led to elution of colistin, however acid was found to be incompatible with the bioassay and no growth was observed on the entire plate. When VF48A extract was eluted with MeCN/H_2O (6:4; Figure 5.3), one zone of inhibition was observed (R_f 0.3); addition of 0.1% TFA was again detrimental to the TLC–bioautography assay.

RC14, MB32 and MB5B extracts were also screened using normal-phase and reverse-phase TLC–bioautography assays. RC14 (skin commensal collected from back of the ear), MB32 (skin commensal collected from collarbone) and MB5B (UV-mutagenesis activated skin commensal from collar bone) extracts exhibited promiscuous activity in TLC–bioautography screen. The zones of inhibition for these extracts were not reproducible; it is possible that the active species were minor components of the extracts and their effective concentration was very low on the plates resulting in no zone of inhibition. Alternatively, degradation of the antibacterial compounds in natural product extracts have also been reported in the past.
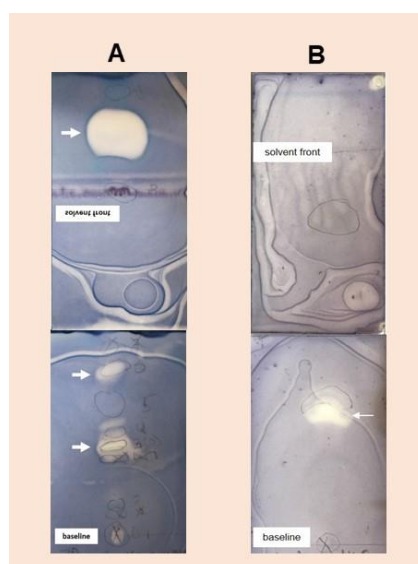
Figure 5.3. TLC–bioautography plates for the selected strains. (A) The activity of P5-25 extract on a normal-phase plate eluted twice with DCM/MeOH (95:5) against *S. aureus* SH1000; (B) The activity of VF48A extract on a reverse-phase plate eluted with MeCN/H$_2$O (60:40) against *E. Coli* CM400.

The extracts were stored at – 4 ºC and TLC chamber was covered with aluminium foil to prevent degradation of sensitive compounds. However, reproducibility and reliability issues persisted. One zone of inhibition was observed consistently near the solvent front for RC14 and MB5B extracts. When this spot was subjected to TLC–MS and TLC–NMR analyses, the spectral data matched with a plasticiser dioctyl-phthalate. Based on these results it is possible that the antibacterial activity recovered in the original screen was coming from this contaminant and that there were no other active compounds present in the extracts. However further work is required to confirm this conclusion. Since the aim

of this project was to find hit strains, further evaluation of these promiscuous strains were out of the scope of this project. Lastly, *Staphylococcus* spp. P5-25 extract exhibited reproducible activity against *S. aureus* SH1000 using normal phase TLC–bioautography assay (Figure 5.3). Therefore, VF48A and *Staphylococcus* spp. P5-25 extracts were ideal candidates for further development. In general, normal-phase TLC plates were most compatible with the assay and facilitated easy visualisation of the zones of inhibition.

5.3.3 Choice of Solvent Systems for TLC–Bioautography Assay

For normal-phase TLC–bioautography assays, various ratios of DCM/MeOH, CHCl$_3$/MeOH, CHCl$_3$/DCM/MeOH, EtOAc/Hexane, EtOH/H$_2$O, EtOAc/^{i}PrOH/H$_2$O were tested to elute the five extracts. Commonly used additives such as methanolic ammonia, formic acid and trifluoroacetic acid were also trialled. For reverse-phase TLC–bioautography assays, MeOH/H$_2$O and MeCN/H$_2$O in various ratios both with and without additives (0.1–0.5% ammonia, 0.1–0.3% TFA) were tested for all five extracts. DCM/MeOH (95:5) solvent mix was found to be most useful solvent system across the board; multiple elutions of the same plate using this solvent system gave better results than more polar solvent systems. Although it was not possible to achieve perfect separation of these complex natural product matrices on a TLC plate, DCM/MeOH mix facilitated effective separation.

For example, when VF48A extract was eluted with EtOAc/^{i}PrOH/H$_2$O (7:2:1) an ill-defined zone of inhibition was found all across the plate up to the solvent front. Similar problem was encountered when methanolic ammonia was added to the solvent mixture (DCM/MeOH 95:5). Addition of 0.1% formic acid resulted in inhibition of bacterial growth on the entire plate. For reverse-phase TLC–bioautography acetonitrile was found to be better eluting solvent than methanol. When eluted with 10% acetonitrile, the extract stuck to the baseline and 70% acetonitrile led to high retention times for the compounds (> 0.5). 60% acetonitrile in deionised water without acid was found to be best solvent system for reverse-phase TLC–bioautography across the board. In conclusion, additives such as ammonia, formic acid and trifluoracetic acid were not compatible with normal-phase as well as reverse-phase TLC–bioautography assay, therefore they should be avoided. Moreover, DCM/MeOH (95:5) for normal-phase and MeCN/H$_2$O for reverse-phase were best solvent systems for all the extracts.

5.4 Solvent Screen for *Staphylococcus* spp. P5-25 and *Bacillus* sp. VF48A Extractions

A sequential solvent system was devised to extract antibacterial compounds based on their polarity and solubility in organic solvents from hit extracts. *Staphylococcus* spp. P5-25 broth (200 mL) was extracted with hexane, methyl-tert-butylether (MTBE, 70mL), diethyl ether (70 mL), isopropylacetate (70 mL) and chloroform (70 mL) in a sequential manner. The extracts were dried and tested for activity against *S. aureus* SH1000 by disc diffusion method and analysed by ^{1}H NMR. No activity was observed for hexane extract. MTBE and diethyl ether extracted almost the same amount of material and showed similar activity (Table 5.5). Isopropylacetate (11 mg) and chloroform (9 mg) extracted higher amount of material than ether solvents and exhibited competing activity against *S. aureus* SH1000.

^{1}H NMR analysis of the four spectra showed complex peaks around 6.65–7.42, 3–4 and 0.8–1.4 ppm; no alkene or anomeric sugar peaks were present. Selective uptake of compounds was not observed in these experiments (indicated by relative peak integration). Therefore, higher antibacterial activity of the ether extracts was most likely due to the order of extraction rather than selective extraction of the antibacterial compounds. P5-25 broth (200 mL) was thereafter extracted with only isopropylacetate (3 × 70 mL) for future studies; the same method was adapted for *Bacillus* sp. VF48A extract.

Table 5.5. Antibacterial activity of P5-25 extracts against *S. aureus* SH1000. Crude extracts were dissolved in methanol and 600 μg/ml was loaded onto the discs.

Extract	Amount (mg)	*S. aureus* SH1000
Hexane	1	-
MTBE	4	++
Diethyl ether	3	++
Isopropylacetate	11	+
Chloroform	9	+
Methanol (control)	-	-

+: 1 to 2 mm (or reduced growth); ++: >2 to 4 mm; +++: > 4 mm

5.5 Purification and characterisation of *Staphylococcus* spp. P5-25 Extract

5.5.1 Semi-purification of *Staphylococcus* spp. P5-25 Extract

Staphylococcus spp. P5-25 extract was analysed by ^{1}H NMR to get an idea about nature of the extract. The spectrum was complex in general, however two doublets at 6.71 and 6.94 ppm coupled in ^{1}H–^{1}H COSY spectrum. These peaks were characteristic of a para-disubstituted system; the upfield shift of these aromatic peaks were suggestive of a methoxy or hydroxy substitution. Based on this hypothesis an alkaline extraction was devised; crude isopropylacetate extract (70 mL) was partitioned against 2 M Na_2CO_3 solution (2 × 50 mL). The remaining organic extract (O1) was dried following standard procedure and tested against *S. aureus* SH1000. The alkaline aqueous solution was neutralised with conc. HCl and back-extracted into ethyl acetate (2 × 50 mL, O2).

O1 and O2 extracts were tested against *S. aureus* SH1000 to follow antibacterial activity of the original extract (isopropylacetate extract); both extracts were still active suggesting the antibacterial compounds in the original extract were not acid or base sensitive. ^{1}H NMR analysis of O2 extract confirmed selective extraction of the targeted compounds.

5.5.2 Prep–HPLC Purification of P5-25O1 and P5-25O2

Preparative–TLC chromatographic purification of P5-25O1 and P5-25O2 was not successful. The compounds interacted strongly with silica resulting in streaked bands and could not be separated even using highly polar solvent systems. Prep–HPLC is a commonly used technique in purification of small amounts of natural products. The extracts were loaded onto a Kinetex^R C18 LC column; acetonitrile, methanol and water systems were screened in varying ratios, gradients and flow rate. Finally, binary solvent system consisted of solvent A: water with 0.1% TFA and solvent B: acetonitrile was used. The elution profile consisted of linear gradient from 5% B to 60% B in the first 30 min, then linear increase to 100% B at 30−31 min followed by isocratic elution (100% B) at 31−34 minutes, and linear decrease to 5% B at 34−35 min followed by 5% B isocratic elution at 35−36 minutes. The flow rate was 15 ml/ min and the peaks were monitored at 210, 220, 230 and 254 nm. Seven fractions were collected at 210 nm and dried in Genevac; **f1** 3.1 mg (6.4 min), **f2** 2.7 mg (8.38 min), **f3** 2.9 mg (8.99 min), **f4** 1.8 mg (10.56 min), **f5** 1.7 mg (10.98 min), **f6** 2.5 mg (11.55 min) and **f7** 3.3 mg (11.86 min).

5.5.3 Characterisation of *Staphylococcus* spp. P5-25 Extract

The dried seven fractions collected by preparative–HPLC chromatography of P5-25 extracts were analysed by IR and NMR spectroscopy, LC–MS, mass spectrometry, and optical rotation values were also recorded. These fractions were identified as a family of 2,5-diketopiperazines: cy(L-Tyr-L-Ile) **58**, cy(L-Leu-L-Pro) **59**, cy(L-Phe-D-Pro) **60**, cy(L-Leu-L-Ile) **61**, cy(L-Leu-L-Leu) **62**, cy(L-Phe-D-Tyr) **63** and cy(L-Phe-L-Leu) **64** (Figure 5.4). This family of compounds has been previously isolated from Fijian marine sponge *Acanthella cavernosa.*[138] Laville *et al.* isolated seven 2,5-diketopiperazines (DKPs) and compared them with synthetic samples to determine unambiguously the L-L absolute configuration of the natural DKPs: cy(L-Phe-L-Leu), cy(L-Phe-L-Ile), cy(L-Phe-L-Val), cy(L-Tyr-L-Ile), cy(L-Leu-L-Ile), cy(L-Phe-L-Thr) and cy(L-Phe-L-Tyr). Other reports of 2,5-diketopiperazines have also been found in the literature, however, full characterisation and absolute configuration assignments are often missing.[139,140,141]

Cy(L-Leu-L-Pro) **59**, cy(L-Phe-D-Pro) **60** and cy(L-Phe-D-Tyr) **63**, showed antibacterial activity against *S. aureus* SH1000 with **59** being the weakest. However, sample sizes were too small for full characterisation, therefore all seven DKPs were synthesised. The bioactivity, MS, NMR and optical rotation data for synthetic samples (see p. 106 for synthesis) was compared with that of natural samples, and literature wherever possible. Literature search for cy(L-Phe-D-Pro) **60** and cy(L-Phe-D-Tyr) **63** in SciFinder, Reaxys and npatlas (Natural Product Atlas) databases showed no positive hits. Therefore, this is the first report of isolation, characterisation and biological activity of these two DKPs.

The characterisation of natural cy(L-Phe-D-Pro) **60** has been described here in detail and rest of the DKPs were characterised using same methodology. Cy(L-Phe-D-Pro) **60** was isolated as a colourless solid and its molecular formula was assigned as $C_{14}H_{16}N_2O_2$ by high resolution EI–HRMS (m/z 244.1177, calculated. for 244.1212). The molecular formula allowed assigning the degree of unsaturations that was eight. In the ^1H NMR spectrum, a multiplet signal at 7.29 ppm indicating the presence of a phenyl group and one broad signal at 5.59 ppm, indicating the presence of an amino group (NH), were observed. Characteristic signals for DKPs at 4.46 (1H, dt, J = 5.0, 1.5 Hz, H-6) and 4.06 ppm (1H, dd, J = 10.5, 6.0 Hz, H-3) were also observed. A detailed analysis of the ^1H–^1H correlation spectroscopy (COSY) spectrum showed connectivity for two proton spin systems, H_3–H_{14}–H_{13}–H_{12} and NH–H_6–H_7–Ph. ^1H–^1H COSY correlations were found for signals at 4.46 and 3.16 ppm, and they were assigned to H-6 and H-7 respectively; the signal at 3.16 ppm (H-7) also coupled with phenyl signals which further confirmed the assignment. The rest of the signals were assigned using same method.

The ^{13}C NMR spectrum showed 14 carbon signals, attributable to two carbonyl carbons at 169.5 and 165.5 ppm, four methylene carbons (21.4, 28.0, 36.8 and 44.6 ppm), two

methine carbons (56.3 and 58.7 ppm), and six aromatic carbons (1 quaternary). All recovered data indicated that compound contained two rings in the structure. The heteronuclear multiple bond correlations (HMQC) of H-12 to C-3, H-3 to C-2, H-14 to C-2 and H-12 to C-5, were observed. This data confirmed presence of a proline moiety and a phenyl moiety. The compound **60** was identified as cy(-L-Phe-D-Pro) and later synthesised alongside other DKPs to confirm their identity and characterisation.

Cy(L-Tyr-L-Ile) **58**   Cy(L-Leu-L-Pro) **59**   Cy(L-Phe-D-Pro) **60**   Cy(L-Phe-L-Leu) **64**

Cy(L-Leu-L-Ile) **61**   Cy(L-Leu-L-Leu) **62**   Cy(L-Phe-D-Tyr) **63**
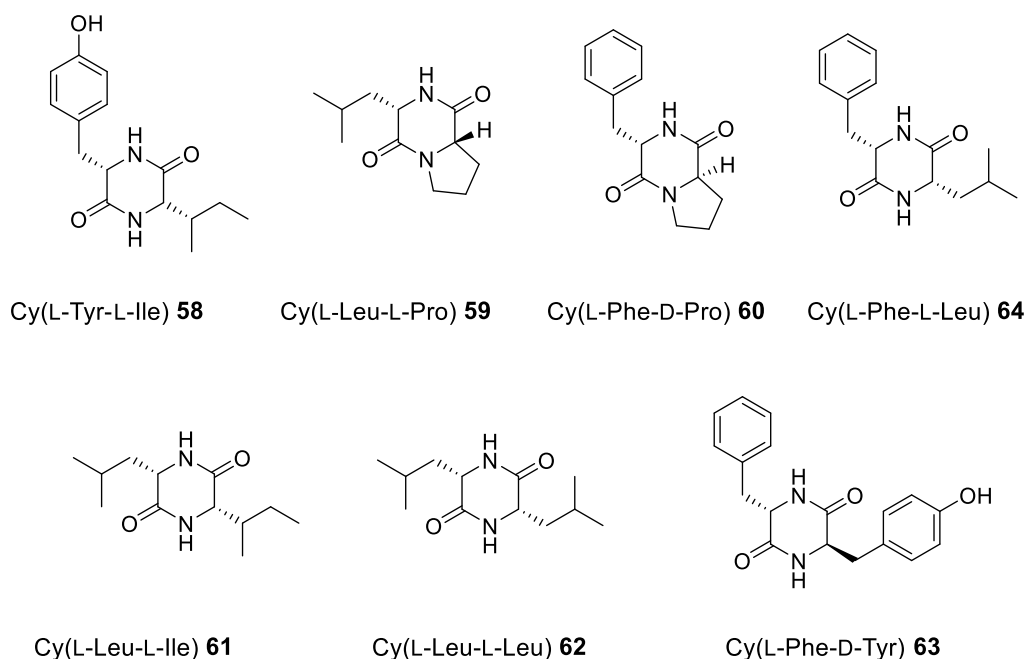
Figure 5.4. The structures of DKPs isolated from *Staphylococcus* spp. P5-25 extract.

5.6 Purification and Characterisation of *Bacillus* sp. VF48A Extract

5.6.1 Purification of *Bacillus* sp. VF48A Extract

Initial LC–MS and ^{1}H NMR analysis of crude *Bacillus* sp. VF48A extract showed similar chemical profile to *Staphylococcus* spp. P5-25 extract. An acid-base purification approach that was previously used for *Staphylococcus* spp. P5-25 extract did not result in semi-purification of the extract, indicating lack of the targeted OH groups. Therefore *Bacillus* sp. VF48A extract (35 mg) was directly purified using preparative HPLC.

After initial screen, an ideal method was found for purification of crude extract. The *Bacillus* sp. VF48A extract (35 mg) was dissolved in methanol (2mL) and filtered. It was then loaded onto Kinetex^R C18 LC Column, 21.2 × 100 mm, 5 μm in 300 μL injections and eluted using gradient solvent system. The binary solvent system consisted of solvent

A: water with 0.1% TFA and solvent B: acetonitrile. The elution profile consisted of linear gradient from 5% B to 32% B in the first 25 min, then linear increase to 100% B at 25−26 min followed by isocratic elution (100% B) at 26−28 minutes, and linear decrease to 5% B at 28−29 min followed by 5% B isocratic elution at 29−30 minutes. The flow rate was 15 ml/ min; the peaks were monitored at 210, 220, 230 and 254 nm and collected at 200 nm.

Fifteen fractions were collected altogether; 10 were identified (and fully characterised) as 2,5-diketopiperazines and surfactin-type compounds (1 mg) were found in fraction 15 (Figure 5.5). The rest of the four fractions were overlapping bands of DKPs as indicated by ^{1}H NMR. Cy(L-Phe-L-Pro-OH) **65** 1.4 mg, cy(L-Leu-D-Pro) **66** 3.9 mg, cy(L-Leu-L-Pro) **59** 4.4 mg, cy(L-Phe-L-Pro) **67** 4.6 mg, cy(L-Phe-D-Pro) **60** 4.2 mg, cy(L-Val-L-Leu) **68** 3.1 mg, cy(L-Phe-L-Tyr) **69** 1.7 mg, cy(L-Tyrp-L-Pro) **70** 1.9 mg and cy(L-Phe-L-Val) **71** 2.1 mg and cy(L-Phe-L-Leu) **62** 2.7 mg. Interestingly **59**, **60** and **64** were also previously found in *Staphylococcus* spp. P5-25 extract. However, since the focus of that project was on finding antibacterial agents against *S. aureus* SH1000 these compounds were not previously tested against *E. coli* CMR400. Furthermore, *Bacillus* sp. VF48A and *Staphylococcus* spp. P5-25 have different genus, however they were both originally collected from human skin commensals.

All compounds were tested against *S. aureus* SH1000 and *E. coli* CMR400 using in-house TLC–bioautography assay. Cy(L-Leu-L-Pro) **59**, cy(L-Phe-D-Pro) **60** and cy(L-Phe-L-Pro) **67** were found active against *S. aureus* SH1000 at 256 µg/ml with cy(L-Phe-D-Pro) being the most potent. Cy(L-Phe-L-Val) **71** and cy(L-Phe-L-Leu) **64** exhibited activity against *E. coli* CMR400 at 256 µg/ml. This is the first report of selective antibacterial activity exhibited by DKPs isolated from *Bacillus* and isolation of cy(L-Phe-D-Pro) **60**, cy(L-Phe-L-Pro-OH) **65** and cy(L-Leu-D-Pro) **66**. Fraction 15 containing surfactin-type compounds showed very weak antibacterial activity against *E. coli* CMR400 at 256 µg/ml. All bioactive DKPs (**59**, **60**, **64**, **67**, **71**) were synthesised to confirm full characterisation and bioactivity of natural DKPs.

There have been reports of DKPs from *Bacillus* in the literature.[142,143] Mohandas *et al.* determined the synergistic effects (discussed later) of diketopiperazines cyclo-(L-Leu-L-Pro) **59** and cyclo-(L-Tyr-D-Pro) purified from a *Bacillus* sp. N strain associated with entomopathogenic nematode *Rhabditis* (*Oscheius*) sp. on the growth of bacteria. Ortiz *et al.* isolated four L-Proline based DKPs from *Bacillus thuringiensis* and *Bacillus endophyticus*. The team then went on to synthesise these DKPs to confirm their characterisation and anti-fungal properties; cyclo-(L-Val-L-Pro) showed a marked inhibition (at 75 mg/ml) against *F. oxysporum* and *Penicillium sp.* fungi whereas cyclo-

(L-Phe-L-Pro) **65** and cyclo-(L-Tyr-L-Pro) showed a slight inhibition against the same fungi, showing the antifungal activity of these compounds.[143]
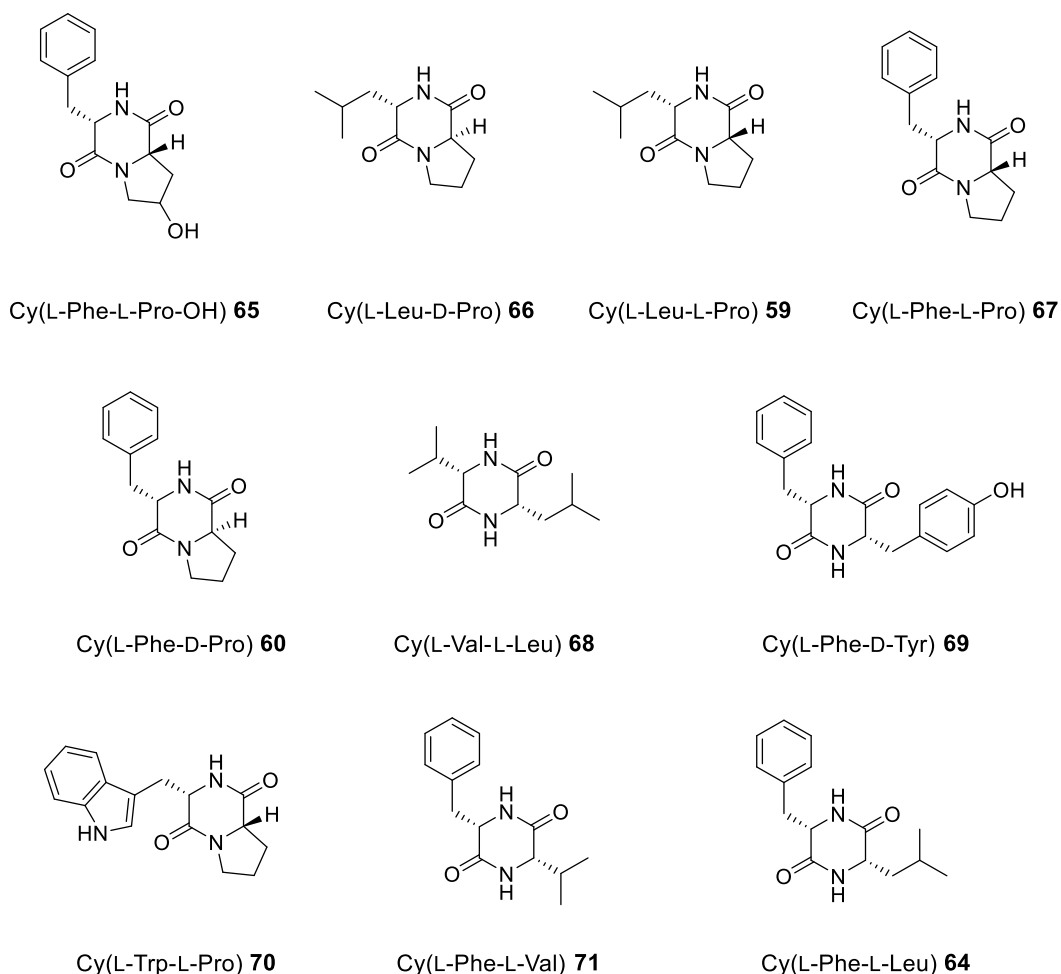

Cy(L-Phe-L-Pro-OH) **65**   Cy(L-Leu-D-Pro) **66**   Cy(L-Leu-L-Pro) **59**   Cy(L-Phe-L-Pro) **67**

Cy(L-Phe-D-Pro) **60**   Cy(L-Val-L-Leu) **68**   Cy(L-Phe-D-Tyr) **69**

Cy(L-Trp-L-Pro) **70**   Cy(L-Phe-L-Val) **71**   Cy(L-Phe-L-Leu) **64**

Figure 5.5. The structures of DKPs isolated from *Bacillus* sp. VF48A extract.

5.6.2 Characterisation of *Bacillus* sp. VF48A Extract

Ten 2,5-diketopiperazines were isolated from VF48A extract by preparative HPLC, and characterised by mass spectrometry, optical rotation studies, NMR and IR spectroscopy: cy(L-Phe-L-Pro-OH) **65**, cy(L-Leu-D-Pro) **66**, cy(L-Leu-L-Pro) **59**, cy(L-Phe-L-Pro) **67**, cy(L-Phe-D-Pro) **60**, cy(L-Val-L-Leu) **68**, cy(L-Phe-L-Tyr) **69**, cy(L-Tyrp-L-Pro) **70** and cy(L-Phe-L-Val) **71** and cy(L-Phe-L-Leu) **64**. All fractions were tested against *S. aureus* SH1000 and *E. coli* CM400 at 256 μg/ml using TLC–bioassay. Cy(L-Leu-L-Pro) **59**, cy(L-Phe-D-Pro) **60** and cy(L-Phe-L-Pro) **67** were found active against *S. aureus* SH1000 with cy(L-Phe-D-Pro) **60** being most potent; whereas cy(L-Phe-L-Val) **71** and cy(L-Phe-L-Leu) **64** exhibited activity against *E. coli* CMR400 at 256 μg/ml; a surfactin-type fraction was

also isolated which was weakly active against *E. coli* CMR400 at 256 µg/ml. Cy(L-Leu-L-Pro) **59** and cy(L-Phe-D-Pro) **60** were previously isolated from our P5-25 extract and exhibited same antibacterial profile. The characterisation of active fractions is discussed here, and the rest of DKPs were assigned in similar manner.

F6 and f7 isolated from VF48A extract were dried on *GeneVac* to give colourless solids and their molecular formulae were assigned as $C_{11}H_{18}N_2O_2$ by high resolution EI–HRMS (m/z 211.1407 [M+H]$^+$, calculated for 211.1428). Based on this molecular formula the degree of unsaturations was four. The molecular formula and subtle difference in NMR spectra for these two fractions were indicative of two isomers of the same compound. ^{1}H NMR analysis of two fractions showed broad signals around 5.78 ppm which were indicative of an amino group; α-protons gave signals at 4.28 and 3.86 ppm for f6, and 4.28 and 4.12 ppm for f7. A detailed analysis of the ^{1}H–^{1}H correlation spectroscopy (COSY) spectra showed connectivity for two proton spin systems: H_3–H_{13}–H_{12}–H_{11} and NH–H_6–H_{10}. Furthermore, two doublets around 0.98 and 1.01 ppm showed correlations with the multiplet at 1.80 ppm confirming presence of an isopropyl moiety.

The ^{13}C NMR spectra showed 11 carbon signals for f6 as well as f7, attributable to two carbonyl carbons at 170.2 and 167.6 ppm for f6, and 171.4 and 167.5 for f7. Four methylene carbons, three methine carbons and two methyl carbons were also found in both spectra. Proline as a common counterpart of the two compounds was easily deduced from the presence of broad methylene multiplets (1.7–3.7 ppm) and their correlations in HSQC and HMBC spectra. Based on this data f6 and f7 were assigned as cy(L-Leu-D-Pro) **66** and cy(L-Leu-L-Pro) **59** respectively. This is the first report of cy(L-Leu-D-Pro) **66**, however cy(L-Leu-L-Pro) **59** has been isolated previously.[140,143] The assignments were further confirmed by comparison with synthetic samples (discussed later) and literature for cy(L-Leu-L-Pro) **59**. [140]

F8 and f9 were assigned as cy(L-Phe-L-Pro) **67** and cy(L-Phe-D-Pro) **60** using similar methodology. Some of the key features for these two compounds have been summarised in

Table 5.6. They were both active against *S. aureus* SH1000 however cy(L-Phe-D-Pro) **60** was significantly more potent. This is the first report of cy(L-Phe-D-Pro) **60** whereas its diastereomer cy(L-Phe-L-Pro) **67** has been previously isolated from various microbial sources.[139,143,144] The molecular formula for both these fractions was assigned as $C_{14}H_{16}N_2O_2$ by high resolution EI-HRMS (m/z 244.1177), calculated for 244.1212. Based on this molecular formula the number of unsaturations was eight.

In the ^{1}H NMR spectra, multiplets around 7.29 ppm were indicative of the presence of a phenyl group and one broad signal at 5.60 ppm of an amino group. The signals for α-protons in ^{1}H NMR were characteristically different for these two compounds: 4.30 ppm (1H, t, J = 4.5 Hz, H-6) and 2.62 ppm (1H, m, H-3) for cy(L-Phe-L-Pro) **67**; 4.45 ppm (1H, dt, J = 5.0, 1.5 Hz, H-6) and 4.07 ppm (1H, dd, J = 10.5, 6.0 Hz, H-3) for cy(L-Phe-D-Pro) **60**. There was a significant upfield shift of H-3 peak from 4.07 ppm in cy(L-Phe-D-Pro) **60** to 2.62 ppm in cy(L-Phe-L-Pro) **67**. Similar trend was observed for H-14b whereas four multiplet signals for H-7a, H-7b, H-13a and H-13b collapsed to two signals for H-13 and H-14 in cy(L-Phe-D-Pro) **60**.

Table 5.6. Comparison of some of the key features of cy(L-Phe-L-Pro) **67** and cy(L-Phe-D-Pro) **60**. + : 1 to 2 mm (or reduced growth); ++ : >2 to 4 mm; +++ : > 4 mm.

Features	Cy(L-Phe-L-Pro) **67**	Cy(L-Phe-D-Pro) **60**
^{1}H NMR (δ/ppm)		
H-3	2.62	4.07
H-6	4.30	4.45
H-7a; 7b	3.20; 3.00	3.16 (2H, dd)
H-14a; H-14b	2.02; 1.68	2.09; 1.23
H-13a; H-13b	1.91; 1.66	1.80 (2H, m)
$[\alpha]^{25}_D$		
Conc. 0.1	+81	-135
Activity by TLC–bioautography assay (256 µg/ml)		
S. aureus SH1000	+	+++
E. Coli CM400	-	-
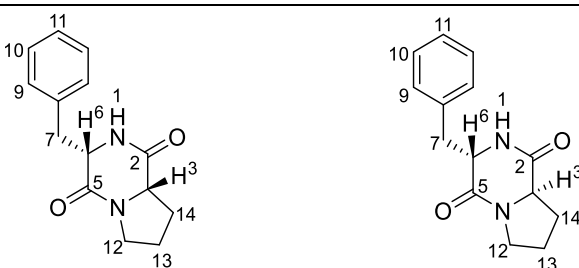
The ^{13}C NMR spectra for the two isomers showed 14 carbon signals each, attributable to two carbonyl carbons around 165–171 ppm, four methylene carbons (21.0–46.0 ppm), two methine carbons (55.0–60.0 ppm), and six aromatic carbons. All recovered data indicated that these compounds contained two rings. A detailed analysis of the [1]H–[1]H correlation spectroscopy (COSY) spectra showed connectivity for two proton spin systems: H_3–H_{13}–H_{12}–H_{11} and NH–H_6–H_7–Ph. The heteronuclear multiple bond correlations (HMBC) of H-6 to C-2, 5, 7, 8 and that of H-3 to C-2, 14 further confirmed assignment of these two protons and proline moiety in cy(L-Phe-D-Pro) **60**. (Table 5.7). All assignments were also compared with synthetic samples (discussed later).

Table 5.7. [1]H–[13]C correlations found in the long range (HMBC) heteronuclear correlation experiment for cy(L-Phe-D-Pro) **60**.
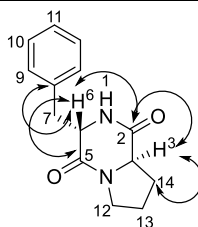
Proton	[13]C correlations
H-3	C-2, 14
H-6	C-2, 5, 7, 8
H-7	C-5, 8, 9
H-12	C-2, 3, 13, 14
H-9	C-7, 10, 11

F13 and f14 exhibited antibacterial activity against *E. coli* CMR400 at 256 µg/ml using TLC–bioautography assay. They were identified as cy(L-Phe-L-Val) **71** and cy(L-Phe-L-Leu) **64**; these compounds have been previously identified but their antibacterial profile against *E. coli* CM400 has never been reported before. Cy(L-Phe-L-Leu) **64** was also isolated from our P5-25 extract previously but it was not tested against *E. coli* CM400. Al-Mourabit *et al.* isolated seven DKPs including cy(L-Phe-L-Val) **71** from the Fijian marine sponge *Acanthella cavernosa*. NMR and circular dichroism (CD) comparison with synthetic L-L DKPs allowed unambiguous assignment of L-L absolute configuration of the natural DKPs.[138] NMR and optical rotation data for cy(L-Phe-L-Val) **71** and cy(L-Phe-L-Leu) **64** was compared with literature and synthetic samples.[138] Cy(L-Phe-L-Val) **71**,

cy(L-Phe-D-Val) **72**, cy(L-Phe-L-Leu) **64** and cy(L-Phe-D-Leu) **73** were synthesised to compare and unambiguously characterise the active diastereomers.

There were similarities and characteristic differences in NMR (Figure 5.6) and optical rotation data for cy(L-Phe-D-Leu) **73** and cy(L-Phe-L-Leu) **64**; a summary has been presented in Table 5.8. In the ^{1}H NMR spectra, multiplets around 7.18–7.31 ppm were indicative of presence of a *mono*-substituted phenyl group and one broad signal around 5.60 ppm of an amino group. The signals for α-protons in ^{1}H NMR spectra were characteristically different for these two compounds: 4.31 ppm (1H, t, J = 4.5 Hz, H-6) and 3.66 ppm (1H, m, H-3) for cy(L-Phe-D-Leu) **73**; 4.26 ppm (1H, t, J = 4.5 Hz, H-6) and 2.77 ppm (1H, dd, J = 6.0, 5.0 Hz, H-3) for cy(L-Phe-L-Leu) **64**. There was a significant upfield shift of H-3 peak from 3.66 ppm in cy(L-Phe-D-Leu) **73** to 2.77 ppm in cy(L-Phe-L-Leu) **64**. On the contrary, downfield shift was observed for H-12 and H-13 in cy(L-Phe-L-Leu) **64**.

Table 5.8. Comparison of some of the key features of cy(L-Phe-L-Leu) **64** and cy(L-Phe-D-Leu) **73**. +: 1 to 2 mm (or reduced growth); ++: >2 to 4 mm; +++: > 4 mm.

Features	Cy(L-Phe-L-Leu) **64**	Cy(L-Phe-D-Leu) **73**
^{1}H NMR (δ/ppm)		
H-3	3.66	2.77
H-6	4.31	4.26
H-12a	0.86	1.54
H-12b	0.08	1.44
H-13	1.42	1.69
$[\alpha]^{25}_D$		
Conc. 0.1	-26	+33
Activity by TLC–bioautography assay (256 µg/ml)		
S. aureus SH1000	-	-
E. Coli CM400	++	-

The ^{13}C NMR spectra for the two isomers showed 13 carbon signals each, attributable to two carbonyl carbons around 167–170 ppm, two methylene carbons (39–44 ppm), three methine carbons (55–60 ppm for C-3 & C-6, 23 ppm for C-13), and six aromatic carbons. All recovered data indicated that these compounds contained one aromatic ring each. A detailed analysis of the ^{1}H–^{1}H correlation spectroscopy (COSY) spectra showed connectivity for two proton spin systems: H_3–H_{12}–H_{13}–$H_{14/15}$ and NH–H_6–H_7–Ph. The heteronuclear multiple bond correlations (HMBC) were also recorded which further confirmed the assignments (Table 5.9); $^{2}J_{C,H}$ correlations were found for H-7/C-6 and H-7/C-8, $^{3}J_{C,H}$ for H-7/C-5 and $^{4}J_{C,H}$ H-7/C-10. Furthermore, H-12a correlated with C-3 and C-13 ($^{2}J_{C,H}$), C-14 and C-15 ($^{3}J_{C,H}$). All assignments were also compared with synthetic samples (discussed later).
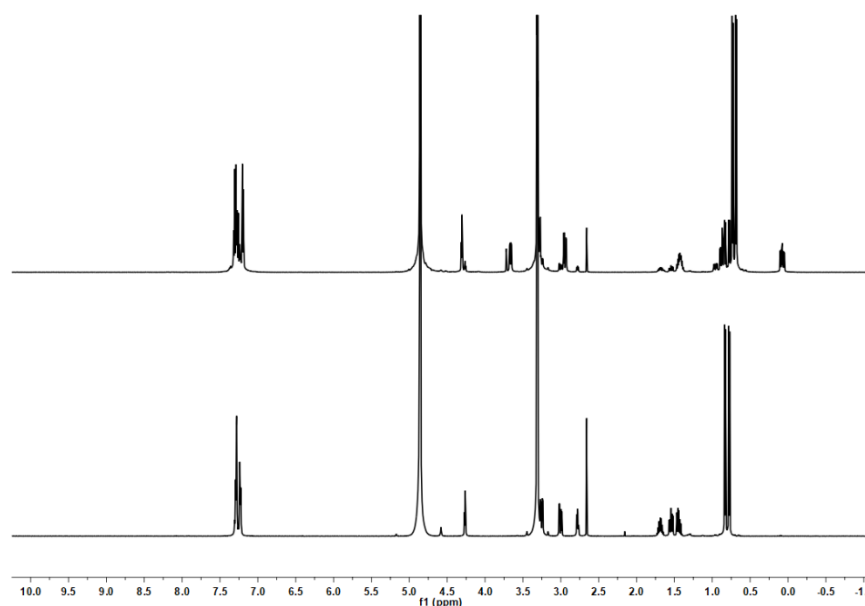

Figure 5.6. Comparison of ^{1}H NMR spectra for cy(L-Phe-L-Leu) **64 and** cy(L-Phe-D-Leu) **73**.

F15 was identified as surfactin-type compounds, however the sample size (1 mg) was too small for full characterisation. This fraction showed weak activity against *E. coli* CMR400 at 256 µg/ml. There have been reports of isolation of surfactin-type compounds from *Bacillus* in the literature. Surfactin is a well-characterised cyclic lipopeptide isolated from *Bacillus subtilis* and one of the most effective biosurfactant known so far. It is a macrolide containing *β*-hydroxy fatty acids (C-13 to C-15 chain length) linked to a cyclic heptapeptide moiety with the sequence L-Glu1->L-Leu2>D-Leu3->L-Val4->L-Asp5- >D-Leu6- >L-Leu7.[145]

^{1}H NMR analysis of the unknown fraction showed a pair of doublets at 7.06 (*J* 8.5 Hz) and 6.73 (*J* 8.5 Hz) indicative of a tyrosine residue; 12 amide protons were observed as broad singlets or doublets in downfield region (7.1–8.6 ppm). There were 11 peaks in characteristic peptidic region of 3.5–4.6 ppm however their relative integration was not consistent with one compound, therefore it was likely that a family of compounds were present in this fraction. The aliphatic region (0.82–1.74 ppm) was complex suggesting a long chain fatty acid moiety. A proline moiety was also indicated by multiplets around 1.2–2.5 ppm.

Table 5.9. [1]H–[13]C correlations found in the long range (HMBC) heteronuclear correlation experiment for cy(L-Phe-L-Leu) **64**.
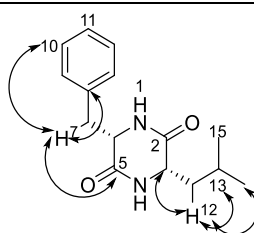
Proton	[13]C correlations
H-7	C-5, 6, 8, 10
H-12a	C-3, 13, 14, 15
H-9	C-7, 8, 10
H-14	C-12, 15
H-15	C-12

There have been several reports of isolation of heptapeptide based biosurfactants from *Bacillus*.[145,146,147] Literature search for related compounds found bacillopeptins to be the closest match for our unknown fraction; ^{1}H NMR and mass data showed high similarity. Kjimiura, Sugiyama and Kaneda isolated three antifungal bacillopeptins from *Bacillus subtilis* FR-2 with *m/z* 1020, 1034 and 1048. The accurate mass analysis of f15 fraction showed masses at 1008, 1022, 1036, 1050, 1064, 1072, 1086 and 1100. Furthermore, characteristic peaks for tyrosine moiety found in ^{1}H NMR spectra for the unknown fraction (6.73 & 7.06 ppm) was in agreement with the published data (6.68 & 7.02 ppm). Since this work was focussed on discovery of small molecule antibacterial agents against *E. coli* CMR400 this fraction was not further investigated or tested for its antifungal properties. The structures of active diketopiperazines have been presented in Figure 5.7.
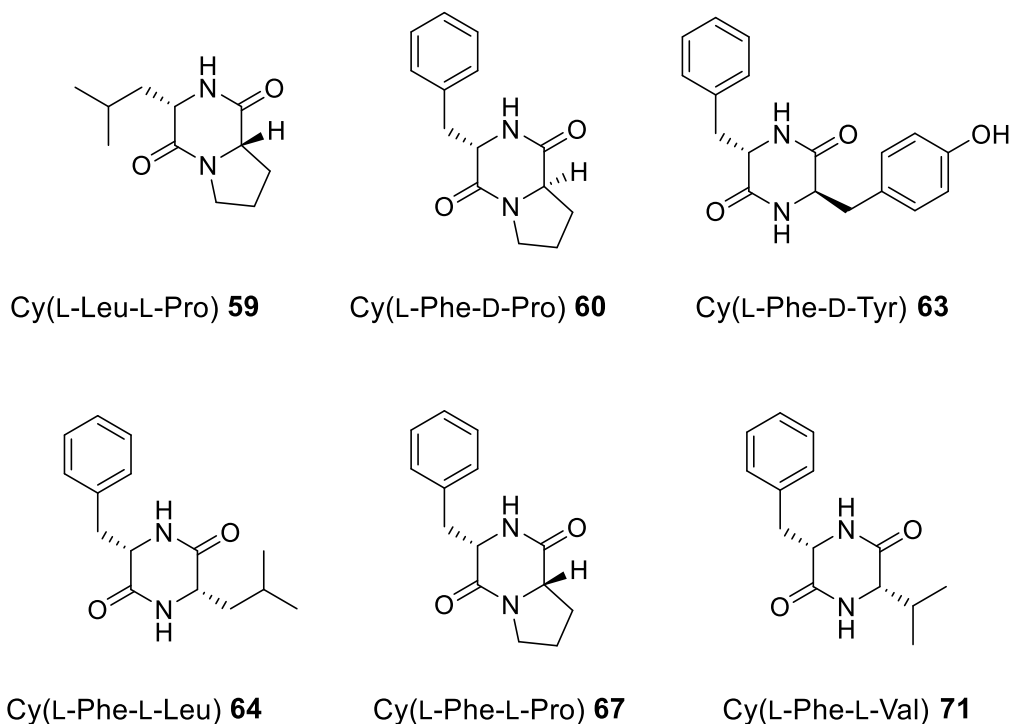
Cy(L-Leu-L-Pro) **59**   Cy(L-Phe-D-Pro) **60**   Cy(L-Phe-D-Tyr) **63**

Cy(L-Phe-L-Leu) **64**   Cy(L-Phe-L-Pro) **67**   Cy(L-Phe-L-Val) **71**

Figure 5.7. The structures of bioactive diketopiperazines. **59**, **60**, **63** and **67** were active against *S. aureus* SH1000. **64** and **71** were active against *E. coli* CMR400.

5.7 Synthesis of 2,5-diketopiperazines (DKPs)

Diketopiperazines are relatively simple cyclodipeptides which consist of rings obtained by the condensation of two α-amino acids that are produced by fungi, bacteria, the plant kingdom, and mammals.[140] Diketopiperazines possess diverse biological activities such as plant-growth promoters, antitumor, antifungal, and antibacterial.[148] They are not only a class of naturally occurring privileged structures that have the ability to bind to a wide range of receptors but they also have a structure that confers high stability and resistance to human digestion that make them attractive scaffolds for drug discovery.[143] Many natural metabolites including alkaloids are biosynthetically derived from diketopiperazines by oxidation and rearrangement reactions.

They represent an interesting tool for medicinal chemistry since their heterocyclic cores provide a good template for further chemical and stereochemical modification. Proline (Pro) and arginine (Arg) units are usually found in biologically active DKPs.[138] DKPs have been isolated from various sources including marine sponge *Acanthella cavernosa,*[138] sponge-associated fungus *Nigrospora oryzae,*[139] green Chinese onion-derived fungus

Talaromyces pinophilus AF-02,[141] *Bacillus endophyticus*,[143] *Bacillus thuringiensis*,[143] *Streptomyces sp.*,[149] and endophytic *Streptomyces* SUK 25.[150]

Many Gram-positive and Gram-negative bacteria communicate *via* production and sensing of small, diffusible signal molecules that coordinate virulence-determinant production and regulate expression of specific genes responsible for communal behaviour. This is known as quorum sensing, and eukaryotes produce quorum-sensing-interfering compounds that have a positive or negative influence on the bacterial signalling network. Hence, quorum sensing represents a novel therapeutic target offering the opportunity to attenuate virulence, and thus control infection, by blocking cell-to-cell communication.

It has been reported that 2,5-diketopiperazines both activate and inhibit quorum sensing in certain Gram-negative bacteria.[151] The cyclic dipeptide cy(L-Phe-L-Pro) **67** is produced by the opportunistic human pathogen *Vibrio vulnificus*, which causes severe wound infection and primary septicemia, and **67** was shown to induce the expression of *Vibrio fischeri* lux genes. Interestingly, of the two enantiomers, only cy(L-Phe-L-Pro) **67** and not cy(D-Phe-D-Pro) **60** was active as a signal molecule controlling the expression of genes important for the pathogenicity of the bacteria *Vibrio spp.*

Thirteen DKPs were synthesised in this work (Table 5.10) and compared with natural DKPs isolated from *Bacillus* sp. VF48A and *Staphylococcus* spp. P5-25 extracts, and tested against *S. aureus* SH1000 and *E. Coli* CMR400. DKPs were synthesised following the previously published method by Al-Mourabit *et al.*[138] Briefly, Boc-protected α-amino acid and α-amino acid ester were stirred in presence of EDC and DMAP in DCM for 10 h; the product was purified using flash chromatography (DCM/MeOH 97:3). The dipeptide coupled product was deprotected using 4 M HCl/dioxane and MeOH (5 mL) and thereafter cyclised in a microwave reactor (140 ºC, 10 min). DKPs were purified in 39–97% yield (Table 5.10); epimerisation was observed for cy(L-Phe-D-Pro) **60**, cy(L-Phe-D-Tyr) **63**, cy(L-Phe-L-Leu) **64**, cy(L-Leu-D-Pro) **66** and cy(L-Phe-L-Val) **71**.

The yields for the synthetic DKPs have been summarised in Table 5.10; cy(L-Phe-L-Tyr) **71**, cy(L-Phe-L-Pro) **59**, cy(L-Phe-D-Val) **72**, cy(L-Phe-D-Leu) **73** and cy(L-Leu-D-Pro) **66** were isolated in 87, 90, 78, 75 and 86% yield respectively. Furthermore, cy(L-Phe-L-Tyr) **69** and cy(L-Phe-L-Pro) **67** gave higher yields (87 and 90%) than their respective *trans*-isomers (61% & 54%). Successful synthesis of cy(L-Phe-L-Pro) **65** has been reported in the literature; it was proposed that higher *cis*-amide content in L-Phe-L-Pro-methyl ester led to facile cyclisation of the dipeptide resulting in 90% yield and no epimerisation was observed.[148] This work is in agreement with the literature; both L-Phe-L-Pro-methyl ester and L-Phe-L-Tyr-methyl ester cyclised to give *cis*-isomers selectively. On the contrary, cy(L-Phe-D-Tyr) **63** and cy(L-Phe-D-Pro) **60** epimerised to give their respective *cis*-

isomers which resulted in a mixture; the ratio for *cis* and *trans* isomers has been summarised in Table 5.11. L-Phe-D-Tyr methyl ester was cyclised following the same protocol as L-Phe-L-Tyr methyl ester, the final product epimerised to give two isomers; cy(L-Phe-D-Tyr) **63** and cy(L-Phe-L-Tyr) **69** were isolated in 27 and 34% respectively (0.8:1). These results imply that cy(L-Phe-L-Tyr) **69** is more stable isomer and therefore favoured. Similarly, cy(L-Phe-L-Pro) **67** was more stable than cy(L-Phe-D-Pro) **60**.

Table 5.10. Synthesis of DKPs and their isolated yields.
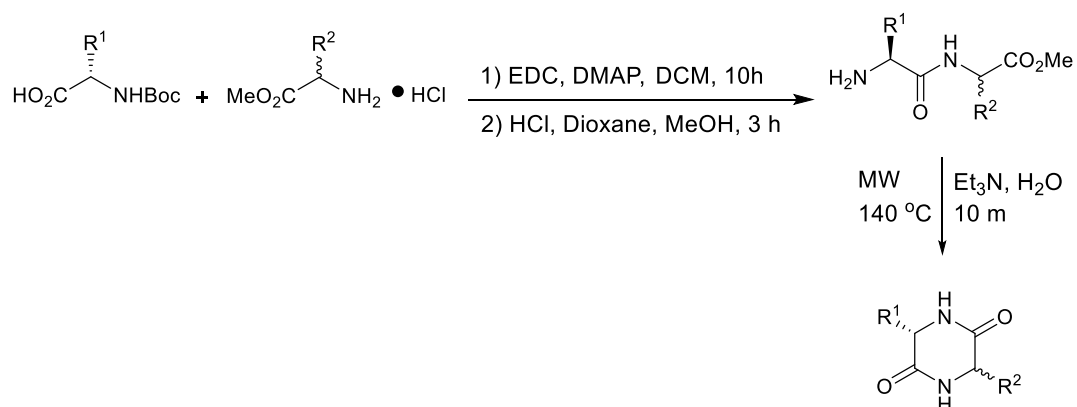
Number	DKP	Yield (%)
58	Cy(L-Tyr-L-Ile)	72
60	Cy(L-Phe-D-Pro)	54
61	Cy(L-Leu-L-Ile)	45
63	Cy(L-Phe-D-Tyr)	61
64	Cy(L-Phe-L-Leu)	54
66	Cy(L-Leu-D-Pro)	86
67	Cy(L-Phe-L-Pro)	90
69	Cy(L-Phe-L-Tyr)	87
71	Cy(L-Phe-L-Val)	43
72	Cy(L-Phe-D-Val)	78
73	Cy(L-Phe-D-Leu)	75

Cy(L-Phe-L-Val) **71**, cy(L-Phe-D-Val) **72**, cy(L-Phe-L-Leu) **64** and cy(L-Phe-D-Leu) **73** were also synthesised in moderate to good yields. L-Phe-D-Val-OMe and L-Phe-D-Leu-OMe cyclised successfully to give only *trans*-isomers in 78 and 75% yields respectively.;

whereas the cyclisation of L-Phe-L-Val-OMe and L-Phe-L-Leu-OMe resulted in lower yields (43 and 52%); furthermore, the cyclised products epimerised to give a mixture of *cis* and *trans* isomers. The steric hindrance between the two side chains is lower in *trans*-isomer than *cis*-isomers in these DKPs leading to higher yield of the *trans*-isomers.

Table 5.11. The ratio of *cis* and *trans* isomers for selected synthetic DKPs.

Di-peptide methyl ester	Ratio of isolated cyclised products	
	Trans-isomer	*Cis*-isomer
L-Phe-D-Tyr-OMe	0.7	1
L-Phe-D-Pro-OMe	0.4	1
L-Phe-L-Val-OMe	1	0.8
L-Phe-L-Leu-OMe	1	0.9

This conclusion was further strengthened when cy(L-Leu-L-Ile) **61** was synthesised in 43% yield; *cis*-configuration at α-carbons resulted in steric hindrance between the side chains. Cy(L-Leu-D-Ile) **72** was not synthesised as this was not one of the isolated or active DKPs from the extract. However, it is recommended for future work that DKPs are synthesised with varying side chains both in *cis*- as well as *trans*-configuration. This would strengthen understanding of the mechanism behind synthesis of these simple yet structurally important and relevant family of compounds. Although DKPs have been isolated from various sources, full characterisation data including absolute configuration studies is scarce in the literature. The small library of DKPs synthesised and fully characterised in this work would initiate reliable database for this family of compounds.

5.8 Comparison of Natural and Synthetic DKPs

Seventeen DKPs were isolated from *Staphylococcus* spp. P5-25 and *Bacillus* sp. VF48A extracts altogether; all DKPs were fully characterised using mass spectrometry, optical rotation studies, IR, 1-D and 2-D NMR spectroscopy. Cy(L-Leu-L-Pro) **59**, cy(L-Phe-D-Pro) **60** and cy(L-Phe-L-Leu) **64** were found in both extracts; whereas the diastereomers cy(L-Phe-D-Tyr) **63** and cy(L-Phe-L-Tyr) **69** were isolated from *Staphylococcus* spp. P5-25 and *Bacillus* sp. VF48A extract respectively. Interestingly two diastereomers were found for Leu-Pro and Phe-Leu-based DKPs in VF48A extract (*Bacillus* sp.): cy(L-Leu-L-

Pro) **59**, cy(L-Leu-D-Pro) **66**, cy(L-Phe-D-Pro) **60** and cy(L-Phe-L-Pro) **67**. Thirteen diketopiperazines (DKPs) were synthesised and compared with natural samples to confirm their assignments and establish their absolute configuration and bioactivity. The assignments were also confirmed with the literature wherever possible. The stacked ^{13}C spectra for natural and synthetic cy(L-Phe-L-Val) **71** samples have been presented in Figure 5.8.
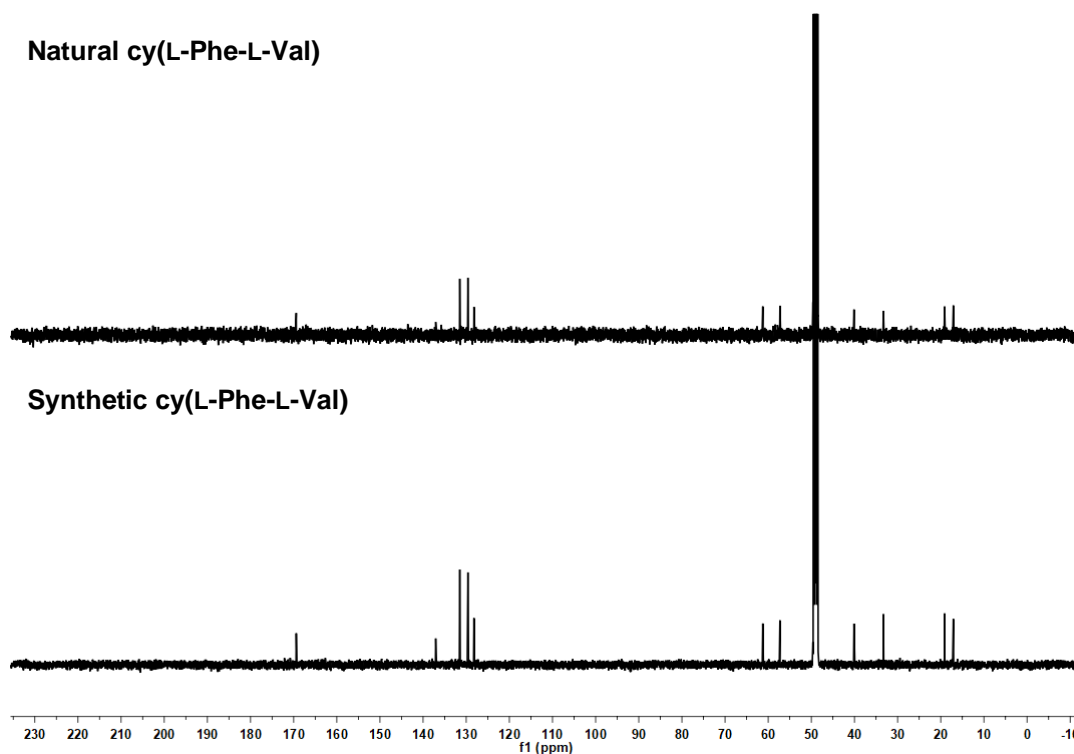

Figure 5.8. Stacked ^{13}C NMR for natural and synthetic cy(L-Phe-L-Val) **71**.

The optical rotation values for synthetic and natural DKPs were recorded in methanol (*c* 0.1) and have been summarised in Table 5.12 for selected DKPs. All optical rotation values for the natural DKPs were in excellent agreement with the synthetic samples. The optical rotation values for cy(L-Phe-L-Val) **71** and cy(L-Leu-L-Pro) **59** were in excellent agreement with the literature values; all readings including the literature ones were recorded at *c* 0.1 in methanol. Cy(L-Leu-L-Ile) **61** gave optical rotation values of -55 and -53 for natural and synthetic samples respectively; Al-Mourabit reported it to be -26, however it was measured in AcOH (*c* 0.3) and direct comparison was difficult; similar pattern was observed for cy (L-Phe-L-Tyr) **69**. No literature references were found for cy(L-Phe-D-Pro) **60**, cy(L-Phe-D-Tyr) **63**, cy(L-Leu-D-Pro) **66**, cy(L-Phe-D-Val) **72** and cy(L-Phe-D-Leu) **73**; this is the first report of isolation and full characterisation of these

DKPs. ^{1}H and ^{13}C NMR data was also compared for the natural and synthetic samples and it was within 0.1% error.

The optical rotation values for natural cy(L-Phe-L-Pro) **67** and cy(L-Phe-D-Pro) **60** were +79 and -117 respectively; these values were within 2% error for the synthetic samples. However, current results were in disagreement with data published for **67** by Tullberg, Grøtli and Luthman.[148] The team did optical rotation studies in methanol (*c* 0.3) and reported their result as -184 as opposed to the positive optical rotation value found in this work. On comparison of NMR data with the published work, a striking resemblance was found between NMR spectra for cy(L-Phe-D-Pro) **60** in current work and the reported NMR data on cy(L-Phe-L-Pro) **67**.

Table 5.12. Specific rotation values for natural and synthetic DKPs in MeOH (*c.* 0.1).[a] *c* 0.3 AcOH; [b] *c* 0.1 MeOH; [c] *c* 0.3 MeOH.

DKP	$[α]_{D(natural)}$	$[α]^{25}_{D(synthetic)}$	$[α]^{25}_{D(literature)}$
Cy(L-Phe-L-Tyr)	-81	-82	-44[a,138]
Cy(L-Phe-D-Tyr)	+49	+48	-
Cy(L-Phe-L-Pro)	+81	+79	-184[148]
Cy(L-Phe-D-Pro)	-115	-117	-
Cy(L-Phe-L-Val)	-94	-95	-95.8[b,150]
Cy(L-Phe-D-Val)	-	+78	-
Cy(L-Phe-L-Leu)	-25	-26	-8[c,148]
Cy(L-Phe-D-Leu)	-	+33	-
Cy(L-Leu-L-Pro)	-311	-310	-310[c,150]
Cy(L-Leu-D-Pro)	+69	+70	-
Cy(L-Leu-L-Ile)	-55	-53	-26[a,138]
Cy(L-Tyr-L-Ile)	-31	-35	-24[a,138]

These two isomers have characteristic differences in their NMR spectra; the peaks for H-3 appear at 2.62 and 4.06 ppm for cy(L-Phe-L-Pro) **67** and cy(L-Phe-D-Pro) **60** respectively in ^{1}H NMR spectra. This was found to be the case for both natural as well as synthetic samples. However, data published by Tullberg, Grøtli and Luthman assigned H-3 to the peak at 3.96 ppm for cy(L-Phe-L-Pro) **67**. The synthetic cy(L-Phe-L-Pro) **67** was obtained in 90% yield as a single isomer and shows characteristic peak for

H-3 and 2.62 ppm which is in agreement with the natural sample. Furthermore, weak antimicrobial activity previously reported for cy(L-Phe-L-Pro) **67** is also in agreement with current work.[149] Based on this work it can be conclude there is a discrepancy in data for cy(L-Phe-L-Pro) **67** in the literature; however striking agreement between natural and synthetic samples in this work confirms reliability of the results.

Brevianamide F **70** (cy(L-Trp-L-Pro) isolated from *Bacillus* sp. VF48A extract has been extensively studied in the literature. It was originally isolated from *Streptomyces* sp. TN58 and exhibited activity against *S. aureus* and *Micrococcus luteus*.[152] Initially cy(L-Trp-L-Pro) and its DL, LD, and DD isomers showed potential for use in the treatment of cardiovascular dysfunction,[153] however they were later shown to be hepatoxic.[154] In current work, cy(L-Trp-L-Pro) showed no activity against the test organisms *S. aureus* SH1000 and *E. coli* CMR400.

Both natural as well as synthetic compounds were tested against *S. aureus* SH1000 and *E. coli* CMR400 using in-house TLC–bioautography assay (Table 5.13). Cy(L-Phe-D-Tyr) **63** and cy(L-Phe-D-Pro) **60** exhibited activity against *S. aureus* SH1000 at 128 µg/ml, whereas cy(L-Phe-L-Pro) **67** and cy(L-Leu-L-Pro) **59** exhibited activity against *S. aureus* SH1000 at 256 µg/ml. Cy(L-Phe-L-Val) **71** and cy(L-Phe-L-Leu) **64** was active against *E. coli* CMR400 at 256 µg/ml. Very similar selectivity and potency was observed for the synthetic analogues. For example, the results for TLC–bioautography assay for natural as well as synthetic cy(L-Phe-D-Pro) **60** has been shown in Table 5.13; bioactivity for rest of the DKPs has also been summarised.

This is the first report of selective antibacterial activity exhibited by DKPs. When cy(L-Phe-L-Tyr) **69** and cy(L-Phe-D-Tyr) **63** were tested against *S. aureus* SH1000 and *E. coli* CMR400, only cy(L-Phe-D-Tyr) **63** showed activity against *S. aureus*; no activity was recovered for either isomers against *E. coli* CMR400. Similarly, cy(L-Phe-D-Pro) **60** was 3 times more potent than cy(L-Phe-L-Pro) **67** against *S. aureus* SH1000, and no activity was obtained against *E. coli* CMR400. Mohandas *et al.* tested cy(L-Leu-L-Pro) **59** and cy(L-Leu-D-Pro) **66** against *S. aureus*, *B. subtilis*, *E. coli* and *P. aeruginosa*; the reported MICs against *S. aureus* were 32 and 64 µg/ml for cy(L-Leu-L-Pro) **59** and cy(L-Leu-D-Pro) **66** respectively.[142] No activity was recovered for cy(L-Leu-D-Pro) **66** in this work and MICs for cy(L-Leu-L-Pro) **59** was 8-fold lower than the reported values. It was possible that this discrepancy was caused by the difference in methods, however when the published method was employed, no bioactivity was recovered against any of the DKPs. Interestingly, only two DKPs showed activity against *E. coli* CMR400 at 256 µg/ml: cy(L-Phe-L-Val) **71** and cy(L-Phe-L-Leu) **64**.

Table 5.13. TLC–bioautography assay results: (A) synthetic cy(L-Phe-D-Pro) **60**; (B) f7 natural cy(L-Leu-L-Pro) **59**, f8 natural cy(L-Phe-L-Pro) **67**, f9 natural cy(L-Phe-D-Pro) **60**. MICs for the synthetic DKPs against *S. aureus* SH1000 and *E. coli* CMR400.
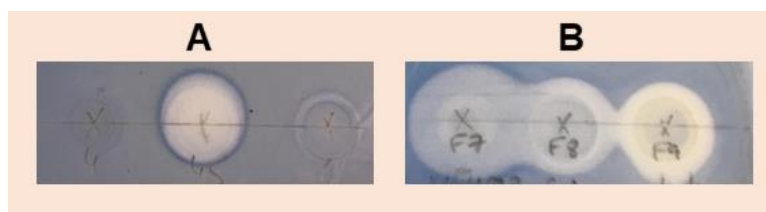
		MIC (µg/ml)	
Number	DKPs	*S. aureus* SH1000	*E. Coli* CMR400
60	Cy(L-Phe-D-Pro)	128	-
63	Cy(L-Phe-D-Tyr)	128	-
67	Cy(L-Phe-L-Pro)	256	-
59	Cy(L-Leu-L-Pro)	256	-
71	Cy(L-Phe-L-Val)	-	256
64	Cy(L-Phe-L-Leu)	-	256
-	Colistin	-	40

There have been reports of synergistic antimicrobial activity of DKPs.[142,144,149] Mohandas *et al.* studied the synergistic effect of cy(L-Leu-L-Pro) **59**, cy(L-Leu-D-Pro) **66** and cy(L-Tyr-D-Pro) using checker board assay and time-kill methods. They found that the combination effects of diketopiperazines were predominately synergistic (FIC index <0.5).[142] Furthermore, time–kill study showed that the growth of the tested bacteria was completely attenuated with 4–12 h of treatment with 50:50 ratios of diketopiperazines. These results suggest that the combination of diketopiperazines may be microbiologically beneficial. In another study, Ki-Hyeong Rhee determined the combined effects of cy(L-Leu-L-Pro) **59** and cy(L-Phe-L-Pro) **67** on the growth of vancomycin-resistant enterococci (VRE) and pathogenic yeasts, as well as determining their anti-mutagenic effects. This drug combination was especially effective against five VRE strains: *Enterococcus faecium* (K-99-38), *E. faecalis* (K-99-17), *E. faecalis* (K-99-258), *E. faecium* (K-01-312) and *E. faecalis* (K-01-511) with MIC values of 0.25–1 mg/l. It was also effective against *Escherichia coli*, *Staphylococcus aureus*, *Micrococcus luteus*, *Candida albicans* and *Cryptococcus neoformans* with MIC values of 0.25–0.5 mg/l.[144]

The published studies support the experimental results in this work and explain the initial potent activity observed for the crude extracts. *Staphylococcus* spp. P5-25 crude extract showed activity at 600 µg/ml against *S. aureus* SH1000 and the MICs of purified

natural/synthetic compounds were in the range of 128–256 μg/ml. *Bacillus* sp. VF48A crude extract showed activity against *E. coli* CMR400 at 600 μg/ml, however only two purified/synthetic DKPs were active against this strain at 256 μg/ml. This could be due to synergistic effect of *E. coli* active DKPs and *S. aureus* active DKPs. More importantly, the surfactin-type compounds found in VF48A extract could also be playing a role as OM-permeabilising (OM outer membrane) agent, facilitating efficient transportation of DKPs across the membrane in *E. coli*. thereby improving their efficacy.

These surfactin-type compounds showed very weak antibacterial activity against *E. coli* at 256 μg/ml on their own, however a synergistic effect between DKPs and these compounds is possible. The detergent effect of surfactin has been reported in the literature which draws on its ability to insert fatty acid chain into the bilipid layer causing disorganisation leading to membrane permeability.[155] Insertion of several surfactin molecules into the membrane can lead to the formation of mixed micelles by self-association and bilayer influenced by fatty chain hydrophobicity ultimately leading to bilayer solubilisation. For future work, it would be interesting to test isolated as well as synthetic DKPs against *S. aureus* SH1000 and *E. coli* CMR400 in presence of surfactin. Furthermore, synergistic studies on DKPs are warranted to confirm bioactivity of the crude extract.

5.9 Conclusion

Antibiotic resistance has become one of the major challenges in healthcare. The problem has been exacerbated by lack of discovery of novel antibacterial drugs. The last clinically useful broad-spectrum antibiotic in a new class to be discovered was daptomycin (in 1986), a lipopeptide that acts against the bacterial cell membrane, but it was not approved until 2003. The lack of new leads necessitated resurrection of previously discarded daptomycin **35**, quinupristin–dalfopristin and fidaxomicin **36**. For efficient discovery and development of novel antibiotics, reliable discovery platforms are required. Some of the examples of such platforms in the literature are prodrugs, species-specific antibiotics, silent operons, revisiting old antibiotics and investigating previously unexploited genera.[99]

In this work, the potential of 'species-specific target' and 'novel sources of antibacterial' approaches have been explored. The human microbiota is a dynamic collection of microbes that have existed within and on us, throughout our evolutionary history. The human microbial composition is diverse across individuals and can also morph along individual lifetimes. Volunteers who are able to give informed consent (>18 y.o.) were recruited from microbiology teaching classes and laboratory members of the Antimicrobial Research Centre, Faculty of Biological Sciences, University of Leeds. They

were asked to collect dry swabs from different body parts. A total of 381 skin swabs and 189 previously plated swabs donated to this project were overlaid with *E. coli* CM400 to screen for antibiotic producers. From the 24 putative antibiotic producers, only 5 isolates retained their activity against *E. coli* CM400 in spot inoculation and spent medium assays. In a parallel study focussed on discovering antibacterial compounds active against *S. aureus* SH1000, out of the 2035 *Staphylococcus spp.* skin isolates screened, 74 exhibited antibacterial activity against *S. aureus* SH1000. Five hit strains were selected after a series of assays and tests.

The process of purifying a natural product extract is a multi-step, time consuming, laborious and resource intensive often with little returns. Therefore, a TLC–bioautography assay was developed for efficient screen of natural product extracts, whereby only the extracts with potential for further development would be taken forward. Colistin was used as positive control as many commercial antibiotic drugs were not active against our multi-drug resistant *E. coli* CM400 strain. TLC–Direct bioautography method was the method of choice to allow maximum contact between active compounds on the TLC plates and cell suspensions. 3-(4,5-dimethylthiazol-2-yl)-2,5-diphenyl tetrazolium bromide (MTT) was used as the staining agent and zone of inhibition was observed as a colourless halo-like zone against a blue-coloured background. The assay was compatible with both normal as well as reverse phase silica plates. However normal-phase silica plates were found compatible with most extracts; their low cost and operational ease further warrants their use in the assay. Additive such as formic acid, trifluoracetic acid, methanolic ammonia were found to be detrimental to the assay; no cell growth was observed on the entire plates.

Five extracts were screened using TLC-bioautography assay against *S. aureus* SH1000 and *E. Coli* CMR400 each and only VF48A and *Staphylococcus* spp. P5-25 extracts were ideal candidates for further development. A family of cyclic dipeptides called 2,5-diketipiperazines were isolated from both strains. Fifteen DKPs were isolated altogether: cy(L-Tyr-L-Ile) **58**, cy(L-Leu-L-Pro) **59**, cy(L-Phe-D-Pro) **60**, cy(L-Leu-L-Ile) **61**, cy(L-Leu-L-Leu) **62**, cy(L-Phe-D-Tyr) **63** and cy(L-Phe-L-Leu) **64** from P5-25 extract, and cy(L-Phe-L-Pro-OH) **65**, cy(L-Leu-D-Pro) **66**, cy(L-Leu-L-Pro) **59**, cy(L-Phe-L-Pro) **67**, cy(L-Phe-D-Pro) **60**, cy(L-Val-L-Leu) **68**, cy(L-Phe-L-Tyr) **69**, cy(L-Tyrp-L-Pro) **70** and cy(L-Phe-L-Val) **71** and cy(L-Phe-L-Leu) **64** from VF48 extract. Furthermore, surfactin-type family of compounds were isolated from VF48A, however the sample size was very small for characterisation. This is the first report of selective antibacterial activity exhibited by DKPs. Interestingly, cy(L-Leu-L-Pro) **59**, cy(L-Phe-D-Pro) **60** and cy(L-Phe-L-Leu) **64** were found in both extracts. Although DKPs have been previously isolated from various sources in nature, this is the first report of isolation of cy(L-Phe-D-Pro) **60**, cy(L-Phe-D-Tyr) **63**, cy(L-Phe-L-Pro-OH) **65** and cy(L-Leu-D-Pro) **66** and cy(L-Phe-D-Val) **72**.

Thirteen DKPs were synthesised in this work and compared with natural DKPs isolated from *Bacillus* sp. VF48A and *Staphylococcus* spp. P5-25 extracts, and test against *S. aureus* SH1000 and *E. coli* CMR400. DKPs were isolated in 39–97% yield; epimerisation was observed for cy(L-Phe-D-Pro) **60**, cy(L-Phe-D-Tyr) **63**, cy(L-Phe-L-Leu) **64**, cy(L-Leu-D-Pro) **66** and cy(L-Phe-L-Val) **71**. Cy(L-Phe-D-Tyr) **63** and cy(L-Phe-D-Pro) **60** exhibited activity against *S. aureus* SH1000 at 128 µg/ml, whereas cy(L-Phe-L-Pro) **67** and cy(L-Leu-L-Pro) **59** exhibited activity against *S. aureus* SH1000 at 256 µg/ml. Cy(L-Phe-L-Val) **71** and cy(L-Phe-L-Leu) **64** was active against *E. coli* CMR400 at 256 µg/ml. Same selectivity and potency was observed for the synthetic analogues.

This is the first report of selective antibacterial activity exhibited by DKPs isolated from *Bacillus*. When cy(L-Phe-L-Tyr) **69** and cy(L-Phe-D-Tyr) **63** were tested against *S. aureus* SH1000 and *E. coli* CMR400, only cy(L-Phe-D-Tyr) **63** showed activity against *S. aureus*; no activity was recovered for either isomers against *E. coli* CMR400. Similarly, cy(L-Phe-D-Pro) **60** was 3 times more potent than cy(L-Phe-L-Pro) **67** against *S. aureus* SH1000, and no activity was recovered against *E. coli* CMR400. Lastly, cy(L-Phe-L-Val) **71** and cy(L-Phe-L-Leu) **66** was active against *E. Coli* CMR400 at 256 µg/ml and resistant to *S. aureus* SH1000. More importantly, the surfactin-type family of compounds found in VF48A extract could also be playing a role as OM-permeabilising (OM outer membrane) agent, facilitating efficient transportation of DKPs across the membrane in *E. coli*. thereby improving their efficacy. The synergistic effect of DKPs and role of surfactin-type compounds needs to be investigated in the future.

Chapter 6 Overall Conclusions and Future Work

6.1 Overall conclusions

In this thesis the diverse potential of natural products for their use in consumer products and as therapeutics was explored. In the first project, blackcurrant was studied extensively as a source for high value chemicals. A series of solvents were screened for their efficiency of extracting polyphenolic compounds including anthocyanins from blackcurrant waste: isopropylacetate, ethyl acetate, methanol, ethanol and water both in presence and absence of 0.1% *v/v* HCl. All extracts were analysed by HPLC, NMR and UV/Vis spectroscopy at every stage of the process to establish dynamic understanding of the extract. The use of a combination of techniques allowed circumvent some of the issues faced when using only one technique to characterise a complex natural product matrix. For example, not all compounds absorb at same wavelength therefore monitoring an extract by HPLC at one wavelength can give false results. Furthermore, overlapping bands in HPLC spectrum would also give inaccurate results. NMR spectroscopy can help resolve some of the issues. A combination of analytical techniques must always be used to accurately characterise a complex natural product mixture. The stability of anthocyanins was also studied, and it was found that even small amount of acid present in extraction solvents can degrade the rutinosides to their corresponding glucosides. This could explain, at least in part, the discrepancy found in reported amounts of anthocyanins in the literature. HPLC and total monomeric anthocyanin assay (TMAC) were compared for their reliability for quantification of anthocyanins in an anthocyanin-rich extract. It was found that TMAC assay was not a reliable technique for quantification of anthocyanins in crude extracts and juices; HPLC should be used instead. This work has been published in Journal of Agricultural and Food Science. [3]

The second part of this thesis was focussed on discovery of antibacterial compounds from crude microbial extracts. These projects were done in close collaboration with Dr Alex O'Neill and his PhD students Dr Nada Nass, Zeyad AlZeyadi and Luiza Galarion. Two strategies were used for this purpose: (1) revisiting previously discarded antibiotic compounds, (2) exploring human microbiota. In the first part of antibiotic project drawing inspiration from success of daptomycin, linezolid and fidaxomicin, previously discarded class of antibacterial agents called the actinorhodins (ACTs) was revisited. This is the first report of full characterisation of **46** in its native form. Full biological evaluation was performed by Nada Nass and this work has been published.[100] These studies revealed that the γ-actinorhodin **46** pharmacophore in fact displays potent antistaphylococcal

activity and possesses many of the requisite properties of a useful antibacterial drug. Last part of this work aimed to explore potential of human microbiota as a source for novel antibiotic compounds. Zeyad alZeyadi and Luiza Galarion initially found several hit extracts active against *S. aureus* SH1000 and multidrug-resistant *E. coli* CMR400 respectively. However, the process of extracting and purifying complex natural product extracts can be a very laborious process. Therefore, a robust TLC-bioautography assay was developed to improve efficiency of the discovery process; this method allows faster screening of the crude extracts and only promising extracts are taken to the next stage. It also gives an idea about nature of the compounds in the extract which in turn helps to plan a targeted purification protocol. Furthermore, the extracts containing sensitive (UV, temperature and solvent sensitive) and easily degradable compounds can also be ruled out. This method also allows dereplication of known compounds which has been an issue in antibiotic discovery in the past. MB32, MB5B, RC14, P5-25 and VFF48A crude extracts were screened using TLC-bioautography assay; P5-25 and VF48A extracts were taken forward to next stage of purification. P5-25 was active against *S. aureus* SH1000 whereas VF48A was active against multi-drug resistant *E. coli* CMR400. Surprisingly both extracts were found to contain a known family of compounds 2,5-diketopiperazines; this is the first report of isolation and full characterisation of these DKPs. Although some of these DKPs have been reported before (assignment based on mass data), full characterisation data is unavailable. All compounds were fully characterised using optical rotation, mass spectrometry, IR, 1-D and 2-D NMR spectroscopy. This study forms basis for data bank for these useful compounds.

Thirteen DKPs were synthesised in this work and compared with natural DKPs isolated from *Bacillus* sp. VF48A and *Staphylococcus* spp. P5-25 extracts and tested against *S. aureus* SH1000 and *E. Coli* CMR400. Cy(L-Phe-D-Tyr) **63** and cy(L-Phe-D-Pro) **60** exhibited activity against *S. aureus* SH1000 at 128 µg/ml, whereas cy(L-Phe-L-Pro) **67** and cy(L-Leu-L-Pro) **59** exhibited activity against *S. aureus* SH1000 at 256 µg/ml. Cy(L-Phe-L-Val) **71** and cy(L-Phe-L-Leu) **64** was active against *E. coli* CMR400 at 256 µg/ml. This is first report of selectivity of bioactivity exhibited by DKPs. Same bioactivity and selectivity was recovered for the synthetic samples too. DKPs were purified in 39–97% yield; epimerisation was observed for cy(L-Phe-D-Pro) **60**, cy(L-Phe-D-Tyr) **63**, cy(L-Phe-L-Leu) **64**, cy(L-Leu-D-Pro) **66** and cy(L-Phe-L-Val) **71**. It was observed that for planar side chains, *cis*-configuration was preferred; therefore cy(L-Phe-D-Pro) **60** and cy(L-Phe-D-Tyr) **63** epimerised efficiently to give cy(L-Phe-L-Pro) **67** cy(L-Phe-L-Tyr) **69** predominantly. Opposite trend was observed for isopropyl and butyl side chains; cy(L-Phe-D-Val) **72** and cy(L-Phe-D-Leu) **73** were preferred isomers. The effect of side chains needs to be further investigated.

6.2 Future Work

The blackcurrant extract was studied extensively in this project and an improved method of extraction has been proposed to Keracol Ltd. This new method would allow access to three product streams of high value chemicals. It would be interesting to see the new method to be scaled up to pilot plant. In the past, pilot scale extraction was found to be more efficient process than lab-scale method. Therefore, same results can be expected for the new method as well. Furthermore, polymeric anthocyanins which make up 18% of the extract should be further investigated. This would form a separate PhD project due to nature of polymers. A detailed study of these polymeric anthocyanins would allow insight into the nature of monomeric sub-units. This is crucial as they could lead to another product stream. Conventionally, polymers are degraded into their monomeric counterparts using acid hydrolysis. However, enzymatic degradation could achieve better yields and specificity.

TLC–bioautography method developed in this project has been very useful in screening crude extracts. In the future it should be developed into TLC–bioautography–MS assay so that the active spots can be identified quickly and dereplicated for known compounds. This work would be good for a Masters project. Firstly, a series of known compounds of varying molecular weights should be shortlisted and made up to same concentration using appropriate solvent. These compounds would then be loaded onto normal phase as well reverse phase silica plates and developed using standard method. The spots from developed plates would be processed and analysed by LC–MS. This would allow us to establish limit of quantification (LoQ) and limit of detection (LoD) of this method. In the next step a series of crude extracts with known chemical composition and bioactivity should be screened using previously established LoQ and LoD parameters. Furthermore, elution methods for these crude extracts should be developed on LC-MS instrument as standard methods (1-minute-long) are unlikely to separate complex mixtures of natural products. Once these systems are place it would be possible to screen tens of bioactive extracts and dereplicate them for known compounds. This would ensure only extracts with novel activity and compounds are taken to the next stage which in turn can potentially speed up process of antibiotic discovery from natural sources.

Lastly, DKPs should be synthesised and synergistic studies should be performed to gain better understanding of their antibacterial activity profile. Furthermore, they should be tested in presence of surfactin-type compounds to understand the role of co-occurring membrane-disorganising compounds in natural extracts. This coupled with TLC–bioautography–LCMS assay would speed up the discovery process dramatically. Although, a detailed study of the effect of side chains on yield and epimerisation of final

DKPs was out of scope of this project, it certainly warrants further work. A systematic study of synthesis of DKPs can help improve yields as well as understanding of these simple yet synthetically useful compounds.

Chapter 7 Experimental

7.1 General Methods

Nuclear magnetic resonance (NMR) spectra were recorded for ^{1}H at 300 and 500 MHz and ^{13}C at 75 and 125 MHz on a Bruker DPX300 or DRX500 spectrometer. Bruker DRX 500 spectrometer was equipped with a multinuclear inverse probe for one-dimensional ^{1}H and two-dimensional heteronuclear single quantum coherence (^{1}H−^{13}C HSQC), heteronuclear multiple bond correlation (^{1}H−^{13}C HMBC), and double quantum filtered correlation (^{1}H−^{1}H COSY). Chemical shifts (δ) are quoted in ppm downfield of tetramethylsilane or residual solvent peaks (3.31 and 49.0 ppm for CD$_3$OD in ^{1}H and ^{13}C, respectively; 110 and 160 ppm for CF$_3$COOD). The coupling constants (J) are quoted in Hz (multiplicities: s singlet, bs broad singlet, d doublet, t triplet, q quartet and apparent multiplicities are described as m). The samples were either dissolved in CD$_3$OD or CD$_3$OD-CF$_3$COOD (95:5, anthocyanins).

The analytical TLC chromatography was carried out using alumina-backed plates coated with silica gel 60 with a fluorescence indicator (20 × 20 cm, Merck) and nanosilica gel C18-100 with a fluorescence indicator (10 × 10 cm; no. 811062). HPLC system (Agilent 1290 infinity series) was equipped with diode-array detector (DAD), binary pump system connected with online degasser and Zorbax Eclipse XDB C18, 150 × 4.6 mm, 5 µm. The flow rate and the injection volume were 1 mL/min and 10 µL respectively. The chromatograms were recorded by scanning the absorption at 190−600 nm. UV/Vis analysis was carried out using a Jasco V630 UV-Vis spectrophotometer. High resolution mass spectra (HRMS) were recorded on a Dionex Ultimate 3000 spectrometer using electron spray ionisation (ESI). All masses quoted are correct to four decimal places. Infrared (IR) spectra were recorded using a PerkinElmer Spectrum One FT-IR spectrophotometer or Bruker Alpha Platinum AR FTIR. Vibrational frequencies are reported in wavenumbers (cm^{-1}).

Liquid chromatography was carried out on Agilent 1200 LC with a Bruker HCT Ultra Ion Trap for MS detection and a photodiode array detector (PAD) for UV/Vis measurements. The electron spray ionisation (ESI) parameters for the positive ionisation (PI) mode were as follows: spray voltage: 4000 V; dry gas flow rate: 10 dm^3 min^{-1}; dry gas temperature:

365 °C; capillary: 60 nA; nebulising pressure: 65 psi; nebulising gas: N_2. The ESI (electrospray ionisation) parameters in the NI (negative ion) mode were as follows: spray voltage 4000 V (applied to the spray tip needle), dry gas 10 dm^3 min^{-1}, dry temperature 365 °C, capillary 60 nA, nebulizer 65 psi, nebulising gas N_2. Solvents were removed under reduced pressure using a Buchi rotary evaporator at 20 mbar, followed by further drying under high vacuum at 0.5 mmHg. To measure the melting points 2-3mm of sample was placed in the bottom of the capillary tube and the tube places in the heating block. The 'melting point' was measured as the range from the appearance of the first liquid droplet until complete melting of the crystals. The measurements were carried out on a Mettler Toledo melting point system

7.2 Materials

All solvents and reagents were purchased from commercial sources. The solvents were HPLC standard and purchased from Sigma Aldrich. Chemicals were purchased from Sigma-Aldrich (Dorset, UK) and Flurochem Ltd. (Glossop, UK) unless stated otherwise. Delphinidin-3-*O*-*β*-glucoside (dp3glc) was purchased from Polyphenol AS, Sandnes, Norway. Amberlite XAD–7HP was prchased from Rohm & Haas, Staines, UK.

Blackcurrant waste was obtained from GlaxoSmithKline (GSK) and more recently from A. R. House Ltd. UK, after the raw fruit grown in the UK was pressed in production of blackcurrant cordial (*Ribena*). The crude waste is referred to as pomace, which comprises the fruit skins (*ca*. 50 wt. %), seeds (*ca*. 45 wt. %) and extraneous matter (*e.g*. berry stalks, ca. 5 wt. %). GSK separated the seeds from this pomace (the seeds are a valuable source of γ-linolenic acid) and removed unwanted stalks; the material received was dried blackcurrant skins. Keracol Ltd. provided their blackcurrant extract for analysis and comparison with the fresh extracts. Natural extracts from microbial sources were provided by PhD students in Dr Alex O'Neill lab. The protocols on how to prepare these natural extracts from broth and agar were developed and provided by the author.

7.3 Biological Studies

7.3.1 Strains and Growth Conditions

Biological evaluation and profiling were done by PhD students in Dr Alex O'Neill group: Dr Nada Nass for *Streptomyces coelicolor* L646, Zeyad alzeyadi for *Staphylococcus aureus* P5–25 and Luiza Galarion for *Bacillus* VF48A projects. Laboratory strains of bacteria and yeast used in this study are listed in Table 1.1. Clinical isolates of *S. aureus*

used for susceptibility testing were part of a culture collection belonging to the Antimicrobial Research Centre, University of Leeds. The actinorhodin overproducer strain Streptomyces coelicolor, L646 (kindly provided by K. McDowall, University of Leeds), was used as the source of γ-actinorhodin and was propagated on ISP medium 2 (Difco) containing 50 µg/ml apramycin at 30 °C. *Staphylococcus aureus* P5–25 and *Bacillus* VF48A were collected from skin samples and sequenced by Zeyad alZeyadi and Luiza Galarion.

Bacteria (except for *S. coelicolor* L646) were routinely cultured in Mueller Hinton broth (MHB) and on Mueller-Hinton agar (MHA) (Oxoid Ltd, Cambridge, UK) at 37 °C for 24 h, whilst *Candida albicans* was grown in Lysogeny broth (LB) and on Lysogeny agar (LA) (Oxoid) at 35 °C for 48 h. *Bacillus* VF48A was grown in Brain Heart Infusion (BHI) whereas *S. aureus* P5-25 was grown in tryptic soy broth (TSB), both at 37 °C overnight.

7.3.2 Spot Inoculation Method

To initially check and confirm the activity of *Bacillus* VF48A, a 2 µL of the isolate grown overnight in Brain Heart Infusion (BHI) broth was spot inoculated on chocolate agar and incubated at 37 °C for 3 days. Plates with mature colonies were each overlaid with 5 ml of soft agar (5 g/L bacteriological agar + 13 g/L nutrient broth in 1 L distilled water) containing 1:10 dilution of OD_{625} = 0.08 (equivalent to 10^8 cells) *E. coli* CM400, or with 1:2 OD_{625} = 0.20 of *Candida albicans* CA6. Plates were incubated at 37 °C for 24 to 48 h and zones of inhibition were measured (ZOI).

7.3.3 Spent Medium Assay

Isolates were grown in 10 ml BHI broth for 3 days and centrifuged at > 4,000 × g for 12 min to pellet cells. The supernatant of each isolate was collected, passed through 0.20 µm Millex ® syringe-driven filter unit (Merck KGaA, Darmstadt, Germany), then used directly. Using a sterile 1 cm cork borer, wells were punched through Mueller-Hinton II agar plates seeded with either *E. coli* CM400 (OD_{625} = 0.08) or *C. albicans* CA6 (OD_{625} = 0.20). A 100 µL of each isolate's filtrate was then added into its corresponding well. The plates were incubated and observed for zones of inhibition (ZOI) the following day.

Table 7.1. The names and sources of strains used in this work. ATCC: American Type Culture Collection; NCTC: National Collection of Type Culture; LGI: Leeds General Infirmary.

Bacterial strains	Genotype or description	Reference
S. aureus SH100	Laboratory strain derivative of strain 8325-4, containing functional *rsbU*	Horsburg *et al.*[156]
S. epidermidis ATCC 14490	Control strain for *Staphylococcus epidermidis* isolated from nose	ATCC
S. haemolyticus 41207	Control strain for *Staphylococcus haemolyticus* isolated from human skin	ATCC
S. pyogenes ATCC 19615	Control strain for *Streptococcus* Group A isolated from pharynx of child following episode of sore throat	ATCC
S. pneumoniae ATCC R6	Non-virulent strain	ATCC
E. faecalis ATCC 29212	Control strain for *Enterococcus faecalis* isolated from urine	ATCC
E. faecium 7634337	Vancomycin resistant enterococci (VRE) strain	LGI
E. coli BW25113	Derivative of *E. coli* K12 strain BD792 (*lacI^q rrnB_{T14}ΔlacZ_{WJ16}hsdR514ΔaraBAD_{AH33}ΔrhaBAD_{LD78}*)	Baba *et al.*[157]
K. pneumoniae K25	Unencapsulated wild-type strain isolated from clinical specimen	NCTC
A. baumannii ATCC 19606	Control strain for *Acinetobacter baumannii* isolated from urine	ATCC
P. aeruginosa PO1	Opportunistic strain of *Pseudomonas* isolated from infected wound	ATCC
S. coelicolor L646	*S. coelicolor* M145 containing an integrating plasmid overexpressing wild-type *atrA,* which leads to hyperproduction of actinorhodin	Towle *et al.*[158]
Candida albicans CA-6	Azole-sensitive strain with normal sterol profile	Martel *et al.*[159]
E. coli CM400	Derivative of *E. coli* MG-1655 strain	Gullo *et al.*[160]

7.3.4 Disc Diffusion Assay

All test organisms were prepared as cell suspension in MHB II by diluting overnight cultures of *E. coli* CM400, *S. aureus* SH1000, *E. faecium* VSE, *K. pneumoniae* D11, *A. baumanii* A1, *P. aeruginosa* PAO11, *E. cloacae* A2 with final OD_{600} 0.08 or *C. albicans* with final OD_{600} 0.20. To seed a plate, a sterile cotton swab was dipped in the cell suspension and spread onto the MHA II plate using electric rotary plater. The crude extracts were dissolved in methanol (2 mL) and sonicated to homogenise the solutions. Using a sterile 6 mm cork borer, wells were punched through MHA II plates freshly seeded with the test organism. 2.5 mg of the crude extract was loaded onto each 6 mm blank antibiotic discs (GE Healthcare Whatman, Little Chalfont, Bucks), then laid on top of the seeded MHA II plates. Methanol was used as a control. Plates were then incubated at 37 °C overnight and resulting diameter of ZOI (zone of inhibition) were measured.

7.3.5 TLC−Bioassay Protocol

All experiments were done in duplicates. The crude extracts were dissolved in methanol (2 mL) and sonicated to homogenise the mixture. Alumina-backed plates coated with silica gel 60 with a fluorescence indicator (20 × 20 cm, Merck) and nanosilica gel C18−100 with a fluorescence indicator (10 × 10 cm; no. 811062) were pre-eluted with methanol and dried with a hair dryer prior to use. 600 µg of the crude extract was loaded onto the plates using a micro-pipette. After air drying the plates were developed in a classic TLC chamber using DCM/MeOH (95:5) or $MeCN/H_2O$ (60:40) for C18 plates. The UV active spots were visualised under UV irradiation (λ= 254 nm); ninhydrin dip was used for the spots which were not UV active on the duplicates. Developed TLC plates were dipped for 10 s in a glass chamber containing the test organism (1:10 of an undiluted overnight culture) in MHB II with 0.05% soft agar and 5% of 2 mg/mL MTT (3-(4,5-dimethylthiazol-2-yl)-2,5-diphenyltetrazolium bromide) dissolved in 0.01 M TES buffer pH 7.2 (Sigma-Aldrich, Frankfurter, DA). Dipped plates were then incubated overnight in a moist environment at 37 °C. Metabolically active cells reduce the colourless MTT to purple or blue coloured formazan, whereas dead cells do not affect the colourless MTT. Therefore, activity of an antibiotic compound is observed as a colourless zone of inhibition against a deep blue background.

7.3.6 Standard Susceptibility Testing

The Minimum Inhibitory Concentrations (MICs) of antibiotics against bacterial isolates was determined by broth microdilution according to Clinical and Laboratory Standards

Institute (CLSI) guidelines (CLSI 2012). Antifungal activity was assessed in essentially the same way, though used LB in place of MHB, and MICs were read after 48 h incubation at 35 °C. Media was supplemented with 4 µg/ml polymyxin B nonapeptide (PMBN) to test the role of membrane permeability on antibiotic delivery against Gram negative bacteria (Vaara 1992). Following incubation, the MIC was defined as the lowest concentration of antibiotic that inhibited all visible growth. MIC determination with appropriate comparator antibiotics was undertaken to permit comparison of the antibacterial activity of the investigated natural products with existing clinical agents against the tester strains. Positive control (growth control) and solvent control were included in each experiment. Susceptibility testing was conducted on a minimum of three independent occasions to ensure reproducibility.

7.3.7 Time-Dependent Killing (time-kill) Studies

Studies to determine the bactericidal activity were carried out on exponential-phase cultures using a method described elsewhere (Ooi *et al*. 2013). Briefly, bacteria were cultured to early exponential phase and diluted to a final density of 10^5–10^6 CFU/ml in MHB and challenged with antibacterial agents at 4x MIC. Time-kill experiments were also performed with bacterial cells in non-growing states. Overnight cultures of SH1000 were harvested by centrifugation and cells were re-suspended in the spent supernatant to 10^5–10^6 CFU/ml before exposure to antibacterial agents. Following antibiotic challenge, bacterial viability was monitored by plating cultures onto MHA, and enumerating colonies after incubation at 37 °C for 18–24 h to allow plotting of log10 CFU/ml versus time. Bactericidal activity was defined as a reduction of ≥ 3 $\log_{10}$ CFU/ml relative to the initial inoculum (Petersen, Jones and Bradford 2007; CLSI 1999). All experiments were performed in three independent cultures and values are expressed as mean ± standard deviation (SD).

7.4 Extraction of Natural Compounds

7.4.1 Extraction of High Value Chemicals from Blackcurrant Waste

Dried blackcurrant fruit epicarp (dried skins, 30 g) were immersed in 600 mL water acidified with 0.1% *v/v* conc. HCl and stirred gently by magnetic follower at room temperature for 2 h. The plant material was filtered off and the resulting aqueous extract was loaded onto an Amberlite XAD-7HP resin (60 g) until the eluent was almost colourless. Resin was then washed with acidified water (0.1% *v/v* conc. HCl, 1L), to get remove small sugar molecules and organic acids, before eluting the polyphenols with

acidified ethanol (0.1% *v/v* conc. HCl, 1L). The collected ethanol fractions were combined and concentrated under vacuum on a rotary evaporator, and then subjected to high vacuum to remove trace solvent, yielding a dark violet amorphous solid (660 mg, yield 2.2%). When ethanol, methanol and aqueous ethanol (1:1) was used as extraction solvents the yields were 0.3%, 2.6% and 1.4% respectively. All the extracts were analysed by UV/Vis and HPLC before and after solid-phase extraction.

^{1}H NMR and HPLC analyses confirmed the presence of four anthocyanins and other polyphenols in the extracts. The dried blackcurrant extract (500 mg) was then dissolved in acidified water (50 mL, 0.1% *v/v* conc. HCl) and partitioned against isopropylacetate (1 × 70 mL) and ethyl acetate (3 × 50 mL) in sequential manner. The organic layers were dried under reduced pressure to give isopropylacetate (yellow amorphous solid, 68.5 mg) and ethyl acetate extracts (yellow amorphous solid, 33 mg), whereas aqueous layer was freeze-dried to afford 398.5 mg (red amorphous solid) extract. These three fractions were further purified by preparative HPLC.

7.4.2 Extraction of γ-actinorhodin (γ-ACT) from *S. coelicolor* L646

S. coelicolor L646 was grown on ISP2 agar at 30 °C for six days, at which point the medium turned deep blue in colour owing to secretion of actinorhodins. The agar was cut into small pieces, and the pigment extracted twice with ethyl acetate at 30 °C for an hour with shaking (200 rpm). The resulting ethyl acetate layers were combined and dried under *vacuo* to give red glassy solid (600 mg). The yield was comparative when agar pieces were extracted with ethyl acetate at room temperature overnight. The yield was 10 times lower when acetone was used as extraction solvent (50 mg). Moreover γ-actinorhodin could not be detected by ^{1}H NMR. The presence of γ-actinorhodin was confirmed by ^{1}H NMR and TLC analyses. No other congeners of actinorhodin were identified in the extract.

7.4.3 Extraction of Diketopiperazines from *Staphylococcus aureus* P5-25

The producer strain was grown overnight in MHB broth 200 ml at 37 °C with agitation, and whole cultures were extracted twice with chloroform (2 × 70 mL). The organic layers were combined and evaporated on *vacuo* to give pale yellow extract (18 mg). The extract was further purified by preparative HPLC. The yield was relatively poor when diethyl ether or isopropylacetate were used as extracting solvents. Sequential extraction with

hexane, isopropylacetate and chloroform did not facilitate selective uptake of the targeted compounds.

7.4.4 Extraction of Diketopiperazines from VF48A

1 L BHI broth was inoculated with the isolate and left to grow at 37 °C with continuous shaking (200 rpm) for 72 h. After incubation, the cell cultures were extracted against ethyl acetate (2 × 300 mL). The organic layers were combined and dried *in vacuo* to give pale yellow glassy solid (30 mg). The extract was further purified by preparative HPLC.

7.5 Analytical HPLC

The extracts were analyed by HPLC at every stage of the extraction and purification. The analytical HPLC system (Agilent 1290 infinity series) was equipped with diode-array detector (DAD), binary pump system connected with online degasser. The flow rate and the injection volume were 1 mL/min and 10 μL respectively. The chromatograms were recorded by scanning the absorption at 190−600 nm.

7.5.1 Analytical HPLC for Blackcurrant Extracts

The anthocyanins were monitored at 520 nm, flavonoids at 350 and hydroxycinnamates at 325 nm. The extracts were loaded on to Zorbax Eclipse XDB C18, 150 × 4.6 mm, 5 μm. For aqueous extract (anthocyanin analysis), the binary solvent system consisted of solvent A: water (0.5% TFA) and solvent B: acetonitrile (0.5% TFA). The elution profile consisted of linear gradient from 5% B to 20% B in the first 20 min, then linear increase to 100% B at 20−23 min followed by isocratic elution (100% B) at 23−24 min, and then linear decrease to 5% B at 24−25 min followed by 5% B isocratic elution at 25−30 min.

For ethyl acetate and isopropylacetate extracts: the binary solvent system consisted of solvent A: water (0.1% TFA) and solvent B: acetonitrile (0.1% TFA). The elution profile consisted of a linear gradient from 5% B to 20% B in the first 30 min, then linear increase to 100% B at 30−33 min followed by isocratic elution (100% B) at 33−34 min, and then linear decrease to 5% B at 34−35 min followed by 5% B isocratic elution at 35−40 min.

7.5.2 Analytical HPLC for γ-Actinorhodin

Purified actinorhodin was loaded onto Hyperclone C18, 150 × 4.6 mm, 5 μm and monitored at 520 nm. The binary solvent system consisted of solvent A: water and solvent B: acetonitrile. The elution profile consisted of linear gradient from 5% B to 20% B in the first 20 min, then linear increase to 100% B at 20−23 min followed by isocratic elution (100% B) at 23−24 min, and then linear decrease to 5% B at 24−25 min followed by 5% B isocratic elution at 25−30 min.

7.5.3 Analytical HPLC for Diketopiperazines from *S. aureus* P5-25 Extract

Purified fractions were loaded onto Ascentis express C18, 150 × 4.6 mm, 5 µm and monitored at 220 nm. The binary solvent system consisted of solvent A: water (0.1% TFA) and solvent B: acetonitrile. The elution profile consisted of linear gradient from 5% B to 95% B in the first 5 min, then linear increase to 100% B at 5−6 min followed by isocratic elution (100% B) at 6−8 min, and then linear decrease to 5% B at 8−9 min followed by 5% B isocratic elution at 9−10 min.

7.5.4 Analytical HPLC Diketopiperazines from VF48A Extract

Purified fractions were loaded onto Ascentis express C18, 150 × 4.6 mm, 5 µm and monitored at 220 nm. The binary solvent system consisted of solvent A: water (0.1% TFA) and solvent B: acetonitrile. The elution profile consisted of linear gradient from 5% B to 95% B in the first 10 min, then linear increase to 100% B at 10−11 min followed by isocratic elution (100% B) at 11−13 min, and then linear decrease to 5% B at 13−14 min followed by 5% B isocratic elution at 14−15 min.

7.6 Preparative HPLC Method Development

The extracts were dissolved in appropriate solvents and filtered before loading onto the preparative columns. The HPLC system (Agilent 1200 infinity series) was equipped with diode-array detector (DAD) and binary pump system connected with online degasser.

7.6.1 Preparative HPLC Method 1

The blackcurrant extract (30 mg) was dissolved in H_2O/EtOH 9:1 (0.1% HCl *v*/*v*, 2 mL). The aqueous extract was filtered and loaded ($\lambda_{collect}$ = 520 nm) on to XBridge^{TM} Prep C18 OBD^{TM} 19 × 100, 5 µm and eluted using gradient solvent system. The binary solvent system consisted of solvent A: water with 0.1% formic acid and solvent B: acetonitrile. The elution profile consisted of linear gradient from 5% B to 20% B in the first 20 min, then linear increase to 100% B at 20−23 min followed by isocratic elution (100% B) at 23−24 minutes, and linear decrease to 5% B at 24−25 min followed by 5% B isocratic elution at 25−30 minutes. The flow rate was 20 ml/min and the peaks were monitored at 254, 285, 325, 350 and 520 nm.

7.6.2 Preparative HPLC Method 2

The blackcurrant extract (30 mg) was dissolved in H_2O/EtOH 9:1 (0.1% HCl *v*/*v*, 2 mL). The aqueous extract was filtered and loaded ($\lambda_{collect}$ = 520 nm) onto XBridge^{TM} Prep C18 OBD^{TM} 19 × 100, 5 µm and eluted using gradient solvent system. The binary solvent

system consisted of solvent A: water with 0.1% formic acid and solvent B: methanol. The elution profile consisted of linear gradient from 5% B to 20% B in the first 20 min, then linear increase to 100% B at 20−23 min followed by isocratic elution (100% B) at 23−24 minutes, and then linear decrease to 5% B at 24−25 min followed by 5% B isocratic elution at 25−30 minutes. The flow rate was 20 ml/min and the peaks were monitored at 254, 285, 325, 350 and 520 nm.

7.6.3 Preparative HPLC Method 3

The blackcurrant extract (30 mg) was dissolved in H_2O/EtOH 9:1 (0.1% HCl v/v, 2 mL). The aqueous extract was and filtered and loaded ($\lambda_{collect}$ = 520 nm) onto XBridge^{TM} Prep C18 OBD^{TM} 21.2 × 250, 5 μm and eluted using gradient solvent system. The binary solvent system consisted of solvent A: water with 0.1% formic acid and solvent B: acetonitrile. The elution profile consisted of linear gradient from 5% B to 20% B in the first 20 min, then linear increase to 100% B at 20−23 min followed by isocratic elution (100% B) at 23−24 minutes, and then linear decrease to 5% B at 24−25 min followed by 5% B isocratic elution at 25−30 minutes. The flow rate was 20 ml/min and the peaks were monitored at 254, 285, 325, 350 and 520 nm.

7.6.4 Preparative HPLC Method 4

The blackcurrant extract (30 mg) was dissolved in H_2O/EtOH 9:1 (0.1% HCl v/v, 2 mL). The aqueous extract was filtered and loaded ($\lambda_{collect}$ = 520 nm) onto XBridge^{TM} Prep C18, 10 × 50, 5 μm and eluted using gradient solvent system. The binary solvent system consisted of solvent A: water with 0.1% formic acid and solvent B: acetonitrile. The elution profile consisted of linear gradient from 5% B to 20% B in the first 20 min, then linear increase to 100% B at 20−23 min followed by isocratic elution (100% B) at 23−24 minutes, and then linear decrease to 5% B at 24−25 min followed by 5% B isocratic elution at 25−30 minutes. The flow rate was 5 ml/min and the peaks were monitored at 254, 285, 325, 350 and 520 nm.

7.6.5 Preparative HPLC Method 5

The blackcurrant extract (30 mg) was dissolved in H_2O/EtOH 9:1 (0.1% HCl v/v, 2 mL). The aqueous extract was filtered and loaded ($\lambda_{collect}$ = 520 nm) onto XBridge^{TM} Prep C18, 10 × 50 mm, 5 μm and eluted using gradient solvent system. The binary solvent system consisted of solvent A: water with 0.1% formic acid and solvent B: acetonitrile. The elution profile consisted of linear gradient from 5% B to 20% B in the first 30 min, then linear increase to 100% B at 30−33 min followed by isocratic elution (100% B) at 33−34 minutes, and then linear decrease to 5% B at 34−35 min followed by 5% B isocratic

elution at 35−40 minutes. The flow rate was 5 ml/min and the peaks were monitored at 254, 285, 325, 350 and 520 nm.

7.6.6 Preparative HPLC Method 6

The blackcurrant extract (30 mg) was dissolved in H_2O/EtOH 9:1 (0.1% HCl *v*/*v*, 2 mL). The aqueous extract was filtered and loaded ($\lambda_{collect}$ = 520 nm) onto XBridge™ Prep C18, 10 × 50, 5 µm and eluted using gradient solvent system. The binary solvent system consisted of solvent A: water with 0.5% formic acid and solvent B: acetonitrile. The elution profile consisted of linear gradient from 5% B to 20% B in the first 30 min, then linear increase to 100% B at 30−33 min followed by isocratic elution (100% B) at 33−34 minutes, and then linear decrease to 5% B at 34−35 min followed by 5% B isocratic elution at 35−40 minutes. The flow rate was 5 ml/min and the peaks were monitored at 254, 285, 325, 350 and 520 nm.

7.6.7 Preparative HPLC Method 7

The blackcurrant extract (20 mg) was dissolved in H_2O/EtOH 9:1 (0.1% HCl *v*/*v*, 2 mL). The aqueous extract was filtered and loaded ($\lambda_{collect}$ = 520 nm) onto XBridge™ Prep C18 10 × 50 mm, 5 µm and eluted using gradient solvent system. The binary solvent system consisted of solvent A: water with 0.1% trifluoroacetic acid and solvent B: acetonitrile. The elution profile consisted of linear gradient from 5% B to 20% B in the first 30 min, then linear increase to 100% B at 30−33 min followed by isocratic elution (100% B) at 33−34 minutes, and then linear decrease to 5% B at 34−35 min followed by 5% B isocratic elution at 35−40 minutes. The flow rate was 5 ml/ min and the peaks were monitored at 254, 285, 325, 350 and 520 nm.

7.6.8 Preparative HPLC Method 8

The blackcurrant extract (20 mg) was dissolved in H_2O/EtOH 9:1 (0.1% HCl *v*/*v*, 2 mL). The aqueous extract was filtered and loaded ($\lambda_{collect}$ = 520 nm) onto XBridge™ Prep C18 10 × 50 mm, 5 µm and eluted using gradient solvent system. The binary solvent system consisted of solvent A: water with 0.5% trifluoroacetic acid and solvent B: acetonitrile. The elution profile consisted of linear gradient from 5% B to 20% B in the first 30 min, then linear increase to 100% B at 30−33 min followed by isocratic elution (100% B) at 33−34 minutes, and then linear decrease to 5% B at 34−35 min followed by 5% B isocratic elution at 35−40 minutes. The flow rate was 5 ml/ min and the peaks were monitored at 254, 285, 325, 350 and 520 nm. This was the finalised method for purification of anthocyanins from blackcurrant extract.

7.6.9 Preparative HPLC Method 9

The dried ethyl acetate and isopropyl acetate extracts (after partitioning experiments with aqueous blackcurrant extract) were dissolved in H_2O/EtOH 1:1 (0.1% HCl *v/v,* 2 mL) and filtered. They were loaded in two different runs ($\lambda_{collect}$ = 520 nm) onto XBridge™ Prep C18 OBD™ 19 × 100 mm, 5 µm and eluted using gradient solvent system. The binary solvent system consisted of solvent A: water and solvent B: acetonitrile (no additive was used). The elution profile consisted of linear gradient from 5% B to 20% B in the first 20 min, then linear increase to 100% B at 20−23 min followed by isocratic elution (100% B) at 23−24 minutes, and linear decrease to 5% B at 24−25 min followed by 5% B isocratic elution at 25−30 minutes. The flow rate was 20 ml/ min and the peaks were monitored at 254, 285, 325, 350 and 520 nm.

7.6.10   Preparative HPLC Method 10

The Z18 extract (18 mg) was dissolved in methanol (2 mL) and filtered. It was then loaded onto Kinetex^R C18 LC Column, 21.2 × 100 mm, 5 µm in 300 µL injections and eluted using gradient solvent system. The binary solvent system consisted of solvent A: water with 0.1% TFA and solvent B: acetonitrile. The elution profile consisted of linear gradient from 5% B to 60% B in the first 30 min, then linear increase to 100% B at 30−31 min followed by isocratic elution (100% B) at 31−34 minutes, and linear decrease to 5% B at 34−35 min followed by 5% B isocratic elution at 35−36 minutes. The flow rate was 15 ml/ min and the peaks were monitored at 210, 220, 230 and 254 nm.

7.6.11   Preparative HPLC Method 11

The VF48A extract (30 mg) was dissolved in methanol (2mL) and filtered. It was then loaded onto Kinetex^R C18 LC Column, 21.2 × 100 mm, 5 µm in 300 µL injections and eluted using gradient solvent system. The binary solvent system consisted of solvent A: water with 0.1% TFA and solvent B: acetonitrile. The elution profile consisted of linear gradient from 5% B to 32% B in the first 25 min, then linear increase to 100% B at 25−26 min followed by isocratic elution (100% B) at 26−28 minutes, and linear decrease to 5% B at 28−29 min followed by 5% B isocratic elution at 29−30 minutes. The flow rate was 15 ml/ min and the peaks were monitored at 210, 220, 230 and 254 nm

7.6.12   Preparative HPLC Method 12

The synthetic samples were dissolved in methanol or DMSO (2 mL) and filtered. They were loaded onto Kinetex^R C18 LC Column, 21.2 × 100 mm, 5 µm in 300 µL injections and eluted using gradient solvent system. The binary solvent system consisted of solvent A: water with 0.1% TFA and solvent B: acetonitrile. The elution profile consisted of linear

gradient from 5% B to 60% B in the first 20 min, then linear increase to 100% B at 20−21 min followed by isocratic elution (100% B) at 21−23 minutes, and linear decrease to 5% B at 23−24 min followed by 5% B isocratic elution at 24−25 minutes. The flow rate was 15 ml/ min and the peaks were monitored at 210, 220, 230 and 254 nm.

7.7 Purification of the Natural Compounds

7.7.1 Purification of Polyphenols from Blackcurrant Extracts

The aqueous layer after liquid-liquid partitioning experiments was dried and 20 mg was re-dissolved in H_2O/EtOH (9:1, 2 ml, acidified with 0.1% *v/v* HCl). It was then purified using method given in section **7.6.7** on semi-preparative HPLC to give anthocyanins. The flow rate was 5 ml/min and five peaks were collected at 520 nm to give delphinidin-3-*O*-*β*-rutinoside (4.5 mg), cyanidin-3-*O*-*β*-rutinoside (4.1 mg), delphinidin-3-*O*-*β*-glucoside (1.6 mg) and cyanidin-3-*β*-*O*-glucoside (0.8mg) and polymeric anthocyanins (4.5 mg).

The isopropylacetate extract (15 mg) and ethyl acetate extract (10 mg) were both dissolved in methanol (2 ml) and purified on a semi-preparative column using method given in section **7.6.8**. The peaks were monitored at 325 for isopropyl acetate and 350 for ethyl acetate extracts. Caffeic acid (3.3 mg), *p*-coumaric acid (5.5 mg), myricetin (2.7 mg) and quercetin (3.5 mg) were purified from the isopropylacetate extract whereas glucosides of myricetin (4.7 mg) and quercetin (3.0 mg) alongside nigrumin-*p*-coumarate (1.5 mg) and nigrumin ferulate (0.7 mg) were isolated from the ethyl acetate extract (10 mg). Myricetin-3-*O*-*β*-rutinoside (0.8 mg) and quercetin-3-*β*-*O*-rutinoside (0.8 mg) were isolated from the aqueous extract (20 mg, monitored at 350 nm) using this method as well. The isolated compounds were characterised using NMR, IR, UV/Vis spectroscopy and accurate mass spectrometry.

7.7.2 Purification of γ-Actinorhodin (γ-ACT)

The dried extract (600 mg) was dissolved in chloroform (100 mL) and washed with aqueous sodium carbonate solution (1 M, 60 mL × 3). The blue aqueous layer was acidified with hydrochloric acid (6 M), and the crude red pigment was obtained by filtration. γ-Actinorhodin was then triturated from methanol (red precipitate, 125 mg, 19%). The identity and purity (95%) of γ-actinorhodin was assessed using mass spectrometry, 1-D NMR, 2-D NMR and infrared spectroscopy and analytical HPLC.

7.7.3 Purification of Diketopiperazines from P5-25 Extract

The Z18 extract (18 mg) was dissolved in methanol (2 mL) and filtered. The extract was then purified using method given in section **7.6.9** on preparative HPLC and the fractions were collected at 210 nm. Cy(L-Tyr-L-Ile) 3.1 mg, cy(L-Leu-D-Pro) 2.7 mg, cy(L-Phe-D-Pro) 2.9 mg, cy(L-Leu-L-Ile) 1.8 mg, cy(L-Leu-L-Leu) 1.7 mg, cy(L-Phe-D-Tyr) 2.5 mg and cy(L-Phe-L-Leu) 3.3 mg.

7.7.4 Purification of Diketopiperazines from VF48A Extract

The VF48A extract (30 mg) was dissolved in methanol (3 mL) and filtered. The extract was then purified using method given in section **7.6.10** on preparative HPLC and the fractions were collected at 200 nm. Cy(L-Phe-L-Pro-OH) 1.4 mg, cy(L-Leu-D-Pro) 3.9 mg, cy(L-Leu-L-Pro) 4.4 mg, cy(L-Phe-L-Pro) 4.6 mg, cy(L-Phe-D-Pro) 4.2 mg, cy(L-Val-L-Leu) 3.1 mg, cy(L-Phe-L-Tyr) 1.7 mg, cy(L-Tyrp-L-Pro) 1.9 mg and cy(L-Phe-L-Val) 2.1 mg and cy(L-Phe-D-Leu) 2.7 mg.

7.8 HPLC Quantification Method (q-HPLC)

The anthocyanins in the post-SPE (solid phase extraction) blackcurrant extract were quantified using calibration graphs for delphinidin-3-O-β-glucoside from samples purified in this work and obtained commercially, using Agilent Chem Software. Delphinidin-3-O-β-glucoside (Dp3glc) was purchased from Polyphenol AS. The isolated as well as commercial samples of Dp3glc were dissolved in buffer pH 1.0 to give 1 mg/mL stock solutions and then several dilutions were prepared. UV/Vis absorption spectra were recorded on-line during HPLC analysis using a photodiode array detector and the external calibration graphs were obtained. Using these calibration graphs and Agilent Chem Software the absolute amount of delphinidin-3-O-β-glucoside and the relative amounts of rest of the anthocyanins were calculated. The relative ratios of the anthocyanins given by HPLC chromatograms and ^{1}H NMR were in good agreement, therefore the difference in molar absorption coefficients was not considered. The amounts of neutral polyphenols are based on their isolated yield. The amounts of individual polyphenols were reflected in the relative peak area of each compound in ^{1}H NMR of the post−SPE extract.

7.9 Total Monomeric Anthocyanin Content (TMAC) Assay

TMAC assay was performed following protocol given by Lee et al (1). Extinction coefficients were calculated for the isolated anthocyanins (Appendix 8). Total anthocyanin content (TA) was calculated using extinction coefficients and molecular weights for delphinidin-3-*O-β*-rutinoside (DOR), delphinidin-3-*O-β*-glucoside (DOG) and cyanidin-3-*O-β*-glucoside (COG) as standards in the equation. The calculated amount was in most agreement with quantitative HPLC (q-HPLC) results when dp3rut was used as standard which is explained by its predominant nature in our extract. The stock solutions were prepared in both pH buffer 1.0 and 4.5 at concentration of 1 mg/mL and several dilutions were prepared to give absorbance between 0.2–1.4. In order to study the co-pigmentation effect, a stock solution for rutin was also prepared in the same way. Mixtures of dp3glc and rutin were screened to achieve absorbance between 0.2–1.4 at 520 (λ_{max} for anthocyanins) and 360 (λ_{max} for rutin); the concentrations of 0.18 and 0.082 mM for dp3glc and rutin respectively were representative of the relative ratios of these compounds in the blackcurrant extract. Therefore, this range was used to study the effect of co-pigmentation TMAC experiment. The samples were measured at 520 nm and 700 nm (for haze correction). The difference between absorbance values at these two pH points gives actual absorbance value for a specific anthocyanin. The following equation is then used to calculate the total monomeric content of a specific sample.

$$\text{TMAC (mg/L)} = (\text{Asp} \times \text{MW} \times \text{DF} \times 1000) / (\varepsilon \times l)$$

Where $A_{sp} = (A_{510} - A_{700})$ pH 1.0 $- (A_{510} - A_{700})$ pH 4.5, M is molar mass 611.2, DF is the dilution factor, ε 7699 M-1 cm-1, l is path length in cm.

7.10 Synthesis of Diketopiperazines: General Methods

General procedure for coupling reaction: the methyl ester of the C-terminal amino acid (1 eq.) and the Boc-protected N-terminal amino acid (1.1 eq.) were dissolved in DCM (10 mL), followed by addition of DMAP (1 eq.). The reaction mixture was stirred for 5 min at room temperature whereupon EDC (1.3 eq.) was added. The reaction was thereafter stirred overnight under nitrogen at room temperature. The crude product was purified by flash chromatography using DCM/MeOH 95:5.

General procedure for deprotection: the pure compound from the coupling reaction was dissolved in MeOH (5 mL), and HCl (4 M in dioxane) (20 eq.) was added. The

reaction mixture was stirred at room temperature for 3 h and then concentrated *in vacuo*, to give deprotected compound.

General procedure for dipeptide cyclisation: the hydrochloride salt of the deprotected dipeptide (1 eq.) was dissolved in H_2O (3 mL) and 2.5 equivalents of triethyl amine was added. The microwave assisted heated reactions were run for 10 min at 140 °C. The crude product precipitated which was then obtained by filtration. Where product did not precipitate, the reaction mixture was extracted with ethyl acetate (40 mL × 3). The organic layers were combined and evaporated *in vacuo*. The crude product was purified by C18 reversed phase preparative HPLC.

7.11 Compound Characterisation: Natural Product
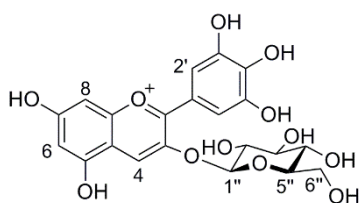
Delphinidin-3-*O*-β-glucopyranoside 16: It was isolated from the aqueous blackcurrant extract using method 7.7.1 (purple solid, 1.6 mg, 7.7%). HPLC: t_R 10.7 min. UV (buffer pH 1.0): λ_{max} nm (log ε) 515 (3.85). ^{1}H NMR (500 MHz, CD$_3$OD/CF$_3$COOD 95:5): δ 8.98 (1H, s, H-4), 7.79 (2H, s, H-2', 6'), 6.88 (1H, d, *J* = 1.5 Hz, H-8) and 6.66 (1H, d, *J* = 1.5 Hz, H-6), 5.32 (1H, d, *J* = 7.5 Hz, H-1''), 3.93 (1H, dd, *J* = 12.3, 2.1 Hz, H-6a''), 3.73 (1H, dd, *J* = 12.3, 6.0 Hz, H-6b''), 3.72 (1H, dd, *J* = 9.0, 7.5 Hz, H-2''), 3.56 (1H, t, *J* = 9.1 Hz, H-3''), 3.54 (1H, ddd, *J* = 9.0, 6.0, 2.1 Hz, H-5'') and 3.47 (1H, dd, *J* = 9.0, 9.1 Hz, H-4''). ^{13}C NMR (125 MHz, CD$_3$OD/CF$_3$COOD 95:5): δ 173.5 (C-7), 160.2 (C-2), 159.1 (C-5), 158.6 (C-4a), 148.8 (C-4'), 147.6 (C-3', 5'), 145.9 (C-3), 136.3 (C-4), 117.6 (C-1'), 115.8 (C-8a), 112.6 (C-2', 6'), 103.7 (C-1''), 103.3 (C-6), 95.0 (C-8), 78.8 (C-5''), 78.1 (C-3''), 74.8 (C-2''), 71.1 (C-4'') and 62.3 (C-6''). IR (neat): ν_{max} 3550-2440, 1680, 1540, 1505, 1310 cm^{-1}. HRMS (ESI) *m/z* calculated for formula C$_{21}$H$_{22}$O$_{12}$ [M+H]$^+$ 466.1027, found 466.1037. The ^{1}H NMR data published in the literature is in agreement with current work.[161]
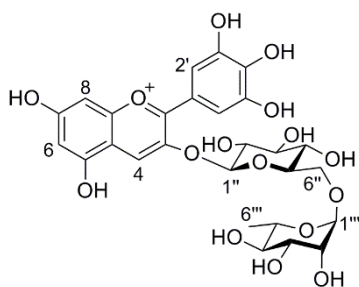
Delphinidin-3-*O*-β-rutinoside 17: It was isolated as purple solid from the aqueous blackcurrant extract using method 1.7.1 (4.5 mg, 22.6%). HPLC: t_R 11.8 min. UV (buffer pH 1.0): λ_{max} nm (log ε) 520 (3.89). ^{1}H NMR (500 MHz, CD$_3$OD/CF$_3$COOD 95:5): δ 8.90 (1H, s, H-4), 7.78 (2H, s, H-2', 6'), 6.88 (1H, d, *J* = 2.0 Hz, H-8) and 6.68 (1H, d, *J* = 2.0 Hz, H-6), 5.30 (1H, d, *J* = 7.5 Hz, H-1''), 4.65 (1H, d, *J* = 1.5 Hz, H-1'''), 4.06

(1H, dd, J = 11.3, 1.8 Hz, H-6a"), 3.80 (1H, dd, J = 3.5, 1.5 Hz, H-2'''), 3.73 (1H, ddd, J = 9.0, 7.2, 1.8 Hz, H-5"), 3.71 (1H, dd, J = 9.0, 7.5 Hz, H-2"), 3.63 (1H, dd, J = 9.5, 3.5 Hz, H-3'''), 3.59 (1H, dd, J = 11.3, 7.2 Hz, H-6b"), 3.57 (1H, m, H-5'''), 3.55 (1H, t, J = 9.0 Hz, H-3"), 3.43 (1H, t, J = 9.0 Hz, H-4"), 3.33 (1H, t, J = 9.0 Hz, H-4''') and 1.15 (3H, d, J = 6.0 Hz, H-6'''). ^{13}C NMR (125 MHz, CD$_3$OD/CF$_3$COOD 95:5): δ 170.3 (C-7), 164.1 (C-2), 159.0 (C-5), 157.6 (C-8a), 147.6 (C-3', 5'), 145.8 (C-4'),144.9 (C-3), 135.4 (C-4), 120.0 (C-1'), 113.1 (C-4a), 112.7 (C-2', 6'), 103.4 (C-6), 103.3 (C-1"), 102.2 (C-1'''), 95.1 (C-8), 78.0 (C-5"), 77.5 (C-3"), 74.7 (C-2"), 73.9 (C-4'''), 72.5 (C-3'''), 71.9 (C-2'''), 71.2 (C-4"), 69.8 (C-5'''), 67.8 (C-6") and 17.9 (C-6'''). IR (neat): v_{max} 3390, 2975, 1650, 1510, 1490 cm^{-1}. HRMS (ESI) calculated for formula C$_{27}$H$_{32}$O$_{16}$ [M+H]$^+$ 612.1681, found 612.1681. The ^{13}C NMR data published in the literature is in agreement with current work.[75]
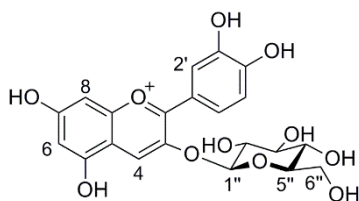
Cyanidin-3-*O*-β-glucopyranoside 18: It was isolated from the aqueous blackcurrant extract using method 1.7.1 (purple solid, 0.8 mg, 4%). HPLC: t_R 12.7 min. UV (buffer pH 1.0): λ$_{max}$ nm (log ε) 510 (3.79). ^{1}H NMR (500 MHz, CD$_3$OD/CF$_3$COOD 95:5): δ 9.04 (1H, s, H-4), 8.27 (1H, dd, J = 8.5, 2.5 Hz, H-6'), 8.06 (1H, d, J = 2.5 Hz, H-2'), 7.02 (1H, d, J = 8.5 Hz, H-5'), 6.91 (1H, d, J = 2.0 Hz, H-8) and 6.69 (1H, d, J = 2.0 Hz, H-6), 5.31 (1H, d, J = 8.0 Hz, H-1"), 3.91 (1H, dd, J = 12.0, 2.0 Hz, H-6a"), 3.72 (1H, dd, J = 12.0, 5.9 Hz, H-6b"), 3.71 (1H, dd, J = 9.0, 7.0 Hz, H-2"), 3.56 (1H, t, J = 9.0 Hz, H-3"), 3.55 (1H, m, H-5"), and 3.44 (1H, t, J = 9.1 Hz, H-4") . HRMS (ESI) calculated for formula C$_{21}$H$_{22}$O$_{11}$ [M+H]$^+$ 449.1027, found 449.1037. The ^{1}H NMR data published in the literature is in agreement with current work.[58]
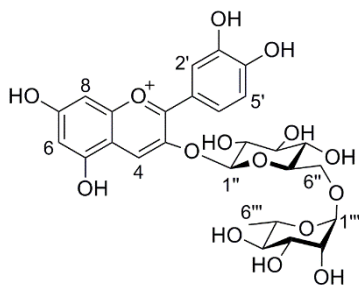
**Cyanidin-3-*O*-β-rutinoside 19:** It was isolated from the aqueous blackcurrant extract using method 1.7.1 (purple solid, 4.1 mg, 20.4%). HPLC: t_R 13.8 min. UV (buffer pH 1.0): λ$_{max}$ nm (log ε) 510 (3.87). ^{1}H NMR (500 MHz, CD$_3$OD/CF$_3$COOD 95:5): δ 8.95 (1H, s, H-4), 8.27 (1H, dd, J = 8.5, 2.5 Hz, H-6'), 8.05 (1H, d, J = 2.5 Hz, H-2'), 7.04 (1H, d, J = 8.5 Hz, H-5'), 6.91 (1H, d, J = 1.5 Hz, H-8) and 6.69 (1H, d, J = 1.5 Hz, H-6), 5.29 (1H, d, J = 7.5 Hz, H-1"), 4.65 (1H, d, J = 1.5 Hz, H-1'''), 4.06 (1H, dd, J = 11.1, 1.5 Hz, H-6a"), 3.80 (1H, dd, J = 3.5, 1.5 Hz, H-2'''), 3.72 (1H, ddd, J = 9.0, 7.0, 1.5 Hz, H-5"), 3.67 (1H, dd, J = 9.0, 7.5 Hz, H-2"), 3.63 (1H, dd, J = 9.3, 3.0 Hz, H-3'''), 3.61 (1H, m, H-5'''), 3.59 (1H, dd, J = 11.1, 7.0 Hz, H-6b"), 3.54 (1H, t, J = 9.0 Hz, H-3"), 3.42 (1H,

t, J = 9.0 Hz, H-4"), 3.53 (1H, m, H-4''') and 1.13 (3H, d, J = 6.0 Hz, H-6'''). ^{13}C NMR (125 MHz, CD$_3$OD/CF$_3$COOD 95:5): δ 170.5 (C-7), 164.2 (C-2), 159.1 (C-5), 157.7 (C-8a), 155.9 (C-4'), 147.5 (C-3'), 145.7 (C-3), 136.2 (C-4), 128.4 (C-6'), 120.3 (C-1'), 118.4 (C-2'), 117.5 (C-5'), 111.8 (C-4a), 103.5 (C-6), 103.4 (C-1"), 102.2 (C-1'''), 95.2 (C-8), 78.0 (C-3"), 77.5 (C-5"), 74.7 (C-2"), 73.9 (C-4"), 72.5 (C-3'''), 71.9 (C-2'''), 71.2 (C-4"), 69.8 (C-5'''), 67.4 (C-6") and 17.9 (C-6'''). IR (neat): ν$_{max}$ 3370, 2955, 1651, 1510, 1490 cm^{-1}. HRMS (ESI) calculated for formula C$_{27}$H$_{32}$O$_{15}$ [M+H]$^+$ 596.1671, found 595.1711. The ^{13}C NMR data published in the literature is in agreement with current work.[75]
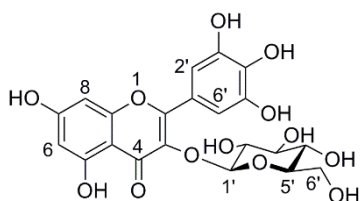
Myricetin-3-*O*-*β*-glucopyranoside 22: It was isolated from the ethyl acetate blackcurrant extract using method 1.7.1 (pale yellow solid, 4.7 mg, 3.1%). HPLC: t$_R$ 12.6 min. UV (EtOH): λ$_{max}$ nm (log ε) 365 (4.23). ^{1}H NMR (500 MHz, CD$_3$OD): δ 7.31 (2H, s, H-2', 6'), 6.40 (1H, d, J = 2.0 Hz, H-8) and 6.22 (1H, d, J = 2.0 Hz, H-6), 5.23 (1H, d, J = 8.0 Hz, H-1"), 3.73 (1H, dd, J = 12.0, 2.3 Hz, H-6a"), 3.62 (1H, dd, J = 12.0, 5.0 Hz, H-6b"), 3.51 (1H, dd, J = 8.9, 8.0 Hz, H-2"), 3.44 (1H, t, J = 8.9 Hz, H-3"), 3.39 (1H, t, J = 9.3 Hz, H-4"), 3.24 (1H, ddd, J = 9.3, 5.0, 2.3 Hz, H-5"). ^{13}C NMR (125 MHz, CD$_3$OD): δ 177.1 (C-4), 163.0 (C-7), 161.4 (C-5), 157.8 (C-2), 157.5 (C-8a), 142.8 (C-3' and C-5'), 137.5 (C-4'), 133.8 (C-3), 119.2 (C-1'), 108.6 (C-2' and C-6'), 102.8 (C-4a), 103.1 (C-1"), 100.0 (C-6), 93.3 (C-8), 77.1 (C-5"), 76.8 (C-3"), 73.8 (C-2"), 69.7 (C-4"), 61.1 (C-6). IR (neat): ν$_{max}$ 3381, 1679, 1610 cm^{-1}. HRMS (ESI$^+$) calculated for formula C$_{21}$H$_{21}$O$_{13}$ [M+H]$^+$ 481.0962, found 481.0974. The ^{1}H NMR data published in the literature is in agreement with current work.[161]
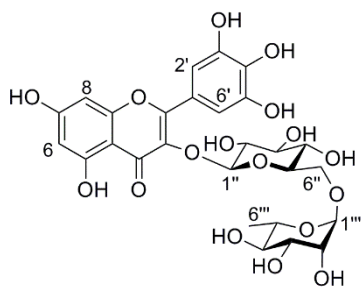

Myricetin-3-*O*-*β*-rutinoside 23: It was isolated from the aqueous blackcurrant extract using method 1.7.1 (pale yellow amorphous solid, 0.8 mg, 3.1%). HPLC: t$_R$ 12.3 min. ^{1}H NMR (500 MHz, CD$_3$OD): δ 7.30 (2H, s, H-2', 6'), 6.41 (1H, d, J = 2.5 Hz, H-8) and 6.22 (1H, d, J = 2.5 Hz, H-6), 5.08 (1H, d, J = 8.0 Hz, H-1"), 4.53 (1H, d, J = 1.3 Hz, H1'''), 3.80 (1H, dd, J = 11.5, 1.5 Hz, H-6a"), 3.63 (1H, dd, J = 3.5, 1.5 Hz, H-2'''), 3.55 (1H, dd, J = 9.5, 3.5 Hz, H-3'''), 3.50 (1H, dd, J = 9.0, 8.0 Hz, H-2"), 3.46 (1H. m, H-5'''), 3.42 (1H, dd, J = 11.5, 5.0 Hz, H-6b"), 3.40 (1H, t, J = 9.0 Hz, H-3") and 1.12 (3H, d, J = 6.0 Hz, H-6'''). HRMS (ESI$^+$) calculated for formula C$_{27}$H$_{31}$O$_{17}$ [M+H]$^+$ 627.1526, found 627.1548. The ^{13}C NMR data published in the literature is in agreement with current work.[75]
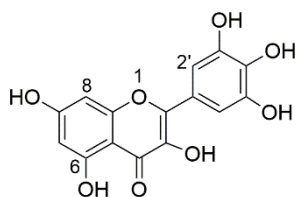
Myricetin 28: It was isolated from the isopropylacetate blackcurrant extract using method 1.7.1 (pale yellow solid, 2.7 mg, 2.5%). HPLC: t_R 19.4 min. UV (EtOH): λ_{max} nm (log ε) 350 (4.33). ^{1}H NMR (500 MHz, CD$_3$OD): δ 7.35 (2H, s, H-2' and 6'), 6.39 (1H, d, J = 2.2 Hz, H-8) and 6.19 (1H, d, J = 2.2 Hz, H-6). HRMS (ESI$^-$) calculated for formula C$_{15}$H$_9$O$_8$ [M-H]$^+$ 317.0400, found 317.0304. The ^{13}C NMR data published in the literature for commercial sample is in agreement with current work.[162]
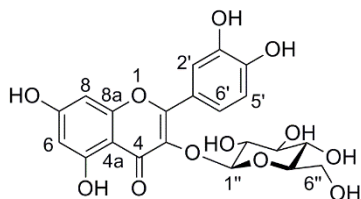
Quercetin-3-O-β-glucopyranoside 24: It was isolated from the ethyl acetate blackcurrant extract using method 1.7.1 (pale yellow amorphous solid, 3 mg, 2%). HPLC: t_R 16.3 min. UV (EtOH): λ_{max} nm (log ε) 345 (4.24). ^{1}H NMR (500 MHz, CD$_3$OD): δ 7.72 (1H, d, J = 2.0 Hz, H-2'), 7.59 (1H, dd, J = 8.5, 2.0 Hz, H-6'), 6.90 (1H, d, J = 8.5 Hz, H-5'), 6.41 (1H, d, J = 2.0 Hz, H-8), 6.22 (1H, d, J = 2.0 Hz, H-6), 5.28 (1H, d, J = 8.0 Hz, H-1''), 3.75 (1H, dd, J = 12.0, 2.5 Hz, H-6a''), 3.60 (1H, dd, J = 12.0, 5.2 Hz, H-6b''), 3.49 (1H, dd, J = 9.1, 8.0 Hz, H-2''), 3.45 (1H, t, J = 9.1 Hz, H-3''), 3.43 (1H, t, J = 9.5 Hz, H-4''), 3.25 (1H, m, H-5'') .^{13}C NMR (125 MHz, CD$_3$OD): 178.1 (C-4), 164.7 (C-7), 161.6 (C-5), 157.6 (C-8a), 157.1 (C-2), 148.5 (C-3'), 144.5 (C-4'), 134.2 (C-3), 121.8 (C-1'), 121.7 (C-6'), 116.2 (C-2'), 114.6 (C-5'), 104.3 (C-4a), 102.9 (C-1''), 98.5 (C-6), 93.3 (C-8), 77.0 (C-5''), (C-3''), 76.7 (C-2''), 74.2 (C-4''), 69.6 (C-6''). IR (neat): v_{max} 3358, 3001, 1638 cm^{-1}. HRMS (ESI) calculated for formula C$_{21}$H$_{21}$O$_{12}$ [M+H]$^+$ 465.1019, found 465.1092. The ^{1}H NMR data published in the literature is in agreement with current work.[161]
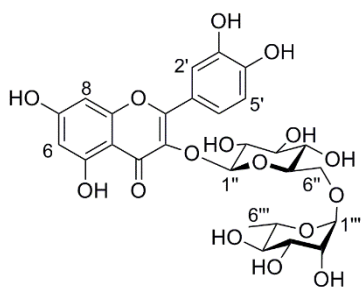
Quercetin-3-O-β-rutinoside 25: It was isolated from the aqueous blackcurrant extract using method 1.7.1 (pale yellow amorphous solid, 0.8 mg, 3.2%). HPLC: t_R 16.1 min. UV (EtOH): λ_{max} nm (log ε) 360 (4.29). ^{1}H NMR (500 MHz, CD$_3$OD): δ 7.68 (1H, d, J = 2.2 Hz, H-2'), 7.64 (1H, dd, J = 8.5, 2.2 Hz, H-6'), 6.89 (1H, d, J = 8.5 Hz, H-5'), 6.43 (1H, d, J = 2.0 Hz, H-8), 6.23 (1H, d, J = 2.0 Hz, H-6), 5.11 (1H, d, J = 8.0 Hz, H-1''), 4.53 (1H, d, J = 1.5 Hz, H-1'''), 3.80 (1H, dd, J = 11.0, 1.5 Hz, H-6a''), 3.63 (1H, dd, J = 3.5, 1.5 Hz, H-2'''), 3.54 (1H, dd, J = 9.5, 3.5 Hz, H-3'''), 3.46 (1H, dd, J = 9.5, 8.0 Hz, H-2''), 3.43 (1H, m, H-5'''), 3.41 (1H, t, J = 9.5 Hz, H-3''), 3.39 (1H, dd, J = 11.0, 5.5 Hz, H-6b''), 3.32 (under solvent peak, H-5''), 3.28 (1H, t, J = 9.5 Hz, H-4'''), 3.26 (1H, d, J = 9.5 Hz, H-4'') and 1.13 (3H, d, J = 6.5 Hz, H-6'''). IR (neat): v_{max} 3310, 2980, 1670, 1610 cm^{-1}. HRMS

(ESI) calculated for formula $C_{27}H_{31}O_{16}$ [M+H]$^+$ 611.1432, found 611.1464. The ^{13}C NMR data published in the literature is in agreement with current work.[75]
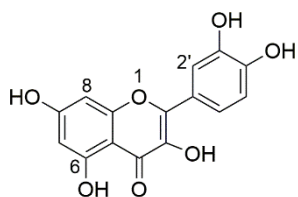
Quercetin 29: It was isolated from the isopropylacetate blackcurrant extract using method 1.7.1 (pale yellow solid, 3.5 mg, 3.2%). HPLC: t_R 26.3 min. UV (EtOH): λ_{max} nm (log ε) 375 (4.32). ^1H NMR (500 MHz, CD₃OD): δ 7.74 (1H, d, J = 2.0 Hz, H-2'), 7.63 (1H, dd, J = 8.5, 2.0 Hz, H-6'), 6.89 (1H, d, J = 8.5 Hz, H-5'), 6.39 (1H, d, J = 2.5 Hz, H-8), 6.19 (1H, d, J = 2.5 Hz, H-6). ^{13}C NMR (125 MHz, CD₃OD): δ 177.4 (C-4), 165.6 (C-7), 162.5 (C-5), 158.3 (C-8a), 148.8 (C-4'), 148.1 (C-2), 146.2 (C-3'), 137.2 (C-3), 124.2 (C-1'), 121.7 (C-6'), 116.2 (C-5'), 116.0 (C-2'), 104.5 (C-4a), 99.3 (C-6), 94.4 (C-8). IR (neat): v_{max} 3480, 3010, 1690, 1610, 1505 cm^{-1}. HRMS (ESI) calculated for formula $C_{15}H_9O_7$ [M-H]$^+$ 301.0353, found 301.0354. The ^{13}C and ^1H NMR data published in the literature is in agreement with current work.[74]
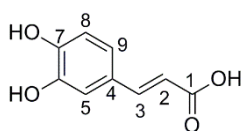
Caffeic acid 30: It was isolated from the isopropylacetate blackcurrant extract using method 1.7.1 (off white solid, 3.3 mg, 3%). HPLC: t_R 2.70 min. UV (EtOH): λ_{max} nm (log ε) 330 (4.34). ^1H NMR (500 MHz, CD₃OD/CF₃COOD 95:5): δ 7.54 (1H, d, J = 16.0 Hz, H-3), 7.04 (1H, d, J = 2.0 Hz, H-5), 6.94 (1H, dd, J = 8.0 and 2.0 Hz, H-9), 6.78 (1H, d, J = 8.0 Hz, H-8) and 6.22 (1H, d, J = 16.0 Hz, H-2). ^{13}C NMR (125 MHz, CD₃OD/CF₃COOD 95:5): δ 171.0 (C-1), 149.5 (C-7), 147.1 (C-3), 146.8 (C-6), 127.8 (C-4), 122.9 (C-9), 116.5 (C-8), 115.5 (C-2), 115.1 (C-5). IR (neat): v_{max} 3476, 3330, 1670, 1620, 1460 cm^{-1}. HRMS (ESI) calculated for formula $C_9H_7O_4$ [M-H]$^+$ 179.0402, found 179.0360. The ^{13}C and ^1H NMR data published in the literature is in agreement with current work.[72]
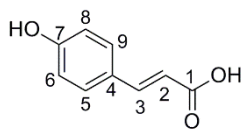
***p*-Coumaric Acid 31:** It was isolated from the isopropylacetate blackcurrant extract using method 1.7.1 (pale yellow solid, 5.5 mg, 5%). HPLC: t_R 19.7 min. UV (EtOH): λ_{max} nm (log ε) 310 (4.39). ^1H NMR (500 MHz, CD₃OD): δ 7.60 (1H, d, J = 16.0 Hz, H-3), 7.45 (2H, d, J = 8.5 Hz, H-5, 9), 6.81 (2H, d, J = 8.5 Hz, H-6, 8), 6.28 (1H, d, J = 16 Hz, H-2); ^{13}C NMR (125 MHz, CD₃OD): δ 171.02 (C-1), 161.15 (C-7), 146.62 (C-3), 131.07 (C-5,9), 127.26 (C-4), 116.81 (C-6,8), 115.65 (C-2). IR (neat): v_{max} 3336, 3026, 1667, 1626, 1446 cm^{-1}. HRMS (ESI) calculated for formula $C_9H_7O_3$ [M-H]$^+$ 163.0503, found 163.0406. No data reference was found in the literature.
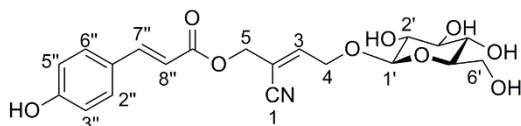
Nigrumin-*p*-coumarate 32: It was isolated from the ethyl acetate blackcurrant extract using method 1.7.1 (yellow glassy solid, 1.5 mg, 1%). HPLC: t_R 19.7 min. UV (MeOH): λ_{max} 310, 211 nm. ^{1}H NMR (500 MHz, CD$_3$OD): δ 7.68 (1H, d, J = 16.0 Hz, H-7"), 7.49 (2H, d, J = 9.0 Hz, H-6" and H-2"), 6.86 (1H, t, J = 6.5 Hz, H-3), 6.82 (2H, d, J = 9.0 Hz, H-3" and H-5"), 6.37 (1H, J = 16.0 Hz, H-8"), 4.82 (1H, s, H-5), 4.66 (1H, dd, J = 14.5, 5.9 Hz, H-4b), 4.54 (1H, dd, J = 14.5, 6.5 Hz, H-4a), 4.36 (1H, d, J = 8.0 Hz, H-1'), 3.88 (1H, dd, J = 12.0, 1.0 Hz, H-6b'), 3.69 (1H, dd, J = 12.0, 5.0 Hz, 6a'), 3.21 (2H, t, J = 8.3 Hz, H-2' and H-5'). IR (neat): v_{max} 3360, 2950, 2850, 2219, 1662, 1480 cm^{-1}. HRMS (ESI) calculated for formula C$_{20}$H$_{22}$NO$_9$ [M-H]$^+$ 420.1706, found 420.1706. The ^{1}H NMR data published in the literature is in agreement with current work.[76]
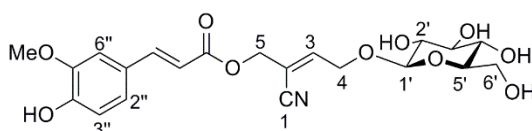
Nigrumin ferulate 33: It was isolated from the ethyl acetate blackcurrant extract using method 1.7.1 (yellow glassy solid, 0.7 mg, 0.5%). HPLC: t_R 20.1 min. UV (MeOH): λ_{max} 324, 210 nm. ^{1}H NMR (500 MHz, CD$_3$OD): δ 7.68 (1H, d, J = 16.0 Hz, H-7"), 7.22 (1H, d, J = 2.0 Hz, H-6"), 7.11 (1H, dd, J = 8.5, 2.0 Hz, H-2"), 6.86 (1H, t, J = 6.5 Hz, H-3), 6.82 (1H, d, J = 8.5 Hz, H-3"), 6.37 (1H, J = 16.0 Hz, H-8"), 4.82 (1H, s, H-5), 4.66 (1H, dd, J = 14.5, 5.9 Hz, H-4b), 4.54 (1H, dd, J = 14.5, 6.5 Hz, H-4a), 4.36 (1H, d, J = 8.0 Hz, H-1'), 3.90 (3H, s, OCH$_3$), 3.88 (1H, dd, J = 12.0, 1.0 Hz, H-6b'), 3.69 (1H, dd, J = 12.0, 5.0 Hz, 6a'), 3.21 (2H, t, J = 8.3 Hz, H-2' and H-5'). IR (neat): v_{max} 3360, 2950, 2840, 2225, 1662, 1450 cm^{-1}. HRMS (ESI) calculated for formula C$_{21}$H$_{24}$NO$_{10}$ [M+H]$^+$ 450.1406, found 450.1389. The ^{1}H NMR data published in the literature is in agreement with current work.[76]

Polymeric anthcyanins: It was isolated from the aqueous blackcurrant extract using method 1.7.1 (dull purple amorphous solid, 4.5 mg, 18%, isolated yield). UV (MeOH/12.1 M HCl, 99.9:0.1): λ_{max} 252, 277, 352, 520 nm. ^{1}H NMR data indicated towards polymeric species with broad aromatic (6.00-7.80 ppm) and sugar region (3.52-4.51 ppm).
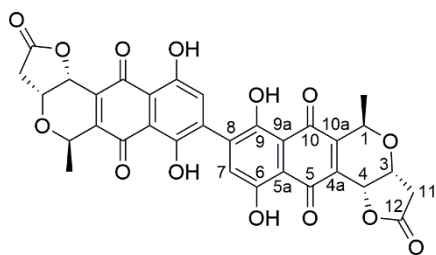
γ-Actinorhodin 46: It was isolated from *S. coelicolor* L646 using method 1.7.2 (red precipitate, 125 mg, 19%). R_F 0.29 (1% MeOH in DCM). HPLC: t_R 25.1 min. ^{1}H NMR (500 MHz, CDCl$_3$): δ 12.80 (1H, s, OH-9), 12.50 (1H, s, OH-6), 7.34 (1H, s, H-7), 5.33 (1H, d, *J* = 3.0 Hz, H-4), 5.19 (1H, q, *J* = 7.0 Hz, H-1), 4.74 (1H, m, H-3), 2.99 (1H, dd, *J* = 17.8, 5.3 Hz, H-11), 2.73 (1H, d, *J* = 17.8 Hz, H-11'), 1.59 (3H, d, *J* = 7.0 Hz, CH$_3$). ^{13}C NMR (125 MHz, CDCl$_3$): δ 176.9 (C-5), 176.6 (C-10), 174.1 (C-12), 165.7 (C-6), 164.9 (C-9), 148.9 (C-10a), 138.0 (C-8), 133.7 (C-7), 133.4 (C-4a), 112.1 (C-9a), 111.7 (C-5a), 68.7 (C-4), 66.8 (C-1), 66.5 (C-3), 37.0 (C-11), 18.5 (CH$_3$). IR (solid): 3502, 2919, 2850, 1790, 1709, 1613, 1575, 1377, 1260 cm^{-1}. HRMS (ESI): *m/z* calculated for formula C$_{32}$H$_{21}$O$_{14}$ [M-H]$^+$ 629.0933; found 629.0922. The ^{1}H NMR data published in the literature is in agreement with current work.[116]
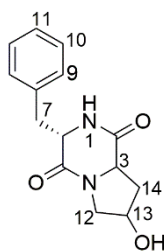
Cy(L-Phe-L-Pro-OH) 65: It was isolated from VF48A extract by preparative HPLC using method 1.7.4 (colourless glassy solid, 1.4 mg, 4.7% extraction yield). HPLC: t_R 9.9 min. $[\alpha]^{25}_D$ = +54 (*c* 0.1, MeOH). ^{1}H NMR (500 MHz, CD$_3$OD): δ 7.31 (2H, d, *J* = 7.5 Hz, H-10), 7.29 (1H, d, *J* = 7.0 Hz, H-11), 7.19 (1H, dd, J = 7.5, 7.0 Hz, H-9), 4.24 (1H, m, H-13), 4.22 (1H, m, H-6), 3.59 (1H, dd, *J* = 12.5, 4.0 Hz, H-12a), 3.27 (1H, dd, *J* =12.5, 6.0 Hz, H-12b), 3.18 (1H, dd, *J* = 13.5, 5.0 Hz, H-7a), 3.00 (1H, dd, *J* = 13.5, 5.0 Hz, H-7b), 2.80 (1H, t, *J* = 8.5 Hz, H-3), 2.23 (1H, m, H-14a), 1.92 (1H, m, H-14b). ^{13}C NMR (125 MHz, CD$_3$OD): δ 169.6 (C-2), 166.3 (C-5), 135.4 (C-8), 129.8 (C-9), 128.3 (C-10), 127.1 (C-11), 67.1 (C-13), 58.2 (C-6), 55.8 (C-3), 52.6 (C-12), 39.5 (C-7), 36.7 (C-14). HRMS (ESI) calculated for formula C$_{14}$H$_{16}$N$_2$O$_3$Na [M+Na]$^+$ 283.3301, found 283.3062. NMR data was not found in the literature.
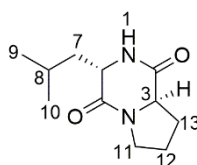
Cy(L-Leu-D-Pro) 66: It was isolated from VF48A extract by preparative HPLC using method 1.7.4 (colourless solid, 3.9 mg, 13% extraction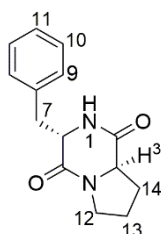 yield). It was also isolated from P5-25 extract by preparative HPLC using method 1.7.3 (colourless solid, 2.7 mg, 15%). HPLC: t_R 11.4 min. $[\alpha]^{25}_D$ = +69 (*c* 0.1, MeOH). ^{1}H NMR (500 MHz, CD$_3$OD): 4.28 (1H, dd, *J* = 9.5, 6.5 Hz, H-3), 3.86 (1H, dd, *J* = 9.5, 5.5 Hz, H-6), 3.57 (1H, m, H-11a), 3.52 (1H, m, H-11b), 2.35 (1H, m, H-13a), 2.03 (1H, m, H-12a), 1.94 (1H, m, H-13b), 1.92 (1H, m, H-12b), 1.79

(1H, m, H-8), 1.67 (1H, ddd, J = 13.5, 9.5, 5.5 Hz, H-7a), 1.58 (1H, ddd, J = 13.5, 8.5, 5.5 Hz, H-7b), 0.98 (3H, d, J = 6.0 Hz, H-10), 0.94 (3H, d, J = 6.5 Hz, H-9). ^{13}C NMR (125 MHz, CD$_3$OD): δ 170.2 (C-2), 167.6 (C-5), 57.9 (C-3), 55.7 (C-6), 45.3 (C-11), 42.2 (C-7), 28.5 (C-13), 24.1 (C-8), 21.9 (C-9), 21.7 (C-12), 20.6 (C-10). IR (neat): ν$_{max}$ 3235, 2953, 2869, 1652, 1447 cm^{-1}. HRMS (ESI[+]) calculated for formula C$_{11}$H$_{19}$N$_2$O$_2$ [M+H][+] 211.1407, found 211.1428. NMR data was not found in the literature.
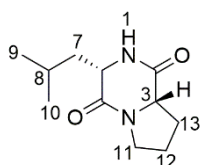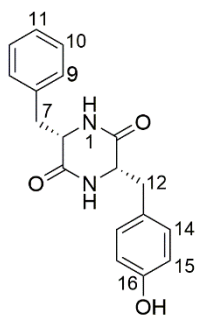
Cy(L-Leu-L-Pro) 59: It was isolated from VF48A extract by preparative HPLC using method 1.7.4 (colourless solid, 4.4 mg, 14.6% extraction yield). HPLC: t$_R$ 12.1 min. [α]$^{25}_D$ = -311 (*c* 0.3, MeOH). ^{1}H NMR (500 MHz, CD$_3$OD): 4.26 (1H, t, J = 8.5 Hz, H-3), 4.12 (1H, dd, J = 10.0, 4.0 Hz, H-6), 3.51 (2H, dd, J = 1.5, 6.0 Hz, H-11), 2.28 (1H, m, H-13a), 2.05 (1H, m, H-13b), 2.01 (1H, m, H-12a), 1.96 (1H, m, H-12b), 1.92 (1H, m, H-7a), 1.87 (1H, m, H-8), 1.52 (1H, m, H-7b), 0.97 (3H, d, J = 6.0 Hz, H-9), 0.95 (3H, d, J = 6.5 Hz, H-10). ^{13}C NMR (125 MHz, CD$_3$OD): δ 171.4 (C-2), 167.5 (C-5), 58.9 (C-3), 53.2 (C-6), 44.9 (C-11), 38.0 (C-7), 27.6 (C-13), 24.6 (C-8), 22.2 (C-12), 21.9 (C-9), 20.6 (C-10). IR (neat): ν$_{max}$ 3236, 2954, 2900, 2869, 1654, 1445 cm^{-1}. HRMS (ESI) calculated for formula C$_{11}$H$_{19}$N$_2$O$_2$ [M+H][+] 211.1407, found 211.1428. The ^{13}C NMR data published in the literature is in agreement with current work.[143]
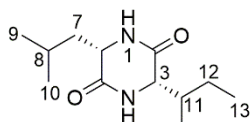
Cy(L-Leu-L-Ile) 61: It was isolated from P5-25 extract by preparative HPLC using method 1.7.3 (colourless solid, 1.8 mg, 10%). HPLC: t$_R$ 8.38 min. [α]$^{25}_D$ = -55 (*c* 0.1, MeOH). ^{1}H NMR (500 MHz, CD$_3$OD): δ 3.95 (1H, dd, J = 9.0, 4.5 Hz, H-6), 3.77 (1H, d, J = 4.5 Hz, H-3), 2.23 (1H, m, H-11), 1.87 (1H, m, H-7a), 1.76 (1H, m, H-8), 1.60 (1H, m, H-7b), 1.09 (1H, m, H-12a), 1.04 (3H, d, J = 7.0 Hz, H-14), 0.97 (9H, m, H-9, 10, 13), 0.90 (1H, m, H-12b). ^{13}C NMR (125 MHz, CD$_3$OD): δ 168.2 (C-2), 168.1 (C-5), 60.2 (C-3), 53.0 (C-6), 43.3 (C-7), 32.3 (C-11), 29.4 (C-12), 24.0 (C-8), 22.3 (C-9), 20.6 (C-10), 18.0 (C-14), 16.5 (C-13). IR (neat): ν$_{max}$ 3190, 3055, 2960, 1661, 1448 cm^{-1}. HRMS (ESI) calculated for formula C$_{12}$H$_{23}$N$_2$O$_2$ [M+H][+] 227.1700, found 227.3001. The ^{1}H NMR data published in the literature is in agreement with current work.[138]
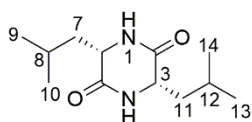
Cy(L-Leu-L-Leu) 62: It was isolated from P5-25 extract by preparative HPLC using method 1.7.4 (colourless solid, 1.7 mg, 9%). HPLC: t_R 10.98 min. $[\alpha]^{25}_D$ = -47 (*c* 0.1, MeOH). ^{1}H NMR (500 MHz, CD$_3$OD): δ 3.90 (2H, m, H-3, 6), 3.77 (1H, d, *J* = 4.5 Hz, H-3), 1.87 (2H, m, H-7a, 11a), 1.71 (2H, m, H-8, 12), 1.63 (2H, m, H-7b, 11b), 0.90 (12H, m, H-9, 10, 13, 14). ^{13}C NMR (125 MHz, CD$_3$OD): δ 169.9 (C-2), 169.8 (C-5), 60.1 (C-3, 6), 44.6 (C-7, 11), 23.9 (C-8, 12), 20.5 (C-9, 10), 20.4 (C-13, 14). IR (neat): v_{max} 3191, 3055, 2960, 1661, 1448 cm^{-1}. HRMS (ESI) calculated for formula $C_{12}H_{23}N_2O_2$ [M+H]$^+$ 227.1700, found 227.3001. The ^{1}H NMR data published in the literature is in agreement with current work.[140]
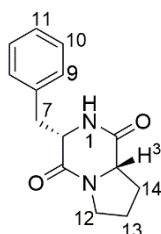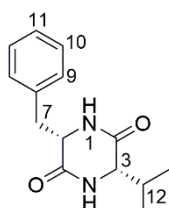
Cy(L-Phe-L-Pro) 67: It was isolated from VF48A extract by preparative HPLC using method 1.7.4 (colourless solid, 4.6 mg, 15.3% extraction yield). HPLC: t_R 13.4 min. $[\alpha]^{25}_D$ = +81 (*c* 0.1, MeOH). ^{1}H NMR (500 MHz, CD$_3$OD): δ 7.30 (2H, t, *J* = 7.5 Hz, H-10), 7.22 (1H, dd, *J* = 7.5, 2.0 Hz, H-11), 7.18 (1H, dd, *J* = 7.5, 2.0 Hz, H-9), 4.20 (1H, t, *J* = 4.5 Hz, H-6), 3.53 (1H, m, H-12a), 3.34 (1H, m, H-12b), 3.20 (1H, dd, *J* =13.0, 4.5 Hz, H-7a), 3.00 (1H, dd, *J* = 13.0, 4.5 Hz, H-7b), 2.62 (1H, m, H-3), 2.02 (H, m, H-14a), 1.91 (1H, m, H-13a), 1.68 (1H, m, H-14b), 1.66 (1H, m, H-13b). ^{13}C NMR (125 MHz, CD$_3$OD): δ 169.9 (C-5), 166.0 (C-2), 135.2 (C-8), 129.9 (C-9), 128.2 (C-10), 127.1 (C-11), 58.4 (C-6), 57.7 (C-3), 44.7 (C-12), 39.6 (C-7), 28.4 (C-14), 21.1 (C-13). IR (neat): v_{max} 3253, 2956, 2890, 1642, 1438 cm^{-1}. HRMS (ESI) calculated for formula $C_{14}H_{17}N_2O_2$ [M+H]$^+$ 245.1270, found 245.1289. The ^{1}H NMR data published in the literature was not in agreement with current work (discussed in detail on p.100).[143]

Cy(L-Phe-D-Pro) 60: It was isolated from VF48A extract by preparative HPLC using method 1.7.4 (colourless glassy solid, 4.2 mg, 14% extraction yield). It was also isolated from P5-25 extract by preparative HPLC using method 1.7.4 (colourless solid, 2.9 mg, 16%). HPLC: t_R 8.99 min. $[\alpha]^{25}_D$ = -135 (*c* 0.1, MeOH). ^{1}H NMR (500 MHz, CD$_3$OD): δ 7.29 (2H, t, *J* = 7.5 Hz, H-10), 7.24 (2H, d, *J* = 7.5 Hz, H-9), 7.23 (1H, t, *J* = 7.5 Hz, H-11), 4.46 (1H, dt, *J* = 5.0, 1.5 Hz, H-6), 4.06 (1H, dd, *J* = 10.5, 6.0 Hz, H-3), 3.54 (1H, m, H-12a), 3.37 (1H, m, H-12b), 3.16 (2H, dd, *J* = 5.0, 2.0 Hz, H-7), 2.09 (1H, m, H-14a), 1.80 (2H, m, H-13), 1.23 (1H, m, H-14b). ^{13}C NMR (125 MHz, CD$_3$OD): δ 169.5 (C-5), 165.5 (C-2), 135.9 (C-8),

129.6 (C-9), 128.3 (C-10), 126.7 (C-11), 58.7 (C-3), 56.3 (C-6), 44.6 (C-12), 36.8 (C-7), 28.0 (C-14), 21.4 (C-13). IR (neat): v_{max} 3251, 3063, 2956,1655, 1447 cm^{-1}. HRMS (ESI) calculated for formula $C_{14}H_{17}N_2O_2$ [M+H]$^+$ 245.1270, found 245.1287. The NMR data was not found in the literature.
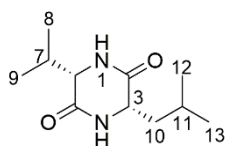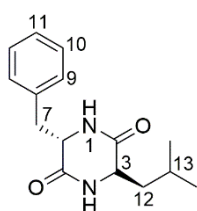
Cy(L-Val-L-Leu) 68: It was isolated from VF48A extract by preparative HPLC using method 1.7.4 (colourless solid, 3.1 mg, 10.3% extraction yield). HPLC: t_R 15.5 min. $[\alpha]^{25}_D$ = -55 (c 0.1, MeOH). ^{1}H NMR (500 MHz, CD$_3$OD): δ 3.94 (1H, ddd, J = 9.0, 4.5, 1.0 Hz, H-3), 3.78 (1H, dd, J = 4.5, 1.5 Hz, H-6), 2.23 (1H, m, H-7), 1.87 (1H, m, H-11), 1.75 (1H, ddd, J = 13.5, 9.0, 4.4 Hz, H-10a), 1.61 (1H, ddd, J = 13.5, 9.0, 4.5 Hz, H-10b), 1.06 (3H, d, J = 7.0 Hz, H-8), 0.97 (3H, d, J = 6.5 Hz, H-9), 0.96 (3H, d, J = 6.5 Hz, H-13), 0.95 (3H, d, J = 6.5 Hz, H-12). ^{13}C NMR (125 MHz, CD$_3$OD): δ 169.9 (C-5), 168.2 (C-2), 60.1 (C-6), 52.8 (C-3), 44.6 (C-10), 32.2 (C-7), 24.1 (C-11), 22.2 (C-9), 20.4 (C-13), 17.8 (C-8), 16.5 (C-12). IR (neat): v_{max} 3291, 2961, 2935, 1661, 1448 cm^{-1}. HRMS (ESI) calculated for formula $C_{11}H_{21}N_2O_2$ [M+H]$^+$ 213.1770, found 213.1846. The ^{1}H NMR data published in the literature is in agreement with current work.[140]

Cy(L-Phe-L-Tyr) 69: It was isolated from VF48A extract by preparative HPLC using method 1.7.4 (colourless solid, 1.7 mg, 5.7% extraction yield). HPLC: t_R 16.1 min. $[\alpha]^{25}_D$ = -81 (c 0.1, MeOH). ^{1}H NMR (500 MHz, CD$_3$OD): δ 7.33 (2H, t, J = 7.5 Hz, H-10), 7.25 (1H, t, J = 7.5 Hz, H-11), 7.11 (2H, d, J = 7.5 Hz, H-9), 6.94 (2H, d, J = 8.5 Hz, H-14), 6.77 (2H, d, J = 8.5 Hz, H-15), 4.08 (1H, ddd, J = 6.7, 4.0, 1.0 Hz, H-3), 4.05 (1H, ddd, J =6.5, 4.0, 1.0 Hz, H-6), 2.81 (1H, dd, J = 13.5, 4.0 Hz, H-7a), 2.72 (1H, dd, J = 14.0, 4.0 Hz, H-12a), 2.19 (H, dd, J = 13.5, 6.5 Hz, H-7b), 2.09 (1H, dd, J = 14.0, 6.7 Hz, H-12b). ^{13}C NMR (125 MHz, CD$_3$OD): δ 169.0 (C-2), 168.3 (C-2), 156.1 (C-16), 137.2 (C-8), 130.9 (C-14), 129.7 (C-9), 128.3 (C-10), 128.2 (C-13), 126.9 (C-11), 115.1 (C-15), 56.4 (C-6), 56.1 (C-3), 39.9 (C-7), 38.9 (C-12). IR (neat): v_{max} 3201, 2961, 1656, 1456 cm^{-1}. HRMS (ESI) calculated for formula $C_{18}H_{18}N_2O_3Na$ [M+Na]$^+$ 333.1520, found 333.1582. The ^{1}H NMR data published in the literature is in agreement with current work.[138]
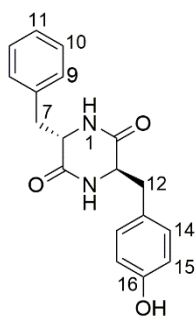
Cy(L-Phe-D-Tyr) 63: It was isolated from P5-25 extract by preparative HPLC using method 1.7.3 (colourless solid, 2.5 mg, 14% extraction yield). HPLC: t_R 16.9 min. $[\alpha]^{25}_D$ = +49 (c 0.1, MeOH). ^{1}H NMR (500 MHz, CD$_3$OD): δ 7.28 (2H, dd, J = 7.2, 6.8 Hz, H-10), 7.22 (1H, d, J = 6.8 Hz, H-11), 7.04 (2H, d, J = 7.2 Hz, H-9), 6.83 (2H, d, J = 8.5 Hz, H-14), 6.68 (2H, d, J = 8.5 Hz, H-15), 3.94 (1H, t, J = 5.0 Hz, H-6), 3.88 (1H, t, J = 4.8 Hz, H-3), 2.59 (1H, m, H-7a), 2.54 (1H, m, H-12a), 2.19 (1H, m, H-7b), 2.15 (1H, m, H-12b). ^{13}C NMR (125 MHz, CD$_3$OD): δ 166.8 (C-2), 166.6 (C-2), 156.6 (C-16), 137.4 (C-8), 125.3 (C-13), 132.3 (C-14), 131.1 (C-9), 129.7 (C-10), 128.2 (C-11), 116.5 (C-15), 59.0 (C-6), 57.7 (C-3), 40.2 (C-7), 30.7 (C-12). IR (neat): v_{max} 3194, 2963, 2923, 1656, 1457 cm^{-1}. HRMS (ESI) calculated for formula C$_{18}$H$_{18}$N$_2$O$_3$Na [M+Na]$^+$ 333.1520, found 333.1582. The NMR data was not found in the literature.
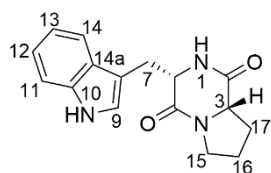
Cy(L-Tryp-L-Pro) 70: It was isolated from VF48A extract by preparative HPLC using method 1.7.4 (colourless glassy solid, 1.9 mg, 6.3% extraction yield). HPLC: t_R 16.5 min. $[\alpha]^{25}_D$ = -50 (c 0.1, MeOH). ^{1}H NMR (500 MHz, CD$_3$OD): δ 7.62 (1H, d, J = 8.0 Hz, H-14), 7.37 (1H, d, J = 8.0 Hz, H-11), 7.12 (1H, s, H-9), 7.11 (1H, dd, J = 8.0, 7.5 Hz, H-12), 7.05 (1H, dd, J = 8.0, 7.5 Hz, H-13), 4.46 (1H, dt, J = 5.0, 1.5 Hz, H-6), 4.05 (1H, dd, J = 11.0, 6.5 Hz, H-3), 3.51 (1H, m, H-15a), 3.32 (1H, dd, J = 11.5, 1.5 Hz, H-7a), 3.30 (1H, m, H-15b), 2.02 (1H, m, H-17a), 1.72 (1H, m, H-16a), 1.52 (1H,m, H-16b), 1.00 (1H, m, H-17b), 0.98 (1H, m, H-7b). ^{13}C NMR (125 MHz, CD$_3$OD): δ 166.4 (C-2), 163.2 (C-5), 137.1 (C-8), 130.9 (C-10a), 115.3 (C-14a), 124.6 (C-9), 121.6 (C-12), 118.7 (C-13), 118.5 (C-14), 113.3 (C-11), 59.1 (C-3), 56.1 (C-6), 44.4 (C-15), 27.7 (C-17), 27.6 (C-7), 20.9 (C-16). IR (neat): v_{max} 3262, 2953, 2925, 1668, 1436 cm^{-1}. HRMS (ESI) calculated for formula C$_{16}$H$_{16}$N$_3$O$_2$Na [M+Na]$^+$ 306.1540, found 306.1554. The ^{1}H NMR data published in the literature is in agreement with current work.[140]

Cy(L-Phe-L-Val) 71: It was isolated from VF48A extract by preparative HPLC using method 1.7.4 (colourless solid, 2.1 mg, 7% extraction yield). HPLC: t_R 18.1 min. $[\alpha]^{25}_D$ = -94 (c 0.1, MeOH). ^{1}H NMR (500 MHz, CD$_3$OD): δ 7.28 (2H, dd, J = 7.5, 7.0 Hz, H-10), 7.23 (2H, d, J = 7.5 Hz, H-9), 7.21 (1H, d, J = 7.0 Hz, H-11), 4.31 (1H, dt, J = 5.0, 1.5 Hz, H-6), 3.64 (1H, dd, J =4.5, 1.5 Hz, H-3), 3.24 (1H, dd, J = 13.5, 5.5 Hz, H-7a), 3.04 (1H, dd, J

= 13.5, 4.5 Hz, H-7b), 1.64 (H, m, H-12), 0.79 (3H, d, J = 7.0 Hz, H-13), 0.43 (3H, d, J = 7.0 Hz, H-14). ^{13}C NMR (125 MHz, CD$_3$OD): δ 168.0 (C-2 & 5), 135.6 (C-8), 130.1 (C-9), 128.2 (C-10), 126.8 (C-11), 59.8 (C-3), 55.9 (C-6), 38.7 (C-7), 31.9 (C-12), 17.7 (C-13), 15.7 (C-14). IR (neat): v_{max} 3187, 2965, 2885, 1660, 1452 cm^{-1}. HRMS (ESI) calculated for formula C$_{14}$H$_{19}$N$_2$O$_2$ [M+H]$^+$ 247.1420, found 247.1451. The ^{1}H NMR data published in the literature is in agreement with current work.[138]

Cy(L-Phe-L-Leu) 64: It was isolated from VF48A extract by preparative HPLC using method 1.7.4 (colourless solid, 2.7 mg, 9% extraction yield). HPLC: t$_R$ 21.4 min. [α]^{25}$_D$ = -25 (c 0.1, MeOH). ^{1}H NMR (500 MHz, CD$_3$OD): δ 7.31 (2H, dd, J = 7.5, 7.0 Hz, H-10), 7.26 (1H, d, J = 7.0 Hz, H-11), 7.19 (2H, d, J = 7.5 Hz, H-9), 4.31 (1H, t, J = 5.0 Hz, H-6), 3.66 (1H, dd, J = 9.8, 4.5 Hz, H-3), 3.26 (1H, dd, J = 14.0, 4.5 Hz, H-7a), 2.95 (1H, dd, J = 14.0, 4.5 Hz, H-7b), 1.42 (1H, m, H-13), 0.87 (1H, ddd, J = 13.8, 9.8, 4.5 Hz, H-12a), 0.73 (3H, d, J = 7.0 Hz, H-14), 0.69 (3H, d, J = 7.0 Hz, H-15), 0.08 (1H, ddd, J = 13.8, 9.4, 4.5 Hz, H-12b). ^{13}C NMR (125 MHz, CD$_3$OD): δ 168.0 (C-2), 167.9 (C-5), 135.4 (C-8), 130.3 (C-9), 128.2 (C-10), 127.1 (C-11), 56.0 (C-6), 56.0 (C-3), 42.7 (C-12), 38.8 (C-7), 23.2 (C-13), 21.9 (C-15), 20.0 (C-14). IR (neat): v_{max} 3195, 2958, 2897, 1668, 1454 cm^{-1}. HRMS (ESI) calculated for formula C$_{15}$H$_{20}$N$_2$O$_2$ [M-Na]$^+$ 283.3400, found 283.1422. The ^{1}H NMR data published in the literature is in agreement with current work.[138]

7.12 Compound Characterisation: Synthetic Compounds
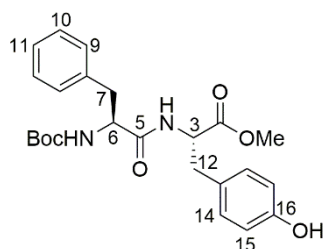
Boc-L-Phe-L-Tyr methyl ester: L-Tyr-OMe (232 mg; 1.00 mmol), Boc-L-phenylalanine (292 mg; 1.10 mmol), DMAP (122 mg; 1.00 mmol) and EDC (192 mg; 1.30 mmol) were reacted in DCM as described in the general procedure. The crude product was purified by flash chromatography using DCM/MeOH (95:5) as eluent. Pure compound was isolated as a colourless solid (287 mg; 65%). ^{1}H NMR (500 MHz, CD$_3$OD): δ 7.24 (2H, dd, J = 7.3, 7.1 Hz, H-10), 7.19 (1H, d, J = 7.1 Hz, H-11), 7.12 (2H, d, J = 7.3 Hz, H-9), 6.91 (2H, d, J = 8.5 Hz, H-14), 6.65 (2H, d, J = 8.5 Hz, H-15), 4.54 (1H, t, J = 5.5 Hz, H-3), 4.19 (1H, t, J = 5.0 Hz, H-6), 3.74 (3H, s , OC$\underline{H}_3$), 3.24 (1H, m, H-12a), 3.22 (1H, m, H-7a),

2.92 (1H, m, H-7b), 2.91 (1H, m, H-12b), 1.29 (9H, C$\underline{H}_3$). ^{13}C NMR (125 MHz, CD$_3$OD): δ 169.9 (C-2), 168.7 (C-2), 166.1 ($\underline{C}$O, Boc), 156.0 (C-16), 136.9 (C-8), 131.2 (C-14), 129.9 (C-9), 127.9 (C-10), 127.0 (C-13), 126.1 (C-11), 115.3 (C-15), 71.9 (C$_q$, Boc), 56.1 (C-6), 53.4 (C-3), 52.1 ($\underline{C}H_3$, ester), 41.9 (C-7), 40.9 (C12), 26.9 ($\underline{C}H_3$, Boc). HRMS (ESI) calculated for formula C$_{24}$H$_{30}$N$_2$O$_6$ [M+Na]$^+$ 465.2103, found 465.2003.
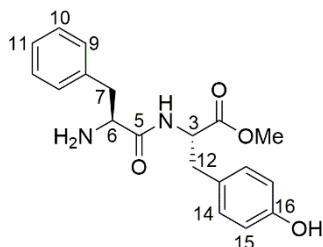

Deboc-L-Phe-L-Tyr methyl ester: *N*-Boc-L-Phe-L-Tyr-OMe (287 mg; 0.650 mmol) was dissolved in MeOH (5 mL) and HCl 4 M in dioxane (3.30 mL; 13.0 mmol) as described in the general procedure. The mixture was concentrated *in vacuo* to give deprotected compound (201 mg; 91%). ^{1}H NMR (500 MHz, CD$_3$OD): δ 7.24 (2H, dd, *J* = 7.3, 7.1 Hz, H-10), 7.19 (1H, d, *J* = 7.1 Hz, H-11), 7.12 (2H, d, *J* = 7.3 Hz, H-9), 6.91 (2H, d, *J* = 8.5 Hz, H-14), 6.65 (2H, d, *J* = 8.5 Hz, H-15), 4.54 (1H, t, *J* = 5.5 Hz, H-3), 4.19 (1H, t, *J* = 5.0 Hz, H-6), 3.74 (3H, s, OC$\underline{H}_3$), 3.24 (1H, m, H-12a), 3.22 (1H, m, H-7a), 2.92 (1H, m, H-7b), 2.91 (1H, m, H-12b), 1.29 (9H, s, C$\underline{H}_3$). ^{13}C NMR (125 MHz, CD$_3$OD): δ 170.4 (C-2), 169.8 (C-2), 156.5 (C-16), 135.9 (C-8), 131.4 (C-14), 130.1 (C-9), 128.2 (C-10), 127.2 (C-13), 126.4 (C-11), 116.3 (C-15), 54.1 (C-6), 53.9 (C-3), 52.4 ($\underline{C}H_3$, ester), 42.6 (C-7), 40.5 (C12). HRMS (ESI$^+$) calculated for formula C$_{19}$H$_{22}$N$_2$O$_4$ [M+Na]$^+$ 365.2019, found 365.2001.
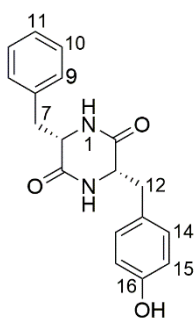
Cy(L-Phe-L-Tyr) 69: L-Phe-L-Tyr-OMe (100 mg; 0.264 mmol) and triethylamine (92 µL; 0.660 mmol) were reacted as described in the general procedure. Pure compound was isolated as colourless solid by filtration (71 mg; 87%). HPLC: t$_R$ 16.1 min. [α]$^{25}_D$ = -82 (*c* 0.1, MeOH). ^{1}H NMR (500 MHz, CD$_3$OD): δ 7.33 (2H, t, *J* = 7.5 Hz, H-10), 7.25 (1H, t, *J* = 7.5 Hz, H-11), 7.11 (2H, d, *J* = 7.5 Hz, H-9), 6.94 (2H, d, *J* = 8.5 Hz, H-14), 6.77 (2H, d, *J* = 8.5 Hz, H-15), 4.08 (1H, ddd, *J* = 6.7, 4.0, 1.0 Hz, H-3), 4.05 (1H, ddd, *J* = 6.5, 4.0, 1.0 Hz, H-6), 2.81 (1H, dd, *J* = 13.5, 4.0 Hz, H-7a), 2.72 (1H, dd, *J* = 14.0, 4.0 Hz, H-12a), 2.19 (1H, dd, *J* = 13.5, 6.5 Hz, H-7b), 2.09 (1H, dd, *J* = 14.0, 6.7 Hz, H-12b). ^{13}C NMR (125 MHz, CD$_3$OD): δ 166.7 (C-2), 166.6 (C-2), 156.4 (C-16), 137.2 (C-8), 130.8 (C-14), 129.8 (C-9), 128.2 (C-10), 128.1 (C-13), 126.4 (C-11), 115.0 (C-15), 55.7 (C-6), 55.4 (C-3), 38.9 (C-7), 38.5 (C-12). IR (neat): ν$_{max}$ 3194, 3086, 3056, 1655, 1458 cm^{-1}. HRMS (ESI) calculated for formula C$_{18}$H$_{18}$N$_2$O$_3$Na [M+Na]$^+$ 333.1520, found 333.1582.
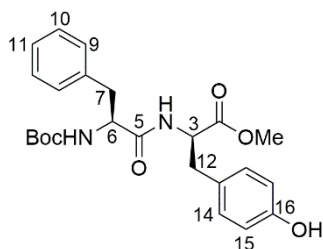
Boc-L-Phe-D-Tyr methyl ester: D-Tyr-OMe (232 mg; 1.00 mmol), Boc-L-phenylalanine (292 mg; 1.10 mmol), DMAP (122 mg; 1.00 mmol) and EDC (192 g; 1.3 mmol) were reacted in DCM as described in the general procedure. The crude product was purified by flash chromatography using DCM/MeOH (95:5) as eluent. Pure compound was isolated as a colourless solid (243 mg; 55%). ^{1}H NMR (500 MHz, CD$_3$OD): δ 7.26 (2H, dd, J = 7.2, 7.0 Hz, H-10), 7.22 (1H, d, J = 7.2 Hz, H-11), 7.10 (2H, d, J = 7.0 Hz, H-9), 6.94 (2H, d, J = 8.4 Hz, H-14), 6.70 (2H, d, J = 8.4 Hz, H-15), 4.61 (1H, dd, J = 8.4, 6.0 Hz, H-3), 3.69 (3H, s, OC$\underline{H}_3$), 3.58 (1H, dd, J = 7.3, 5.0 Hz, H-6), 2.96 (1H, dd, J = 14.0, 6.0 Hz, H-12a), 2.91 (1H, dd, J = 13.5, 5.0 Hz, H-7a), 2.80 (1H, dd, J = 14.0, 8.4 Hz, H-12b), 2.69 (1H, dd, J = 13.5, 7.3 Hz, H-7b), 1.32 (9H, s, C$\underline{H}_3$). ^{13}C NMR (125 MHz, CD$_3$OD): δ 1672.1 (C-2), 171.7 (C-2), 167.9 ($\underline{C}$O, Boc), 156.0 (C-16), 137.2 (C-8), 129.9 (C-14), 129.1 (C-9), 128.1 (C-10), 127.1 (C-13), 126.4 (C-11), 114.9 (C-15), 71.0 (C$_q$, Boc), 55.8 (C-6), 53.8 (C-3), 51.3 ($\underline{C}$H$_3$, ester), 40.9 (C-7), 36.4 (C-12), 27.5 ($\underline{C}$H$_3$, Boc). HRMS (ESI$^+$) calculated for formula C$_{24}$H$_{30}$N$_2$O$_6$ [M+Na]+ 465.2103, found 465.2003.
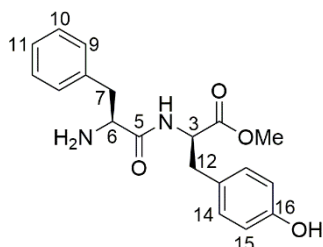
Deboc-L-Phe-D-Tyr methyl ester: N-Boc-L-Phe-D-Tyr-OMe (243 mg; 0.550 mmol) was dissolved in MeOH (5 mL) and HCl 4M in dioxane (2.80 mL; 11.0 mmol) as described in the general procedure. The mixture was concentrated *in vacuo* to give deprotected compound (149 mg; 79%). ^{1}H NMR (500 MHz, CD$_3$OD): δ 7.25 (2H, dd, J = 7.5, 7.0 Hz, H-10), 7.22 (1H, d, J = 7.5 Hz, H-11), 7.11 (2H, d, J = 7.0 Hz, H-9), 6.92 (2H, d, J = 8.5 Hz, H-14), 6.68 (2H, d, J = 8.5 Hz, H-15), 4.52 (1H, dd, J = 8.2, 6.1 Hz, H-3), 3.74 (3H, s, OC$\underline{H}_3$), 3.58 (1H, dd, J = 7.0, 5.0 Hz, H-6), 3.01 (1H, dd, J = 13.5, 6.1 Hz, H-12a), 2.94 (1H, dd, J = 13.0, 5.0 Hz, H-7a), 2.85 (1H, dd, J = 13.5, 8.0 Hz, H-12b), 2.72 (1H, dd, J = 13.0, 7.0 Hz, H-7b). ^{13}C NMR (125 MHz, CD$_3$OD): δ 173.4 (C-2), 171.9 (C-2), 156.2 (C-16), 137.5 (C-8), 129.7 (C-14), 128.9 (C-9), 128.0 (C-10), 126.9 (C-13), 126.2 (C-11), 116.4 (C-15), 55.8 (C-6), 54.2 (C-3), 51.4 ($\underline{C}$H$_3$, ester), 41.6 (C-7), 36.2 (C12). HRMS (ESI$^+$) calculated for formula C$_{19}$H$_{22}$N$_2$O$_4$ [M+Na]$^+$ 365.2019, found 365.2001.
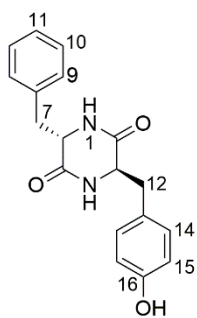
Cy(L-Phe-D-Tyr) 63: L-Phe-D-Tyr-OMe (100 mg; 0.264 mmol) and triethylamine (92 µL; 0.660 mmol) were reacted as described in the general procedure. Two isomers were isolated by preparative HPLC using method 1.6.11: cy(L-Phe-D-Tyr) as colourless powder (22 mg; 27%) and cy(L-Phe-L-Tyr) as colourless powder (28 mg; 34%). HPLC: t_R 16.9 min. $[\alpha]^{25}_D$ = +48 (c 0.1, MeOH). ^{1}H NMR (500 MHz, CD$_3$OD): δ 7.28 (2H, dd, J = 7.2, 6.8 Hz, H-10), 7.22 (1H, d, J = 6.8 Hz, H-11), 7.04 (2H, d, J = 7.2 Hz, H-9), 6.83 (2H, d, J = 8.5 Hz, H-14), 6.68 (2H, d, J = 8.5 Hz, H-15), 3.94 (1H, t, J = 5.0 Hz, H-6), 3.88 (1H, t, J = 4.8 Hz, H-3), 2.59 (1H, m, H-7a), 2.54 (1H, m, H-12a), 2.19 (1H, m, H-7b), 2.15 (1H, m, H-12b). ^{13}C NMR (125 MHz, CD$_3$OD): δ 166.8 (C-2), 166.6 (C-2), 156.6 (C-16), 137.4 (C-8), 125.3 (C-13), 132.3 (C-14), 131.1 (C-9), 129.7 (C-10), 128.2 (C-11), 116.5 (C-15), 59.0 (C-6), 57.7 (C-3), 40.2 (C-7), 30.7 (C-12). IR (neat): v_{max} 3194, 2963, 2923, 1656, 1456 cm^{-1}. HRMS (ESI) calculated for formula C$_{18}$H$_{18}$N$_2$O$_3$Na [M+Na]$^+$ 333.1520, found 333.1582.
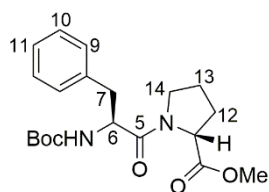
Boc-L-Phe-L-Pro methyl ester: L-Pro-OMe (166 mg; 1.00 mmol), Boc-L-phenylalanine (292 mg; 1.10 mmol), DMAP (122 mg; 1.00 mmol) and EDC (192 g; 1.3 mmol) were reacted in DCM as described in the general procedure. The crude product was purified by flash chromatography using DCM/MeOH (95:5) as eluent. Pure compound was isolated as a colourless powder (263 mg; 70%). ^{1}H NMR (500 MHz, CD$_3$OD): δ 7.31 (2H, m, H-9), 7.29 (2H, m, H-10), 7.23 (1H, m, H-11), 4.65 (1H, dd, J = 8.5, 4.5 Hz, H-6), 4.45 (1H, dd, J = 8.0, 6.0 Hz, H-3), 3.75 (1H, m, H-14a), 3.72 (3H, s, OCH$_3$), 3.38 (1H, m, H-14b), 3.03 (1H, dd, J = 14.0, 4.5 Hz, H-7a), 2.80 (1H, dd, J = 14.0, 8.5, H-7b), 2.24 (1H, m, H-12a), 1.95 (2H, m, H-13), 1.91 (1H, m, H-12b), 1.91 (9H, s, CH$_3$). ^{13}C NMR (125 MHz, CD$_3$OD): δ 172.5 (C-2), 171.7 (C-5), 168.1 (CO, Boc), 138.9 (C-8), 129.2 (C-10), 128.1 (C-9), 126.4 (C-11), 79.1 (C$_q$, Boc), 59.2 (C-3), 53.8 (C-6), 51.1 (CH$_3$, ester), 48.2 (C-14), 37.1 (C-7), 28.8 (C-12), 27.0 (CH$_3$, Boc), 24.1 (C-13). IR (neat): v_{max} 3228, 2956, 2890, 1642, 1438 cm^{-1}. HRMS (ESI$^+$) calculated for formula C$_{20}$H$_{29}$N$_2$O$_5$ [M+H]$^+$ 377.2000, found 377.1562.
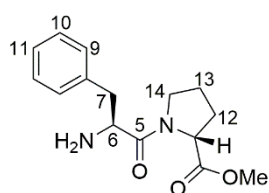
Deboc-L-Phe-L-Pro methyl ester: N-Boc-L-Phe-L-Pro-OMe (263 mg; 0.700 mmol) was dissolved in MeOH (5 mL) and HCl 4M in dioxane (3.6 mL; 14.0 mmol) as described in the general procedure. The mixture was concentrated *in vacuo* to give pure deprotected compound (164 mg; 85%). ^{1}H NMR (500 MHz, CD$_3$OD): δ 7.39 (2H, m, H-

10), 7.33 (1H, m, H-11), 7.36 (2H, m, H-9), 4.50 (1H, dd, J = 8.7, 4.8 Hz, H-3), 4.40 (1H, t, J = 7.0, H-), 3.76 (3H, s, OC$\underline{H}_3$), 3.61 (1H, m, H-14a), 3.25 (1H, dd, J = 13.8, 6.9 Hz, H-7a), 3.08 (1H, m, H-7b), 3.06 (1H, m, H-14b), 2.26 (1H, m, H-12a), 1.94 (1H, m, H-12b), 1.93 (2H, m, H-13). ^{13}C NMR (125 MHz, CD$_3$OD): δ 171.9 (C-2), 167.2 (C-5), 133.9 (C-8), 129.6 (C-10), 128.7 (C-9), 127.6 (C-11), 59.3 (C-3), 53.0 (C-6), 51.4 ($\underline{C}$H$_3$, ester), 46.9 (C-14), 36.5 (C-7), 28.6 (C-12), 24.1 (C-13). HRMS (ESI) calculated for formula C$_{15}$H$_{21}$N$_2$O$_3$ [M+H]$^+$ 276.1500, found 277.1562.
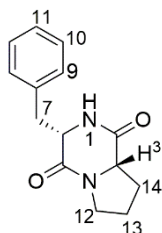
Cy(L-Phe-L-Pro) 67: L-Phe-L-Pro-OMe (100 mg; 0.362 mmol) and triethylamine (125 µL; 0.905 mmol) were reacted as described in the general procedure. Pure compound was isolated from reaction mixture as colourless powder by extracting with ethyl acetate three times (79 mg; 90%). HPLC: t$_R$ 13.4 min. [α]^{25}$_D$ = +79 (c 0.1, MeOH). ^{1}H NMR (500 MHz, CD$_3$OD): δ 7.30 (2H, m, H-9), 7.27 (1H, m, H-11), 7.18 (2H, dd, J = 7.0, 3.0, Hz, H-10), 4.20 (1H, t, J = 4.5 Hz, H-6), 3.63 (1H, m, H-12a), 3.31 (1H, m, H-12b), 3.19 (1H, dd, J = 13.8, 4.5 Hz, H-7a), 2.99 (1H, dd, J = 13.8, 4.5 Hz, H-7b), 2.62 (1H, m, H-3), 2.02 (1H, m, H-14a), 1.90 (1H, m, H-13a), 1.88 (1H, m, H-14b), 1.85 (1H, m, H-13b). ^{13}C NMR (125 MHz, CD$_3$OD): δ 169.9 (C-5), 168.0 (C-2), 136.3 (C-8), 129.9 (C-10), 128.3 (C-9), 127.1 (C-11), 58.3 (C-6), 57.7 (C-3), 44.7 (C-12), 39.7 (C7), 28.4 (C14), 21.1 (C-13). IR (neat): v_{max} 3228, 2956, 2890, 1642, 1437 cm^{-1}. HRMS (ESI) calculated for formula C$_{14}$H$_{17}$N$_2$O$_2$ [M+H]$^+$ 245.1200, found 245.1302.
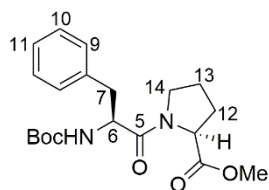
Boc-L-Phe-D-Pro methyl ester: D-Pro-OMe (166 mg; 1.00 mmol), Boc-L-phenylalanine (292 mg; 1.10 mmol), DMAP (122 mg; 1.00 mmol) and EDC (192 g; 1.30 mmol) were reacted in DCM as described in the general procedure. The crude product was purified by flash chromatography by using DCM/MeOH (95:5) as eluent. Pure compound was isolated as a colourless powder (226 mg; 60%). ^{1}H NMR (500 MHz, CD$_3$OD): δ 7.21 (2H, m, H-9), 7.21 (2H, m, H-10), 7.19 (1H, m, H-11), 4.53 (1H, m, H-3), 4.19 (1H, m, H-3), 3.63 (3H, s, OC$\underline{H}_3$), 3.46 (1H, m, H-14a), 2.93 (1H, dd, J = 12.8, 6.0 Hz, H-7a), 2.83 (1H, dd, J = 12.8, 9.4, H-7b), 2.62 (1H, m, H-14b), 1.86 (1H, m, H-12a), 1.78 (1H, m, H-13a), 1.76 (1H, m, H-12b), 1.46 (1H, m, H-13b), 1.36 (9H,s, C$\underline{H}_3$). ^{13}C NMR (125 MHz, CD$_3$OD): δ 172.5 (C-2), 170.7 (C-5), 168.4 ($\underline{C}$O, Boc), 136.2 (C-8), 129.3 (C-9), 128.4 (C-10), 126.9 (C-11), 79.9 (C$_q$, Boc), 58.8 (C-6), 53.5 (C-3), 52.1 ($\underline{C}$H$_3$, ester), 46.8 (C-14), 39.6 (C7), 28.9 (C12), 28.2 ($\underline{C}$H$_3$, Boc), 24.3 (C-13). HRMS (ESI) calculated for formula C$_{20}$H$_{29}$N$_2$O$_5$ [M+H]$^+$ 377.2000, found 375.1562.

150
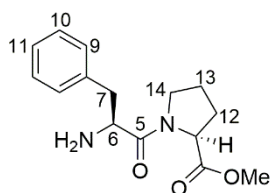
Deboc-L-Phe-D-Pro methyl ester: *N*-Boc-L-Phe-L-Pro-OMe (226 mg; 0.60 mmol) was dissolved in MeOH (5 mL) and HCl 4 M in dioxane (3.10 mL; 12.0 mmol) as described in the general procedure. The mixture was concentrated *in vacuo* to give pure deprotected compound (203 mg; 90%). ^{1}H NMR (500 MHz, CD$_3$OD): δ 7.24 (2H, dd, J = 8.4, 7.2 Hz, H-10), 7.19 (1H, d, J = 8.4 Hz, H-11), 7.13 (2H, d, J = 7.2 Hz, H-9), 3.66 (2H, m, H-3, 6), 3.63 (3H, s, OCH$_3$), 3.42 (1H, m, H-14a), 3.04 (1H, dd, J = 13.6, 4.8 Hz, H-7a), 2.79 (1H, dd, J = 13.6, 8.0 Hz, H-7b), 2.51 (1H, m, H-14b), 1.84 (1H, m, H-12a), 1.81 (1H, m, H-13a), 1.75 (1H, m, H-12b), 1.39 (1H, m, H-13b). ^{13}C NMR (125 MHz, CD$_3$OD): δ 175.4 (C-2, 5), 137.2 (C-8), 129.3 (C-9), 128.6 (C-10), 126.9 (C-11), 55.9 (C-3, 6), 52.0 (CH$_3$, ester), 45.9 (C-14), 41.0 (C-7), 27.9 (C-12), 24.1 (C-13). HRMS (ESI) calculated for formula C$_{15}$H$_{21}$N$_2$O$_3$ [M+H]$^+$ 276.1500, found 277.1562.
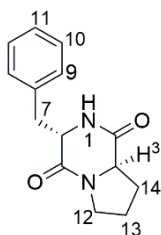
Cy(L-Phe-D-Pro) 60: L-Phe-D-Pro-OMe (100 mg; 0.362 mmol) and triethylamine (125 µL; 0.905 mmol) were reacted as described in the general procedure. Two isomers were isolated by preparative HPLC using method 1.6.11: cy(L-Phe-D-Pro) as colourless powder (15 mg; 17%) and cy(L-Phe-L-Pro) as colourless powder (35 mg; 40%). HPLC: t$_R$ 8.99 min. [α]$^{25}_D$ = -137 (*c* 0.1, MeOH). ^{1}H NMR (500 MHz, CD$_3$OD): δ 7.30 (2H, t, J = 7.4 Hz, H-10), 7.24 (2H, d, J = 7.4 Hz, H-9), 7.23 (1H, d, J = 7.4 Hz, 11), 4.45 (1H, dt, J = 5.0, 1.5 Hz, H-6), 4.06 (1H, ddd, J = 10.5, 6.0, 1.5, H-3), 3.54 (1H, m, H-12a), 3.36 (1H, m, H-12b), 3.16 (2H, dd, J = 5.0, 2.0 Hz, H-7), 2.09 (1H, m, H-14a), 1.80 (2H, m, H-13), 1.22 (1H, m, H-14b). ^{13}C NMR (125 MHz, CD$_3$OD): δ 169.4 (C-2), 165.5 (C-5), 136.3 (C-8), 129.6 (C-9), 128.3 (C-10), 126.6 (C-11), 58.7 (C-3), 56.2 (C-6), 44.6 (C-12), 36.8 (C-7), 27.9 (C-14), 21.4 (C-13). IR (neat): v_{max} 3203, 3063, 2956, 1665, 1448 cm^{-1}. HRMS (ESI) calculated for formula C$_{14}$H$_{17}$N$_2$O$_2$ [M+H]$^+$ 245.1200, found 245.1302.
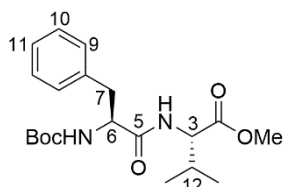
Boc-L-Phe-L-Val methyl ester: L-Val-OMe (168 mg; 1.00 mmol), Boc-L-phenylalanine (292 mg; 1.10 mmol), DMAP (122 mg; 1.00 mmol) and EDC (192 g; 1.3 mmol) were reacted in DCM as described in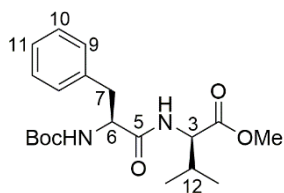 the general procedure. The crude product was purified by flash chromatography using DCM/MeOH (95:5) as eluent. Pure compound was isolated as a colourless powder (303 mg; 80%). ^{1}H NMR (500 MHz, CD$_3$OD): δ 7.28 (2H, m, H-10), 7.23 (2H, m, H-9), 7.21 (1H, m, H-11), 4.38 (1H, dd, J =

9.5, 5.5 Hz, H-6), 4.35 (1H, d, J = 6.0 Hz, H-3), 3.70 (3H, s, OC$\underline{H}_3$), 3.11 (1H, dd, J = 13.5, 5.5 Hz, H-7a), 2.85 (1H, dd, J = 13.5, 9.5, H-7b), 2.15 (1H, m, H-12), 1.38 (9H, s, C$\underline{H}_3$), 0.97 (3H, d, J = 6.0 Hz, H-13), 0.95 (3H, d, J = 6.0 Hz, H-14). ^{13}C NMR (125 MHz, CD$_3$OD): δ 173.1 (C-5), 171.8 (C-2), 156.2 ($\underline{C}$O, Boc), 137.1 (C-8), 128.9 (C-9), 127.9 (C-10), 126.2 (C-11), 79.2 (C$_q$, Boc), 57.2 (C-3), 55.8 (C-6), 50.9 ($\underline{C}H_3$, ester), 37.7 (C-7), 30.6 (C-12), 27.1 ($\underline{C}H_3$, Boc), 18.1 (C-13), 17.0 (C-14). HRMS (ESI) calculated for formula C$_{20}$H$_{30}$N$_2$O$_5$ [M+Na]$^+$ 401.2200, found 401.2235.
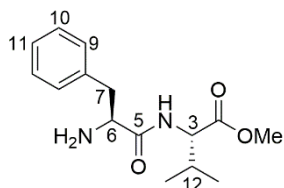
Deboc-L-Phe-L-Val methyl ester: *N*-Boc-L-Phe-L-Val-OMe (303 mg; 0.800 mmol) was dissolved in MeOH (5 mL) and HCl 4 M in dioxane (4.10 mL; 16.0 mmol) as described in the general procedure. The mixture was concentrated in *vacuo* to give pure deprotected compound (223 mg; 82%). ^{1}H NMR (500 MHz, CD$_3$OD): δ 7.37 (2H, dd, J = 7.5, 6.5 Hz, H-10), 7.33 (1H, d, J = 7.5 Hz, H-11), 7.32 (2H, dd, J = 6.5 Hz, H-19), 4.37 (1H, d, J = 5.5 Hz, H-3), 4.19 (1H, dd, J = 8.5, 6.0 Hz, H-6), 3.64 (3H, s, OC$\underline{H}_3$), 3.28 (1H, dd, J = 14.0, 6.0 Hz, H-7a), 3.02 (1H, dd, J = 14.0, 8.5, H-7b), 2.18 (1H, m, H-12), 0.98 (3H, d, J = 7.0 Hz, H-14), 0.96 (3H, d, J = 6.0 Hz, H-13). ^{13}C NMR (125 MHz, CD$_3$OD): δ 171.4 (C-2), 168.5 (C-5), 134.1 (C-8), 129.2 (C-9), 128.7 (C-10), 127.5 (C-11), 68.1 (C-3), 64.1 (C-6), 61.2 ($\underline{C}H_3$, ester), 37.3 (C-7), 30.4 (C-12), 17.9 (C-13), 17.1 (C-14). HRMS (ESI) calculated for formula C$_{15}$H$_{23}$N$_2$O$_3$ [M+H]$^+$ 279.1600, found 279.1728.
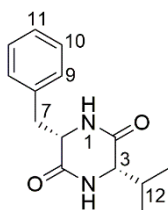
Cy(L-Phe-L-Val) 71: L-Phe-L-Val-OMe (100 mg; 0.360 mmol) and triethylamine (125 µL; 0.905 mmol) were reacted as described in the general procedure. Two isomers were isolated by preparative HPLC using method 1.6.11: cy(L-Phe-L-Val) as colourless powder (20 mg; 20%) and cy(L-Phe-D-Val) as colourless powder (18 mg; 23%). HPLC: t$_R$ 18.1 min. [α]$^{25}_D$ = -95 (*c* 0.1, MeOH). ^{1}H NMR (500 MHz, CD$_3$OD): δ 7.28 (2H, dd, J = 7.5, 7.0 Hz, H-10), 7.23 (2H, d, J = 7.5 Hz, H-9), 7.21 (1H, d, J = 7.0 Hz, H-11), 4.31 (1H, t, J = 5.0 Hz, H-6), 3.65 (1H, d, J =4.5 Hz, H-3), 3.23 (1H, dd, J = 13.5, 5.5 Hz, H-7a), 3.04 (1H, dd, J = 13.5, 5.0 Hz, H-7b), 1.64 (H, m, H-12), 0.79 (3H, d, J = 7.0 Hz, H-13), 0.44 (3H, d, J = 7.0 Hz, H-14). ^{13}C NMR (125 MHz, CD$_3$OD): δ 168.0 (C-2 & 5), 135.6 (C-8), 130.1 (C-9), 128.2 (C-10), 126.8 (C-11), 59.8 (C-3), 55.9 (C-6), 38.7 (C-7), 31.9 (C-12), 17.7 (C-13), 15.7 (C-14). IR (neat): v_{max} 3187, 2965, 2932, 2886, 1660, 1452 cm^{-1}. HRMS (ESI) calculated for formula C$_{14}$H$_{19}$N$_2$O$_2$ [M+H]$^+$ 247.1420, found 247.1451.
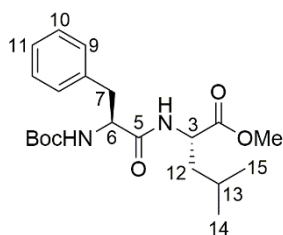
Boc-L-Phe-D-Val methyl ester: D-Val-OMe (168 mg; 1.00 mmol), Boc-L-phenylalanine (292 mg; 1.10 mmol), DMAP (122 mg; 1.00 mmol) and EDC (192 g; 1.30 mmol) were reacted in DCM as described in the general procedure. The crude product was purified by flash chromatography using DCM/MeOH (95:5) as eluent. Pure compound was isolated as a colourless powder by filtration (265 mg; 70%). ^{1}H NMR (500 MHz, CD$_3$OD): δ 7.27 (2H, d, J = 7.5 Hz, H-9), 7.25 (2H, dd, J = 7.5, 7.0 Hz, H-10), 7.20 (1H, m, H-11), 4.38 (1H, dd, J = 8.5, 6.5 Hz, H-6), 4.26 (1H, d, J = 6.0 Hz, H-3), 3.70 (3H, s, OC$\underline{H}_3$), 3.05 (1H, dd, J = 13.8, 6.5 Hz, H-7a), 2.84 (1H, dd, J = 13.8, 8.5, H-7b), 2.06 (1H, m, H-12), 1.38 (9H,s, C$\underline{H}_3$), 0.86 (3H, d, J = 6.0 Hz, H-13), 0.82 (3H, d, J = 6.0 Hz, H-14). ^{13}C NMR (125 MHz, CD$_3$OD): δ 173.1 (C-5), 171.8 (C-2), 156.1 ($\underline{C}$O, Boc), 137.1 (C-8), 129.0 (C-9), 128.1 (C-10), 126.2 (C-11), 79.2 (C$_q$, Boc), 57.8 (C-3), 56.0 (C-6), 50.9 ($\underline{C}$H$_3$, ester), 38.0 (C7), 30.6 (C12), 27.3 ($\underline{C}$H$_3$, Boc), 17.8 (C-13), 17.1 (C14). HRMS (ESI) calculated for formula C$_{20}$H$_{30}$N$_2$O$_5$ [M+Na]$^+$ 401.2200, found 401.2066.
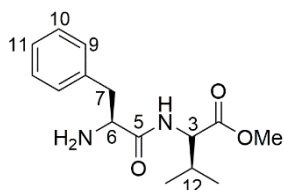
Deboc-L-Phe-D-Val methyl ester: *N*-Boc-L-Phe-L-Val-OMe (265 mg; 0.700 mmol) was dissolved in MeOH (5 mL) and HCl 4M in dioxane (3.60 mL; 14.0 mmol) as described in the general procedure. The mixture was concentrated in *vacuo* to give pure deprotected compound (140 mg; 72%). ^{1}H NMR (500 MHz, CD$_3$OD): δ 7.37 (2H, d, J = 7.0 Hz, H-9), 7.31 (2H, dd, J = 7.5, 7.0 Hz, H-10), 7.30 (1H, d, J = 7.5 Hz, H-11), 4.37 (1H, d, J = 5.5 Hz, H-6), 4.22 (1H, t, J = 7.5 Hz, H-3), 3.71 (3H, s, OC$\underline{H}_3$), 3.18 (1H, dd, J = 13.8, 7.5 Hz, H-7a), 3.08 (1H, dd, J = 13.8, 5.5, H-7b), 2.05 (1H, m, H-12), 0.80 (3H, d, J = 7.0 Hz, H-14), 0.78 (3H, d, J = 6.0 Hz, H-13). ^{13}C NMR (125 MHz, CD$_3$OD): δ 171.2 (C-2), 168.5 (C-5), 134.2 (C-8), 129.1 (C-10), 128.8 (C-9), 127.5 (C-11), 58.1 (C-6), 54.1 (C-3), 51.2 ($\underline{C}$H$_3$, ester), 37.5 (C-7), 30.2 (C-12), 17.9 (C-13), 17.1 (C-14). HRMS (ESI) calculated for formula C$_{15}$H$_{23}$N$_2$O$_3$ [M+H]$^+$ 279.1600, found 279.1727.
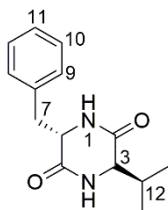

Cy(L-Phe-D-Val) 72: L-Phe-D-Val-OMe (100 mg; 0.360 mmol) and triethylamine (125 μL; 0.905 mmol) were reacted as described in the general procedure. Pure compound was isolated as colourless powder by extracting reaction mixture with ethyl acetate three times (69 mg; 78%). HPLC: t$_R$ 16.7 min. [α]$^{25}_D$ = +78 (*c* 0.1, MeOH). ^{1}H NMR (500 MHz, CD$_3$OD): δ 7.28 (1H, m, H-11), 7.27 (2H, m, H-10), 7.22 (2H, dd, J = 7.5, 2.0 Hz, H-9),

4.29 (1H, t, $J = 4.5$ Hz, H-6), 3.26 (1H, dd, $J = 13.5$, 4.5 Hz, H-7a), 3.01 (1H, dd, $J = 13.5$, 4.5 Hz, H-7b), 2.94 (1H, d, $J = 2.8$ Hz, H-3), 2.15 (1H, m, H-12), 0.90 (3H, d, $J = 7.0$ Hz, H-13), 0.83 (3H, d, $J = 7.0$ Hz, H-14). ^{13}C NMR (125 MHz, CD$_3$OD): δ 168.3 (C-2, 5), 135.1 (C-8), 130.1 (C-9), 128.1 (C-10), 126.9 (C-11), 59.1 (C-3), 55.6 (C-6), 38.9 (C-7), 31.6 (C-12), 17.1 (C-13), 15.2 (C-14). IR (neat): v_{max} 3176, 2961, 2878, 1664, 1450 cm^{-1}. HRMS (ESI) calculated for formula $C_{14}H_{19}N_2O_2$ [M+H]$^+$ 247.1420, found 247.1451.

Boc-L-Phe-L-Leu methyl ester: L-Leu-OMe (182 mg; 1.00 mmol), Boc-L-phenylalanine (292 mg; 1.10 mmol), DMAP (122 mg; 1.00 mmol) and EDC (192 g; 1.30 mmol) were reacted in DCM as described in the general procedure. The crude product was purified by flash chromatography using DCM/MeOH (95:5) as eluent. Pure compound was isolated as a colourless powder (318 mg; 81%). ^{1}H NMR (500 MHz, CD$_3$OD): δ 7.29 (2H, m, H-10), 7.27 (2H, m, H-9), 7.22 (1H, m, H-11), 4.49 (1H, dd, $J = 9.5$, 5.5 Hz, H-3), 4.33 (1H, dd, $J = 9.0$, 5.5 Hz, H-6), 3.69 (3H, s, OC$\underline{H}_3$), 3.11 (1H, dd, $J = 13.5$, 5.5 Hz, H-7a), 2.81 (1H, dd, J = 14.0, 9.0, H-7b), 1.62 (1H, m, H-12), 1.37 (9H, s, C$\underline{H}_3$), 1.71 (1H, m, H-13), 0.96 (3H, d, $J = 6.5$ Hz, H-14), 0.92 (3H, d, $J = 6.5$ Hz, H-15). ^{13}C NMR (125 MHz, CD$_3$OD): δ 173.0 (C-5), 172.8 (C-2), 156.2 ($\underline{C}$O, Boc), 137.2 (C-8), 129.0 (C-9), 128.0 (C-10), 126.2 (C-11), 79.2 (C$_q$, Boc), 55.7 (C-6), 51.3 ($\underline{C}$H$_3$, ester), 50.7 (C-6), 40.4 (C-12), 37.7 (C-7), 27.2 ($\underline{C}$H$_3$, Boc), 24.2 (C-13), 21.9 (C-14), 20.4 (C-15). HRMS (ESI) calculated for formula $C_{21}H_{32}N_2O_5$ [M+Na]$^+$ 415.2300, found 415.2215.
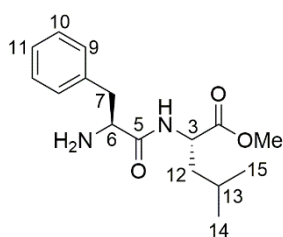

Deboc-L-Phe-L-Leu methyl ester: *N*-Boc-L-Phe-L-Leu-OMe (318 mg; 0.810 mmol) was dissolved in MeOH (5 mL) and HCl 4 M in dioxane (4.1 mL; 16.2 mmol) as described in the general procedure. The mixture was concentrated *in vacuo* to give pure deprotected compound (213 mg; 90%). ^{1}H NMR (500 MHz, CD$_3$OD): δ 7.39 (1H, d, $J = 7.0$ Hz, H-11), 7.38 (2H, d, $J = 7.5$, 7.0 Hz, H-10), 7.34 (2H, d, $J = 7.0$ Hz, H-9), 4.61 (1H, dd, $J = 9.0$, 6.0 Hz, H-3), 4.13 (1H, dd, $J = 8.8$, 5.3 Hz, H-6), 3.71 (3H, s, OC$\underline{H}_3$), 3.31 (1H, dd, $J = 14.5$, 5.3 Hz, H-7a), 3.01 (1H, dd, J = 14.5, 8.8, H-7b), 1.70 (1H, m, H-13), 1.64 (1H, dd, $J = 12.0$, 9.0, H-12a), 1.62 (1H, dd, $J = 12.0$, 9.0 Hz, H-12b), 0.97 (3H, d, $J = 6.5$ Hz, H-14), 0.94 (3H, d, $J = 6.5$ Hz, H-15). ^{13}C NMR (125 MHz, CD$_3$OD): δ 172.4 (C-2), 168.2 (C-5), 134.1 (C-8), 129.2 (C-10), 128.8 (C-9), 127.5 (C-11), 64.1 (C-6), 61.4 ($\underline{C}$H$_3$, ester), 60.9 (C-3), 37.1 (C-7), 40.1 (C-12), 24.5 (C-

13), 21.9 (C-14), 20.3 (C-15). HRMS (ESI) calculated for formula $C_{16}H_{25}N_2O_3$ $[M+H]^+$ 293.1800, found 293.1887.
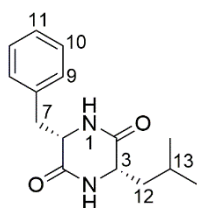
Cy(L-Phe-D-Leu) 73: L-Phe-L-Leu-OMe (100 mg; 0.342 mmol) and triethylamine (119 µL; 0.856 mmol) were reacted as described in the general procedure. Two isomers were isolated by preparative HPLC using method 1.6.11: cy(L-Phe-L-Leu) as colourless powder (25 mg; 26%) and cy(L-Phe-D-Leu) as colourless powder (23 mg; 28%). HPLC: t_R 22.2 min. $[\alpha]^{25}_D$ = +33 (c 0.1, MeOH). ^{1}H NMR (500 MHz, CD$_3$OD): δ 7.29 (2H, m, H-10), 7.28 (1H, m, H-11), 7.23 (2H, dd, J = 7.3, 2.3 Hz, H-9), 4.26 (1H, t, J = 4.5 Hz, H-6), 3.25 (1H, dd, J = 13.5, 4.5 Hz, H-7a), 3.01 (1H, dd, J = 13.5, 4.5 Hz, H-7b), 2.77 (1H, dd, J = 6.0, 5.0 Hz, H-3), 1.69 (H, m, H-13), 1.54 (1H, ddd, J = 13.0, 8.0, 5.0 Hz, H-12a), 1.44 (1H, ddd, J = 13.0, 7.0, 6.0 Hz, H-12b), 0.83 (3H, d, J = 6.5 Hz, H-14), 0.78 (3H, d, J = 6.5 Hz, H-15). ^{13}C NMR (125 MHz, CD$_3$OD): δ 169.9 (C-2), 168.8 (C-5), 135.1 (C-8), 130.1 (C-9), 128.1 (C-10), 127.0 (C-11), 56.1 (C-6), 52.0 (C-3), 40.8 (C-12), 39.2 (C-7), 23.7 (C-13), 21.8 (C-14), 20.9 (C-15). IR (neat): v_{max} 3288, 2957, 2831, 1650, 1456 cm^{-1}. HRMS (ESI) calculated for formula $C_{15}H_{21}N_2O_2$ $[M+H]^+$ 261.1500, found 261.1595.
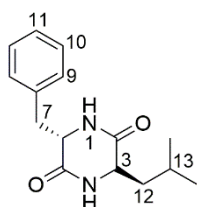
Cy(L-Phe-L-Leu) 64: It was isolated by preparative HPLC using method 1.6.11 (colourless solid, 23 mg, 26%). HPLC: t_R 21.4 min. $[\alpha]^{25}_D$ = -26 (c 0.1, MeOH). ^{1}H NMR (500 MHz, CD$_3$OD): δ 7.30 (2H, dd, J = 7.5, 7.0 Hz, H-10), 7.26 (1H, d, J = 7.0 Hz, H-11), 7.20 (2H, d, J = 7.5 Hz, H-9), 4.30 (1H, t, J = 4.5 Hz, H-6), 3.66 (1H, dd, J = 10.0, 4.5 Hz, H-3), 3.29 (1H, dd, J = 13.5, 4.5 Hz, H-7a), 2.95 (1H, dd, J = 13.5, 4.5 Hz, H-7b), 1.42 (H, m, H-13), 0.87 (1H, ddd, J = 14.0 9.5, 4.5 Hz, H-12a), 0.74 (3H, d, J = 7.0 Hz, H-14), 0.69 (3H, d, J = 7.0 Hz, H-15), 0.08 (1H, ddd, J = 14.0, 10.0, 5.0 Hz, H-12b). ^{13}C NMR (125 MHz, CD$_3$OD): δ 169.2 (C-2), 167.5 (C-5), 135.4 (C-8), 130.4 (C-9), 128.2 (C-10), 127.1 (C-11), 56.0 (C-6), 52.7 (C-3), 43.8 (C-12), 38.8 (C-7), 23.2 (C-13), 21.9 (C-14), 20.0 (C-15). IR (neat): v_{max} 3195, 2958, 2897, 1668, 1454 cm^{-1}. HRMS (ESI) calculated for formula $C_{15}H_{21}N_2O_2$ $[M+H]^+$ 261.1500, found 261.1594.
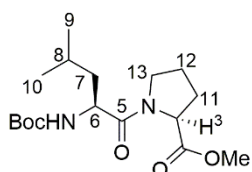
Boc-L-Leu-D-Pro methyl ester: D-Pro-OMe (166 mg; 1.00 mmol), Boc-L-leucine (254 mg; 1.10 mmol), DMAP (122 mg; 1.00 mmol) and EDC (192 mg; 1.30 mmol) were reacted in DCM as described in the general procedure. The crude product was purified by flash chromatography using DCM/MeOH (95:5) as eluent. Pure compound was isolated as a

colourless powder (318 mg; 93%). ^{1}H NMR (500 MHz, CD$_3$OD): δ 4.46 (1H, dd, J = 9.1, 5.5 Hz, H-6), 4.38 (1H, dd, J = 9.3, 5.3 Hz, H-3), 3.69 (3H, s, OC$\underline{H}_3$), 3.61 (1H, m, H-13a), 3.53 (1H, m, H-13b), 3.03 (1H, dd, J = 14.0, 4.5 Hz, H-7a), 2.21 (2H, m, H-7), 2.03 (2H, m, H-12), 1.98 (2H, m, H-11), 1.67 (1H, m, H-8), 1.43 (9H, s, C$\underline{H}_3$). ^{13}C NMR (125 MHz, CD$_3$OD): δ 172.5 (C-2), 170.3 (C-5), 169.1 ($\underline{C}$O, Boc), 79.1 (C$_q$, Boc), 59.3 (C-3), 51.2 (C-6), 50.6 ($\underline{C}$H$_3$, ester), 46.8 (C-13), 40.5 (C-7), 28.6 (C-11), 27.3 ($\underline{C}$H$_3$, Boc), 24.3 (C-12), 22.2 (C-8). HRMS (ESI) calculated for formula C$_{17}$H$_{31}$N$_2$O$_5$ [M+H]$^+$ 343.2200, found 343.2206.
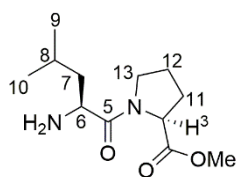
Deboc-L-Leu-D-Pro methyl ester: *N*-Boc-L-Leu-D-Pro-OMe (318 mg; 0.930 mmol) was dissolved in MeOH (5 mL) and HCl 4 M in dioxane (4.90 mL; 19.0 mmol) as described in the general procedure. The mixture was concentrated in *vacuo* to give pure deprotected compound (203 mg; 90%). ^{1}H NMR (500 MHz, CD$_3$OD): δ 4.49 (1H, dd, J = 8.7, 5.5 Hz, H-6), 4.31 (1H, dd, J = 8.8, 5.3 Hz, H-3), 3.74 (3H, s, OC$\underline{H}_3$), 3.59 (1H, m, H-13a), 3.51 (1H, m, H-13b), 2.64 (1H, m, H-7a), 2.59 (1H, m, H-7b), 2.03 (2H, m, H-12), 1.98 (2H, m, H-11), 1.59 (1H, m, H-8). ^{13}C NMR (125 MHz, CD$_3$OD): δ 171.8 (C-2), 169.9 (C-5), 58.3 (C-3), 53.2 (C-6), 50.2 ($\underline{C}$H$_3$, ester), 44.8 (C-13), 39.5 (C-7), 28.4 (C-11), 24.1 (C-12), 21.9 (C-8). HRMS (ESI) calculated for formula C$_{12}$H$_{23}$N$_2$O$_3$ [M+H]$^+$ 243.1200, found 243.1606.
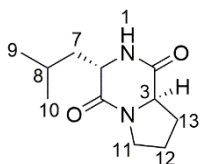
Cy(L-Leu-D-Pro) 66: L-Phe-D-Pro-OMe (100 mg; 0.413 mmol) and triethylamine (143 µL; 1.03 mmol) were reacted as described in the general procedure. Two isomers were isolated by preparative HPLC using method 1.6.11: cy(L-Leu-D-Pro) as colourless solid (55 mg; 63%) and cy(L-Leu-L-Pro) as colourless solid (20 mg; 23%). It was isolated from. HPLC: t$_R$ 11.4 min. [α]^{25}$_D$ = +70 (*c* 0.1, MeOH). ^{1}H NMR (500 MHz, CD$_3$OD): δ 4.27 (1H, dd, J = 8.9, 6.5 Hz, H-3), 3.86 (1H, dd, J = 9.5, 5.5 Hz, H-6), 3.58 (1H, m, H-11a), 3.50 (1H, m, H-11b), 2.34 (1H, m, H-13a), 2.03 (1H, m, H-12a), 2.01 (1H, m, H-12a), 1.95 (1H, m, H-13b), 1.92 (1H, m, H-12b), 1.78 (1H, m, H-8), 1.69 (1H, ddd, J = 13.5, 9.5, 5.0 Hz, H-7a), 1.57 (1H, ddd, J = 13.5, 8.5, 5.5 Hz, H-7b), 0.99 (3H, d, J = 6.0 Hz, H-10), 0.96 (1H, d, J = 6.0 Hz, H-9). ^{13}C NMR (125 MHz, CD$_3$OD): δ 170.2 (C-2), 167.7 (C-5), 57.9 (C-3), 55.7 (C-6), 45.3 (C-11), 32.2 (C-7), 28.5 (C-13), 24.1 (C-8), 21.9 (C-9), 21.7 (C-12), 20.5 (C-10). IR (neat): v$_{max}$ 3235, 2953, 2869, 1652, 1447 cm^{-1}. HRMS (ESI$^+$) calculated for formula C$_{11}$H$_{19}$N$_2$O$_2$ [M+H]$^+$ 211.1400, found 211.1499.
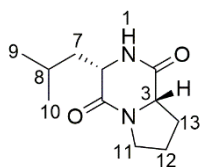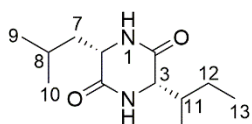
Cy(L-Leu-L-Pro) 59: It was isolated as colourless solid (20 mg; 23%) by preparative HPLC using method 1.6.11. HPLC: t_R 12.1 min. $[\alpha]^{25}_D$ = -310 (c 0.1, MeOH). ^{1}H NMR (500 MHz, CD$_3$OD): δ 4.27 (1H, dd, J = 8.9, 6.0 Hz, H-3), 4.14 (1H, dd, J = 9.0, 5.5 Hz, H-6), 3.52 (2H, m, H-11), 2.31 (1H, m, H-13a), 2.02 (1H, m, H-13b), 2.01 (1H, m, H-12a), 1.95 (1H, m, H-12b), 1.91 (1H, m, H-7a), 1.90 (1H, m, H-8), 1.52 (1H, H-7b), 0.98 (3H, d, J = 6.0 Hz, H-10), 0.96 (1H, d, J = 6.0 Hz, H-9). ^{13}C NMR (125 MHz, CD$_3$OD): δ 171.4 (C-5), 167.5 (C-2), 135.4 (C-8), 58.9 (C-3), 53.2 (C-6), 45.0 (C-11), 38.0 (C-7), 27.7 (C-13), 24.4 (C-8), 22.2 (C-12), 21.9 (C-9), 20.7 (C-10). IR (neat): v_{max} 3236, 2954, 2869, 1654, 1455 cm^{-1}. HRMS (ESI) calculated for formula $C_{11}H_{19}N_2O_2$ [M+H]$^+$ 211.1400, found 211.1454.
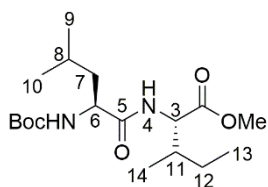
Boc-L-Leu-L-Ile methyl ester: L-Ile-OMe (182 mg; 1.00 mmol), Boc-L-leucine (254 mg; 1.10 mmol), DMAP (122 mg; 1.00 mmol) and EDC (192 mg; 1.30 mmol) were reacted in DCM as described in the general procedure. The crude product was purified by flash chromatography using DCM/MeOH (95:5) as eluent. Pure compound was isolated as a colourless solid (322 mg; 90%). ^{1}H NMR (500 MHz, CD$_3$OD): δ 3.86 (1H, dd, J = 9.0, 4.5 Hz, H-6), 3.62 (1H, d, J = 4.5 Hz, H-3), 3.69 (3H, s, OC$\underline{H}_3$), 2.20 (1H, m, H-11), 1.92 (1H, m, H-7a), 1.69 (1H, m, H-8), 1.56 (1H, m, H-7b), 1.42 (9H, s, C$\underline{H}_3$), 1.20 (1H, m, H-12a), 1.09 (3H, d, J = 7.0 Hz, H-14), 0.97 (9H, m, H-9, 10, 13), 0.86 (1H, m, H-12b). ^{13}C NMR (125 MHz, CD$_3$OD): δ 169.2 (C-2), 169.0 (C-5), 159.8 ($\underline{C}$O, Boc), 79.3 (C$_q$, Boc), 54.2 (C-6), 51.9 (C-3), 50.9 ($\underline{C}$H$_3$, ester), 44.5 (C-7), 29.1 (C-12), 27.2 ($\underline{C}$H$_3$, Boc), 24.9 (C-8), 22.6 (C-9), 20.9 (C-10), 18.8 (C-14), 17.2 (C-13). HRMS (ESI) calculated for formula $C_{18}H_{35}N_2O_5$ [M+H]$^+$ 359.2500, found 359.2488.
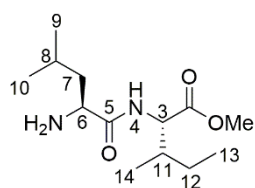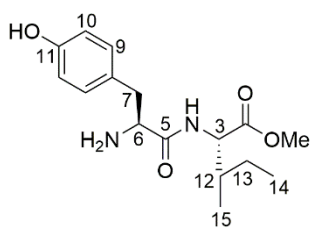
Deboc-L-Leu-L-Ile methyl ester: N-Boc-L-Leu-L-Ile-OMe (322 mg; 0.900 mmol) was dissolved in MeOH (5 mL) and HCl 4M in dioxane (4.6 mL; 18.0 mmol) as described in the general procedure. The mixture was concentrated *in vacuo* to give pure deprotected compound (209 mg; 90%). ^{1}H NMR (500 MHz, CD$_3$OD): δ 3.82 (1H, d, J = 8.9, 4.3 Hz, H-6), 3.59 (1H, d, J = 5.0 Hz, H-3), 3.69 (3H, s, OC$\underline{H}_3$), 2.18 (1H, m, H-11), 1.94 (1H, m, H-7a), 1.72 (1H, m, H-8), 1.56 (1H, m, H-7b), 1.24 (1H, m, H-12a), 1.06 (3H, d, J = 7.0 Hz, H-10), 0.95 (9H, m, H-9, 13, 14), 0.85 (1H, m, H-12b). ^{13}C NMR (125 MHz, CD$_3$OD): δ 171.2 (C-2), 170.0 (C-5), 59.5 (C-3), 52.4 (C-6), 51.2 ($\underline{C}$H$_3$, ester), 44.1 (C-7), 31.1 (C-11), 28.9 (C-12), 24.2 (C-8), 22.4 (C-9), 20.6 (C-10), 18.4 (C-14), 17.0 (C-13). HRMS (ESI) calculated for formula $C_{13}H_{27}N_2O_3$ [M+H]$^+$ 259.1900, found 259.3001.

Cy(L-Leu-L-Ile) 61: L-Leu-L-Ile-OMe (100 mg; 0.387 mmol) and triethylamine (134 µL; 0.968 mmol) were reacted as described in the general procedure. Pure compound was isolated as colourless solid by filteration (39 mg; 45%) by filtration. HPLC: t_R 8.38 min. $[\alpha]^{25}_D$ = -53 (*c* 0.1, MeOH). ^{1}H NMR (500 MHz, CD$_3$OD): δ 3.94 (1H, dd, *J* = 9.0, 4.5 Hz, H-6), 3.77 (1H, d, *J* = 4.5 Hz, H-3), 3.69 (3H, s, OC$\underline{H}_3$), 2.23 (1H, m, H-11), 1.87 (1H, m, H-7a), 1.76 (1H, m, H-8), 1.60 (1H, m, H-7b), 1.09 (1H, m, H-12a), 1.04 (3H, d, *J* = 7.0 Hz, H-14), 0.97 (9H, m, H-9, 10, 13), 0.90 (1H, m, H-12b). ^{13}C NMR (125 MHz, CD$_3$OD): δ 168.2 (C-2), 168.1 (C-5), 60.2 (C-3), 53.0 (C-6), 43.3 (C-7), 32.3 (C-11), 29.4 (C-12), 24.0 (C-8), 22.3 (C-9), 20.6 (C-10), 18.0 (C-14), 16.5 (C-13). IR (neat): v_{max} 3190, 3054, 2960, 1662, 1448 cm^{-1}. HRMS (ESI) calculated for formula C$_{12}$H$_{23}$N$_2$O$_2$ [M+H]$^+$ 227.1700, found 227.3001.
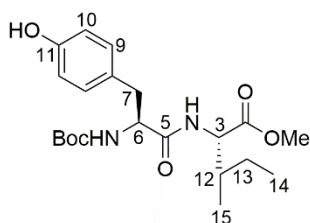
Boc-L-Tyr-L-Ile methyl ester: L-Ile-OMe (182 mg; 1.00 mmol), Boc-L-Tyr (309 mg; 1.10 mmol), DMAP (122 mg; 1.00 mmol) and EDC (192 g; 1.30 mmol) were reacted in DCM as described in the general procedure. The crude product was purified by flash chromatography using DCM/MeOH (95:5) as eluent. Pure compound was isolated as a colourless powder (297 mg; 77%). ^{1}H NMR (500 MHz, CD$_3$OD): δ 6.99 (2H, d, *J* = 8.5 Hz, H-9), 6.67 (2H, d, *J* = 8.5 Hz, H-10), 4.17 (1H, d, *J* = 5.5 Hz, H-6), 3.66 (1H, d, *J* = 5.0 Hz, H-3), 3.74 (3H, s, OC$\underline{H}_3$), 3.15 (1H, dd, *J* = 13.5, 5.5 Hz, H-7a), 2.88 (1H, dd, J = 14.0, 9.0, H-7b), 1.69 (1H, m, H-12), 1.37 (9H, m, C$\underline{H}_3$), 0.90 (6H, d, *J* = 6.9 Hz, H-14, 15), 0.80 (2H, m, H-13). ^{13}C NMR (125 MHz, CD$_3$OD): δ 169.0 (C-5), 167.8 (C-2), 157.6 (C-11), 156.2 ($\underline{C}$O, Boc), 133.2 (C-9), 127.5 (C-8), 116.5 (C-10), 79.4 (C$_q$, Boc), 58.7 (C-3), 56.3 ($\underline{C}$H$_3$, ester), 55.7 (C-6), 37.8 (C-12), 36.5 (C-7), 27.2 ($\underline{C}$H$_3$, Boc), 23.2 (C-13), 14.6 (C-15), 11.4 (C-14). HRMS (ESI) calculated for formula C$_{21}$H$_{33}$N$_2$O$_6$ [M+Na]$^+$ 409.2300, found 409.2215.

Deboc-L-Tyr-L-Ile methyl ester: *N*-Boc-L-Tyr-L-Ile-OMe (297 mg; 0.800 mmol) was dissolved in MeOH (5 mL) and HCl 4 M in dioxane (3.8 mL; 15.0 mmol) as described in the general procedure. The mixture was concentrated *in vacuo* to give pure deprotected compound (252 mg; 88%). ^{1}H NMR (500 MHz, CD$_3$OD): δ 6.90 (2H, d, *J* = 8.4 Hz, H-9), 6.61 (2H, d, *J* = 8.4 Hz, H-10), 4.09 (1H, d, *J* = 5.0 Hz, H-6), 3.68 (1H, d, *J* = 5.0 Hz, H-3), 3.75 (3H, s, OC$\underline{H}_3$), 3.20 (1H, dd, *J* =

13.0, 5.0 Hz, H-7a), 2.85 (1H, dd, J = 13.0, 9.1 Hz, H-7b), 1.67 (1H, m, H-12), 0.88 (6H, d, J = 7.0 Hz, H-14, 15), 0.75 (2H, m, H-13). ^{13}C NMR (125 MHz, CD$_3$OD): δ 167.0 (C-5), 166.2 (C-2), 156.2 (C-11), 132.2 (C-9), 127.5 (C-8), 115.5 (C-10), 58.7 (C-3), 55.7 (CH$_3$, ester), 54.9 (C-6), 36.8 (C-12), 35.8 (C-7), 23.2 (C-13), 14.4 (C-15), 11.2 (C-14). HRMS (ESI) calculated for formula $C_{16}H_{25}N_2O_4$ [M+Na]$^+$ 309.1700, found 309.2015.
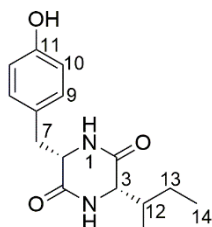
Cy(L-Tyr-L-Ile) 58: L-Tyr-L-Ile-OMe (100 mg; 0.350 mmol) and triethylamine (121 µL; 0.870 mmol) were reacted as described in the general procedure. Pure compound was isolated as colourless solid by filteration (70 mg; 72%) by filtration. HPLC: t$_R$ 6.40 min. [α]$^{25}_D$ = -35 (c 0.1, MeOH). ^{1}H NMR (500 MHz, CD$_3$OD): δ 6.97 (2H, d, J = 8.1 Hz, H-9), 6.63 (2H, d, J = 8.1 Hz, H-10), 4.11 (1H, t, J = 4.5 Hz, H-6), 3.56 (1H, t, J = 4.5 Hz, H-6), 3.06 (1H, dd, J = 13.5, 3.3 Hz, H-7a), 2.72 (1H, dd, J = 13.5, 4.5 Hz, H-7b), 1.42 (1H, m, H-12), 0.80 (6H, d, J = 6.9 Hz, H-14, 15), 0.70 (2H, m, H-13). ^{13}C NMR (125 MHz, CD$_3$OD): δ 166.4 (C-5), 164.5 (C-2), 156.1 (C-11), 131.3 (C-9), 126.2 (C-8), 114.7 (C-10), 58.8 (C-3), 55.2 (C-6), 37.8 (C-12), 36.8 (C-7), 23.1 (C-13), 14.6 (C-14), 11.6 (C-14). IR (neat): v_{max} 3251, 2969, 2879, 1652, 1514 cm^{-1}. HRMS (ESI) calculated for formula $C_{15}H_{21}N_2O_2$ [M+H]$^+$ 277.1500, found 277.1393.

References

1   J. B. Harborne and C. A. Williams, *Nat. Prod. Rep.*, 2005, **15**, 631.

2   T. Coultate and R. S. Blackburn, *Color. Technol.*, 2018, **134**, 165–186.

3   S. Farooque, P. M. Rose, M. Benohoud, R. S. Blackburn and C. M. Rayner, *J. Agric. Food Chem.*, 2018, **66**, 12265–12273.

4   H. B. S, *Prog. Clin. Biol. Res.*, 1988, **280**, 121.

5   F. Pina, M. J. Melo, C. A. T. Laia, A. J. Parola and J. C. Lima, *Chem. Soc. Rev.*, 2012, **41**, 869–908.

6   Ø. M. Andersen and M. Jordheim, *Encycl. Life Sci.*, 2010, **2**, 1–12.

7   A. G. Newsome, C. A. Culver and R. B. Van Breemen, *J. Agric. Food Chem.*, 2014, **62**, 6498–6511.

8   M. Rubinskiene, I. Jasutiene, P. R. Venskutonis and P. Viskelis, *J. Chromatogr. Sci.*, 2005, **43**, 478–482.

9   A. K. Landbo and A. S. Meyer, *J. Agric. Food Chem.*, 2001, **49**, 3169–3177.

10   F. Pina, *J. Agric. Food Chem.*, 2014, **62**, 6885–6897.

11   R. L. Stoddard and J. S. McIndoe, *J. Chem. Educ.*, 2013, **90**, 1032–1034.

12   T. Fossen, Ø. M. Andersen and L. Cabrita, *Food Chem.*, 2000, **68**, 101–107.

13   T. A. Holton and E. C. Cornish, *Plant Cell*, 2007, **7**, 1071.

14   T. Furukawa, T. Akutagawa, H. Funatani, T. Uchida, Y. Hotta, M. Niwa and Y. Takaya, *Bioorganic Med. Chem.*, 2012, **20**, 2002–2009.

15   E. Soubeyrand, C. Basteau, G. Hilbert, C. Van Leeuwen, S. Delrot and E. Gomès, *Phytochemistry*, 2014, **103**, 38–49.

16   S. Park, D. H. Kim, J. Y. Lee, S. H. Ha and S. H. Lim, *J. Agric. Food Chem.*, 2017, **65**, 5287–5298.

17   K. R. Markham, K. S. Gould, C. S. Winefield, K. A. Mitchell, S. J. Bloor and M. R. Boase, *Phytochemistry*, 2000, **55**, 327–336.

18   A. Castañeda-Ovando, M. de L. Pacheco-Hernández, M. E. Páez-Hernández, J. A. Rodríguez and C. A. Galán-Vidal, *Food Chem.*, 2009, **113**, 859–871.

19   B. V. Chandler and K. A. Harper, *Aust. J. Chem.*, 1962, **15**, 114–120.

20   C. Frøytlog, R. Slimestad and Ø. M. Andersen, *J. Chromatogr. A*, 1998, **825**, 89–95.

21   R. Slimestad and H. Solheim, *J. Agric. Food Chem.*, 2002, **50**, 3228–3231.

22   K. Torskangerpoll and Ø. M. Andersen, *Food Chem.*, 2005, **89**, 427–440.

23   X. Wu, L. Gu, R. L. Prior and S. McKay, *J. Agric. Food Chem.*, 2007, **52**, 7846–7856.

24   Ø. M. Andersen, T. Fossen, K. Torskangerpoll, A. Fossen and U. Hauge, *Phytochemistry*, 2004, **65**, 405–410.

25   M. H. Wathon, N. Beaumont, M. Benohoud, R. S. Blackburn and C. M. Rayner, *Color. Technol.*, 2019, **135**, 5–16.

26   I. Iliopoulou, D. Thaeron, A. Baker, A. Jones and N. Robertson, *J. Agric. Food Chem.*, 2015, **63**, 7066–7073.

27   G. R. Takeoka, L. T. Dao, G. H. Full, R. Y. Wong, L. A. Harden, R. H. Edwards and J. D. J. Berrios, *J. Agric. Food Chem.*, 2002, **45**, 3395–3400.

28   M. Jordheim, T. Fossen and Ø. M. Andersen, *J. Agric. Food Chem.*, 2006, **54**, 3572–3577.

29   L. Cabrita and Ø. M. Andersen, *Phytochemistry*, 1999, **52**, 1693–1696.

30   C. Qin, Y. Li, W. Niu, Y. Ding and R. Zhang, *Czech J. Food Sci*, 2010, **28**, 117–126.

31   M. Jordheim, K. H. Enerstvedt and Ø. M. Andersen, *J. Agric. Food Chem.*, 2011, **59**, 7436–7440.

32   M. Jordheim, K. Aaby, T. Fossen, G. Skrede and Ø. M. Andersen, *J. Agric. Food Chem.*, 2007, **55**, 10591–10598.

33   N. Saito, F. Tatsuzawa, K. Toki, K. Shinoda, A. Shigihara and T. Honda, *Phytochemistry*, 2011, **72**, 2219–2229.

34   L. Mäkilä, O. Laaksonen, A. L. Alanne, M. Kortesniemi, H. Kallio and B. Yang, *J. Agric. Food Chem.*, 2016, **64**, 4584–4598.

35   A. Degenhardt, H. Knapp and P. Winterhalter, *J. Agric. Food Chem.*, 2000, **48**, 338–343.

36   V. Gavrilova, M. Kajdžanoska, V. Gjamovski and M. Stefova, *J. Agric. Food Chem.*, 2011, **59**, 4009–4018.

37   G. M. Khoo, M. R. Clausen, H. L. Pedersen and E. Larsen, *Food Chem.*, 2012, **132**, 1214–1220.

38   S. Cyboran, D. Bonarska-Kujawa, H. Pruchnik, R. Zyłka, J. Oszmiański and H. Kleszczyńska, *Food Res. Int.*, 2014, **65**, 47–58.

39   W. Aneta, O. Jan, M. Magdalena and W. Joanna, *Int. J. Food Sci. Technol.*, 2013, **48**, 715–726.

40   M. P. Kähkönen, J. Heinämäki, V. Ollilainen and M. Heinonen, *J. Sci. Food Agric.*, 2003, **83**, 1403–1411.

41   J. Giné Bordonaba and L. A. Terry, *J. Agric. Food Chem.*, 2008, **56**, 7422–7430.

42   V. Nour, F. Stampar, R. Veberic and J. Jakopic, *Food Chem.*, 2013, **141**, 961–966.

43   Y. Tian, J. Liimatainen, A. L. Alanne, A. Lindstedt, P. Liu, J. Sinkkonen, H. Kallio and B. Yang, *Food Chem.*, 2017, **220**, 266–281.

44   I. García-Estévez, R. Jacquet, C. Alcalde-Eon, J. C. Rivas-Gonzalo, M. T. Escribano-Bailón and S. Quideau, *J. Agric. Food Chem.*, 2013, **61**, 11560–11568.

45   L. Y. Foo, Y. Lu, A. B. Howell and N. Vorsa, *J. Nat. Prod.*, 2000, **63**, 1225–1228.

46   J. Souquet, V. I. R. Cheyner, F. Brossaud and M. Moutounet, *Phytochemistry*, 1996, **43**, 509–512.

47   D. Y. Xie and R. A. Dixon, *Phytochemistry*, 2005, **66**, 2127–2144.

48   Y. Wang, A. P. Singh, W. J. Hurst, J. A. Glinski, H. Koo and N. Vorsa, *J. Agric. Food Chem.*, 2016, **64**, 2190–2199.

49   H. S. Lee and V. Hong, *J. Chromatogr. A*, 1992, **624**, 221–234.

50   J. M. Kong, L. S. Chia, N. K. Goh, T. F. Chia and R. Brouillard, *Phytochemistry*, 2003, **64**, 923–933.

51   G. J. McDougall, S. Gordon, R. Brennan and D. Stewart, *J. Agric. Food Chem.*, 2005, **53**, 7878–7885.

52   J. G. Bordonaba, P. Crespo and L. A. Terry, *Food Chem.*, 2011, **129**, 1265–1273.

53   Y. Lu and L. Y. Foo, *Tetrahedron Lett.*, 2001, **42**, 1371–1373.

54   P. Heffels, F. Weber and A. Schieber, *J. Agric. Food Chem.*, 2015, **63**, 7532–7538.

55   E. N. Kananykhina and I. V Pilipenko, *Production*, 2000, **36**, 118–120.

56   P. Goiffon J., P. Mouly P. and M. Gaydou E., *Anal. Chim. Acta*, 1999, **382**, 39–50.

57   I. L. F. Nielsen, G. R. Haren, E. L. Magnussen, L. O. Dragsted and S. E. Rasmussen, *J. Agric. Food Chem.*, 2003, **51**, 5861–5866.

58   Ø. M. Andersen, S. Refn, H. Lönnberg, L. H. J. Lajunen, A. Karjalainen, J.-E. Berg, M. Bartók, I. Pelczer and G. Dombi, *Acta Chem. Scand.*, 2008, 42b, 462–468.

59   T. Eisele, M. M. Giusti, H. Hofsommer, S. Koswig, D. A. Krueger, S. Kupina, S. K. Martin, B. K. Martinsen, T. C. Miller, F. Paquette, A. Ryabkova, G. Skrede, U. Trenn and J. D. Wightman, *J. AOAC Int.*, 2005, **88**, 1269–1278.

60   E. A. Dufton, School of Design, University of Leeds, 2018.

61   H. Peixoto, M. Roxo, S. Krstin, T. Röhrig, E. Richling and M. Wink, *J. Agric. Food Chem.*, 2016, **64**, 1283–1290.

62   A. Bunea, D. Rugină, Z. Sconţa, R. M. Pop, A. Pintea, C. Socaciu, F. Tăbăran, C. Grootaert, K. Struijs and J. VanCamp, *Phytochemistry*, 2013, **95**, 436–444.

63   X. Zhang, Y. Yang, Z. Wu and P. Weng, *J. Agric. Food Chem.*, 2016, **64**, 2582–2590.

64   A. Olejnik, K. Kowalska, M. Olkowicz, W. Juzwa, R. Dembczyński and M. Schmidt, *J. Agric. Food Chem.*, 2016, **64**, 7710–7721.

65   B. Gordon, *Ger. Hist.*, 2003, **16**, 222–238.

66   K. Jiménez-Aliaga, P. Bermejo-Bescós, J. Benedí and S. Martín-Aragón, *Life Sci.*, 2011, **89**, 939–945.

67   M. C. Walton, T. K. McGhie, G. W. Reynolds and W. H. Hendriks, *J. Agric. Food Chem.*, 2006, **54**, 4913–4920.

68   United States Patent Application Publication, 2014.

69   R. Slimestad, Ø. M. Andersen, G. W. Francis, A. Marston and K. Hostettmann, *Phytochemistry*, 1995, **40**, 1537–1542.

70   J. Oliveira, N. F. Brás, M. A. Da Silva, N. Mateus, A. J. Parola and V. De Freitas, *Phytochemistry*, 2014, **105**, 178–185.

71   J. Oliveira, M. Alhinho Da Silva, N. Teixeira, V. De Freitas and E. Salas, *J. Agric. Food Chem.*, 2015, **63**, 7636–7644.

72   R. W. Teng, D. Z. Wang, Y. S. Wu, Y. Lu, Q. T. Zheng and C. R. Yang, *Magn. Reson. Chem.*, 2004, **43**, 92–96.

73   W. P. Slichter, *Rubber Chem. Technol.*, 2011, **34**, 1574–1600.

74   M. Miyazawa and M. Hisama, *Biosci. Biotechnol. Biochem.*, 2003, **67**, 2091–2099.

75   Y. Lu and L. Yeap Foo, *Food Chem.*, 2003, **80**, 71–76.

76   Y. Lu, L. Y. Foo and H. Wong, *Phytochemistry*, 2002, **59**, 465–468.

77   J. Lee, C. Rennaker and R. E. Wrolstad, *Food Chem.*, 2008, **110**, 782–786.

78   B. Fu, H. Li, X. Wang, F. S. C. Lee and S. Cui, *J. Agric. Food Chem.*, 2005, **53**, 7408–14.

79   S. G. Lee, T. M. Vance, T. G. Nam, D. O. Kim, S. I. Koo and O. K. Chun, *J. Food Meas. Charact.*, 2016, **10**, 562–568.

80   X. Wu, G. R. Beecher, J. M. Holden, D. B. Haytowitz, S. E. Gebhardt and R. L. Prior, *J. Agric. Food Chem.*, 2006, **54**, 4069−4075.

81   C. Sanchez-Moreno, G. Cao, B. OU and R. L. Prior, *J. Agric. Food Chem.*, 2003, **51**, 4889−4896.

82   F. Santos, C.M.; Gomez, B.; Goncalves, L. M.; Oliveira, J. Rocha, S.; Coelho, M.; Rodriguer, J. A.; Freitas, V.; Aquilar, *J. Brazalian Chem. Soc.*, 2014, **25**, 1029–1035.

83   N. Terasawa, A. Saotome, Y. Tachimura, A. Mochizuki, H. Ono, M. Takenaka and M. Murata, *J. Agric. Food Chem.*, 2007, **55**, 4154–4159.

84   P. G. Kapasakalidis, R. A. Rastall and M. H. Gordon, *J. Agric. Food Chem.*, 2006, **54**, 4016–4021.

85   P. M. Rose, V. Cantrill, M. Benohoud, A. Tidder, C. M. Rayner and R. S. Blackburn, *J. Agric. Food Chem.*, 2018, **66**, 6790–6798.

86   H. Matsumoto, S. Hanamura, T. Kawakami, Y. Sato and M. Hirayama, *J. Agric. Food Chem.*, 2001, **49**, 1541–1545.

87   T. S. Crofts, A. J. Gasparrini and G. Dantas, *Nat. Rev. Microbiol.*, 2017, **15**, 422–434.

88   A. Akter, School of Molecular and Cellular Biology, Faculty of Biological Sciences, The University of Leeds, 2018.

89   C. L. Ventola, *Pharm. Ther.*, 2015, **40**, 277–83.

90   R. I. Aminov, *Front. Microbiol.*, 2010, **1**, 1–7.

91   I. Chopra, L. Hesse and A. J. O'Neill, *J. Appl. Microbiol.*, 2003, **92**, 4S-15S.

92   O. Genilloud, *Nat. Prod. Rep.*, 2017, **34**, 1203–1232.

93   K. Lewis, *Nature*, 2012, **485**, 439–440.

94   J. O'neill, *Tackling Drug-Resistant Infections Globally: Final Report and Recommendations*, 2016.

95   A. Cannatelli, T. Giani, A. Antonelli, L. Principe, F. Luzzaro and G. M. Rossolini, *Antimicrob. Agents Chemother.*, 2016, **60**, 3257–3258.

96   K. Lewis, *Nat. Rev. Drug Discov.*, 2013, **12**, 371–387.

97   T. S. Crofts, A. J. Gasparrini and G. Dantas, *Nat. Rev. Microbiol.*, 2017, **15**, 422–434.

98   L. L. Silver, *Clin. Microbiol. Rev.*, 2011, **24**, 71–109.

99   G. D. Wright, *Nat. Prod. Rep.*, 2017, **34**, 694–701.

100   N. M. Nass, S. Farooque, C. Hind, M. E. Wand, C. P. Randall, J. M. Sutton, R. F.

Seipke, C. M. Rayner and A. J. O'Neill, *Sci. Rep.*, 2017, **7**, 1–11.

101 K. Lewis, *Nat. Rev. Drug Discov.*, 2013, **12**, 371–87.

102 G. D. Wright, *Chem. Biol.*, 2012, **19**, 3–10.

103 J. Masschelein, M. Jenner and G. L. Challis, *Nat. Prod. Rep.*, 2017, **34**, 712–783.

104 L. L. Ling, T. Schneider, A. J. Peoples, A. L. Spoering, I. Engels, B. P. Conlon, A. Mueller, T. F. Schäberle, D. E. Hughes, S. Epstein, M. Jones, L. Lazarides, V. A. Steadman, D. R. Cohen, C. R. Felix, K. A. Fetterman, W. P. Millett, A. G. Nitti, A. M. Zullo, C. Chen and K. Lewis, *Nature*, 2015, **517**, 455–9.

105 L. Song, M. Jenner, J. Masschelein, C. Jones, M. J. Bull, S. R. Harris, R. C. Hartkoorn, A. Vocat, I. Romero-Canelon, P. Coupland, G. Webster, M. Dunn, R. Weiser, C. Paisey, S. T. Cole, J. Parkhill, E. Mahenthiralingam and G. L. Challis, *J. Am. Chem. Soc.*, 2017, **139**, 7974–7981.

106 W. K. Mousa, B. Athar, N. J. Merwin and N. A. Magarvey, *Nat. Prod. Rep.*, 2017, **34**, 1302–1331.

107 F. Alberti, D. J. Leng, I. Wilkening, L. Song, M. Tosin and C. Corre, *Chem. Sci.*, 2019, **10**, 453–463.

108 N. M. Nass, School of Molecular and Cellular Biology, Faculty of Biological Sciences, The University of Leeds, 2017.

109 H. Brockmann and H. Pini, *Chem. Ber.*, 1947, **34**, 190–191.

110 H. Brockmann, H. Pini and O. V. Plotho, *Chem. Ber.*, 1950, **83**, 161–167.

111 P. Brockmann, H.; Christiansen, *Chem. Ber.*, 1970, **103**, 708–717.

112 P. Christiansen, University of Gottingen, 1970.

113 H. Brockmann and E. Hieronymus, *Chem. Berichte*, 1965, **88**, 1379–1390.

114 L. F. Wright and D. A. Hopwood, *J. Gen. Microbiol.*, 1976, **96**, 289–297.

115 C.-J. and F. H. G. Gorst-Allman, C, P. Rudd,B. A. M. Chang, *J. Org. Chem.*, 1981, **46**, 455–456.

116 L. V Bystrykh, J. K. Herrema, F. Malpartida, D. A. Hopwood, L. Dijkhuizen, J. A. N. K. Herrema, L. V Bystrykh and M. A. Ferna, *J. Bacteriol.*, 1996, **178**, 2238–2244.

117 H. W. Moore, *Science (80-.).*, 1977, **197**, 527–532.

118 R. Moore, H. W. & Czerniak, *Med. Res. Rev.*, 1981, **1**, 249–280.

119 M. Nishiyama, T., Hashimoto, Y., Kusakabe, H., Kumano, T. & Kobayashi, *Proc. Natl. Acad. Sci. USA*, 2014, **111**, 17152–17157.

120 C. P. Randall, K. R. Mariner, I. Chopra and A. J. O'Neill, *Antimicrob. Agents Chemother.*, 2013, **57**, 637–639.

121 I. O'Neill, A. J., Miller, K., Oliva, B. & Chopra, *J Antimicrob Chemother*, 2004, **54**, 1127–1129.

122 D. L. Higgins, R. Chang, D. V. Debabov, J. Leung, T. Wu, K. M. Krause, E. Sandvik, J. M., Q. G. Hubbard, Kone´ Kaniga, Donald E. Schmidt, Jr., R. T. Cass, D. E. Karr, B. M. Benton and P. P. Humphrey, *Antimicrob Agents Chemother*, 2005, **49**, 1127–1134.

123 J. K. Hobbs, K. Miller, A. J. O'Neill and I. Chopra, *J. Antimicrob. Chemother.*, 2008, **62**, 1003–1008.

124 S. J. Clements, M. O., Watson, S. P. & Foster, *J Bacteriol*, 1999, **181**, 3898–3903.

125 I. Imlay, J. A. & Fridovich, *J Biol Chem*, 1991, **266**, 6957–6965.

126 P. C. Dorrestein, S. K. Mazmanian and R. Knight, *Immunity*, 2014, **40**, 824–832.

127 *The Human Microbiome Project Consortium: Structure, function and diversity of the healthy human microbiome*, Nature Publishing Group, 2012, vol. 486.

128 C. Chatterjee, M. Paul, L. Xie and W. A. van der Donk, *Chem. Rev.*, 2005, **105**, 633–684.

129 J. Oh, A. L. Byrd, C. Deming, S. Conlan, H. H. Kong, J. A. Segre, B. Barnabas, R. Blakesley, G. Bouffard, S. Brooks, H. Coleman, M. Dekhtyar, M. Gregory, X. Guan, J. Gupta, J. Han, S. L. Ho, R. Legaspi, Q. Maduro, C. Masiello, B. Maskeri, J. McDowell, C. Montemayor, J. Mullikin, M. Park, N. Riebow, K. Schandler, B. Schmidt, C. Sison, M. Stantripop, J. Thomas, P. Thomas, M. Vemulapalli and A. Young, *Nature*, 2014, **514**, 59–64.

130 C. Otto, M. and Vuong, *Microbes Infect.*, 2002, **4**, 481–489.

131 P. Perry, A. and Lambert, *Expert Rev. Anti. Infect. Ther.*, 2014, **9**, 1149–1156.

132 M. A. Zimmermann, M. and Fischbach, *Chem. Biol.*, 2010, **17**, 925–930.

133 F. C. B. M. A. Wyatt, W. Wang, C. M. Roux and P. M. D. and N. A. M. D. E. Heinrichs, *Science (80-.).*, 2010, **329**, 294–296.

134 E. M. Alvarez, C. B. White, J. Gregory, G. C. Kydd, A. Harris, H. H. Sun, A. M. Gillium and R. Cooper, *J. Antibiot. (Tokyo).*, 2012, **48**, 1165–1167.

135 J. Chu, X. Vila-Farres, D. Inoyama, M. Ternei, L. J. Cohen, E. A. Gordon, B. V. B. Reddy, Z. Charlop-Powers, H. A. Zebroski, R. Gallardo-Macias, M. Jaskowski, S. Satish, S. Park, D. S. Perlin, J. S. Freundlich and S. F. Brady, *Nat. Chem. Biol.*, 2016, **12**, 1004–1006.

136 E. M. Grzelak, C. Hwang, G. Cai, J. W. Nam, M. P. Choules, W. Gao, D. C. Lankin, J. B. McAlpine, S. G. Mulugeta, J. G. Napolitano, J. W. Suh, S. H. Yang, J. Cheng, H. Lee, J. Y. Kim, S. H. Cho, G. F. Pauli, S. G. Franzblau and B. U. Jaki, *ACS Infect. Dis.*, 2016, **2**, 294–301.

137 R. N. Mshana, G. Tadesse and G. Abate, *J. Clin. Microbiol.*, 1998, **36**, 1214–1219.

138 A. Al-Mourabit, R. Laville, T. Binh Nguyen, C. Moriou, S. Petek and C. Debitus, *Heterocycles*, 2014, **90**, 1351.

139 L. Ding, W. Yuan, Q. Peng, H. Sun and S. Xu, *Chem. Nat. Compd.*, 2016, **52**, 969–970.

140 R. He, B. Wang, T. Wakimoto, M. Wang, L. Zhu and I. Abe, *J. Braz. Chem. Soc.*, 2013, **24**, 1926–1932.

141 M. M. Zhai, H. T. Niu, J. Li, H. Xiao, Y. P. Shi, D. L. Di, P. Crews and Q. X. Wu, *J. Agric. Food Chem.*, 2015, **63**, 9558–9564.

142 S. N. Kumar, J. V. Siji, B. Nambisan and C. Mohandas, *Appl. Biochem. Biotechnol.*, 2012, **168**, 2285–2296.

143 E. Sansinenea, F. Salazar, J. Jiménez, Á. Mendoza and A. Ortiz, *Tetrahedron Lett.*, 2016, **57**, 2604–2607.

144 K. H. Rhee, *Int. J. Antimicrob. Agents*, 2004, **24**, 423–427.

145 I. Grangemarda, J. Bonmatinb, J. Bernillon, L. De Biochimie, S. Bioorganique

and U. C. Bernard, *J. Antibiot. (Tokyo).*, 1999, **52**, 363–373.

146 A. Mhammedi, F. B. Peypoux, F. Besson and G. Michel, *J. Antibiot. (Tokyo).*, 2012, **35**, 306–311.

147 Y. Kajimura, M. Sugiyama and M. Kaneda, *J. Antibiot. (Tokyo).*, 1995, **48**, 1095–103.

148 M. Tullberg, M. Grøtli and K. Luthman, *Tetrahedron*, 2006, **62**, 7484–7491.

149 K. H. Rhee, *J. Microbiol. Biotechnol.*, 2006, **16**, 158–162.

150 M. M. Alshaibani, N. Mohamadzin, J. Jalil, N. M. Sidik, S. J. Ahmad, N. Kamal and R. Edrada-Ebel, *J. Microbiol. Biotechnol.*, 2017, **27**, 1249–1256.

151 A. D. Borthwick, *Chem. Rev.*, 2012, **112**, 3641–3716.

152 L. Mehdi, R. B. A; Shaaban, K.A.; Rebai, I.K.; Smaoui, S.; Bejar, S.; Mellouli, *J. Nat. Prod. Res.*, 2009, **23**, 1095–1107.

153 M. P. amie H, Kilian G, Dyason K, *J. Pharm. Pharmacol.*, 2002, **54**, 1659–1665.

154 M. P. Jamie H, Kilian G, *Pharmazie*, 2002, **57**, 638–642.

155 M. J. le Maire M, Champeil P, *Biochim. Biophys. Acta*, 2000, **1508**, 86–111.

156 J. K. L. S. J. F. Horsburgh, M. J., J. L. Aish, I. J. White, L. Shaw, *J. Bacteriol.*, 2002, **184**, 5457–5467.

157 T. Baba, T. Ara, M. Hasegawa, Y. Takai, Y. Okumura, M. Baba, K. A. Datsenko, M. Tomita, B. L. Wanner and H. Mori., *Mol. Syst. Biol.*, 2006, **2**, 1–11.

158 J. E. Towle, School of Molecular and Cellular Biology, Faculty of Biological Sciences, University of Leeds, 2007.

159 N. Martel, C. M., J. E. Parker, O. Bader, M. Weig, U. Gross, A. G. S. Warrilow and D. E. K. and S. L. K. Rolley, *Antimicrob. Agents Chemother.*, 2010, **54**, 4527–4533.

160 F. Gullo, V.P., McAlpine, J., Lam, K.S., Baker, D., Petersen, *J Ind Microbiol Biotechnol*, 2006, **33**, 523–531.

161 K. Kazuma, N. Noda and M. Suzuki, *Phytochemistry*, 2003, **62**, 229–237.

162 J. C. Merlin, A. Statoua, J. P. Cornard, M. Saidi-Idrissi and R. Brouillard, *Phytochemistry*, 1993, **35**, 227–232.

Appendices

Appendix A1
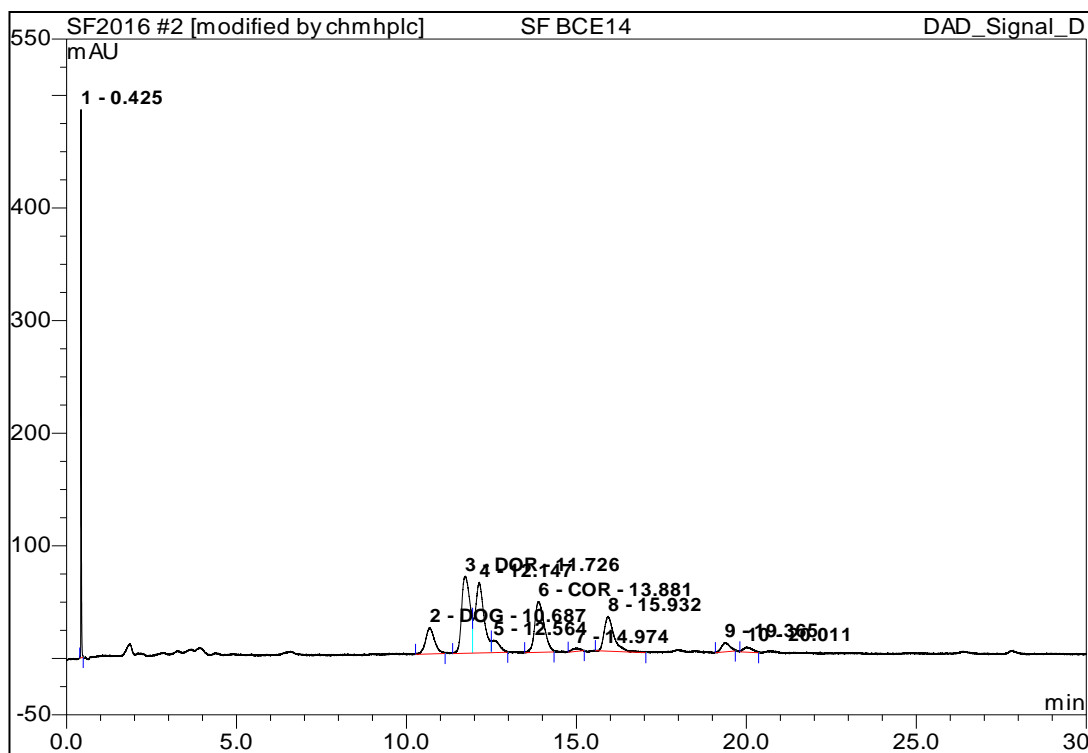
The HPLC chromatogram for post-SPE blackcurrant extract at 350 nm when eluted with 0.5% TFA in the mobile phase.

Appendix A2
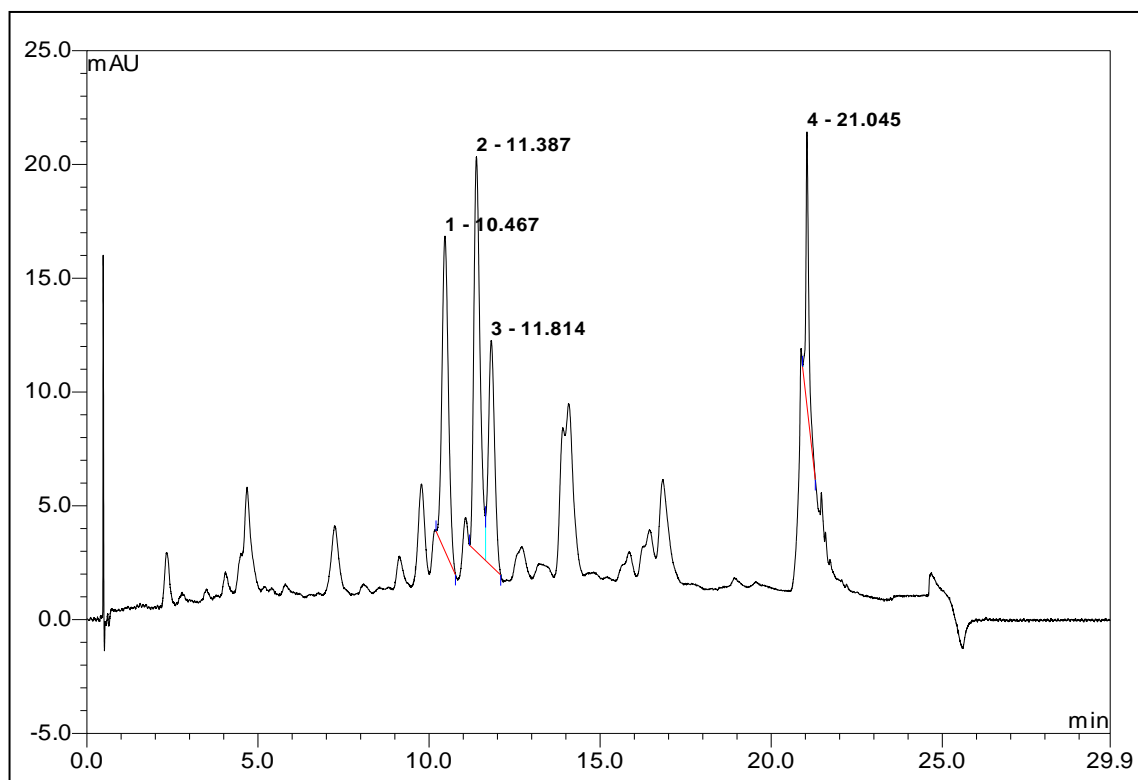
The HPLC chromatogram for post-SPE blackcurrant extract at 350 nm when eluted with 0.1% TFA in the mobile phase.
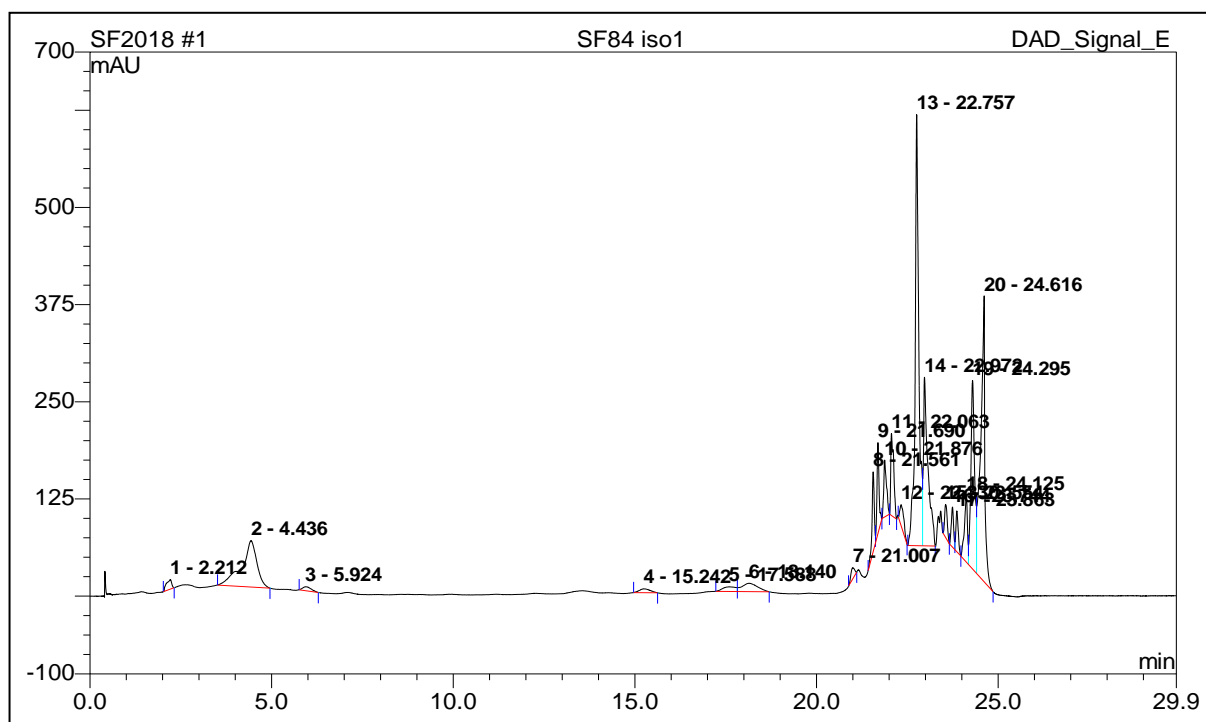
Appendix A3
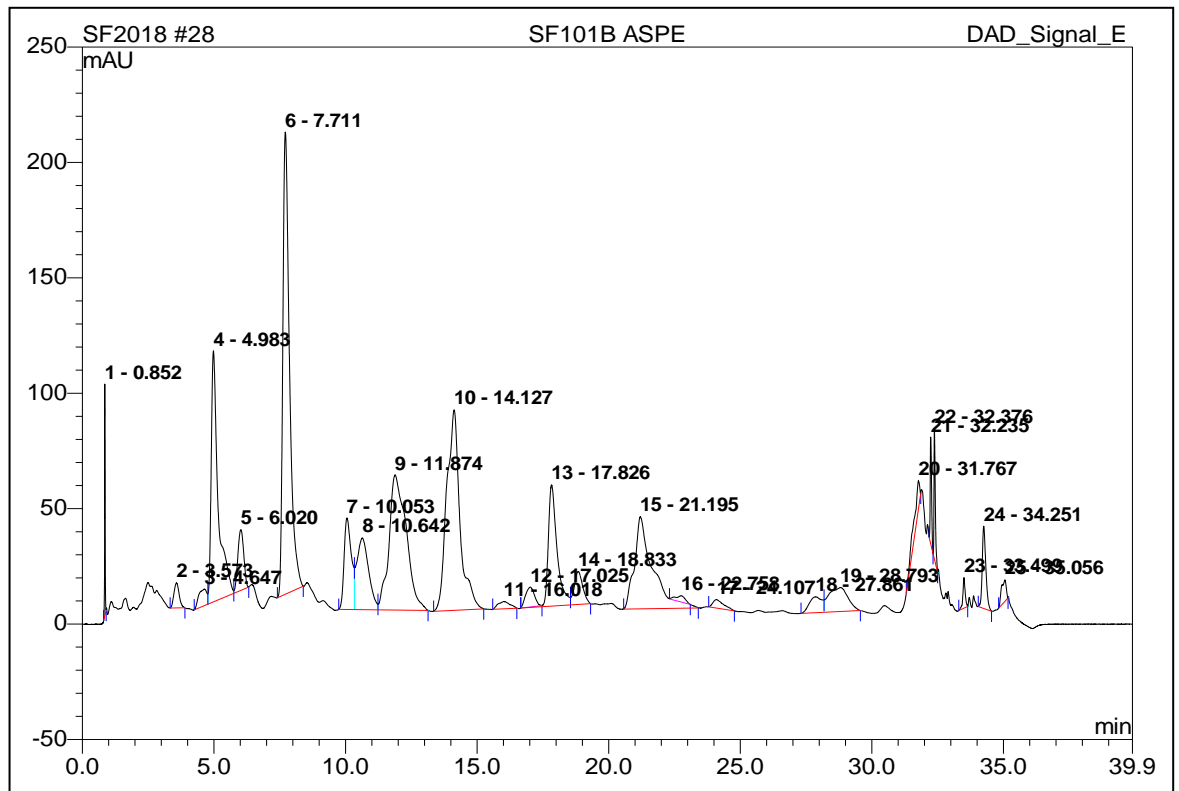
The HPLC chromatogram for methanolic blackcurrant extract at 325 nm.
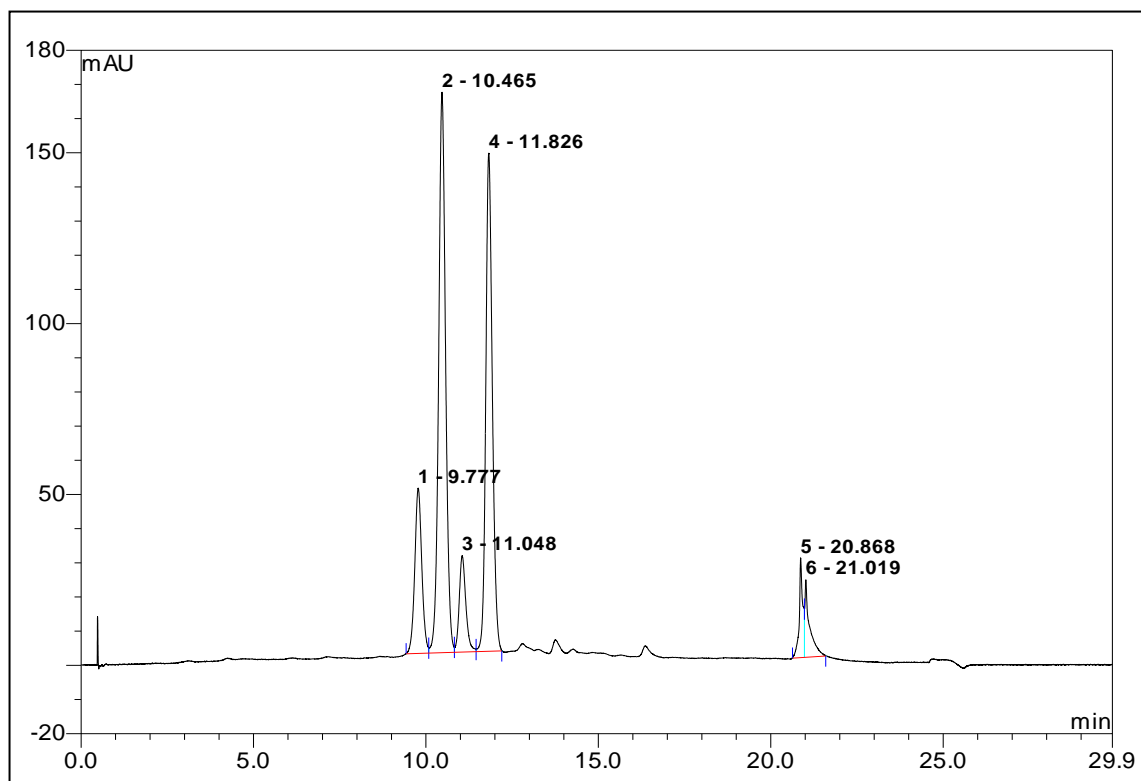
Appendix A4
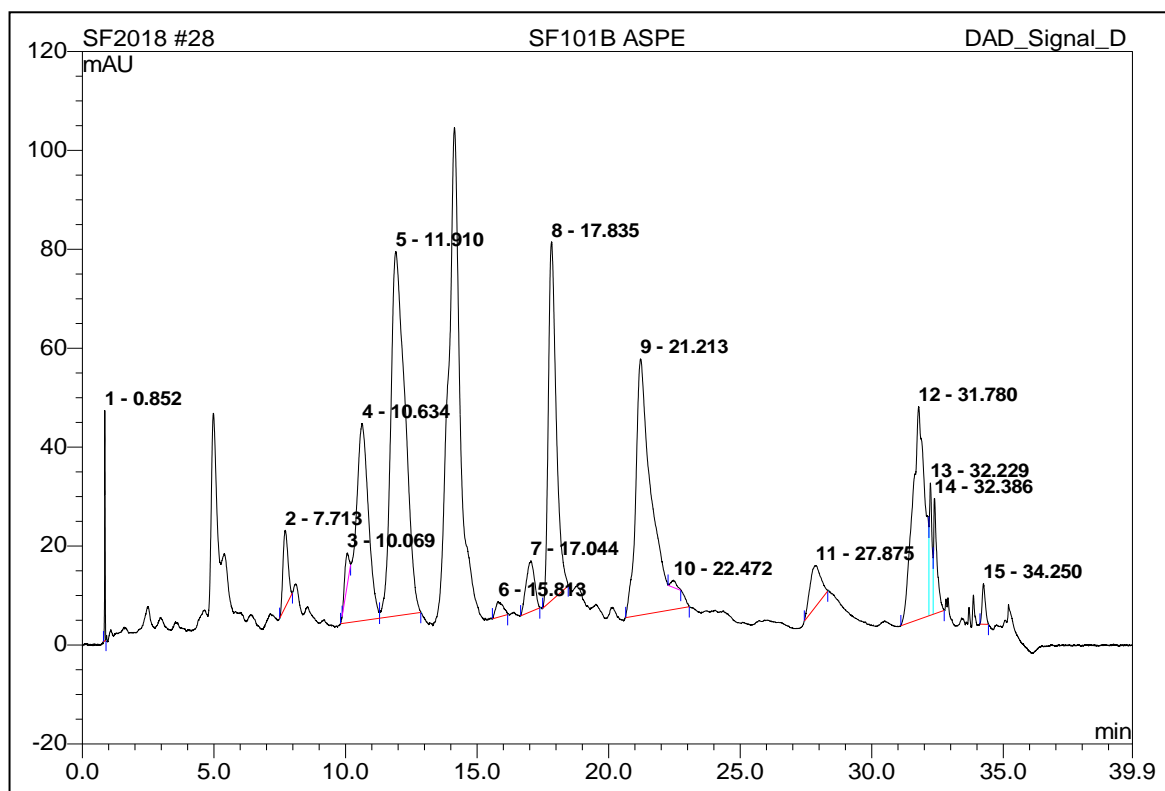
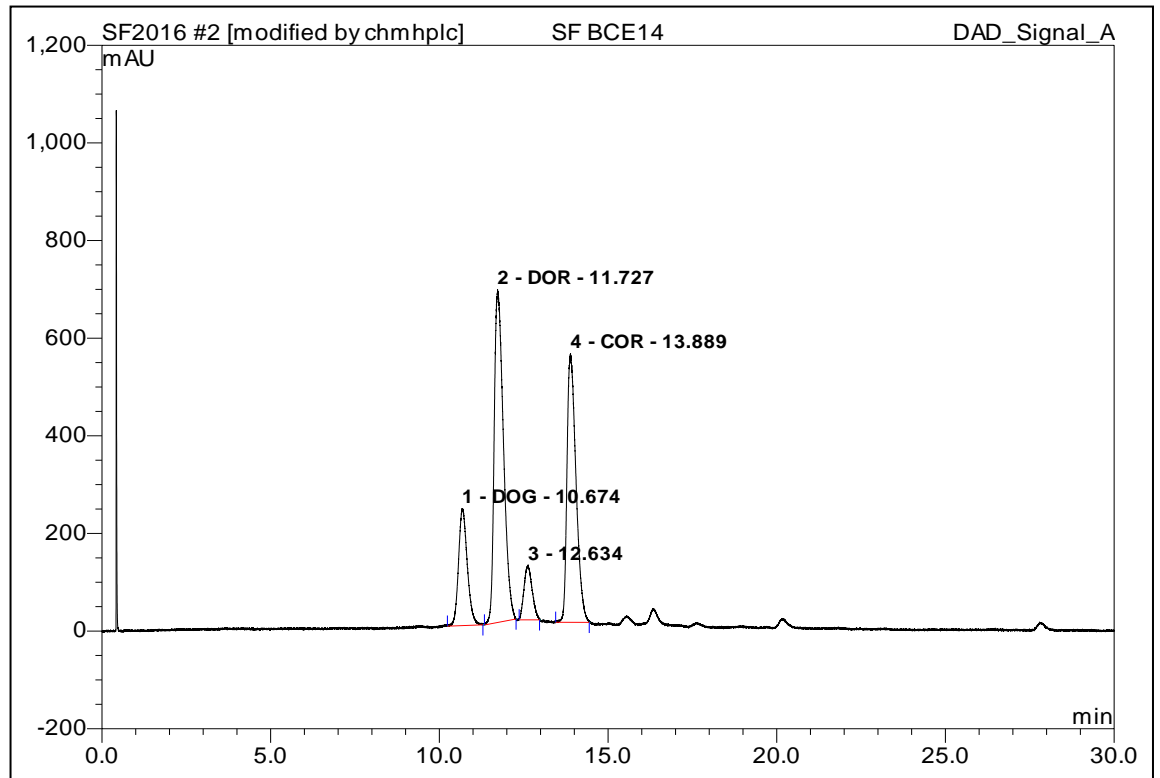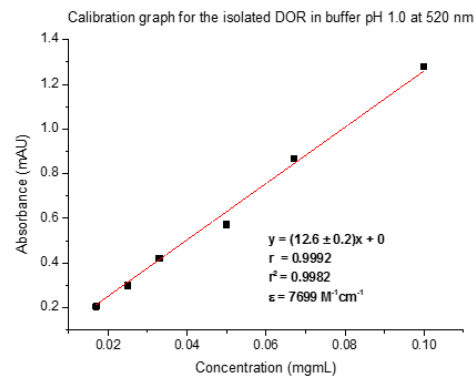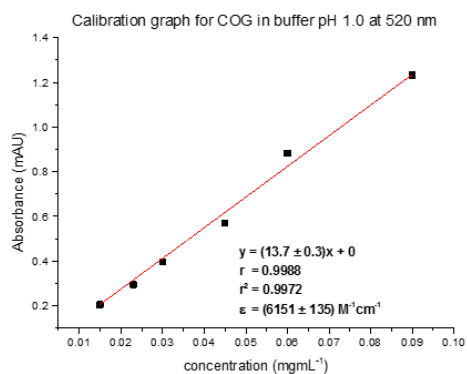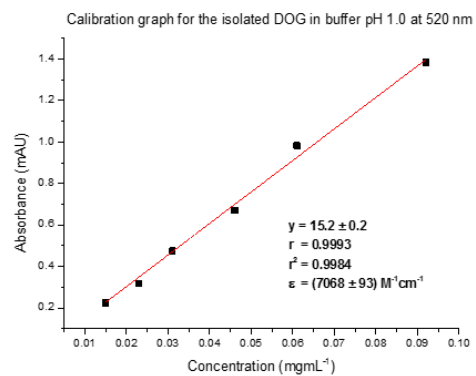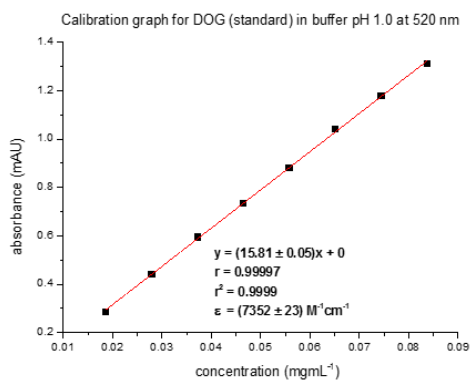The HPLC chromatogram for methanolic blackcurrant extract at 350 nm.

Appendix A5

The HPLC chromatogram for isopropylacetate blackcurrant extract at 325 nm.

Appendix A6

The HPLC chromatogram for post-SPE aqueous extract at 520 nm eluted with 0.1% TFA in the mobile phase.

Appendix A7

The HPLC chromatogram for post-SPE aqueous extract at 520 nm when eluted with 0.5% TFA in the mobile phase.

Appendix A8

Calibration graph for DOG (standard) in buffer pH 1.0 at 520 nm

$y = (15.81 \pm 0.05)x + 0$
$r = 0.99997$
$r^2 = 0.9999$
$\varepsilon = (7352 \pm 23)$ M^{-1}cm^{-1}

Calibration graph for the isolated DOG in buffer pH 1.0 at 520 nm

$y = 15.2 \pm 0.2$
$r = 0.9993$
$r^2 = 0.9984$
$\varepsilon = (7068 \pm 93)$ M^{-1}cm^{-1}

Calibration graph for COG in buffer pH 1.0 at 520 nm

$y = (13.7 \pm 0.3)x + 0$
$r = 0.9988$
$r^2 = 0.9972$
$\varepsilon = (6151 \pm 135)$ M^{-1}cm^{-1}

Calibration graph for the isolated DOR in buffer pH 1.0 at 520 nm

$y = (12.6 \pm 0.2)x + 0$
$r = 0.9992$
$r^2 = 0.9982$
$\varepsilon = 7699$ M^{-1}cm^{-1}

The calibration graphs for extinction coefficient studies for anthocyanins isolated from blackcurrant extract.

Appendix B1
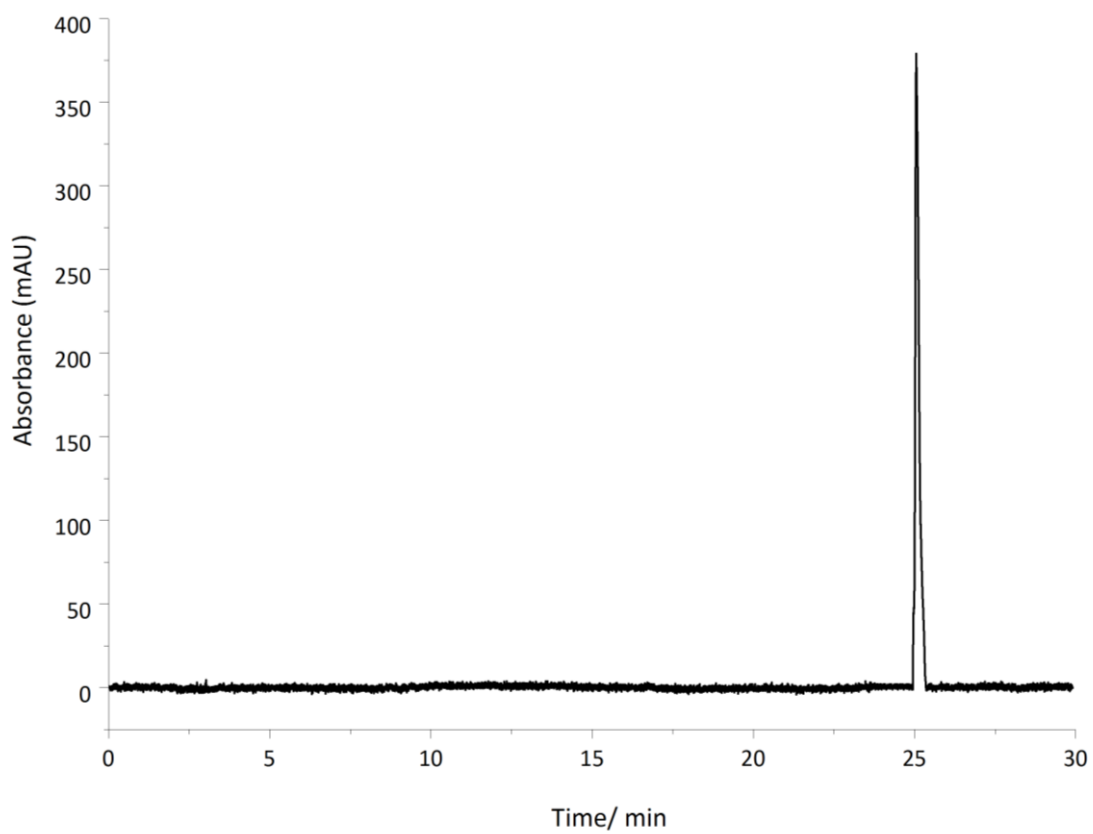
The HPLC chromatogram for γ-actinorhodin **46** at 520 nm.
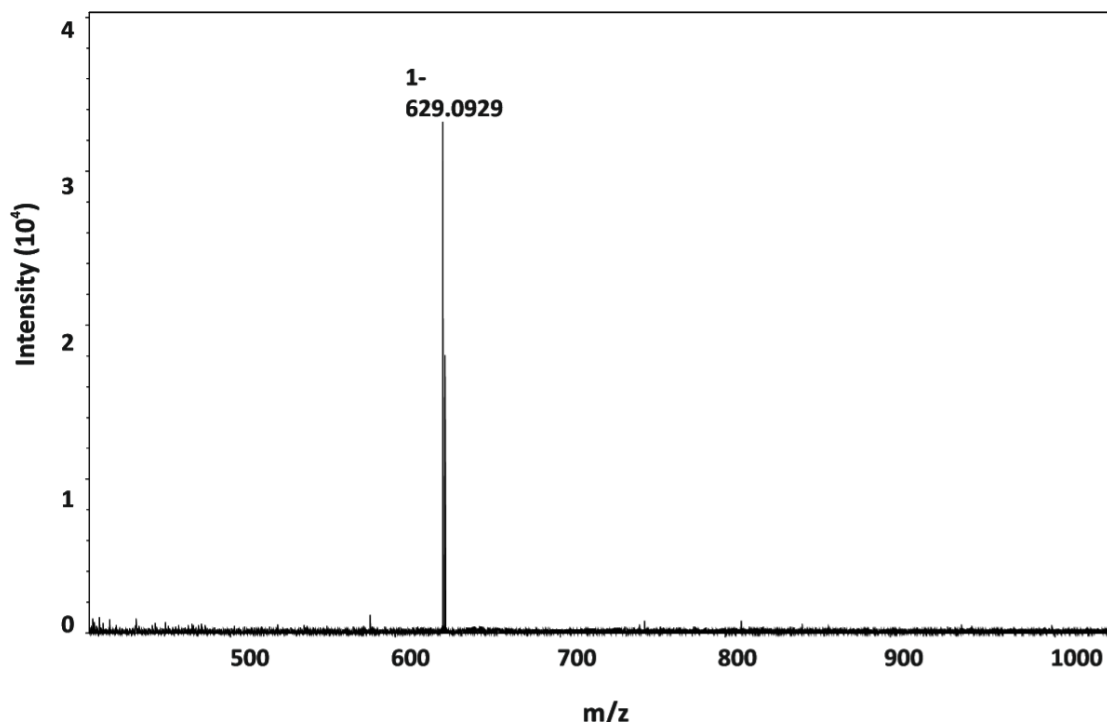
The mass spectrum for γ-actinorhodin **46**.
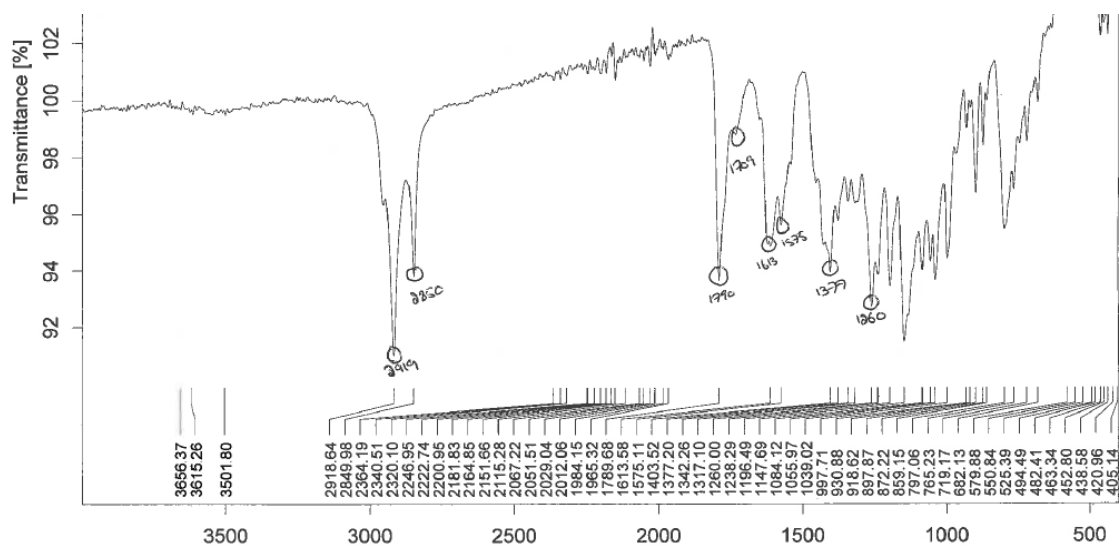
The IR spectrum for γ-actinorhodin **46**.
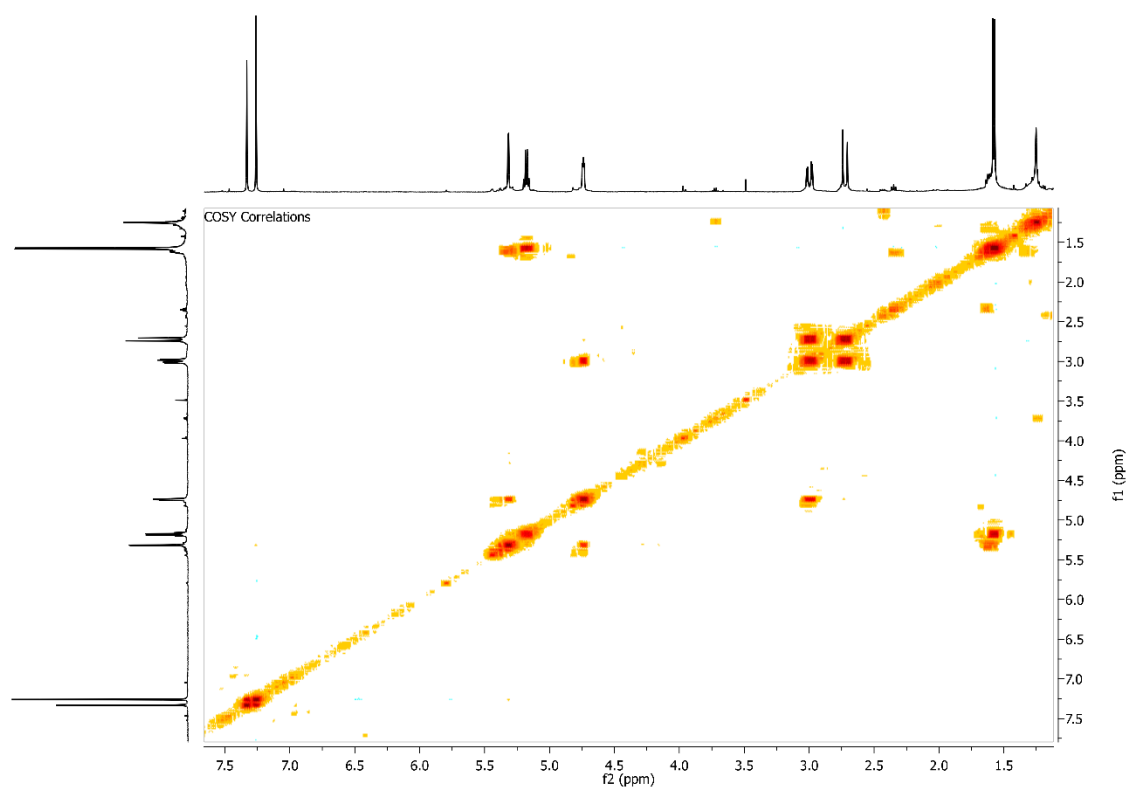
Appendix B4
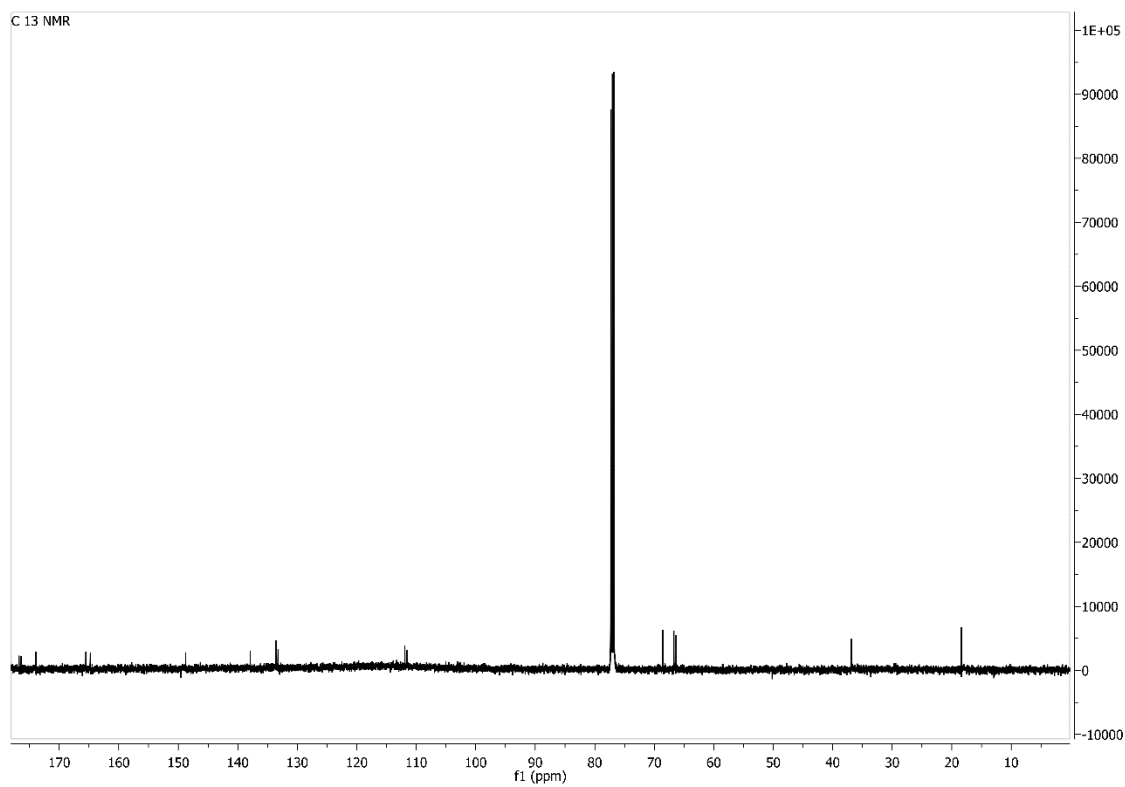
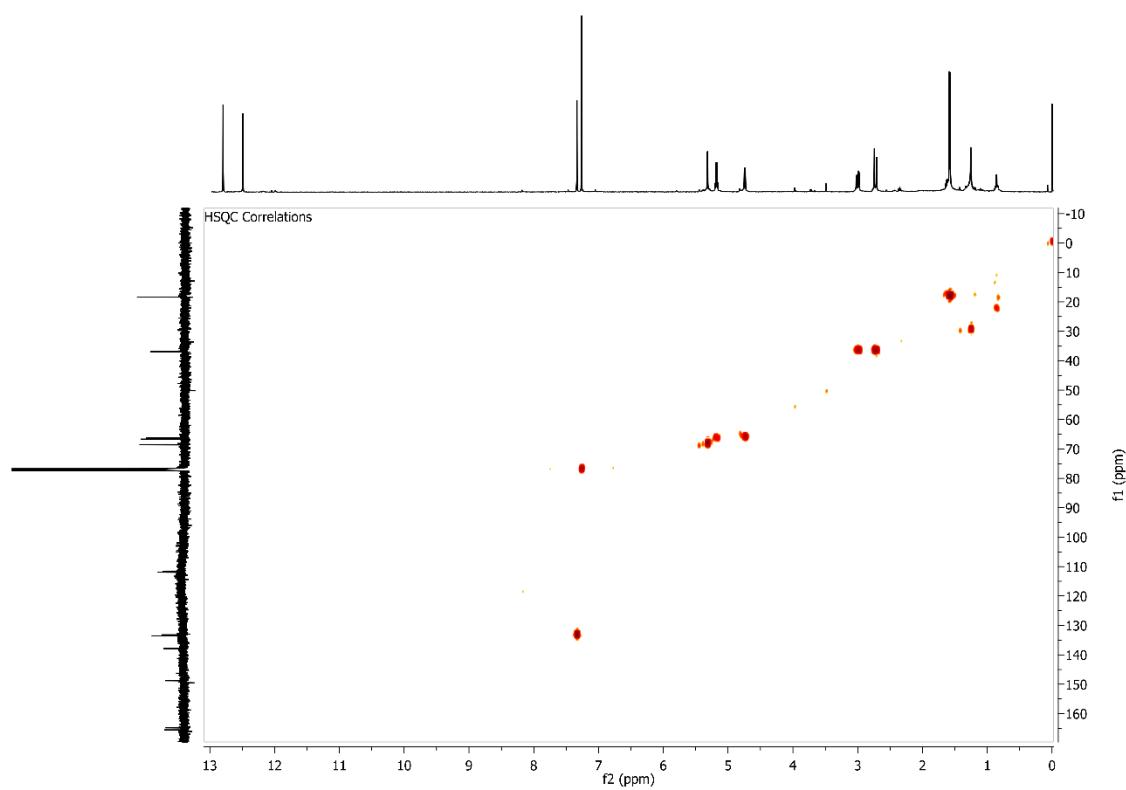The ^{13}C NMR spectrum for γ-actinorhodin **46** (400 MHz, CDCl$_3$ 77.1 ppm).

Appendix B5
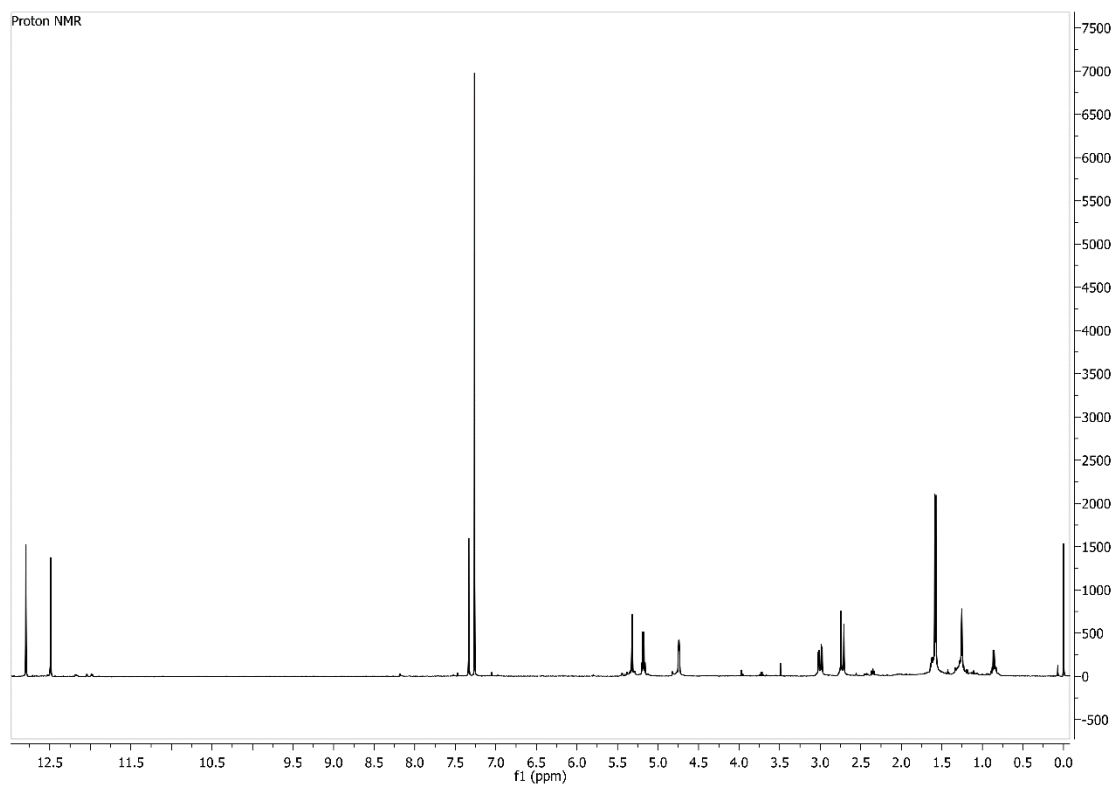
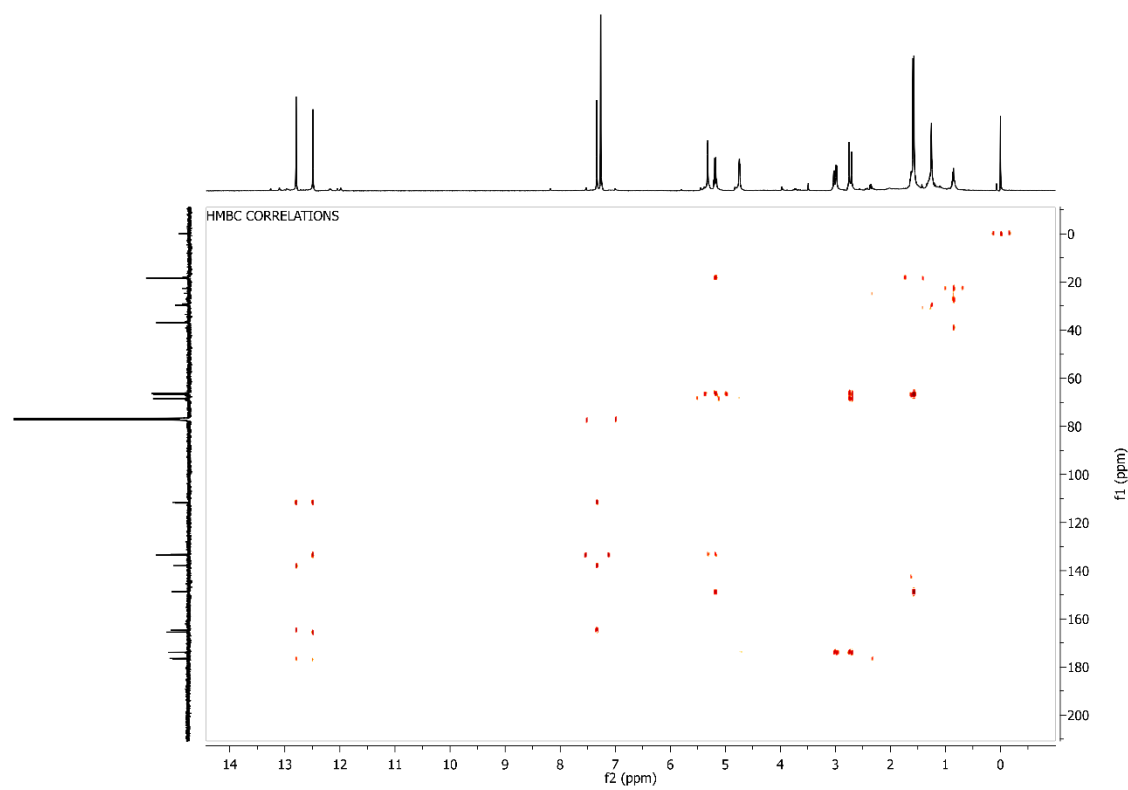The ^{1}H NMR spectrum for γ-actinorhodin **46** (400 MHz, CDCl$_3$ 7.26 ppm).

Appendix B6

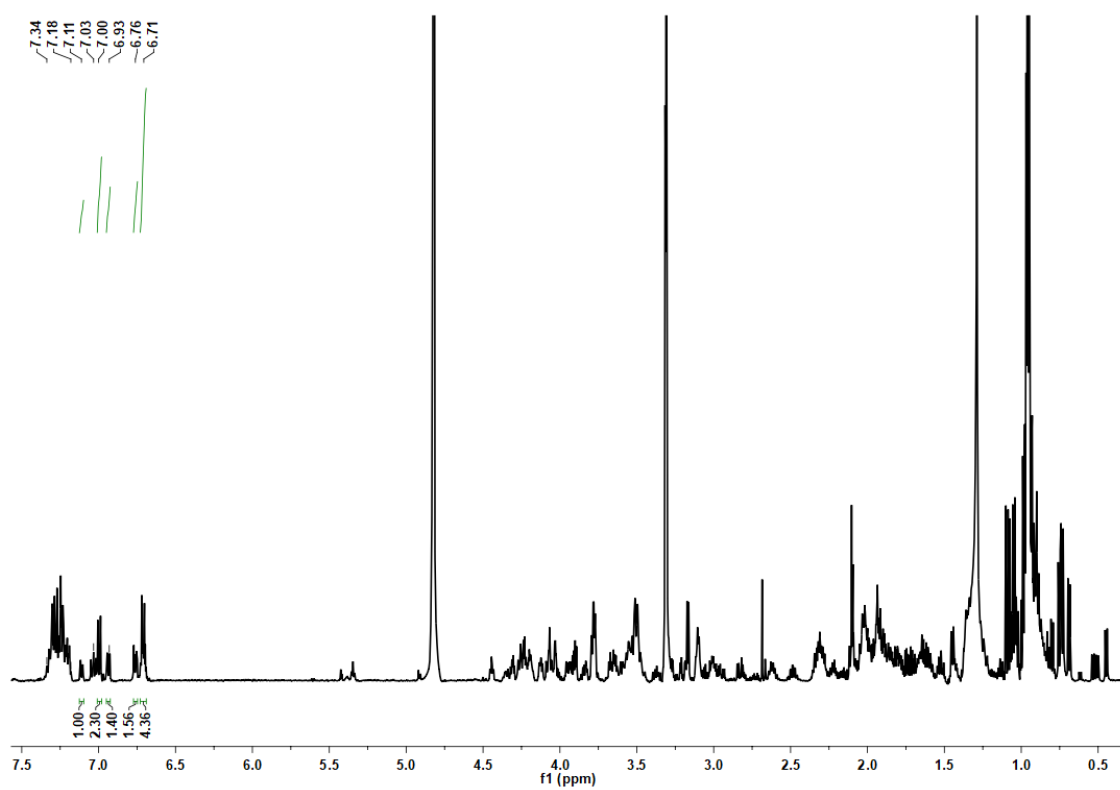The ^{1}H-^{1}H COSY NMR spectrum for γ-actinorhodin **46** (400 MHz, CDCl$_3$ 7.26 ppm).

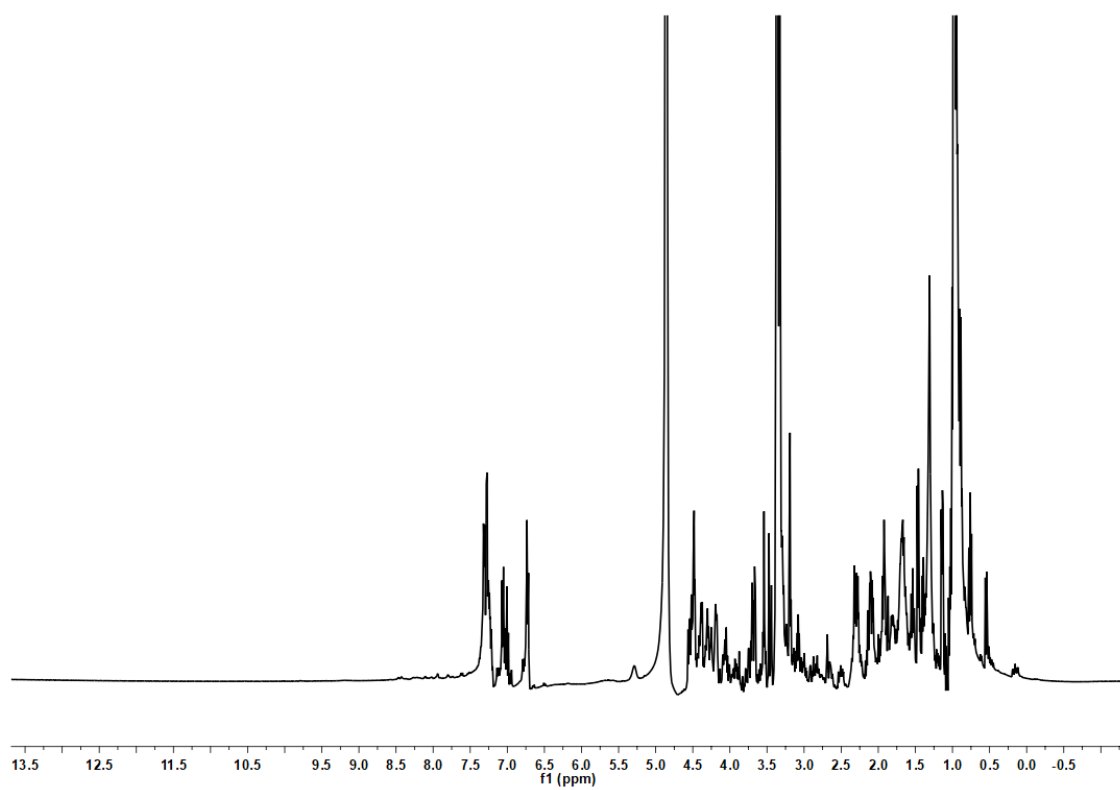The ^{1}H-^{13}C HSQC NMR spectrum for γ-actinorhodin **46**.

The ^{1}H-^{13}C HMBC NMR spectrum for γ-actinorhodin **46**.

Appendix C

The ^{1}H NMR spectrum for P5-25 crude extract.

Appendix D

The ^{1}H NMR spectrum for VF48A crude extract.